



NTNU – Trondheim
Norwegian University of
Science and Technology

Graphene Oxide as Reinforcement in Epoxy Based Nanocomposites.

Elizabeth Martine Svendsen

Chemical Engineering and Biotechnology

Submission date: June 2014

Supervisor: Wilhelm Robert Glomm, IKP

Co-supervisor: Finn Knut Hansen, Forsvarets forskningsinstitutt

Norwegian University of Science and Technology
Department of Chemical Engineering

Problem description

This problem was suggested by Finn Knut Hansen, UiO/FFI.

Graphene and graphene oxide (GO) have received much attention lately, and are promising materials for various applications. For use in nanocomposite materials graphene oxide is interesting because it has built-in reactive groups and is relatively easy to manufacture in large quantities. However, strong oxidation weakens the graphene structure so that GO can have both advantages and disadvantages. Reduced graphene oxide (RGO) is therefore an option, as some of the graphite structure will be retained, but RGO may still have functional groups. In the specialization project graphene oxide was made by chemical oxidation of graphite powder dispersed in strong acids and permanganate. RGO was also obtained by thermal reduction in vacuum.

The thesis will continue methods for the preparation of GO and RGO developed in the specialization project. Large quantities will be produced and will be used in nanocomposites based on epoxy polymers. This type of nanocomposites are very interesting to investigate for improvement of mechanical properties in tensile and shear action of advanced materials in for example air -space and marine applications. Nanocomposites will be produced by different strategies of dispersion and reaction with the active surface groups of GO and RGO. These will further be tested mechanically and thermally and compared with pure polymers.

Assignment given: January 6th, 2014

Supervisor: Wilhelm R. Glomm, NTNU/SINTEF

Co-supervisor: Finn Knut Hansen, UiO/FFI

Preface

This thesis was written as a final part of a master's degree at the department of Chemical Engineering, at the Norwegian University of Science and Technology (NTNU). The report was written during the subject TKJ4900 M.Sc. in Chemical Engineering. The M.Sc. thesis is a continuation of a research project which took place during the autumn of 2013 and was part of the course TKP4520 "Specialization project in Colloid and Polymer Chemistry". The experimental work of the study was undertaken between the end of January 2014 and the middle of May 2014 and has been carried out at the laboratory at the Norwegian Defence Research Establishment (FFI), Kjeller. The topic was suggested by Professor Finn Knut Hansen at FFI/University of Oslo (UiO).

I would like to thank my co-supervisor Professor Finn Knut Hansen at FFI/UiO for giving me the opportunity to work with this project and for advice during the thesis, and my main supervisor Professor Wilhelm R. Glomm for guidance with the report structure and proof reading of my report. I am very grateful to Tomas Roll Frømyr, PhD student and researcher at FFI, and Torbjørn Olsen researcher at FFI, for always having their door open for questions, and for much needed aid and advices. I would also like to thank Bernt Brønmo Johnsen, PhD at FFI for help with the three point flexural test and for useful comments on my results, Spyros Diplas, head of research at (SINTEF/UIO), for his assistance with the XPS analysis, and Nadia Karim, PhD student for proofreading my report. I would also like to thank all other FFI employees for being friendly and showing interest in my thesis, and for making the stay at FFI enjoyable. Lastly, I would like to thank Dag Erik for his encouragement and for being more than understanding and patient during many years of studying, as well as friends and family for their support.

Declaration of compliance

I declare that this is an independent work according to the exam regulations of the Norwegian University of Science and Technology (NTNU).



Place and date: Kjeller, June 2nd, 2014 Signature: Elizabeth Martine Svendsen

Abstract

Graphene oxide has received much attention in recent years because of its many promising properties. Graphene oxide can be used to produce graphene in large quantities, and in addition graphene oxide has many promising properties itself, such as its high level of dispersion in polar solvents, and good compatibility with various polymers. Addition of nanoparticles in composite materials have been tested for many years, and in recent years carbon nanotubes have been in focus as a reinforcement. Graphene oxide is considered very promising for reinforcement of composite materials and several studies have shown improvements in Young's Modulus-, tensile strength, and fracture toughness by adding graphene oxide into nanocomposites.

In this thesis, the way in which the mechanical properties of epoxy composite materials were affected by addition of various forms of graphene oxide was studied. The same epoxy resin (Araldite LY556) was used in all experiments, while other parameters were changed. Various experiments were performed with addition of graphene oxide, exfoliated graphene oxide and functionalized graphene oxide. Both water and acetone were used as solvents, para-phenylenediamine and XB3473 were used for the functionalization of the graphene oxide, and two different hardeners were used (XB3473 and isophorone diamine). Experiments with the dispersion of graphene oxide in various solvents were first performed. Graphene oxide was dispersed in an ultrasonic bath and by using ultrasonic horn. The graphene oxide dispersions were analyzed in a disk centrifuge. This data was used for the further experiments when transferring graphene oxide into the epoxy. The graphene oxide was wet transferred into the epoxy in either water or acetone. The functionalized graphene oxide was analyzed with XPS.

Despite the fact that previous studies have shown promising results for the reinforcement of composites with graphene oxide, the same impressive improvements were not found in this M.Sc. thesis. Problems with homogeneous dispersion were possibly the cause of these findings. The XPS indicated a successful functionalization of graphene oxide with para-phenylenediamine.

Sammendrag (Norwegian summary)

Grafen oksid har fått mye oppmerksomhet de siste årene pga. sine mange ettertraktede egenskaper. Grafen oksid kan blant annet brukes for å fremstille grafen i store kvanta, i tillegg til at grafen oksid selv har mange ettertraktede egenskaper, som blant annet god kompatibilitet med ulike polymerer og høy dispergeringsgrad i polare løsemidler. Tilsats av nanopartikler til komposittmaterialer har lenge vært prøvd ut, og de siste årene har karbonnanorør vært mest i fokus. Grafen oksid er ansett som svært lovende for forsterkning av komposittmaterialer. Flere undersøkelser har vist forbedringer i Youngs modul, strekkfasthet, og bruddseighet ved tilsats av grafen oksid til nanokompositter.

I denne masteroppgaven ble det sett på hvordan tilsats av ulike former for grafen oksid påvirker de mekaniske egenskapene til epoksybaserte komposittmaterialer. Samme epoksyresin (Araldite LY556) ble benyttet i alle forsøkene, mens andre parametere ble endret underveis. Det ble gjort forsøk med grafen oksid, eksfoliert grafen oksid og funksjonalisert grafen oksid. Både vann og aceton ble brukt som løsningsmidler, parafenyldiamin og XB3473 ble brukt til funksjonalisering av grafen oksid, og det ble benyttet to ulike herdere (XB3473 og isoforondiamin). Det ble først gjort forsøk med dispergering av grafen oksid i ulike løsningsmidler, hvor dispergering i ultralydbad og med ultralydhorn ble benyttet og undersøkt på disksentrifuge. Disse dataene ble videre brukt til overføring til epoksymateriale. Grafen oksid i alle former ble overført i løst form i enten vann eller aceton. Funksjonaliser grafen oksid ble undersøkt med XPS.

På tross av at tidligere studier har vist lovende resultater for forsterkning av kompositter med grafen oksid, ble det ikke funnet forbedringer ved tilsats av i denne masteroppgaven. Problemer med homogen dispergering er muligens årsaken til disse funnene. XPS resultatene indikerte en suksessfull funksjonalisering av grafen oksid med parafenyldiamin.

Table of Contents

PROBLEM DESCRIPTION	I
PREFACE.....	III
ABSTRACT	V
SAMMENDRAG (NORWEGIAN SUMMARY)	VII
ABBREVIATIONS.....	XIII
LIST OF SYMBOLS	XV
1 INTRODUCTION.....	1
1.1 CONTEXT.....	1
1.2 AIM OF THE PROJECT AND STRUCTURE OF THE REPORT.....	2
2 THEORY.....	3
2.1 COMPOSITES.....	3
2.2 EPOXY POLYMERS	4
2.3 GRAPHENE AND GRAPHENE OXIDE	5
2.3.1 <i>Exfoliation and reduction of GO</i>	10
2.3.2 <i>Functionalization</i>	12
2.4 DISPERSION AND STABILITY IN SOLUTION.....	13
2.4.1 <i>Surface and interfacial tension</i>	14
2.4.2 <i>Zeta Potential</i>	15
2.5 PREPARATION OF NANOCOMPOSITES	17
2.5.1 <i>Graphene oxide in epoxy</i>	17
2.5.2 <i>Dispersion in composites</i>	18
2.6 MECHANICAL PROPERTIES.....	20
2.7 PREVIOUS STUDY	23
3 EXPERIMENTAL	27
3.1 MATERIALS.....	27
3.2 METHODS	29
3.2.1 <i>Preparation of GO</i>	29
3.2.2 <i>Exfoliation of GO</i>	31
3.2.3 <i>Dispersing GO</i>	32
3.2.3.1 <i>Dispersing EXGO (300 °C) with ultrasonic bath</i>	32

3.2.3.2	Dispersing as- prepared GO in ultrasonic bath	32
3.2.3.3	Dispersing as-prepared GO with horn-type ultrasonicator	33
3.2.4	<i>Particle size distribution of GO dispersions</i>	34
3.2.5	<i>Functionalization of as- prepared GO</i>	35
3.2.5.1	Functionalization of GO with diamine XB3473	35
3.2.5.2	Functionalization of GO with para-phenylenediamine (PPDA).....	36
3.2.6	<i>X-Ray photoelectron spectroscopy</i>	37
3.2.7	<i>Effect of pH</i>	38
3.2.8	<i>Zeta potential</i>	38
3.2.9	<i>Optical microscope</i>	38
3.2.10	<i>Pre-tests of epoxy/water dispersion</i>	38
3.2.11	<i>Surface tension and interfacial tension</i>	39
3.2.12	<i>Preparation of epoxy in distilled water and acetone</i>	40
3.2.13	<i>Preparation of composites</i>	41
3.2.13.1	Nanocomposites with epoxy system Araldite LY556/XB3473	43
3.2.13.2	Epoxy system Araldite LY556/isophorone diamine	44
3.2.13.3	FGO (PPDA) in distilled water and IPDA	45
3.2.14	<i>Preparation of epoxy composite testing rods</i>	45
3.2.15	<i>Dynamic mechanical analysis</i>	46
3.2.16	<i>Three-point flexural bending test</i>	47
4	RESULTS AND DISCUSSION	49
4.1	DISPERSION OF GO	49
4.1.1	<i>Dispersing EXGO (300 °C) in ultrasonic bath</i>	49
4.1.2	<i>Dispersing as- prepared GO with ultrasonic bath</i>	51
4.1.3	<i>Dispersing GO in acetone with ultrasonic horn</i>	52
4.1.4	<i>Dispersing GO in distilled water with ultrasonic horn</i>	53
4.2	X-RAY PHOTOELECTRON SPECTROSCOPY	55
4.2.1	<i>Surface composition</i>	55
4.2.2	<i>Functional groups</i>	58
4.3	EFFECT OF PH	61
4.4	ZETA POTENTIAL	63
4.5	SURFACE TENSION AND INTERFACIAL TENSION.....	64
4.6	OPTICAL MICROSCOPE	66
4.6.1	<i>GO in acetone</i>	66
4.6.2	<i>Epoxy with FGO (XB3473) in distilled water</i>	66
4.6.3	<i>Epoxy with FGO (PPDA) in acetone</i>	68
4.6.4	<i>EXGO (1000 °C) in distilled water and SDS</i>	69
4.6.5	<i>EXGO (300 °C) in acetone</i>	70

4.6.6	<i>FGO (PPDA) in distilled water (XB3473/LY556)</i>	70
4.6.7	<i>FGO (PPDA) in distilled water (IPDA/LY556)</i>	74
4.7	DYNAMIC MECHANICAL ANALYSIS AND THREE-POINT FLEXURAL BENDING TEST.....	79
4.8	PREPARATION OF COMPOSITES	88
4.9	DISCUSSION/SUMMARY	92
4.10	FUTURE WORK.....	98
5	CONCLUSION	99
6	REFERENCES	101
	APPENDICES	I

Abbreviations

¹³ C-NMR	Nuclear magnetic resonance spectroscopy to carbon 13
AFM	Atomic force microscopy
CCG	Chemically converted graphene
CNT	Carbon nanotube
CVD	Chemical vapour deposition
DCS	Disc centrifuge
DGEBA	Diglycidyl ether of bisphenol-A
DLS	Dynamic light scattering
DMA	Dynamic mechanical analysis
DMTA	Dynamic mechanical thermal analysis
DSC	Diffraction scanning calorimeter
e.g.	for example
ECH	Epichlorohydrine
EXGO	Exfoliated GO
FFI	Norwegian Defence Research Establishment
FGO	Functionalised GO
FGS	Functionalized graphene
FTIR	Fourier transform infrared (spectroscopy)
GO	Graphene oxide
GPL	Graphene platelets
IEP	Isoelectric point
IPDA	Isophorone diamine

MIBK	Methyl isobutyl ketone
MWCNT	Multi walled carbon nanotube
NTNU	Norwegian University of Science and Technology
PAA	Poly (acrylic acid)
PAN	Poly (acrylonitrile)
PMMA	Poly (methyl methacrylate)
PPDA	p-phenylenediamine
PVA	Poly vinyl alcohol
RGO	Reduced GO
SDS	Sodium dodecyl sulphate
SEM	Scanning electron microscope
Silane-f-GO	silane functionalized graphene oxide
SWCNT	Single walled carbon nanotube
TEM	Transmission electron microscope
T _g	Glass transition temperature
TGA	Thermo gravimetric analysis
TPU	Thermoplastic polyurethane
TRGO	Thermally reduced graphene oxide
UiO	University of Oslo
UL	Ultrasonic treatment
XPS	X-ray photoelectron spectroscopy
XRD	X-Ray diffraction

List of symbols

A	original cross section area through which a force is applied (mechanics)
a	particle radius
d	specimen thickness (mm) (Mechanics)
D_{ST}	Stokes' spherical diameter (μm) (Particle size distribution)
E	Young's modulus (mechanics)
E'	Storage modulus (mechanics)
E''	Loss modulus (mechanics)
E_f	Flexural strain (mechanics)
ϵ	dielectric constant
ϵ	Strain (mechanics)
ϵ_{fB}	flexural strain (mechanics)
F	force exerted on an object under tension (mechanics)
κ	the inverse of the Debye screening length
L	length of support span (mm) (Mechanics)
l	change in length (mechanics)
Δl_0	original length of an object (mechanics)
η	Viscosity
σ	Stress (mechanics)
σ_{fM}	Flexural stress (mechanics)
ρ_p	mass density of the particles (kg/m^3)
ρ_f	mass density of the fluid (kg/m^3)
R	cross-head speed (mm/min) (Mechanics)
R	particle radius
ζ	Zeta potential
Ψ_δ	Stern potential

U_E	Electrophoretic mobility
μ	viscosity of the liquid
v_s	particle's settling velocity (m/s)
W_d	fractional mass (g/m) (particle size distribution)
Z	straining of the outer fibre (mm/mm/min=0.01) (Mechanics)

1 Introduction

1.1 Context

A lot of attention has been directed towards graphene and graphene oxide lately as their many extraordinary properties are expected to be valuable in a variety of applications. Among others, graphene based materials are predicted to give improvements in food packaging, medicine, faster internet, insulators, and nanocomposite materials [1]. Polymer nanocomposites with incorporated graphene based materials have especially received considerable attention. Different studies have shown improvements in properties such as Young's modulus, tensile strength, and stiffness of nanocomposites when graphene or graphene oxide is added [2].

Composite materials with matrices based on epoxy resins are frequently applied in the automotive-, airspace- and marine industries [3]. By the modification of molecular architecture and structure of the epoxy matrices, the mechanical property profile can be improved. Increasing the crosslink density of the epoxy material can possibly improve the stiffness and strength. Conversely the behaviour of highly cross-linked epoxy matrices can be undesirably brittle and can lead to spontaneous failure [3]. Providing epoxy matrices with high toughness and simultaneously maintaining the thermo-mechanical properties is a challenge, and this is therefore an area of heavy research [3].

Addition of nanoparticles in epoxy polymers appears to affect and improve the properties of the composite. Addition of nanoparticles in composite materials can potentially improve properties like strength, stiffness, flame resistance, thermal conductivity, electrical conductivity, and optical clarity [2]. A common problem with nanoparticles dispersed in a polymer matrix, is that they agglomerate very easily and it is difficult to obtain a good dispersion [4-7]. In addition, poor interfacial adhesion between polymer and nanoparticle has been reported to be a problem [4].

Previously, most of the research on the incorporation of nanoparticles has been related to carbon nanotubes (CNTs), clay, silica and alumina [4-7]. More recently, however, considerable interest and research has been directed towards graphene and graphene oxide due to its many exceptional properties. Large scale production of graphene, however, is a problem. Recent research has shown promising results by using graphene oxide as a precursor for graphene production. In addition, graphene oxide has its own beneficial properties e.g. a

high level of dispersion in polar solvents, dispersibility in various matrices and better compatibility with polymers compared to CNT's.

1.2 Aim of the project and structure of the report

This M.Sc. thesis is a continuation of a specialization project carried out during the fall of 2013 as part of the course TKP4520 "Specialization project in Colloid and Polymer Chemistry" at NTNU. During the specialization project, graphene oxide (GO) was prepared by chemical oxidation of graphite powder, and later characterized with scanning electron microscope (SEM), Fourier transform infrared spectroscopy (FTIR), X-Ray photoelectron spectroscopy (XPS), atomic force microscopy (AFM), thermo gravimetric analysis (TGA), dynamic light scattering (DLS), disc centrifuge (DCS) and differential scanning calorimetry (DSC). In addition, the GO was exfoliated with different methods using ultrasonic and thermal treatments.

The aim of the thesis is to investigate whether the addition of GO can improve the mechanical properties of nanocomposites based on an epoxy system. During the thesis, firstly the dispersion of GO in different solvents and optimization of duration of the ultrasonic treatment was assessed. As prepared GO, functionalised GO with diamine and exfoliated GO were dispersed in either distilled water, acetone, methyl isobutyl ketone (MIBK), or distilled water with sodium dodecyl sulphate (SDS), and added to the epoxy system. XB3473 and paraphenylenediamine were used for the functionalization of GO. The different epoxy composites were further analysed with dynamic mechanical analysis (DMA) and three-point flexural bending test. The results were first analysed in the dedicated instrument programs, followed by plotting original data values in Origin Pro.

Chapter 2 contains background theory about composites, epoxy resins, preparation of graphene oxide, issues related to the manufacturing, processing and use of epoxy based composite matrices, mechanical properties, and a literature survey. A description of materials and experimental methods used throughout the M.Sc. thesis is given in Chapter 3. Chapter 4 includes the obtained results with the related discussions, a summarizing discussion of the overall results, and suggestions for further work. The conclusion is presented in Chapter 5, followed by the bibliography in Chapter 6. The various raw data files of DMA, Three point flexural bending test and Zeta potential, are attached as Appendices. Data sheet, Risk assessment, tables of surface and interfacial tension and characteristic binding energies for XPS analyses are also attached in Appendices.

2 Theory

In order to get a better understanding of the previous work done with respect to graphene oxide as reinforcement in epoxy based nanocomposites, a literature survey was conducted. The aim was to get an overview of the methods that were used, the problems and challenges, and the advantageous properties that could be obtained. This chapter will focus on some background theory about composites, epoxy polymers, graphene oxide, different dispersions and mechanical properties, and a section of previous study are included in Section 2.7.

2.1 Composites

A composite is a material formed of two or more constituents, usually a matrix and reinforcement. The advantage of a composite material is that the properties of each constituent are combined to produce a single material with better properties than the individual components separately [8]. The reinforcing phase provides the strength and stiffness to the composite, and usually consists of particles or fibres. The matrix, often a polymer, is used for maintaining orientation and spacing, in addition to protecting the reinforcement against the environment and abrasion. In other words, the polymer matrix is the “glue” holding the fibres (carbon fibres, glass fibres etc.) together [8]. Composites with incorporated particles, platelets or fibres with at least one dimension in the range between 1-100 nm, are called nanocomposites [9]. The idea of using nanoparticles in combination with composite material was first proposed by Toyota Central Research Laboratories in Japan in the 1990s. The laboratory tried to incorporate a small amount of nanofiller with Nylon-6 composite, and the results showed improvements in both thermal and mechanical properties [4].

Composites, especially high strength carbon- and glass fibres, have the ability to enhance mechanical properties and reduce component weight [8]. Some of the most interesting applications are found in air- and spacecraft industries where resins and fibres are combined to produce complex composite structures [7]. Low weight and high strength are important factors in aircraft-, automobile-, and space industries, as it is possible to increase the free space for additional fuel and payload, and potentially save energy [8]. Aircraft, aerospace-, defence-, ship-, car-, and sports equipment industries all try to bring forward new materials

with low weight and high strength. Advanced materials, like fibre- reinforced polymeric composites are made of ductile polymer matrices which contribute to light weight and chemical resistance, combined with high strength fibres [10]. Addition of nanoparticles in composites can potentially increase the mechanical strength and stiffness of the composite [11]. Changes in the glass transition temperature (T_g) of the polymer matrix is another potential effect of adding nanoparticles to a composite [7].

2.2 Epoxy polymers

Epoxy polymers consist of two components; the epoxy resin and the hardener or curing agent [12]. Epoxy resins comprise a class of thermoset materials first discovered during the late 1930s. They are chemically compatible with most substrates and are well suited to composite applications due to their tendency to wet surfaces easily [13]. Epoxies have many beneficial properties such as: high strength; low shrinkage; good adhesion to various substrates; effective electrical insulation; chemical and solvent resistance; low cost and low toxicity [7]. Diglycidyl ether of bisphenol-A (DGEBA) is the simplest and most widely used epoxy resin today. DGEBA is produced by a reaction of bisphenol A with epichlorohydrine (ECH). Bisphenol A is a compound with two phenol functional groups [12]. The number of repeating chains (n) in an epoxy resin varies from 0 to 25 and the end use applications of the resin depend on the number of chains. For the DGEBA n is almost zero (0.2) [13;14]. The chemical structure of DGEBA is shown in Figure 1.

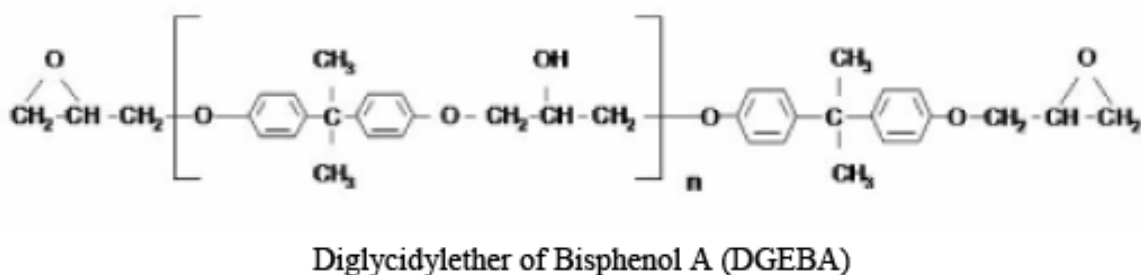


Figure 1- The simplest epoxy resin, bisphenol A [15].

Epoxy resins are normally in a viscous state, but harden with treatment, addition of hardener, and through curing. Different hardeners can be mixed with the epoxy resin for condensation curing of the composite and multiple combinations of resin and hardener are available. Predetermined ratios of resin and hardener are used for the mixing, and different curing

temperatures are required for the mix to cure and give the best polymer properties. The hardener normally reacts with the polymer forming a cross-linking network. The cure kinetics and the glass transition temperature (T_g) of the epoxy are dependent on the chemical nature of the hardener because the hardener controls the cross-link nature [12]. The hardener is an oligomer with low molecular weight and contains one or more epoxy groups per molecule that can crosslink. High temperature curing systems generally have higher glass transition temperature, strength and stiffness, compared to the curing systems used at room temperature. Typically, high temperature curing systems are aromatic amines or acid anhydrides, while aliphatic amines are used as room temperature curing agents [16].

2.3 Graphene and graphene oxide

Graphene is an allotrope of carbon, and is often called “the mother of all graphitic forms” (Figure 2), as it is considered to be the building block for other sp^2 carbon allotropes (nanotubes, graphite and fullerenes). Graphene can be wrapped up into Bucky balls, rolled into nanotubes or stacked into graphite [17-19].

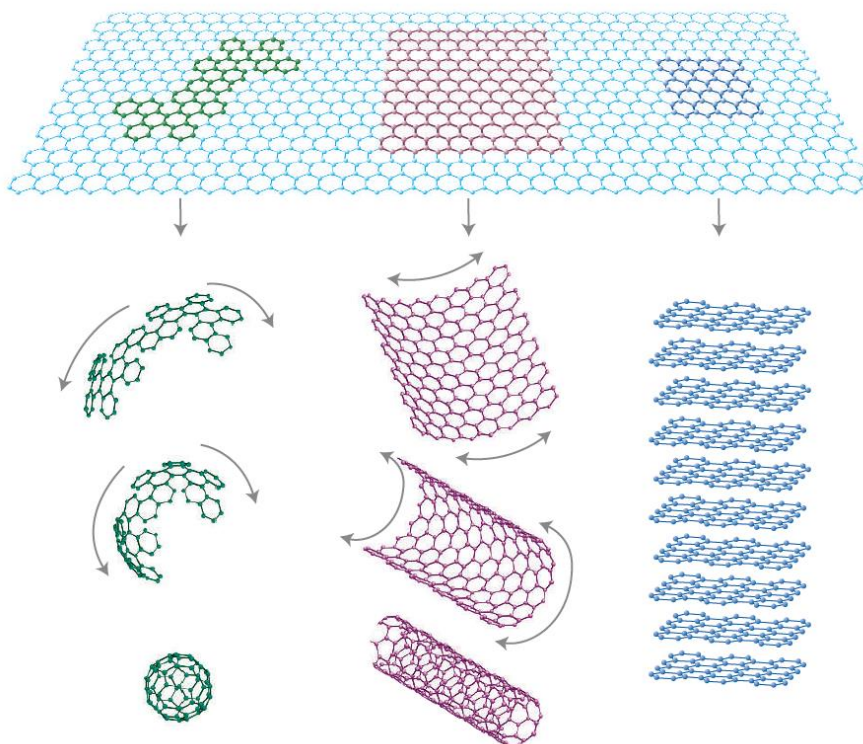


Figure 2- Graphene is the mother of all graphitic forms. The picture shows a single graphene sheet, a Bucky ball, a carbon nanotube, and graphite layers [17].

Graphene consists of a single layer sheet of carbon arranged in a chicken wire (hexagonal) lattice of sp^2 carbon. To date, graphene is considered the strongest material on earth [5]. Graphene has a high surface-to-volume ratio which is very advantageous for easy binding to different matrices [20]. Single layer, defect free graphene is said to have an intrinsic tensile strength higher than any other material [21].

Figure 3 shows the structure of graphene.

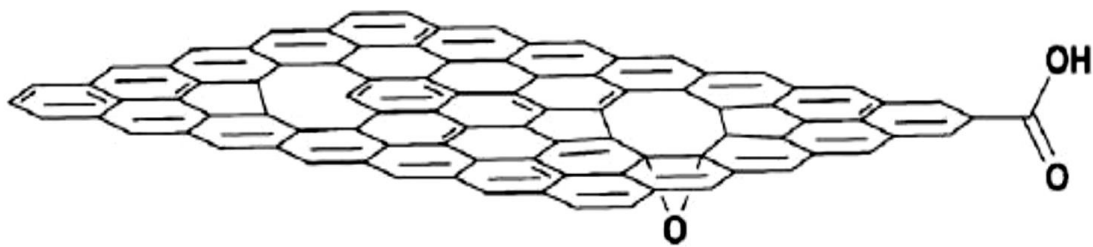


Figure 3 – Structure of graphene [22].

Graphene can be prepared through many different methods, including top-down methods like mechanical cleavage and liquid phase exfoliation, or bottom-up methods like chemical vapour deposition (CVD) [23]. Large scale production of graphene is a problem, however, recent research has shown promising results by using graphene oxide (GO) as a precursor for graphene production.

When GO is used as a precursor for graphene production graphite is oxidized to graphite oxide. Mechanical or chemical exfoliation of graphite oxide produces single layer graphene oxide sheets. The GO is then reduced to chemically converted graphene (CCG). An illustration of the various steps of the preparation of CCG by chemical reduction of graphene oxide is presented in Figure 4.

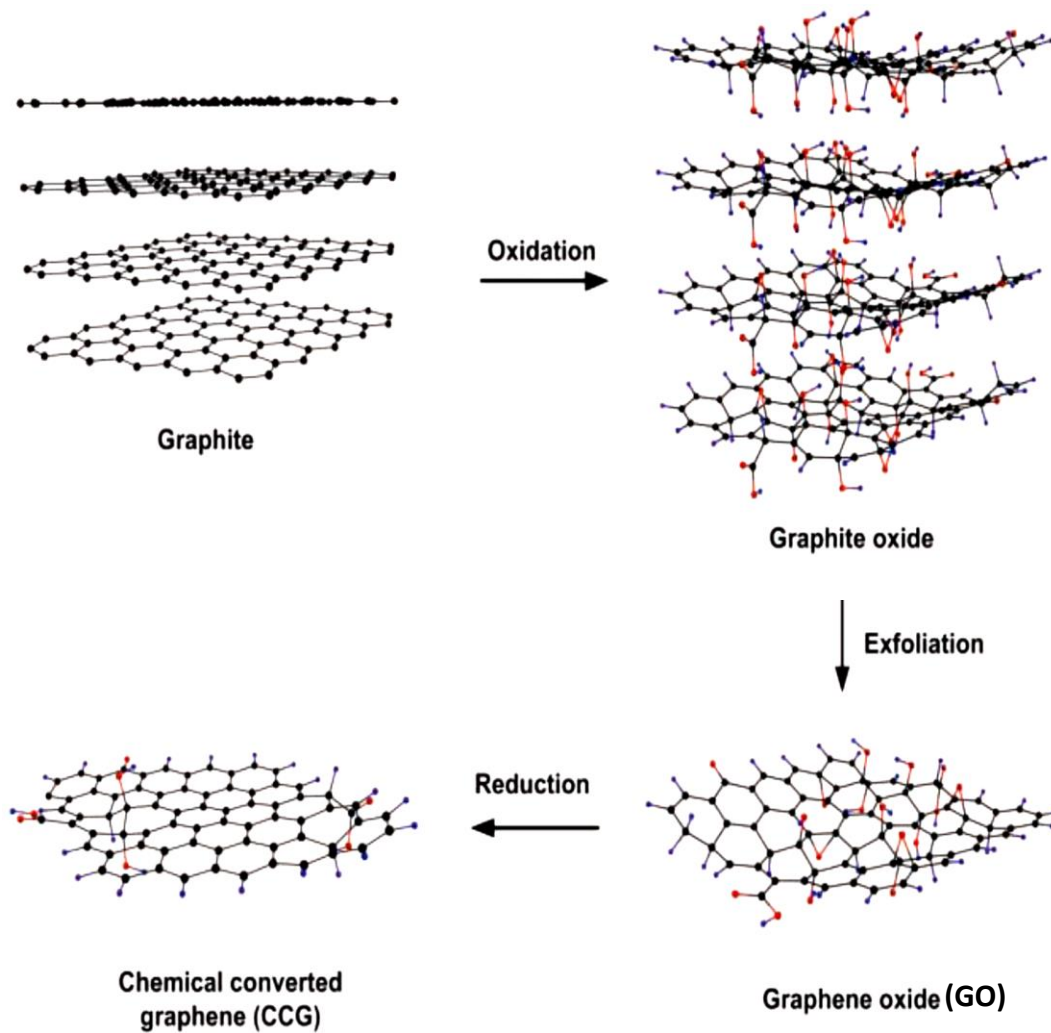


Figure 4- Preparation of chemically converted graphene (CCG) by reduction of graphene oxide [24]. Graphite is initially oxidized to graphite oxide, followed by mechanical or chemical exfoliation to produce single layer graphene oxide sheets. The GO is reduced to chemically converted graphene.

GO is easier to manufacture compared to graphene and can be produced from graphite powder which is readily available and cheap. In addition to being a route for graphene production, graphene oxide has many advantageous properties itself, such as its high level of dispersion in polar solvents, its dispersibility in various matrices and better compatibility with polymers compared to pristine graphene [25]. GO have almost the same structure as graphene but consist of a single layer of sp^2 -hybridized carbon which is enriched with oxygen-containing groups like epoxy and carboxyl [22]. Though there is a common theory that the carboxylic groups are located on the edges of the GO flake, and hydroxyl, epoxide and other functional groups are located at the basal plane, the exact structure of graphene oxide is unknown [26]. As researchers from different laboratories use different preparation methods,

and no single definitive characterisation technique is available, different structures are possible and have been proposed during years of research. One possible structure of GO is shown in Figure 5 [26].

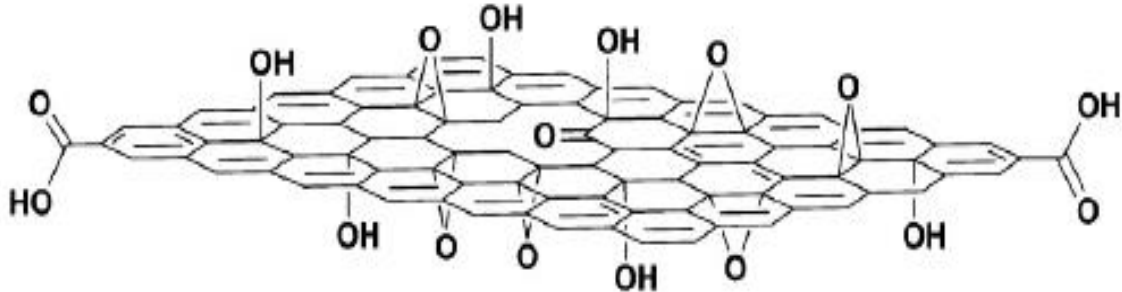


Figure 5: Structure of Graphene oxide [22].

The most common method for the production of GO is chemical oxidation of graphite. B.C. Brodie is considered the first person to produce GO, and his production method was used for many years. Brodie’s method involves the graphitic oxide (graphene oxide) being synthesized by using potassium chlorate and fuming nitric acid [27]. In 1957, Hummers and Offerman proposed a new preparation method for GO, and “Hummers’ method” became the most common preparation method. In “Hummers’ method”, graphite is oxidized through various steps with a water free mixture of concentrated sulphuric acid, sodium nitrate and potassium permanganate [27]. The different steps in “Hummers’ methods are illustrated in Figure 6.

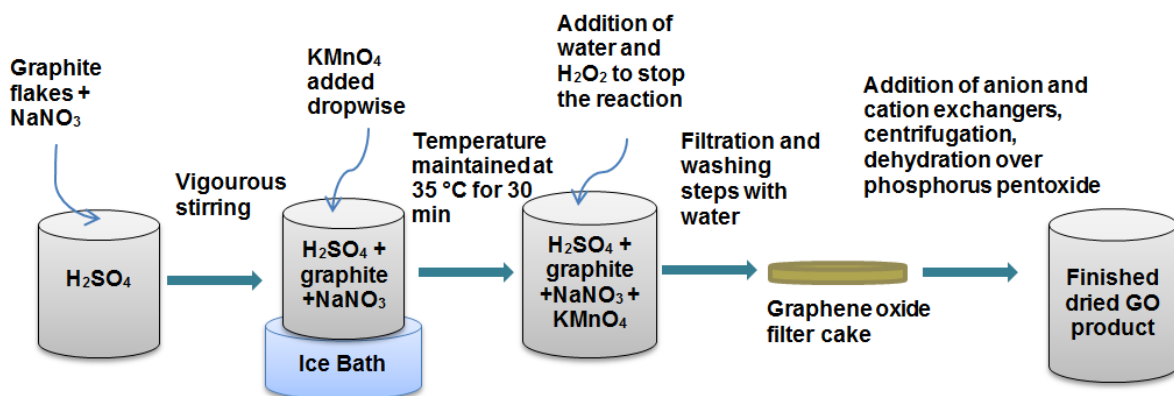


Figure 6–Illustration of the different steps in Hummers’ method.

In 2010, Marcano et al. proposed an Improved Hummers method where a mix of phosphoric acid and sulphuric acid was utilized. Marcano et al. claimed their method to be easier and safer than Hummers method, whilst also capable of producing GO of higher quality and with higher yield [28]. The improved Hummers' method uses a combination of sulphuric acid and phosphoric acid, excludes the NaNO_3 , and increases the amount of KMnO_4 to improve the efficiency of the oxidation process. Production of toxic gases is eliminated by excluding the use of sodium nitrate [28]. The reaction of potassium permanganate with sulphuric acid can cause detonation when heated to temperatures above $55\text{ }^\circ\text{C}$ or if in contact with organic compounds [29]. This reaction occurs in Hummers' method and lot of care must be taken to prevent detonation. In the method by Marcano et al., however, the temperature does not exceed $50\text{ }^\circ\text{C}$, and the risk of detonation is eliminated [28]. The structure of as-prepared GO obtained by using the improved Hummers' method during the specialization project of the autumn of 2013, is presented in Figure 7.

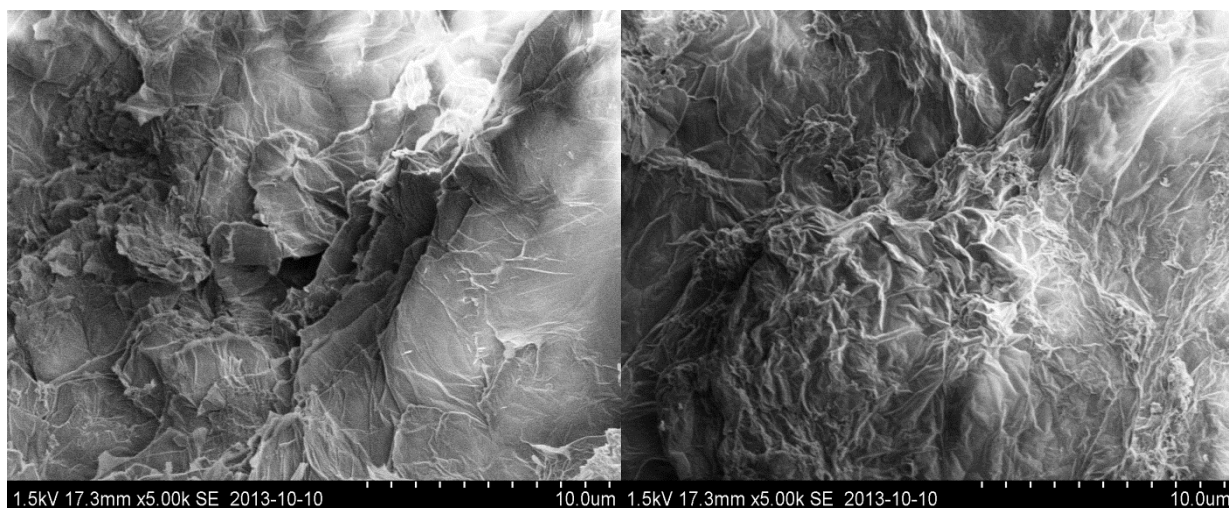


Figure 7 – SEM pictures of as-prepared GO produced by the modified version of Marcano et al. during the specialization project performed during the autumn of 2013 [30].

The search for new methods for GO and graphene production is still ongoing, and researchers are trying to find an optimal preparation method which is not too time consuming, produces a high yield and good quality graphene oxide, is easy to perform, and has few or no hazardous steps [25].

2.3.1 Exfoliation and reduction of GO

Whilst exfoliation of GO can be done with different methods, solvent- based or thermal exfoliation techniques are the most common [31;32]. Solvent-based exfoliation is often performed by ultrasonication or mechanical stirring which increases the interlayer spacing of GO, resulting in colloidal suspensions of GO [31]. The oxygen-containing groups of GO expand the interlayer distance and make the layers hydrophilic, and the oxidized layers can therefore be exfoliated in water [25]. It has been found that sonication produces suspensions that consist primarily of single layer GO platelets. The sonication process, however, fragments the GO platelets by reducing their lateral dimensions. Mechanical stirring is a gentler method and results in GO platelets with larger dimensions compared to sonication, but the exfoliation is very slow and produces a low yield [31].

GO has different physical properties compared to graphene. For example, GO is electrically insulating, but it is possible to reduce graphene oxide sheets by removing the oxygen-containing groups to get a structure similar to pristine graphene and thus restore the conductivity [33]. Chemical - or thermal reduction of GO sheets can be done to generate bulk quantities of graphene platelets. Chemical reduction is performed by using reducing agents such as sodium borohydride or hydrazine monohydrate [31].

Exfoliation of GO can be done by thermal annealing. Some researchers have tried to exfoliate GO by rapid heating at high temperature ($\sim 1050\text{ }^{\circ}\text{C}$) in an inert atmosphere [34], while others have tried lower temperatures ($\sim 200\text{-}400\text{ }^{\circ}\text{C}$) and high vacuum for a longer time period [35].

Figure 8 is an illustration of a high temperature and a low temperature exfoliation procedure.

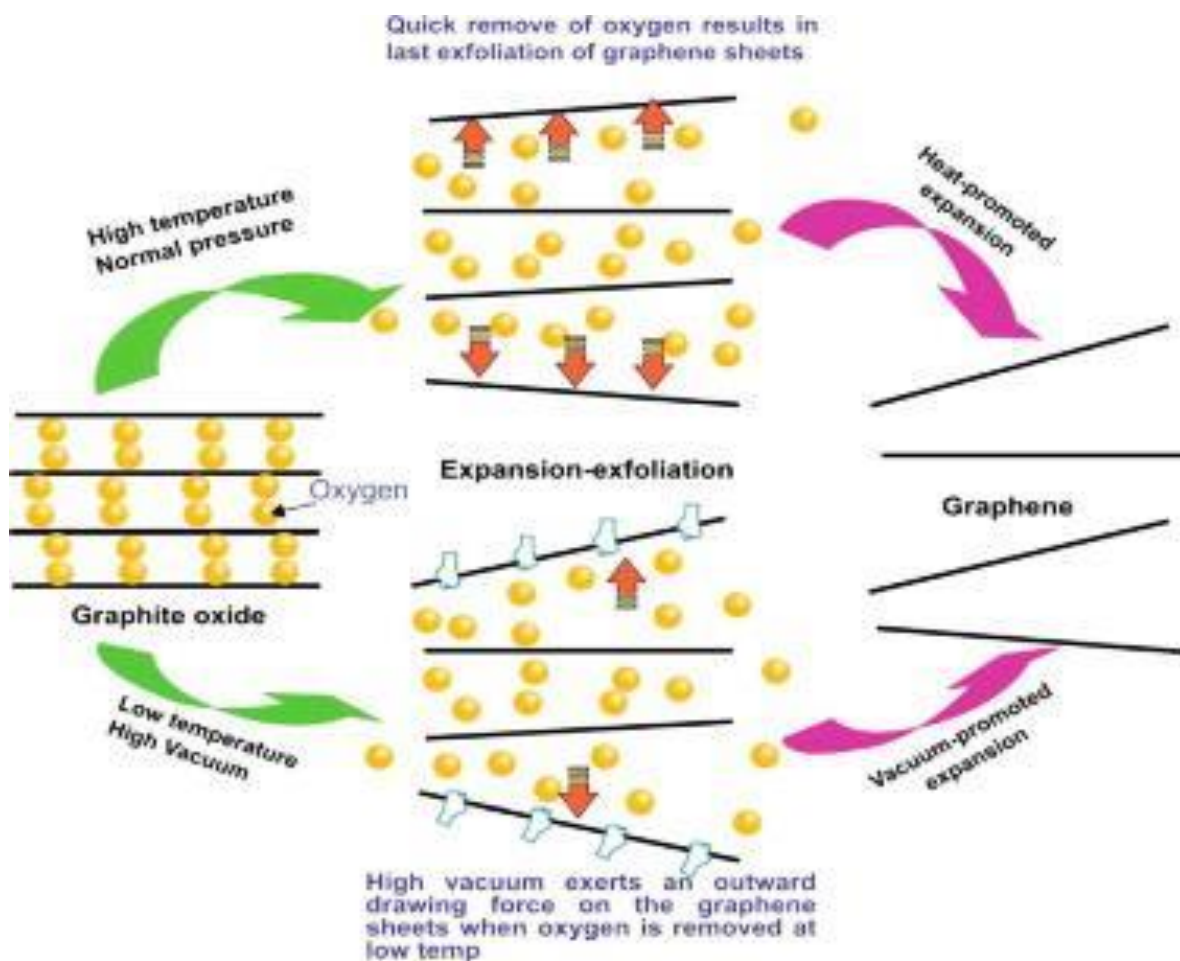


Figure 8 - Schematic presentation of thermal exfoliation of GO. The sequence on the top shows exfoliation of GO at high temperature under atmospheric pressure, while the sequence at bottom shows exfoliation of GO at low temperature (as low as 200 °C) under high vacuum [35].

The oxygen-containing groups on GO are decomposed into gases by the rapid increase in temperature. The gases produced cause a pressure increase between the layers of GO, and this in turn causes a separation of the layers. In addition to being exfoliated at the high temperature, GO is also reduced into a graphene-like structure by the thermal treatment and is called reduced GO (RGO) [25].

Figure 9 shows SEM images of thermally exfoliated GO (RGO) obtained during the specialization project of the autumn of 2013.

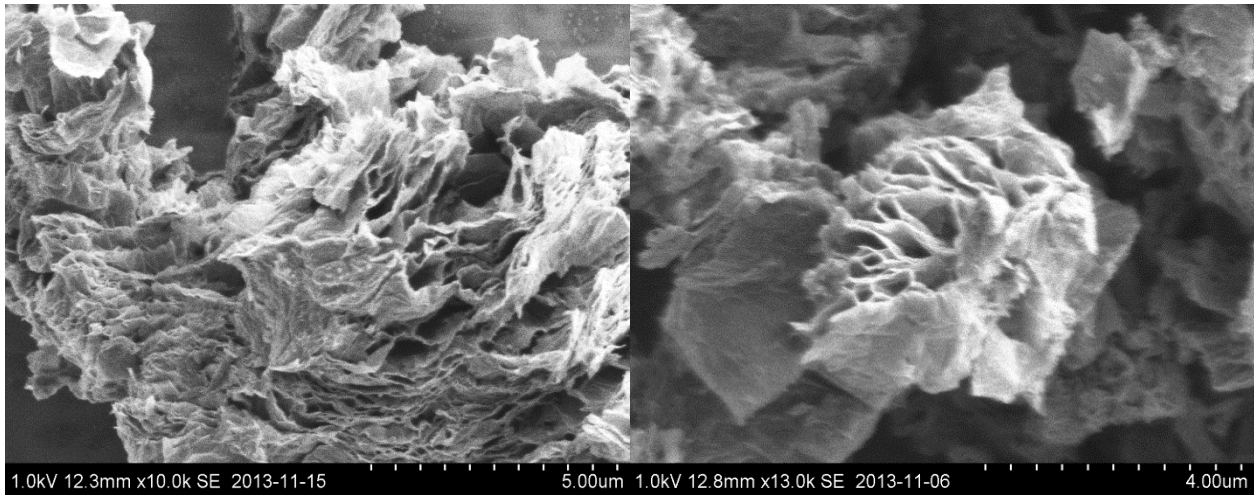


Figure 9 - SEM images of thermally exfoliated GO obtained during the specialization project of the autumn of 2013 [30].

The high temperature, however, can cause the produced graphene sheets to be small and wrinkled as some carbon is always removed during the decomposition process. The release of carbon dioxide therefore leads to structural damage of the graphene sheets, which affects their properties, in particular the electric properties [25]. This may not necessarily be a disadvantage for the use of RGO in nanocomposites.

2.3.2 Functionalization

It has been proposed that the surface of highly crystalline graphene is chemically inert. The inert surface can potentially react with other molecules by physisorption, which is adsorption caused by weak molecular attractive interaction forces from permanent or induced dipoles (dispersion forces/van der Waals forces) [36]. Different chemical groups (carboxyl, carbonyl, amines and hydrogenated (CH)) could react with the chemically reactive edges of graphene [19].

A variety of transformations of GO is possible because of its oxygen based functional groups. Additions of other chemical functionalities to GO using various chemical reactions are possible, and this is known as functionalized GO (FGO). GO can be functionalized both covalently and non-covalently [29]. The other functional groups can react through various

reactions with the different oxygen containing groups on GO. Functionalization of GO may enhance compatibility with different polymer matrices, and make GO dispersions more stable. Reactions where amines or isocyanates are used for the functionalization of GO are the most common [31].

2.4 Dispersion and stability in solution

GO has a high level of dispersion in polar solvents and water [11]. The dispersibility of GO is affected by the solvent and by the amount of surface oxygenated groups [26]. A good dispersion is also dependent on the particle size distribution, homogenous spatial distribution and temporal stability [37].

There are different methods for the dispersion of nanoparticles into solutions and composites, but sonication and three-roll mill is the most common. Sonication can be performed in either a bath-sonicator or in a horn-sonicator. During sonication the liquid is irradiated by a transducer with a high pressure sound field, and this sound field causes cavitations which release energy. In an ultrasonic bath the sound field is almost uniform, and gives the advantage of homogenous treatment of the suspension. The bath sonicator, however, gives a much lower sound pressure compared to a horn-type sonicator [38]. A horn-type sonicator generates a high-intensity sound field localized at the resonating horn tip, and the intensity decreases with the distance from this tip [39].

The dispersing result is affected by a variety of parameters during ultrasonication, including energy input; viscosity of the fluid; temperature; power density; ultrasonic frequency; and morphology of the GO particles [39].

Research on CNT's have shown that ultrasonic treatment of the CNT dispersions caused bent tubes and buckling effects, and when the sonication time was increased, the more serious damage and breakage of small graphitic layers on the CNT's was observed [40]. Sonication can also cause substantial damage to the GO platelets. The distribution of sizes and the dimensions can differ, and it can cause breakage of the graphitic structure [29].

2.4.1 Surface and interfacial tension

Surface- and interfacial tensions arise because of an imbalance in the intermolecular forces acting on the molecules at the interface [36]. Molecules in the bulk phase of a liquid are attracted equally from all directions, and the attractive forces will get close to zero. Molecules at the surface, however, become unilateral attracted by molecules that lie within. The forces acting over the interfacial area against molecules in the gas phase can be neglected, and the surface tension of a liquid (the other phase is a gas), is almost only determined by the intermolecular forces in the liquid. The interfacial tension between two liquids is determined by the intermolecular forces between the molecules in both phases, and in addition by the forces acting across the phase boundaries [36;41].

Figure 10 illustrates the intramolecular attractive forces in air, liquid and surface.

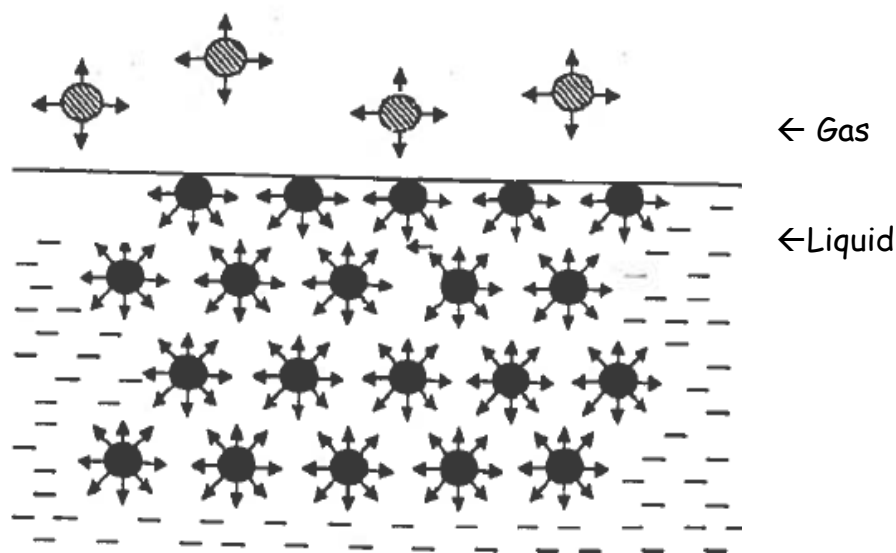


Figure 10 – Intramolecular attractive forces in air, liquid and surface [36].

Surface tension for a liquid is defined as the amount of energy or work needed to increase the surface by a unit area [36]. The surface forces want to minimize the surface area. The surface- and interfacial forces are dependent on which liquid is present, and which gas is present on the upper side [41].

2.4.2 Zeta Potential

A charged surface will influence the distribution of neighbouring ions in a polar media. Ions with similar charge (co ions) will repel each other, while ions with opposite charge (counter ions) will attract at the surface. The different behaviour and the thermal movement of the ions will cause the formation of an electrical double layer around each particle, which consists of the charged surface and an outer diffuse part with counter ions. The diffuse part is, according to Stern, divided in two layers; the Stern layer which is the inner part of the layer with ions that are specific adsorbed at the charged surface, and the Goy- Chapman layer, which is the diffuse layer ranging from x to infinity. The potential inside the Stern layer decreases quickly because specific adsorbed ions neutralize some of the surface charges and the potential flattens. The stern potential (ψ_δ) is considered approximately equal to the electrical potential at the shear plane between a charged surface and the dispersion media. This potential is called the zeta potential (ζ) [36]. Figure 11 illustrates Stern's model of the electrical double layer with shear plane and zeta potential.

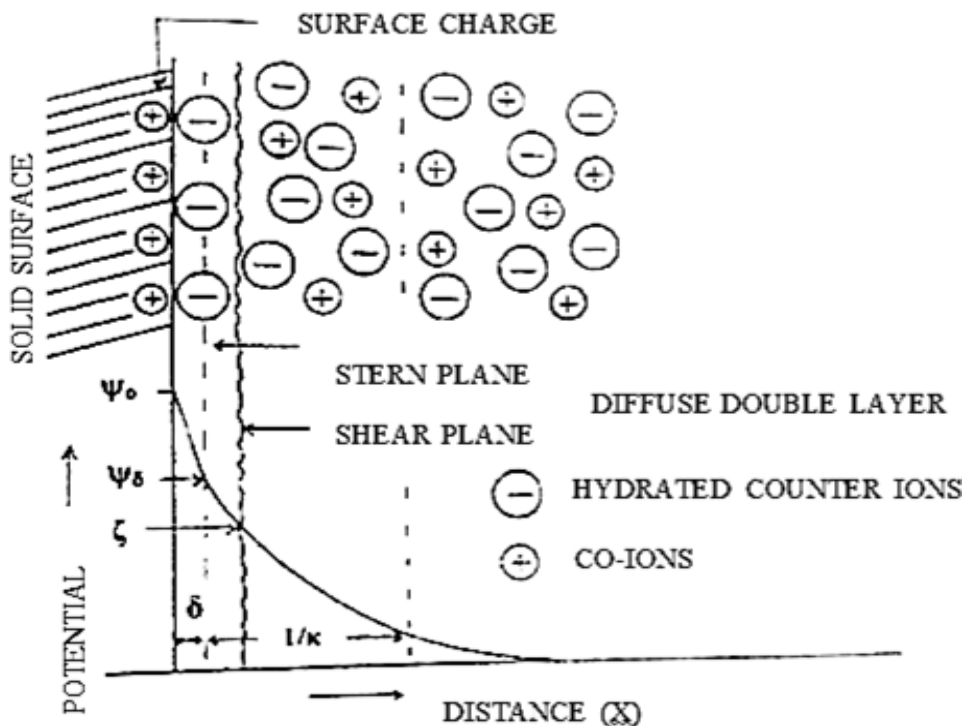


Figure 11 - Schematic view of Stern's model of the electrical double layer with among others the zeta potential (ζ), the Shear plane, the Stern plane, and ions marked. [36].

Electro kinetic techniques can be employed to calculate electrophoretic mobility and zeta potential. Electro kinetic phenomena are those that occur when the mobile part (the outer layer) of the electrical double layer moves relative to the stationary part (the inner part) under the influence of an electrical field. The electrophoretic mobility can be decided through electro kinetic methods. The electrophoretic mobility is defined as the ratio between the linear particle speed and the electrical field strength [36]. The electrophoretic mobility can further be used to calculate the Zeta potential by the Henry equation given in Equation 1,

$$\zeta = \frac{1.5 \cdot \eta \cdot U_E}{f(\kappa a) \cdot \varepsilon} \quad (1)$$

where ζ is the Zeta potential, U_E is the electrophoretic mobility, η is the viscosity, ε is the dielectric constant, a is the particle radius, and κ is the inverse of the Debye screening length [36]. When $\kappa a \ll 1$ the particle can be considered as a point charge which are moving in an electrical field, and the Hückel equation (Equation 2) is used

$$\zeta = \frac{1.5 \cdot \eta \cdot U_E}{\varepsilon} \quad (2)$$

When $\kappa a \gg 1$, the double layer can be considered as if it was a flat, and the Smoluchowski's equation (Equation 3) can be used to calculate the zeta potential,

$$\zeta = \frac{\eta \cdot U_E}{\varepsilon} \quad (3)$$

Smoluchowski's equation gives the relation between the electrophoretic mobility and the zeta potential for a plane surface, if the thickness of the electrical double layer is much smaller than the particle radius.

The zeta potential of a solution can greatly inform aspects of the stability of the dispersion in water. A high negative or positive zeta potential will cause the particles to repel each other,

and agglomeration of particles will be less probable. If the zeta potential has a low negative or positive value, however, the repulsive forces between the particles will be too weak to keep the particles from agglomerating. The zeta potential is usually strongly dependant on pH. A high pH will cause a highly negative zeta potential and a low pH will cause a positive zeta potential [42]. The pH where there is no charge, and the zeta potential is zero, is called the isoelectric point (IEP) [36]. The IEP is important because the colloidal system is normally least stable at this point [42;43].

2.5 Preparation of nanocomposites

Nanofiller and polymer matrix can be mixed by different methods, but the most common methods are solution blending, melt mixing, and in situ polymerization [11].

During the solution mixing of polymer composites, the filler is dispersed in a suitable solvent by, for example, ultra-sonication. The polymer is then incorporated and the solvent is removed by evaporation [1]. During the solution mixing process the polymer coats the individual graphene sheets, and after the solvent is removed, the sheets are interconnected [11]. When melt blending is used, the reinforcement phase is dispersed in the polymer matrix through high temperature and shear forces. Undergoing high temperature, the polymer matrix becomes soft, leading to an easier dispersion or intercalation of the GO or RGO reinforcement phase [1;11]. Melt blending has the advantage of not using (toxic) solids, but unfortunately the higher viscosity of the composite during increased filler loading makes the dispersion of graphene sheets less effective compared to solution blending [1;11]. In addition, the shear forces during the melt blending can cause buckling, rolling or shortening of graphene sheets [1].

In situ polymerization starts with dispersion of GO or RGO in the liquid monomer before polymerization is initiated by either heat or radiation [1;11].

2.5.1 Graphene oxide in epoxy

GO is dispersible in a wide variety of polymers [22]. The presence of epoxy and hydroxyl groups on the basal plane, and the carboxyl and carbonyl groups on the sheet edges of GO, makes GO ideal for dispersion in matrices. Furthermore, active sites which facilitate chemical bonds make the interface between polymer and graphene nanosheets good [44;45].

Many different preparation methods have been studied, with varying results. Direct mixing of graphene particles and polymer melt is not suitable for effective dispersal of nanolayers of graphene, according to recent studies [46]. Graphene has a high surface area and surface energy and this makes it difficult to disperse by polymer melt shear [46].

In order to obtain good nanocomposites with superior mechanical properties, the dispersion of GO in the polymer and the bonding between GO and the matrix must be good [47]. When adding GO to epoxy, wet transfer is recommended. Dispersion of GO powder directly in viscous epoxy often leads to poor dispersion. GO sheets tend to restack when added in a dry state and the sheets are strongly bonded together by hydrogen bonds. To ensure effective dispersion of GO in polymer, restacking of the graphenic sheets must be avoided [47], and this may be achieved by wet transfer. When GO is transferred into an organic phase and wet transferred to the epoxy resin, restacking and agglomeration of GO sheets can be avoided because the organic solvent keeps the nanosheets separated by acting as a spacer [47].

When composites with GO are made, the most common method of transferring the GO into the epoxy matrix, is by dispersing GO (or sometimes functionalized graphene oxide (FGO)) into the organic solvent and mixing it with the epoxy resin. The solvent is then removed from the epoxy using various techniques such as rotavapor or a vacuum oven [47].

2.5.2 Dispersion in composites

High specific surface area is a special characteristic of nanoparticles, and this property is beneficial for the creation of a large interface in the composite. Small particles have a higher surface-to-volume ratio, and particles at nano scale have a higher fraction of atoms localized at the surface compared to particles on the micro scale [3].

The addition of nanoparticles doesn't always influence the bulk composite material positively. Sometimes the nanoparticles can lead to a reduction of the composites performance rather than an enhancement [6]. Maintenance of a stable dispersion of graphene is a major challenge when graphene sheets are dispersed in the polymer resin. Secondary agglomeration during curing can occur, and must be avoided [48]. Research has shown that due to the strong van der Waals forces, nanofiller tend to re-agglomerate even within uncured polymers. High

temperature during curing seems to increase the likelihood of the graphene sheets re-agglomerating [48;49]. Increased curing time also seems to increase the tendency of the graphene sheets to re-agglomerate [48]. The dispersion of isolated graphene layers within the polymer matrix, and the interfacial bonding between graphene sheets and the polymer matrix affects thermal and mechanical properties of the composite [19;48]. Pure graphene has a tendency to aggregate in the form of layers, by layer stacking due to the van der Waals interactions. Additionally pure graphene is poorly compatible with polymer matrices. GO, interacts more strongly with polymers because of its hydroxyl and epoxy groups on the sheet, and the carbonyl and carboxyl groups at the edges [19]. In addition, GO is more easily dispersed in different solvents, and its surface is easier to modify via insertion of amines and ester functionalities for example, which can stabilize dispersions [19].

A challenge of introducing nanoparticles instead of larger particles is that fine nanoparticles have a stronger tendency to form agglomerates [4]. Brownian forced hydrodynamic motions in colloidal systems result in collisions between the dispersed particles. If the attractive van der Waals forces become larger than the repulsive forces, the particles agglomerate in the matrix [36]. Agglomerates can remain even after vigorous processing [6]. Even ultrasonication of graphenic sheets in organic solvent for a long period of time does not guarantee a good dispersion especially for high graphenic contents [47]. Because of the high surface area, high aspect ratio and strong inter-particle interactions of nanoparticles, they tend to stick together and form micro particles which do not have the same advantageous qualities [47]. The presence of agglomerates is inconvenient because agglomerates limit the effect of the nanofiller and their potential benefits will not be fully exploited [39].

Interfacial adhesion between polymer and particles decides how easy the particles are dispersed in the polymer. A good dispersion is achieved when the interfacial adhesion between the particles and the surrounding polymer is high, and when there are only individual particles in the solution [50]. Interfacial adhesion and dispersion of the filler material is important for producing homogenous nanocomposites. High surface area and nanoparticle incompatibility with polymer matrix can lead to difficulties with the dispersion of nanoparticles [6]. Dispersion of the nanofiller is a crucial step when making polymer nanocomposites. The quality of the dispersion affects the whole matrix of the nanocomposite

and the final properties of the composite. A homogenous and well dispersed system is therefore a key focus when making a nanocomposite [33].

Nanoparticles can give greater interfacial contact area with a polymer matrix compared to micron-sized particles. This effect is caused by the higher specific surface area of nanoparticles. The number of particles will be higher for nanoparticles compared to micron-sized particles, even with the same volume fraction added, and this causes the inter particle distance to be smaller for nanofiller [12]. The reinforcing effect of the nanofiller is dependent on the interfacial compatibility. The high increase in interfacial area causes the properties of the composite to be dominated by the properties of the interface or the interphase [7]. Reduced and exfoliated GO as a filler material is believed to be promising because it seems to give enhanced interfacial adhesion with the epoxy matrix, probably caused by its hydroxyl, carboxyl, and epoxide functional groups on the surface [12]. Nanoparticles also have a lot more polymer interphase surrounding the particles compared to micro particles because of the high surface area. This interphase influences the composite properties, among others the composite stiffness may be greatly enhanced and the glass transition temperature of the polymer can be changed [39].

2.6 Mechanical properties

When polymers are used in different engineering applications it is crucial to have knowledge about the mechanical properties. It is necessary to know the stiffness of the polymer, the material strength, and the rheological properties of the polymer [51]. How much the polymer deflects under a given load and what level of stress the polymer can support before it breaks or deforms, is decisive when selecting a polymer. Furthermore, the hardness, ability to withstand cyclic loading (fatigue), resistance to loading in the presence of an organic solvent, and the toughness of the material are other important mechanical properties [51].

A materials resistance against elastic deformation during applied stress is called Young's modulus, or elastic modulus, E . Young's modulus can be calculated as the slope of the linear portion of the plot below the yield point in a stress-strain curve [12]. The stress-strain curve is illustrated in Figure 12 .

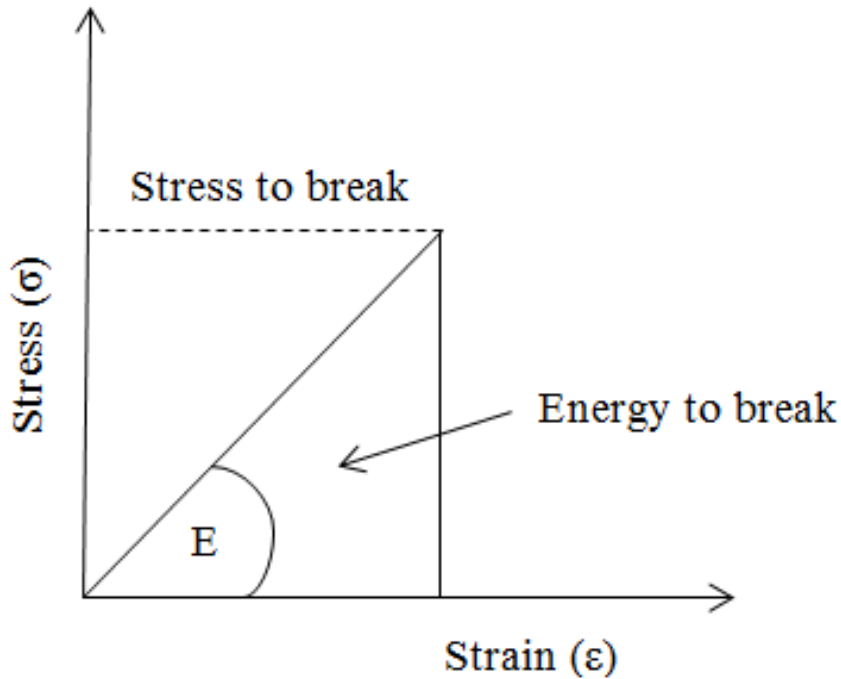


Figure 12 – Stress/strain diagram for a material hypothetical that obeys Hooke's law all the way to failure [51].

Equation 4 shows Hooke's law with the equation for the calculation of Young's modulus (E),

$$E = \frac{\text{stress}}{\text{strain}} = \frac{\sigma}{\varepsilon} = \frac{F/A}{\Delta l/l_0} = \frac{Fl_0}{A\Delta l} \quad , \quad (4)$$

where E is the Young's modulus, F is the force exerted on an object under tension, A is the original cross-sectional area through which the force is applied, Δl is the change in length, and l_0 is the original length of the object [51].

The endpoint of the material elasticity is given by the yield point. When a bending mode is used during the deformation testing, the modulus is reported as flexural modulus. The maximum strength a material can withstand is referred to as the tensile strength, or in bending mode as the flexural strength [12]. Figure 13 shows the setup of a three- point flexural bending test.

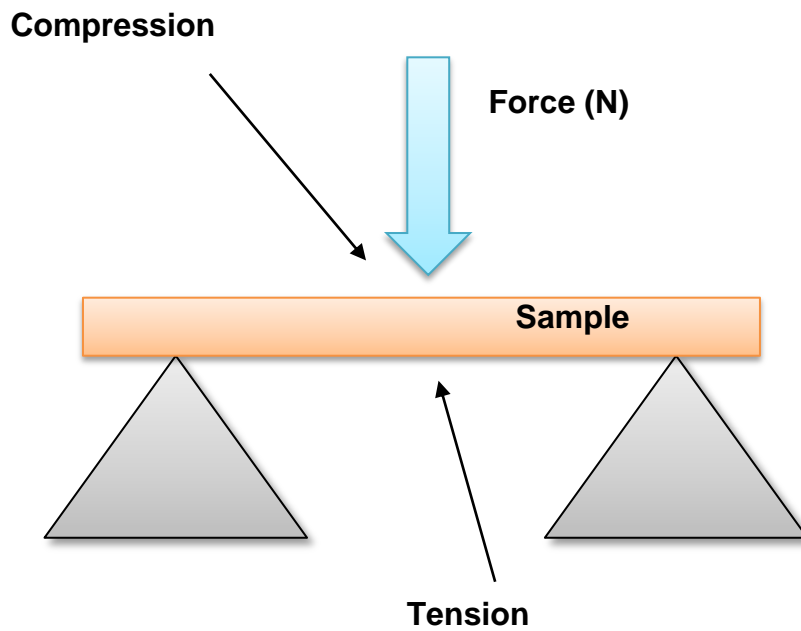


Figure 13 – Illustration of a three –point flexural bending test.

During a three- point flexural bending test, a specimen is placed on two supports and a load is applied at the centre of the specimen. The specimen is under tensile stress at the convex surface (the lower surface) and under compressive stress at the concave surface (the upper surface) during the test. The materials flexural strength is the load at yield. The flexural modulus gives a value of the stiffness of a material under bending. The higher the flexural modulus, the stiffer the material is.

Temperature plays an important role for the mechanical properties of an epoxy polymer [12], and it is sometimes appropriate to test the materials at temperatures that simulate the intended use environment. The glass transition temperature (T_g) is a physical property for polymers. The properties of a polymer are strongly related to T_g [19]. The behaviour near T_g is critical for high-temperature applications and for the processing of polymer composites [19]. The region below T_g is called the glassy region, and in this region the polymer behaves like a rigid solid. In general, the value of T_g of most epoxy polymers varies between room temperature and 260 °C, and is dependent on the molecular structure of the polymer [12].

Filler loading, the particle size, and the interfacial adhesion between particle and matrix influence the mechanical properties of a composite [39]. The composite stiffness is not

dependent on the particle/matrix adhesion, but the particle loading plays a significant role. The composite toughness and strength are particularly influenced by particle/matrix adhesion, but the particle size and loading also affect the toughness and strength considerably [39].

2.7 Previous study

A wide range of work has been done with respect to incorporating of GO into polymer based nanocomposites. Among others, researchers have succeeded in homogenous dispersion of graphene and graphene oxide in poly (methyl methacrylate) (PMMA), poly (acrylonitrile) (PAN), poly (acrylic acid) (PAA), polyester, epoxy resin, thermoplastic polyurethane (TPU), and poly vinyl alcohol (PVA) [5].

In the present thesis, the topic is epoxy based composites, and other composite systems will therefore not be covered in this review. In addition, only mechanical and thermal properties will be discussed and electrical properties, conducting properties etc. will not be covered.

In a study performed by Rafiee et al. the properties of graphene platelets (GPL) (multiple graphene sheets that are stacked together) were compared to CNTs as additive for epoxy, and the epoxy with graphene platelets showed promising results compared to CNTs [32]. While single walled carbon nanotube (SWCNT) showed a 3 % increase of Young's modulus compared to pristine epoxy, the graphene platelets showed an increase of 31 %. The tensile strength of epoxy was improved by 40 % by addition of graphene platelets, while multi walled carbon nanotubes (MWCNT) showed an increase of 14 %. In addition, the fracture toughness of the epoxy nanocomposite showed a 53 % increase with graphene platelets, compared to 20 % improvement with MWCNT. The graphene used in the study was thermally reduced graphene oxide, and the study was performed for epoxy nanocomposites at fixed weight fraction of 0.1 ± 0.002 %. It was proposed that the enhanced properties were caused by the enhanced specific area of graphene platelets, the improved mechanical adhesion at the nanofiller - matrix interface, and the two-dimensional geometry of graphene platelets [32].

In another study, performed by Rafiee et al., functionalised graphene (FGS) was compared with CNTs dispersed in an epoxy matrix. The graphene used in the study was prepared by oxidizing graphite and exfoliate is through thermal exfoliation by rapid heating (1050°C) in a quartz tube. The functionalized graphene was dispersed in an epoxy matrix through solution mixing with acetone and an ultrasonic probe sonicator. The study showed that functionalised graphene sheets were remarkably effective as nanofiller. A weight content of only 0.125 % of functionalised graphene sheets was needed to increase the fracture toughness of epoxy by ~ 65 % and the fracture energy by ~115 %. These properties were also present when CNTs were used as nanofiller, but a two orders of magnitude higher weight fraction of CNTs was required, compared with graphene in order to achieve the same result [52].

Yang et al. performed a study where GO was employed in an epoxy nanocomposite by mixing a GO aqueous dispersion with epoxy resin through a two-phase extraction. The GO aqueous dispersion and epoxy resin were heated (50 °C) and stirred in an oil bath and left standing to sediment for several hours to phase separate the water and remove it. XPS, SEM, FTIR, TGA, transmission electron microscope (TEM) and AFM were used as characterization techniques and compression tests were performed. When a 0.0375 wt. % loading of chemically converted GO sheets were applied to the epoxy resin significant improvements in mechanical properties were achieved. The compressive failure had an improvement of 48.3 % and the toughness showed remarkable 1185.2 % increase compared to the epoxy system without graphene oxide [53].

The effect of as-produced GO and silane functionalised GO (silane f-GO) on the mechanical properties of composites were investigated by Wan et al. [54]. The silane f-GO and the as-produced GO were dispersed in acetone by sonication and further mixed with a DGEBA epoxy resin by sonication. The solution was processed by using a planetary ball mill, and further degassed at 80 °C for 12 hours in vacuum to remove solvent, before adding a hardener. The samples were characterized by using TEM, X-Ray diffraction (XRD), XPS, Dynamic mechanical thermal analysis (DMTA), TGA and flexural tests [54]. When the interface and microstructure in the composites were studied, it was obvious that agglomerates and gaps between matrix and aggregates were present in the as produced GO composites. In case of the silane-f-GO composite, however, the dispersion of particles was obtained, no clusters/agglomerates were observed, and no gaps were observed. The as- produced GO and

the silane-f-GO composites showed an increase in storage modulus of 12 % and 27 % respectively, compared to the neat epoxy in the glassy state, and 30 % and 52 % increase in storage modulus respectively, in the rubbery state compared to the neat epoxy. A small increase in T_g was also observed for the reinforced composites compared to the neat epoxy. Tensile and flexural tests were also performed and showed an increase in tensile strength and modulus, flexural strength and modulus for both reinforced composites compared to the neat composite. The silane-f-GO showed larger improvement compared to the as-produced GO [54].

A study of fracture toughness and failure mechanisms of graphene based epoxy composites was performed by Chandrasekaran et al. [55]. Three different nanofillers were used in the experiment; thermally reduced graphene oxide (TRGO), graphite nano-platelets (GNP) and MWCNT. The epoxy system used in the study was diglycidyl ether of bisphenol A (Araldite LY556) with an anhydride hardener (Aradur CH917) and imidazole accelerator (DY070). The different fillers were mixed in dry state into the epoxy by using a three-roll mill. SEM was used to characterize the dispersion, and whilst a fairly good dispersion was seen, some primary agglomerates were visible, and TRGO seemed to have better dispersion than GNP. Fracture tests were performed by using a three point bending test. TRGO showed the most significant improvements in toughening effect with 40 % increase, while GNP and MWCNT showed 24 % and 8 % improvement respectively. When the fracture surfaces were studied, the MWCNT showed a smooth surface only slightly rougher than pure epoxy with crack bridging, de-bonding and pull-out of nano-tubes. GNP and TRGO, however, showed a much rougher fracture surface with several small and different height fracture surfaces, and narrow bands at the boundary of the fracture surface parallel to crack growth direction. The flow pattern of the fracture surface was formed around the agglomerates. TRGO showed less crack formation compared to GNP [55].

Gudarzi et al. studied the effect of wet transferring of functionalised GO in an epoxy based composite system. GO was functionalised with p-Phenylenediamine (PPDA) and dissolved in distilled water before the FGO was transferred into Epon828 epoxy resin with isophorone diamine (IPDA) hardener. The FGO was characterized with SEM, optical microscope, FTIR, XRD, XPS and AFM, and the nanocomposite was investigated by rheological measurements, and a three-point flexural test. Their results showed that the FGO was well dispersed and had

a good bonding with the epoxy, the Young's modulus showed a 30 % increase with 0.4 vol % FGO, a 12 % increase in ultimate strength, and the flexural modulus had an increase from 2800 ± 25 MPa to 3670 ± 60 MPa [47]. Figure 14 show a schematic illustration of diamine bonding to GO and the transferal of GO particles from water to epoxy phase after functionalization.

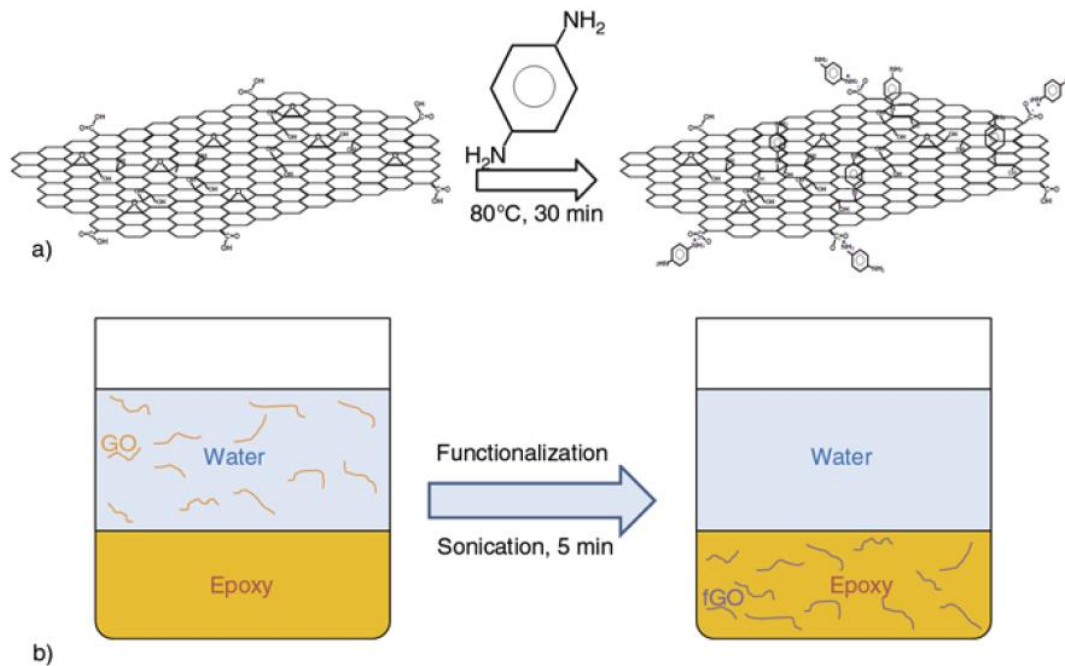


Figure 14 – a) Schematic illustration of diamine bonding to GO. b) Illustration of transferring GO sheets from water to epoxy phase after functionalization [47].

The method by Gudarzi et al. [47] was used as a template for the preparation of composites during the thesis.

3 Experimental

The various techniques and materials used in the experimental part of the thesis are described in the following sections. The method for the preparation of GO, the functionalization of GO, and the various techniques for the characterization of dispersions and functionalization will be described in detail.

3.1 Materials

Synthetic graphite powder, < 20 μm from Sigma-Aldrich (CAS. 7782-42-5) was used as graphite source for the GO production. Diethyl ether, puriss p.a. ACS reagent iso ($\geq 99.8\%$). Sigma-Aldrich, Potassium permanganate, pro analysis, EMSURE[®] ISO Sulphuric Acid (95-97 %) pro analysis Merck, Kebo, Hydrogen peroxide, pro analysis (30 %) Merck, Kebo and ortho-phosphoric acid (85 %) pro analysis Merck, Kebo were used during the preparation of GO. Technical Hydrochloric acid (35 %) VWR international and Absolute alcohol prima (ethanol) Kemetyl Norge AS, were used in the washing steps of GO. Acetone pro analysis, EMSURE[®] from Merck were used for the dispersion of GO, FGO and EXGO. Dodecane, Gradient Cap Fluid from CPS Instruments Inc. was used for the disc centrifuge testing, Sucrose AnalaR[®], BDH from VWR International was used for the production of Sucrose gradient.

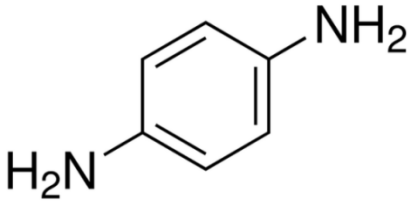
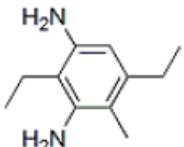
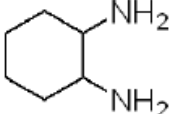
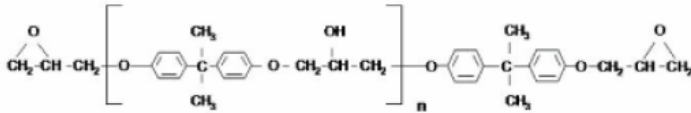
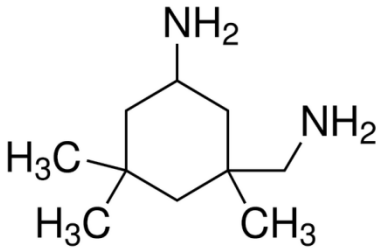
Ammonia solution, 32 %, extra pure, from Merck, and Sodium hydroxide pellets extra pure, from Merck KGaA, Germany, UN182 were used for the pH neutralization of FGO. Sodium dodecyl sulphate specially purified for biochemical work, 88.0 %, Prod 44215, from BDH Chemicals Ltd Poole England, was used for the dispersion of GO in distilled water. Diamine (Formulated amine hardener, XB3473, from Huntsman, Batch AAC0186100) and p-phenylenediamine ($\geq 99.0\%$ (GC/NT), CAS 106-50-3, LOT#BCBKS235V, 78429-100G, from Sigma Aldrich, were used for the functionalization of GO.

The epoxy used in the present study was a bisphenol- A- based epoxy (Araldite LY556, Batch nr. AAB 150990, exp. Date 09-2018, from Huntsman), and the curing agent used was Formulated amine hardener, XB3473 (Batch AAC0186100 from Huntsman).

Isophorone diamine (IPDA), (5-Amino-1, 3, 3-trimethylcyclohexanemethylamine, mixture of cis and Trans, $\geq 99\%$) was used as the low temperature hardener and was purchased from Sigma Aldrich, Germany. Trenmitten TREN's E, from Haufler Industrievertretungen were used as the release agent for the coating of metal moulds. Table show the chemical structures of the different amines, hardeners and epoxy resin used in the experimental work.

A risk assessment of the experimental work can be studied in Appendix C.

Table 1 – Chemical structures of the amines, hardeners and epoxy resin used in the experimental work.

Chemical	Chemical structure
para-phenylenediamine (PPDA) [56]	
The two components of the XB3473 amine [15]	<div style="display: flex; justify-content: space-around; align-items: center;"> <div style="text-align: center;">  <p>Diethyltoluenediamine</p> </div> <div style="text-align: center;">  <p>1,2-diaminocyclohexane</p> </div> </div>
The epoxy resin Araldite LY556 [15]	 <p>Diglycidylether of Bisphenol A (DGEBA)</p>
Isophorone diamine (IPDA) [57]	

3.2 Methods

3.2.1 Preparation of GO

Residual batches of GO from the specialization project from the autumn of 2013 were used in the thesis, and in addition, three additional batches of GO were made during the M.Sc. thesis with the following procedure (Figure 15).

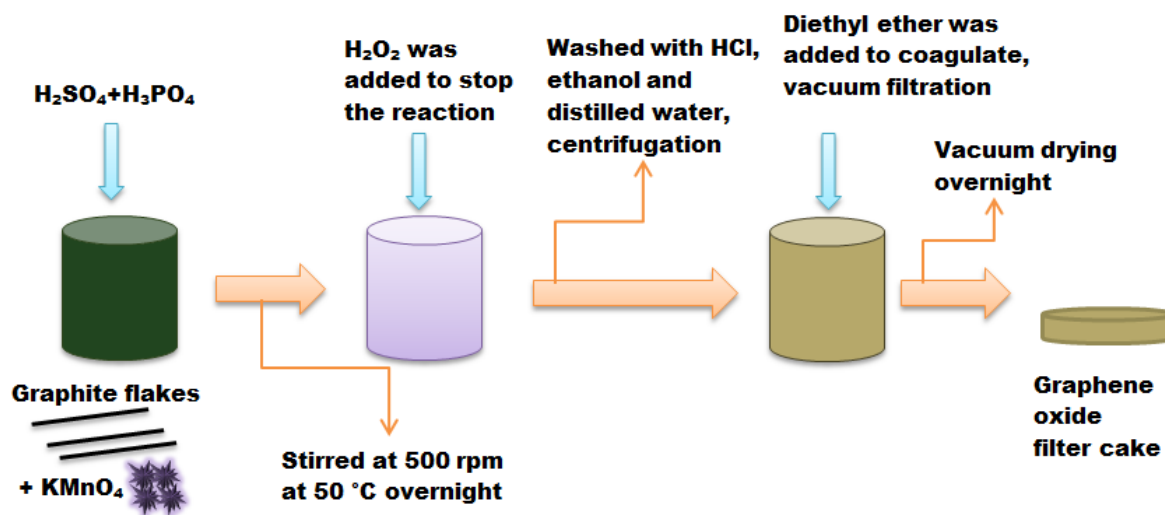


Figure 15 – A schematic illustration of the modified improved Hummers' method used for the preparation of as-prepared GO.

GO was prepared by a modified version of the improved Hummers' method first prepared by Marcano et al. [28]. Powdered graphite (0.5 g) was mixed with KMnO_4 (3.0 g) in a round bottom flask. A 9:1 mix of H_2SO_4 (60 ml) and H_3PO_4 (6.7 ml) was then added slowly and dropwise to the mixture during stirring and over an ice bath until it was well mixed. The colour of the mixture turned dark green at this point. The mixture was further heated to 50° C and stirred (500 rpm) overnight for approximately 20h. During the night, the mixture turned brownish. The solution was cooled to room temperature before poured into ice (100 mL) with H_2O_2 (0.5 mL). This step caused an increase in temperature, and the solution almost boiled. The solution was again cooled to room temperature at which point it turned dark purple. The solution was centrifuged in a Kubota 5400 centrifuge in 3500 rpm for 1 hour immediately after cooling. The supernatant was decanted away and the solid matter was re-dispersed in distilled water (~10 mL in each tube). The total amount of solution was combined in one centrifuge tube and went through various washing steps by centrifugation (30 min, 3500 rpm) of the solution (30 min, 3500 rpm), and re-dispersal in distilled water, hydrochloric acid and

absolute ethanol (2 x). Some of the different steps during the preparation of GO are shown in Figure 16.



Figure 16- A: Preparation of GO before washing, B: GO after dispersing in distilled water. C: GO after cleaning in HCl, D: GO after dispersed in ethanol, E: GO dispersed in water [30].

After the washing steps the solution was centrifuged for 30 min at 3500 rpm. The supernatant was decanted away and the remaining material was coagulated with diethyl ether (>98 %, 33mL). The resulting solution was filtered over an AN1200 (1.2 μm) membrane filter and the solid obtained at the filter was vacuum-dried overnight in a vacuum oven at room temperature. Figure 17 presents the finished as-prepared GO product after coagulation with diethyl ether, evaporation in rotavapor, and vacuum drying.



Figure 17 - As prepared GO, finished product.

The as-prepared GO can be used in different forms before adding it into the epoxy system. Figure 18 show some of the possible different pathways for GO used as reinforcement in epoxy. A more in detailed description of each step like dispersion, exfoliation, functionalization and preparation of composite are given in the various sections following.

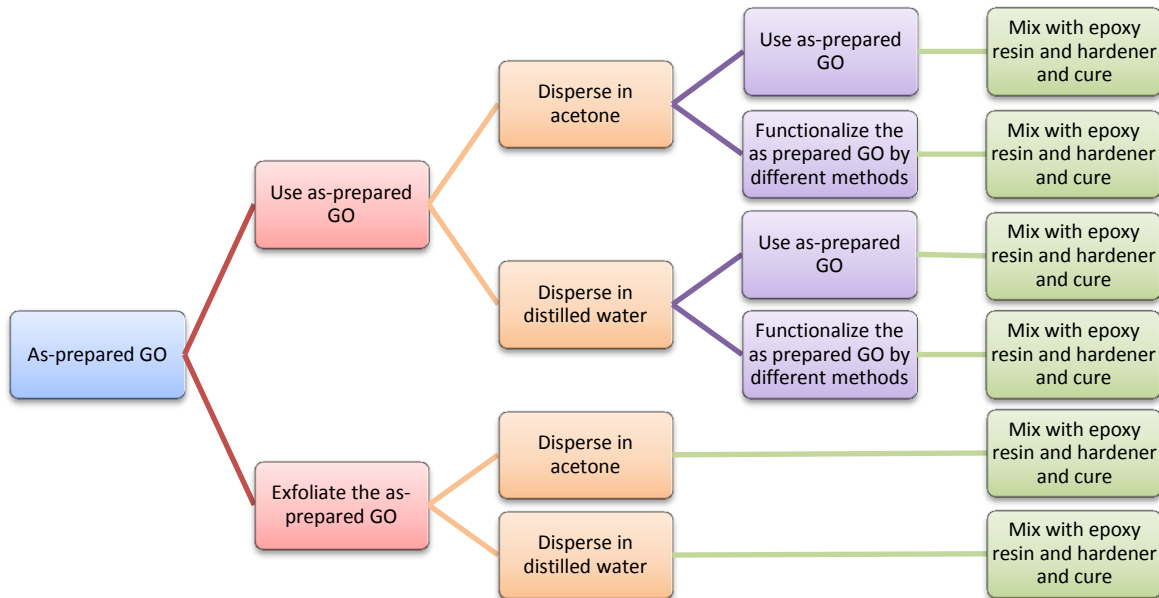


Figure 18 – Illustration of how the as- prepared GO can be used in epoxy composites.

3.2.2 Exfoliation of GO

Exfoliated GO which was prepared during the specialization project during the autumn of 2013 was used in the thesis. The exfoliated GO that was used was made by two methods. GO (100 mg) was put in a custom made glass tube which was evacuated and sealed at the end (Figure 19). A muffle oven was heated to 300 °C, and the glass tube with GO sample was placed in the oven for 10 minutes.



Figure 19 - Custom made glass tube with GO sample before thermal exfoliation [30].

During the second method, the GO (100 mg) was placed in a custom made quartz tube that was evacuated and sealed at the end. A muffle oven was heated to 1000 °C, and the tube with GO was held in the oven for approximately 30 seconds.

3.2.3 Dispersing GO

Different dispersions of GO were made in the first part of the experimental work to find an optimal method and solvent for the dispersion of GO particles. The various methods and solvents are describes in the following sections.

3.2.3.1 Dispersing EXGO (300 °C) with ultrasonic bath

EXGO (300 °C, 0.05 wt. %) was dispersed in MIBK in a plastic centrifuge tube, and shaken for some seconds. GO (300 °C 0.05 wt. %) was dispersed in MIBK and the stabilization agent; Disperbyk 2150((D2150, Byk additives, heated to 50 °C before use), (0.4 wt. %)) in another plastic centrifuge tube and shaken for some seconds. The GO/MIBK solutions were then exposed to an ultrasonic bath (Bandelin Sonorex Digital 10 P, 352 kHz, 480 W) (100 % power)) for different time intervals (0 min, 1min, 5 min, 30 min,1h, 2h and 4 h).

3.2.3.2 Dispersing as- prepared GO in ultrasonic bath

During the specialization project, an optimum time of two hours for the dispersing of GO in distilled water in ultrasonic bath, was found. It was therefore decided to go directly to a sonication time of 2 hours, because acetone was expected to give more or less the same results as distilled water. GO (100 mg) was dispersed in acetone (20 ml) in a plastic tube and exposed to the ultrasonic bath (100 % power) for 2 hours. The Acetone/GO mix was diluted with distilled water (1:10) before analysing on the disc centrifuge. A sucrose gradient was used before the sample and a 377 nm standard was exposed to ultrasonic bath for 1 minute and analysed before the sample was added.

Both a dispersion of as-prepared GO in acetone, and as-prepared GO in distilled water were made after the same procedure.

3.2.3.3 Dispersing as-prepared GO with horn-type ultrasonicator

GO (0.25 g) was dispersed in acetone (100 g), with a horn-type ultrasonicator (Branson Digital Sonifier[®] S-450D, 25kHz, 400 W). During the horn sonication, the tip of the horn was placed into the dispersion, and the power delivered was controlled by setting the amplitude of the tip of the resonating horn to 20 %. The temperature was controlled by a cooling jacket with a set maximum temperature of 30 °C. The dispersion was exposed to the ultrasonication horn for different time intervals (10 min, 30 min, 1h, and 2 h). A sample from the dispersion was collected by a syringe extended by a flexible tube, and diluted by distilled water (1:5) before analysing by the disc centrifuge (described in section 3.2.4.). Figure 20 shows the experimental setup of the horn ultrasonicator with cooling jacket and temperature control.

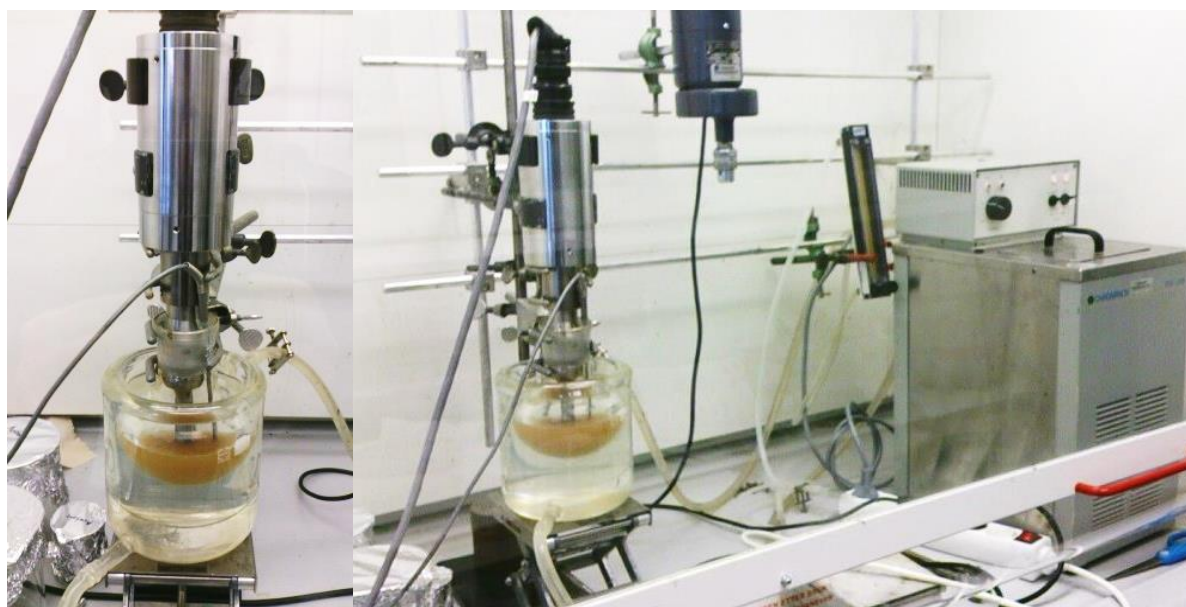


Figure 20 – Horn-type ultrasonicator with cooling jacket and temperature control (acetone and GO in the round bottom flask).

The same procedure were done for both a dispersion of as-prepared GO in acetone and as-prepared GO in distilled water.

3.2.4 Particle size distribution of GO dispersions

The particle size distributions of the GO dispersions were determined by DCS (disc centrifuge) DC24000 from CPS instruments Inc.

The DCS uses differential centrifugal sedimentation in a liquid with a density gradient to separate the particles by size [37;38]. Particles are exposed to centrifugal acceleration in a rotating hollow disc with a fluid inside, and the settling velocity of the particles is measured as a function of their diameter. Based on different size and shape, the particles will sediment at different velocities towards the outer edge of the rotating disc [37]. The disc centrifuge was used with a detector with a 405 nm light source [38].

A density gradient is added in the disc centrifuge to stabilise the sedimentation process and to avoid formation of streams. In addition, a calibration standard is needed before each sample measurement to adjust parameters [37]. The sedimentation velocity increases proportional to the squared particle diameter, so small particles sediment more slowly than big particles. Stokes sedimentation equation is shown in Equation 5.

$$v_s = \frac{2}{9} \cdot \frac{(\rho_p - \rho_f)}{\mu} \cdot g R^2 \quad (5)$$

,where v_s is the particle's settling velocity (m/s) (vertically downwards if $\rho_p > \rho_f$, upwards if $\rho_p < \rho_f$), g is the gravitational acceleration (m/s^2), ρ_p is the mass density of the particles (kg/m^3), and ρ_f is the mass density of the fluid (kg/m^3), R is the radius and μ is the viscosity of the liquid [58].

The sedimentation velocity also depends on the friction ratio. The friction ratio is a measure of the viscous resistance of a particle in a fluid and its deviation from a spherical shape. The friction ratio of a spherical particle is equal to 1 and spherical particles will therefore sediment faster than other particle shapes [36]. Deviation from a spherical shape will therefore be measured in the centrifuge as a hydrodynamic diameter smaller than a sphere of the same volume [36;37].

For the samples with MIBK and Disperbyk, automatic gradient injection was used. The gradient was injected in different concentrations to make the baseline, before a gradient cap

fluid, D 2.150 (0.5 mL), was injected. A calibration standard, 516 nm (0.2 mL) was treated in ultrasonic bath for 1 minute and injected before every sample injection. The gradient was changed between each or every second sample injection. 0.1 mL of the sample was injected and the centrifuge was run at 24000rpm.

Sucrose solutions were used as a density gradient when the samples were dispersed in water and acetone. The sucrose gradient was injected manually before every second experiment to make the baseline. The gradient consisted of nine different ratios of 8 and 2 % sucrose solution with a total volume of 1.6 mL each. The ratios were as follows, 8 % sucrose solution of 1.6, 1.4, 1.2, 1.0, 0.8, 0.6, 0.4, 0.2, and 0 mL with the rest of the content being 2 % sucrose solution. After adding the gradient series, a gradient cap fluid dodecane (0.5 mL) was added. The program was started, the baseline was automatically adjusted and a standard (H₂O 377 nm STD, 0.1 mL) was injected. GO solution was diluted 1:5 in distilled water and sonicated 1 minute in bath sonicator immediately before analysis. 0.1 mL of the sample was injected and the disk centrifuge was run at 24000 rpm.

Stokes' spherical diameter, D_{ST} , which is the equivalent hard sphere diameter having the same sedimentation rate as the measured particles were used for the reporting of the size in the particle size distribution [37;38].

3.2.5 Functionalization of as- prepared GO

In this thesis, two different diamines for the functionalization of GO were tested. The two techniques will be explained in Section 3.2.5.1 and Section 3.2.5.2.

3.2.5.1 Functionalization of GO with diamine XB3473

Diamine (Hardener XB3473, 1.0g) was added to the GO/distilled water – solution that had been exposed to the ultrasonic horn for 2 hours (as described in Section 3.2.3.3). The dispersion with diamine was then put on a magnetic stirrer (500 rpm) and heated to 80 °C for 30 minutes to complete the reaction. The solution got a dark brown, almost black, colour. The solution was further cooled to room-temperature and washed with distilled water several times to remove excess diamine. During the washing steps a centrifuge (Sorwall WX Ultra-

80) was used (10000 rpm for 30 min, and 20000 rpm for 15 min), and five washing steps was performed. Two batches of this type of FGO were made during the thesis.

3.2.5.2 Functionalization of GO with para-phenylenediamine (PPDA)

GO (0.25 g) was added in a round bottom flask with distilled water (100 g), and exposed to the ultrasonic horn (20 % amplitude) for 2 hours. PPDA (1.0126 g) was dissolved in warm distilled water (~70 °C, ~30 mL) and added to the GO/distilled water – solution that had been exposed to the ultrasonic horn for 2 hours. The solution was then heated to 80 °C at 500 rpm for 30 minutes on a magnet stirrer. Figure 21 shows some of the steps in the production of FGO with PPDA.

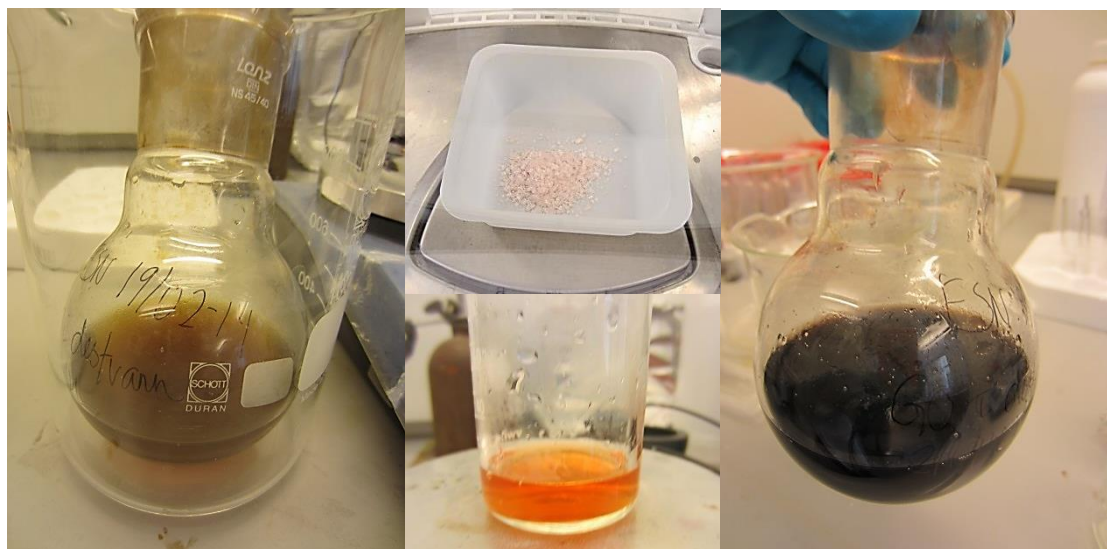


Figure 21- First picture; GO in distilled water. Pictures in the middle; PPDA flakes, and PPDA dispersed in hot distilled water. Last picture; PPDA added to the GO/distilled water solution.

The solution was then distributed in four centrifuge tubes and centrifuged in the Sorwall WX Ultra-80 at 20 000 rpm for 10 minutes. The supernatant was decanted away and the remaining solid was washed with distilled water several times to remove excess diamine. During the washing steps the same centrifuge was used (8000 rpm for 10 min and 5min). Three batches of this type of FGO were made during the thesis. One of the dispersions made were washed with acetone and dispersed in acetone instead of distilled water.

Figure 22 show FGO (PPDA) in distilled water.

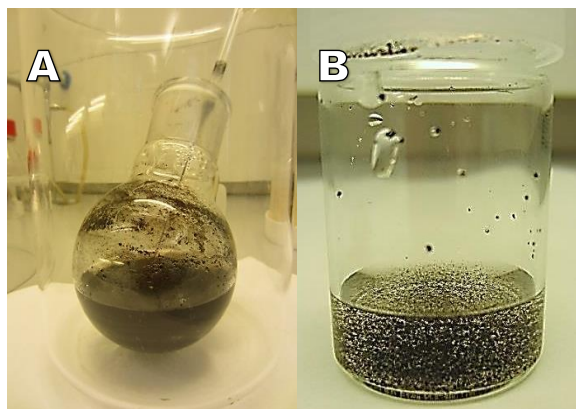


Figure 22 – A: FGO (PPDA) in distilled water before washing steps. B: FGO (PPDA) in distilled water, diluted.

3.2.6 X-Ray photoelectron spectroscopy

After the functionalization, the FGO was analysed by XPS to see if the functionalization with PPDA had been successful.

XPS can be used to determine the elemental composition of a materials surface and the chemical or electronic state of the elements. In addition, an XPS analysis can give information about relative ratios of the elements detected, hybridization of carbons on the surface of a material, and information about the purity of a material [59].

XPS analysis was performed in a KRATOS AXIS ULTRA-DLD by Spyros Diplas, head of research at SINTEF/UiO. One sample of FGO (PPDA) dispersed in water was dried in a vacuum oven and analysed in the XPS by using monochromatic Al K α radiation ($h\nu = 1486$ eV). The spectra were obtained at zero angle of emission ($\theta = 0^\circ$) with the lenses in hybride mode, which means that both the magnetic and the electrostatic lenses were used. Survey scan spectra were acquired in the kinetic energy range of 0-1200, and pass energy of 160 eV with a step size of 1 eV. The high resolution peaks were acquired at pass energy of 20 eV ans a step size of 0.1 eV. The XPS KRATOS AXIS ULTRA-DLD can perform surface sensitive analysis to a depth of about 10 nm. The XPS spectra were analysed by the program Casa XPS (Casa Software ltd.).

3.2.7 Effect of pH

The pH in a sample of FGO (PPDA) was adjusted to check if colour changes in the dispersion were a pH effect or if the colour change was a result of the functionalization with PPDA.

NaOH pellets (0.37 g) were dissolved in distilled water (100 g) to get a NaOH solution of approximately 0.1 M. A few drops of this NaOH solution were added to the FGO (PPDA) in distilled water to investigate the effect of pH on the FGO. Additional drops were added until the pH had reached approximately pH 9.

Ammonia (32 %, a few drops) was also added to a new sample of FGO (PPDA) in distilled water. Additional drops were added to reach a pH of 9-10.

3.2.8 Zeta potential

The Zeta potential of a dispersion of FGO (PPDA) in distilled water was performed to investigate the stability of the dispersion at different pH.

Measurements of the Zeta potential of FGO (PPDA) in distilled water was performed on a Zetasizer 3000 (Malvern Instruments) at UiO with help from professor Finn Knut Hansen. The zeta potential is measured by electrophoresis using the Doppler Effect with dynamic light scattering. The electrophoretic mobility is measured and the zeta potential is calculated by Smoulochowski's equation (Equation 3, Section 2.4.2). The FGO dispersion was diluted approximately 1:10, and injected into the Zetasizer. The sample absorption was set to 0.71 and the refractive index to 1.74 [60]. During the analysis, the pH of the solution was measured and adjusted by addition of ammonium and HCl, to find the isoelectric point, and to find how the Zeta potential varied with pH.

3.2.9 Optical microscope

A Leica optical microscope was used during the experimental work to inspect the different GO-, FGO-, and EXGO dispersion during processing. The microscope was typically used at either 10 X or 40 X magnifications.

3.2.10 Pre-tests of epoxy/water dispersion

To check the possible effect of water on the epoxy resin, epoxy (Araldite LY556, 25.5663 g) was added to a round bottom flask with distilled water (100 mL). It was first tried to mix the

epoxy with the water by stirring with an agitator for some minutes. Then the solution was mixed with a horn-type sonicator for 5 minutes at 20 % amplitude. The solution was further put on a magnetic stirrer (500 rpm, 100 °C) for 5-10 minutes. The solution formed a white, milk-like emulsion. The solution was again sonicated with a horn sonicator for 5 minutes at 20 % amplitude. The solution got even more emulsion-like. The epoxy/water emulsion was evaporated in a rotavapor for about 1.5-2 h to get rid of the water. The mixture had at this time got a clear, transparent appearance. Then the solution was put in a vacuum chamber on a magnet stirrer at 100 rpm and 100 °C, for several hours (Friday-Monday). The vacuum chamber on the magnetic stirrer and the epoxy with air bubbles are shown in Figure 23.

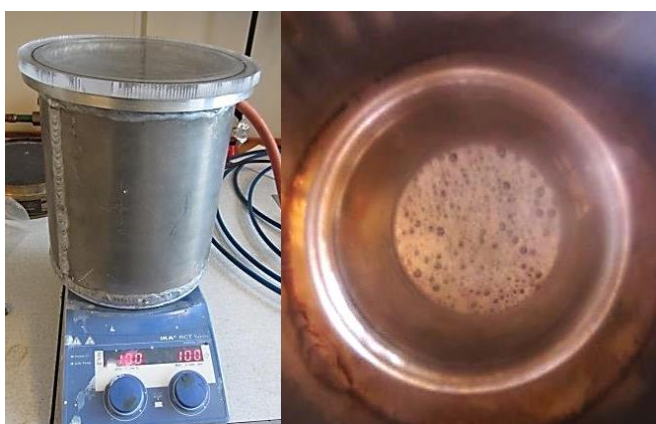


Figure 23 – Vacuum chamber on a magnetic stirrer to the left and epoxy with air bubbles on the right.

The epoxy/water solution was cooled to room temperature before hardener (XB3473, 5.75 g) was added, and well mixed into the epoxy/water dispersion. Air bubbles were removed in a vacuum chamber until no bubbles were left. The solution was cast in treated metal moulds, and cured at 120 °C for 2 hours, 160 °C for 2 hours and 180 °C for 2 hours. The cured samples were allowed to cool slowly in the oven to room temperature.

3.2.11 Surface tension and interfacial tension

The surface- and interfacial tension of epoxy in air and epoxy in water were measured to check for the presence of surface active agents in the epoxy resin. The surface- and interfacial tension were measured by a drop shape analysis on a goniometer from ramé-hart Instruments (by Finn Knut Hansen).

3.2.12 Preparation of epoxy in distilled water and acetone

To investigate the possible effect of water or acetone on the epoxy resin, neat epoxy was dispersed in either distilled water or acetone.

Epoxy (Araldite LY556, 40 g) was added to a round bottom flask with distilled water (100 mL). The solution was sonicated with a horn sonicator for 5 minutes at 20 % amplitude, which leads to a relatively unstable epoxy in water emulsion. The emulsion was let standing for the epoxy to sediment, and afterwards the top layer of water was removed by a pipette until there was no visible water left. The rest of the emulsion was evaporated in a rotavapor in a water bath at 40 °C for about 1.5-2 h to get rid of the remaining water. This finally gave a clear, transparent appearance, but with still some water left. Then the solution was put in a vacuum chamber on a magnet stirrer at 100 rpm and 40 °C, for several hours during night. The solution was cooled to room temperature before hardener (XB3473, 9.2 g) was added, and well mixed into the solution. Air bubbles were removed in a vacuum chamber, until no bubbles were left. The solution was poured into beforehand treated metal moulds. The composite was put in a vacuum oven for about half an hour at 40 °C to get rid of remaining air bubbles. The composite in the metal moulds was cured in an oven, first at 120 °C for 2 hours, then 160 °C for 2 hours and 180 °C for 2 hours. The cured samples were allowed to cool slowly in the oven to room temperature.

The same procedure was followed for an epoxy with acetone.

3.2.13 Preparation of composites

A variety of epoxy based composites were made during the experimental work of the M.Sc. thesis. A scheme of the different versions of epoxy composites with GO made is presented in Figure 24.

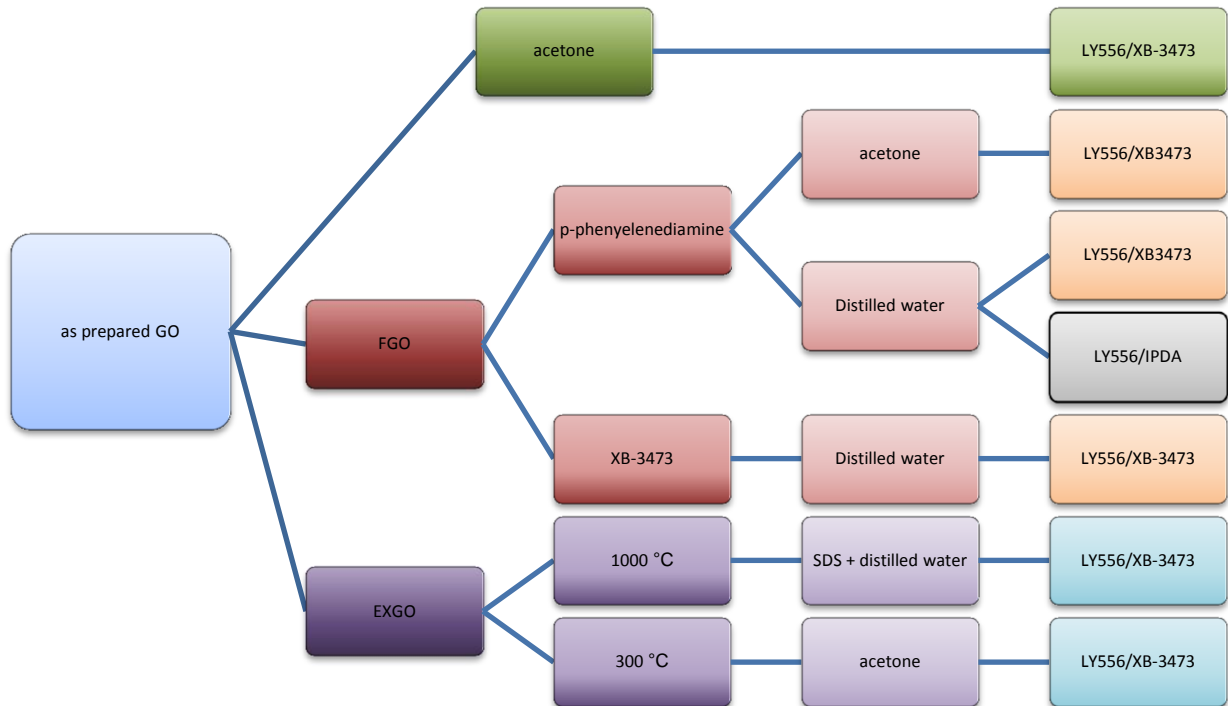


Figure 24 –Scheme of the different versions of epoxy matrixes with GO made during the M.Sc. thesis.

The procedure of the preparation of neat epoxy and epoxy nanocomposites reinforced with GO, FGO or EXGO are described in more detail in Section 3.2.13.1, 3.2.13.2. and 3.2.13.3. Approximately the same procedure were used for epoxy reinforced with GO, EXGO, and FGO.

Differences in curing cycle, amounts of GO/FGO/EXGO, solvent, epoxy resin, and hardener and different time in ultrasonic treatment are summarized in Table 2.

Table 2 – Preparation of composites, with reinforcements, solvents, dispersion with ultrasonic horn and curing cycle presented for all the composites.

Epoxy system	Reinforcement	Solvent	Dispersion with ultrasonic horn (20 % amplitude)	Curing cycle
LY556/XB3473 (mixing ratio 100:23) (approximately 40 g resin and 9.2 g hardener)	FGO (XB3473) (0.25 g GO, 1 g XB3473)	Distilled water (100 g)	2 h before resin added +5min after resin added	2h/120°C+2h/160°C+2h/180°C
	FGO (PPDA) (0.25 g GO, 1 g PPDA)	Distilled water (100 g)	2 h before resin added +5min after resin added	2h/120°C+2h/160°C+2h/180°C
	FGO (PPDA) (0.25 g GO, 1 g PPDA)	Acetone (100 g)	2 h before resin added + 5min after resin added	2h/120°C+2h/160°C+2h/180°C
	EXGO (300 °C) (0.02 g)	Acetone (50 g)	1.5 h before resin added + 1.5 min after resin added	2h/120°C+2h/160°C+2h/180°C
	EXGO (1000 °C) (0.08 g) SDS (0.08 g)	Distilled water and SDS (50 g)	2 h before resin added + 5min after resin added	2h/120°C+2h/160°C+2h/180°C
	As prepared GO (0,25 g)	Acetone (100 g)	2 h before resin added + 1 h after resin added	2h/120°C+2h/160°C+2h/180°C
	-	Acetone (100 g)	1h after resin added	2h/120°C+2h/160°C+2h/180°C
	-	Distilled water (100 g)	5min after resin added	2h/120°C+2h/160°C+2h/180°C
LY556/ IPDA (mixing ratio 100:22.7) Approximately 40.8 g resin and 9.3 g hardener	FGO (PPDA) (0.25 g GO, 1g PPDA)	Distilled water (100 g)	2 h before resin added+ 5 min after resin added + 5 min after solvent removed	4h/30°C+1.5h/80°C+1.5h/150°C
	-	-	-	4h/30°C+1.5h/80°C+1.5h/150°C
	-	-	-	24h/ room temperature+2h/100°C

3.2.13.1 Nanocomposites with epoxy system Araldite LY556/XB3473

Neat epoxy polymer specimens of Araldite LY556/XB3473 were made to have a reference for further experiments.

Neat epoxy polymer specimens were prepared by first mixing the epoxy resin and the hardener at the ratio 100:23 by weight. The mix was stirred manually by a Teflon coated stirring rod to get an even distribution. Air bubbles were removed by degassing in a vacuum chamber, before the blend was cast into metal moulds coated with two layers of release agent. The blend was cured in an oven for 2 hours at 120 °C, 2 hours at 160 °C, and 2 hours at 180 °C.

GO/FGO/EXGO was dispersed in distilled water or acetone by sonication with a horn-type ultrasonicator (Branson Digital Sonifier® S-450D, 25 kHz, 400W). During the horn sonication, the tip of the horn was placed into the dispersion, and the power delivered was controlled by setting the amplitude at the tip of the resonating horn to 20 %. The temperature was controlled by a cooling jacket with a set maximum temperature of 30 °C. After sonication for 2 hours, epoxy resin (~ 40g) was added to the GO dispersion and mixed thoroughly before again sonicating with the horn-type sonicator for 5 minutes. The solvent (water or acetone) was evaporated in a rotavapor (Figure 25). The rotavapor was kept at a temperature of ~40-60°C when distilled water was used as the solvent, and ~ 80 °C for dispersion with acetone. Figure 25 shows the epoxy sample installed in the rotavapor for the removal of acetone in the sample.



Figure 25 – Epoxy solution in rotavapor for the removal of solvent (acetone).

When most of the solvent had been removed, the blend was put in a vacuum chamber with stirring at (70 °C) overnight to remove remaining solvent. The epoxy blend was cooled to room temperature before hardener (XB3473, ~ 9.2 g) was added, and thoroughly mixed into the epoxy blend. Air bubbles were removed by degassing in a vacuum chamber, before the blend was cast into metal moulds coated with two layers of release agent. The metal moulds with epoxy blend were again put in a vacuum chamber at room temperature to remove the last remaining's of air bubbles. The composite was cured in an oven for 2 hours at 120 °C, 2 hours at 160 °C, and 2 hours at 180 °C. The cured samples were allowed to cool slowly in the oven to room temperature.

3.2.13.2 *Epoxy system Araldite LY556/isophorone diamine*

Neat epoxy polymer specimens of the epoxy system Araldite LY556/isophorone diamine were made as a reference for a composite with FGO (PPDA).

Hardener (IPDA) and epoxy resin (Araldite LY556) were added in a round bottom flask (250 mL) in the ratio 100:22.7 by weight and was thoroughly mixed with a Teflon coated stirring rod. Air bubbles were removed by degassing in a vacuum chamber, and thereafter the blend was cast into metal moulds coated with two layers of release agent. The epoxy was cured at room temperature for 24 hours and then post cured at 100°C for 2 hours. The cured samples were allowed to cool slowly in the oven to room temperature.

Hardener (IPDA) and epoxy resin (Araldite LY556) were added in a round bottom flask (250 mL) in the ratio 100:22.7 by weight and was thoroughly mixed with a Teflon coated stirring rod. Air bubbles were removed by degassing in a vacuum chamber, and thereafter the blend was cast into metal moulds coated with two layers of release agent.

The epoxy was cured at room temperature for 4 hours and then post cured at 80 °C for 1.5 hour and 150 °C for 1.5 hour. The ramp rate between 30°C and 80°C was 0.5 °C /min, and 1 °C /min between the 80 °C and 150 °C step. The cured samples were allowed to cool slowly in the oven to room temperature.

3.2.13.3 FGO (PPDA) in distilled water and IPDA

A new neat epoxy polymer specimen of the epoxy system Araldite LY556/isophorone diamine with a different curing cycle were made as a reference for a composite with FGO (PPDA).

FGO (PPDA) dispersed in distilled water was exposed to ultrasonic horn for 2 x 5 min at 20 % amplitude, before epoxy resin (Araldite LY556, ~ 40.8 g) was added. The epoxy/GO/distilled water blend was again exposed to ultrasonic horn for 5 min at 20 % amplitude, before the water was evaporated for 3-4 hours in a rotavapor. After evacuation in the rotavapor, the solution was put in a vacuum chamber on a magnet stirrer at 70 °C and 50 rpm overnight, to make sure all water had been removed. Additional 2-3 hours in the vacuum chamber were needed, before all remaining water was removed. The epoxy/FGO mix was again treated with ultrasonic horn for 5 min, before hardener (IPDA, ~ 9.2 g) was added and properly mixed into the epoxy resin with FGO. Approximately 1.5 hour in vacuum chamber with varying pressure was needed to remove air bubbles, before casting into metal moulds and allowing the epoxy to cure in room temperature for 1 hour. The metal moulds with epoxy was then placed in a regulated oven for further curing at 30 °C for 5 hours, 80 °C for 1.5 hour and 150 °C for 1.5 hour. During the temperature changes the temperature were raised with approximately 1°C /minute and 0.5 °C /minute, and the epoxy was allowed to cool slowly to room temperature after curing.

3.2.14 Preparation of epoxy composite testing rods

The metal moulds used for the preparation of epoxy composite testing rods had to be lubricated with two layers of release agent and the screws with grease, before the epoxy was added to the moulds. Each layer of release agent had to dry for 1 hour at 60 °C. After curing, the longitudinal sides of the test specimens were polished in a grinding machine with a P320 SiC paper with water lubrication until a smooth surface and an even thickness were obtained. The specimen width and thickness of every specimen was measured by a digital micrometer (Micromar 40EWR, MahrIP65) before analysis. Figure 26 shows some of the steps in the preparation of epoxy rods.

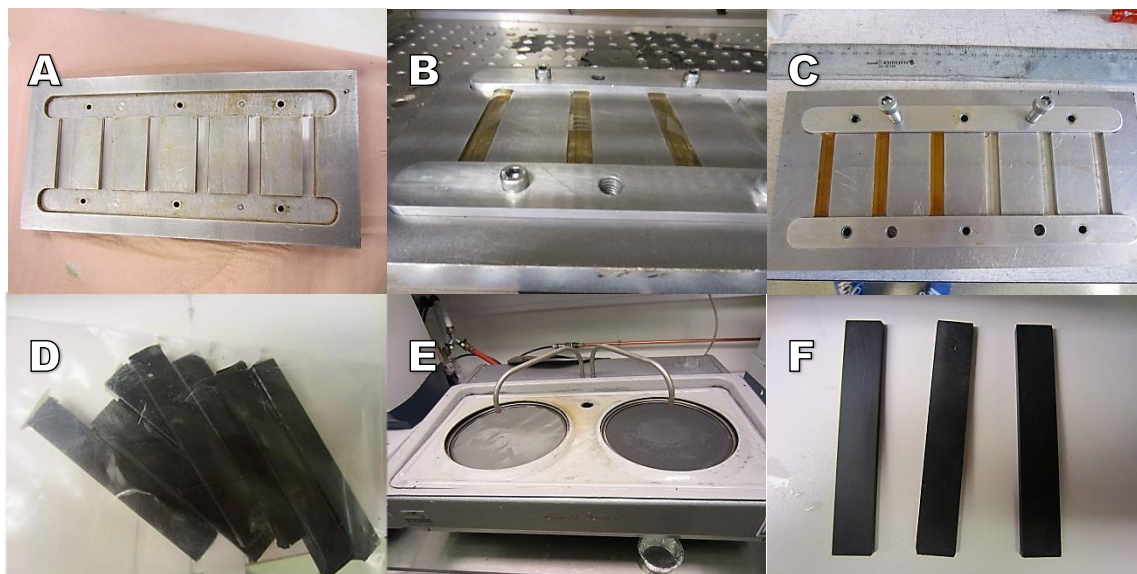


Figure 26 – Preparation of epoxy composite testing rods. A: metal mould, B: during curing, C: after curing, D: epoxy rods, E: grinding machine, F: epoxy rods after grinding.

3.2.15 Dynamic mechanical analysis

The various composites and neat epoxies were analysed by dynamical mechanical analysis to be able to compare the mechanical properties of the composites.

DMA was performed on a DMA Q800 Dynamic Mechanical Analyser from TA Instruments.

Rectangular specimens with dimensions of typically 60 mm x 9.7 mm x 2.9 mm (length x width x thickness) were used. The specimen thickness was measured at nine different locations on the specimen and the width was measured at a minimum of three different locations on the specimen using a digital micrometer (Mircomar40EWR). The average values were used in the analysis. The DMA was conducted using a 3-point bending clamp. The specimen was placed in the clamp, and aligned as accurately as possible. During the analysis the oscillation frequency was set to 1 Hz, the pre-load force was set to 0.01 N, the heating rate was 5 °C/min, and the force track was set to 125 %. The start temperature for each sample was set to 28 °C, and the heating was performed until a temperature of 250 °C was reached. A minimum of three replicate specimens were tested for the different sample series.

The program TA Universal Analysis was used to analyse the results. The value of the storage modulus, E' , was measured at a temperature of 35 °C, while the T_g of the epoxy polymer is

reported as the peak value of the loss modulus, E'' . The setup of the specimen in the DMA is presented in Figure 27.

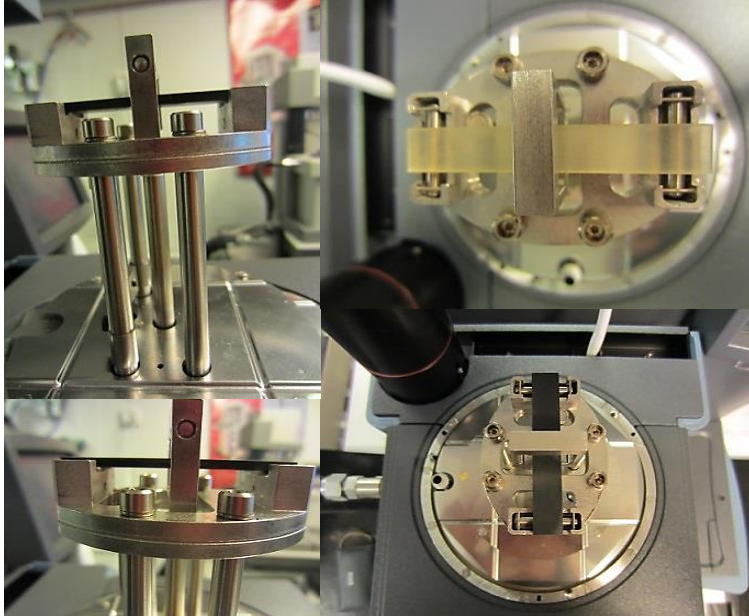


Figure 27 - Epoxy rods aligned in the 3-point -bending mode in the DMA Q800.

3.2.16 Three-point flexural bending test

The flexural properties of the different composites were determined according to Procedure A in “ASTM D 790-03 [61]. The testing was performed in a Zwick BZ2.5/TN1S material testing machine equipped with a 2.5 kN load cell.

Rectangular specimens were loaded in a three-point bending mode. The specimens typically had a size of 60 mm x 9.7 mm x 2.9 mm (length x width x thickness) and were machined from moulded samples. The specimen thickness was measured at nine different locations on the specimen and the width was measured at a minimum of three different locations on the specimen using a digital micrometer (Mircomar40EWR). The average value was used in the analysis. The specimens were resting on two supports while a loading nose was pushing with a downward force in the middle of the supports. The support span was adjusted according to the thickness and selected span-to depth ratio (the ratio of the distance between the support spans and the specimen thickness). The span-to-depth ratio during the testing was 16 to 1. The load was applied at the crosshead speed calculated from Equation 6,

$$R = \frac{ZL^2}{6d} \quad , \quad (6)$$

where R is the crosshead speed (rate of movement of the loading nose) (mm/min), Z is the straining in the outer fibre (mm/mm/min =0.01), L is the length of the support span (mm), and d is the specimen thickness (mm). L was calculated from Equation 7,

$$L = d \times 16 \quad , \quad (7)$$

where d is the nominal specimen thickness (mm).

Five replicate specimens were tested for each testing series (each type of condition). Flexural modulus (the modulus of elasticity in bending), E_B (MPa), flexural stress, σ_{fM} (MPa), and flexural strain, ε_{fB} (%) were calculated by the test software (testXpert II). The set up of the three-point flexural bending test is shown in Figure 28.

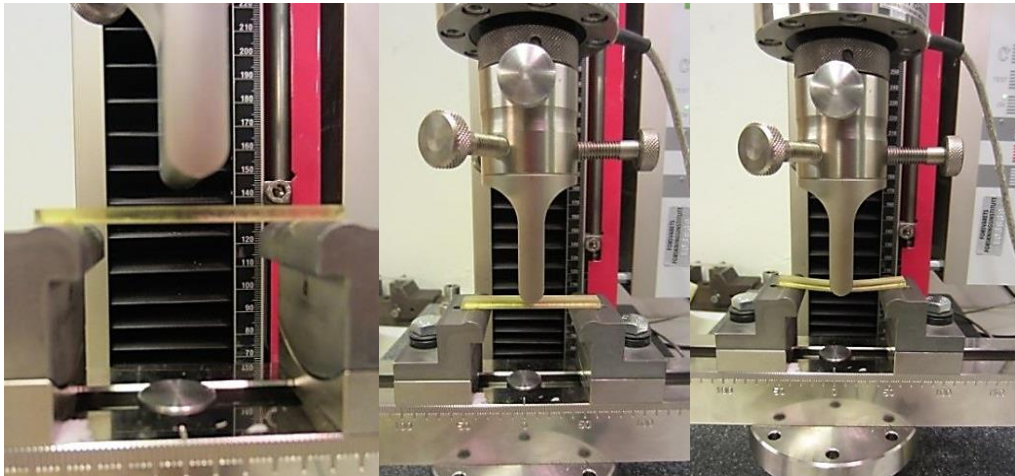


Figure 28 - Three-point flexural bending test in the Zwick BZ2.5/TNIS material testing machine.

4 Results and discussion

This chapter presents the results of the various experiments and analyses performed during the thesis. The results are discussed under each experiment performed, and a summary of the total results and experiments are discussed in a summarizing discussion.

4.1 Dispersion of GO

The first analyses in the experimental work of the M. Sc. thesis were done to investigate the dispersion of the GO particles in different solvents and ultrasonic treatment at different time intervals. These tests were performed to find the optimal dispersion method for the GO in solution for further application in the epoxy composites. Both ultrasonic horn and ultrasonic bath were used for the dispersion.

4.1.1 Dispersing EXGO (300 °C) in ultrasonic bath

EXGO (300°C) was dispersed in MIBK and MIBK with the stabilization agent; Disperbyk. The dispersions were sonicated in an ultrasonic bath (denoted by UL in the figure (Figure 29)) for different time intervals. EXGO has a structure more similar to that of graphene, and EXGO is therefore less dispersible in water and polar solvents compared to as-prepared GO. Disperbyk was used as dispersion agent in one of the EXGO/MIBK dispersions. Disperbyk has been successfully used for CNT's [38] and was presumed to make the EXGO/MIBK dispersion more stable.

Figure 29 show the results of the particle size distribution of EXGO (300°C) in MIBK and in MIBK with the Disperbyk stabilizing agent obtained by analysis in disc centrifuge.

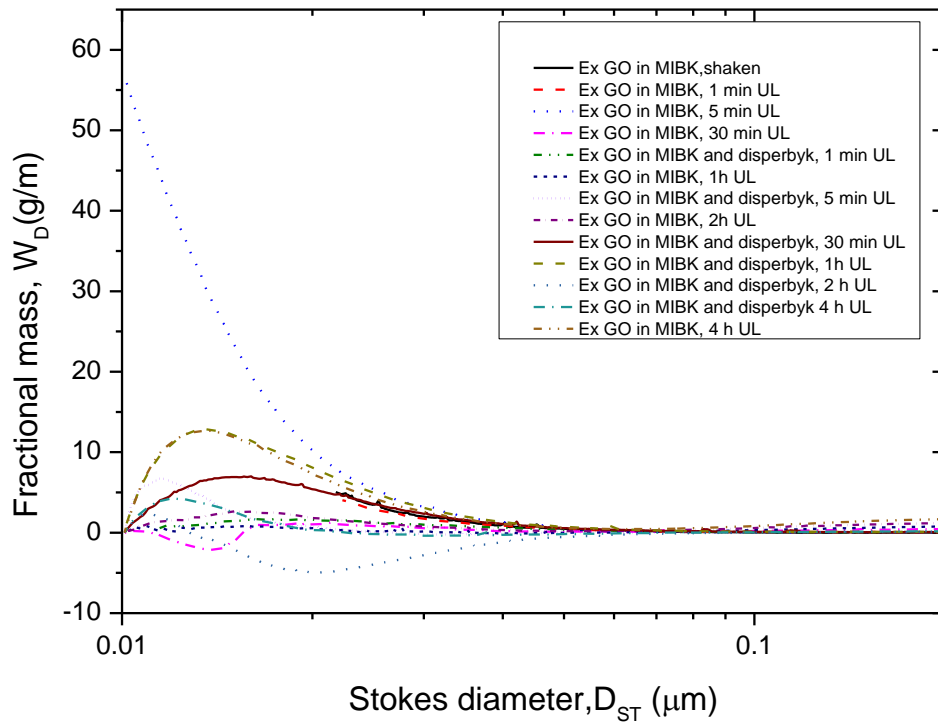


Figure 29 - Disc centrifuge results of dispersion of EXGO in MIBK and MIBK with Disperbyk at different treatment lengths in the ultrasonic bath.

The graph (Figure 29) shows that no distinct top or clear distribution exists. This indicates a poor and unstable dispersion. However, there is a tendency of peak formation between 10-20 nm as the sonication time in the ultrasonic bath was increased. The same trend was visible for both the solution with the Disperbyk and the one without. The graph shows that the lines are inconsistent as time goes by, and this means that the results are varying and are not very reliable. The blue dotted upper line is showing increasing fractional mass after some time. This behaviour is probably caused by drift in the baseline, and is not reliable.

4.1.2 Dispersing as- prepared GO with ultrasonic bath

To compare the dispersion of GO in acetone and water, the dispersions were analysed in a disc centrifuge after two hours of treatment in an ultrasonic bath. Figure 30 shows the results from the analysis in disc centrifuge.

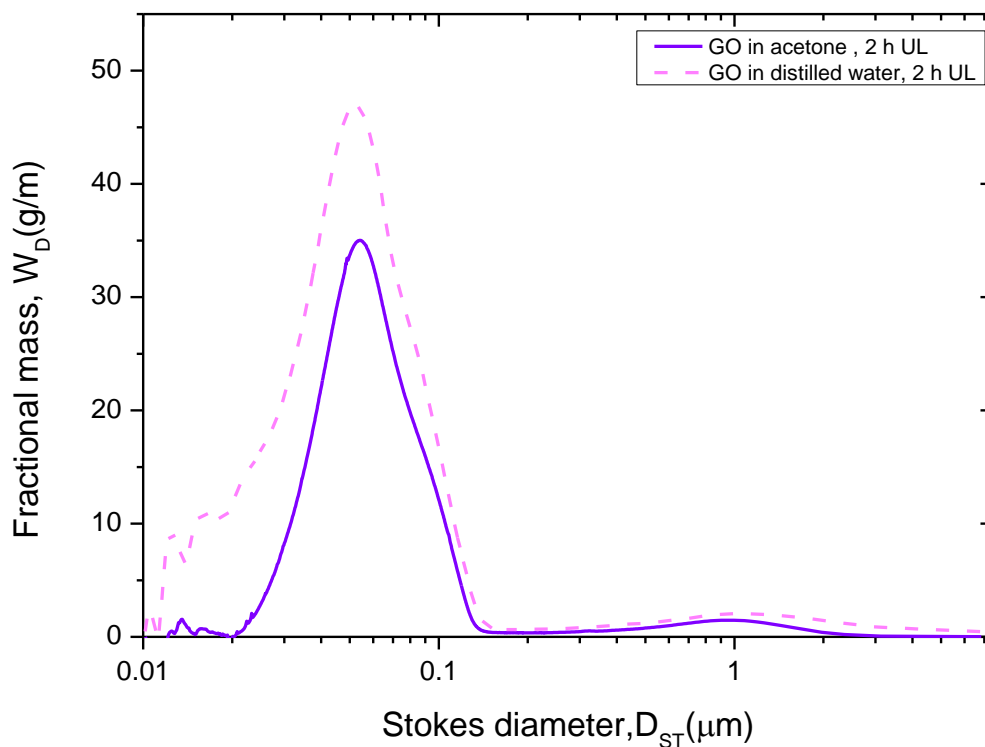


Figure 30 – Result of analysing the dispersion of GO in acetone and distilled water in disc centrifuge after treatment in ultrasonic bath. Stokes diameter corresponds to the particle size.

As shown in Figure 30 the Stokes diameter of the GO particles in both acetone and in distilled water became approximately 50 - 60 nm. Stokes diameter corresponds to the particle size of GO. The results show similar values for acetone and distilled water. The peak is higher for GO dispersed in distilled water compared to the peak of GO dispersed in acetone. This difference is however, not assumed to be significant, and can be caused by different amounts of GO in the two samples. Based on this experiment it is assumed that the dispersion of GO in acetone is similar with GO dispersed in distilled water, which indicates that acetone is a good solvent for exfoliation, and as a dispersing medium.

4.1.3 Dispersing GO in acetone with ultrasonic horn

A gradual increase in treatment with ultrasonic horn was introduced to a dispersion of GO in acetone, and the dispersion was analysed by the disc centrifuge. Figure 31 shows the results from the dispersion of GO in acetone after exposure to sonication in an ultrasonic horn for different time intervals.

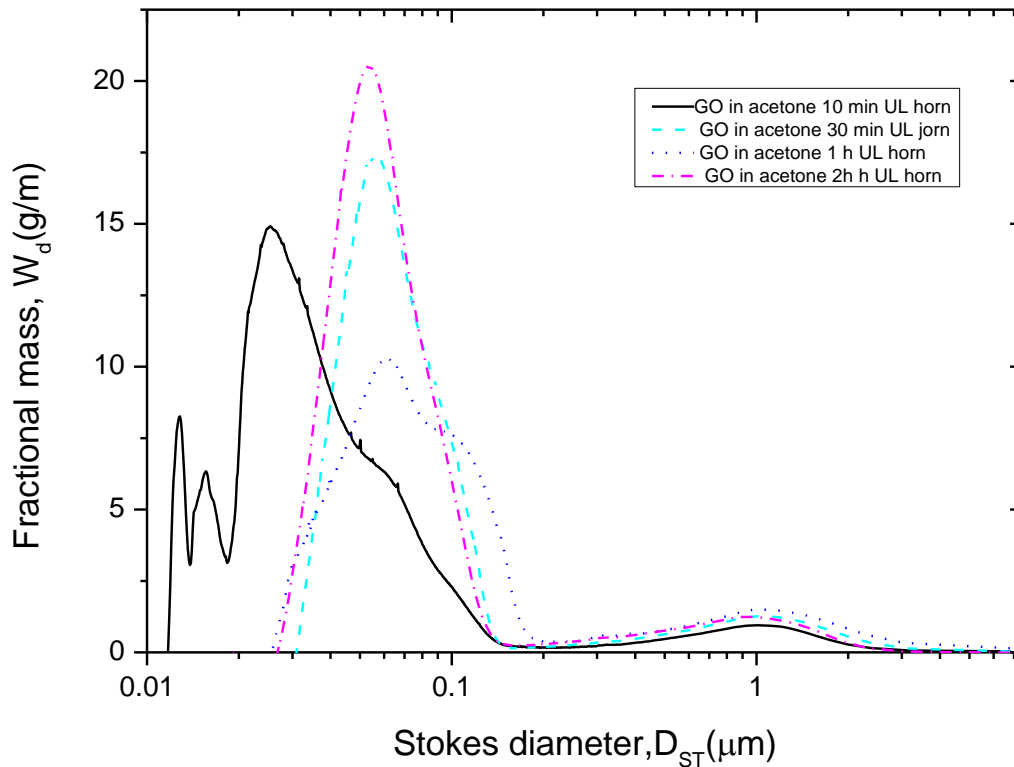


Figure 31 – Result of analysing the dispersion of GO in acetone in disc centrifuge after treatment with ultrasonic horn for different time intervals. Stokes diameter corresponds to the particle size.

The figure (Figure 31) shows that the dispersion becomes smoother after increased treatment with ultrasonic horn. The size of the particles shows a bimodal pattern with the highest peak around 50-60nm and a smaller peak around 1 μm . The bimodal pattern indicates that the samples consisted of particles of two different sizes. After increased time of ultrasonic treatment, the peak with the large particles was reduced, while the number of particles in the lower area increased. The peak around 1 μm is assumed to be caused by agglomerated GO flakes.

4.1.4 Dispersing GO in distilled water with ultrasonic horn

GO in distilled water was exposed to ultrasonic horn at gradually increased time intervals, and was analysed by the disc centrifuge. Figure 32 shows the results from the dispersion of GO in distilled water after exposure to sonication in an ultrasonic horn for different time intervals.

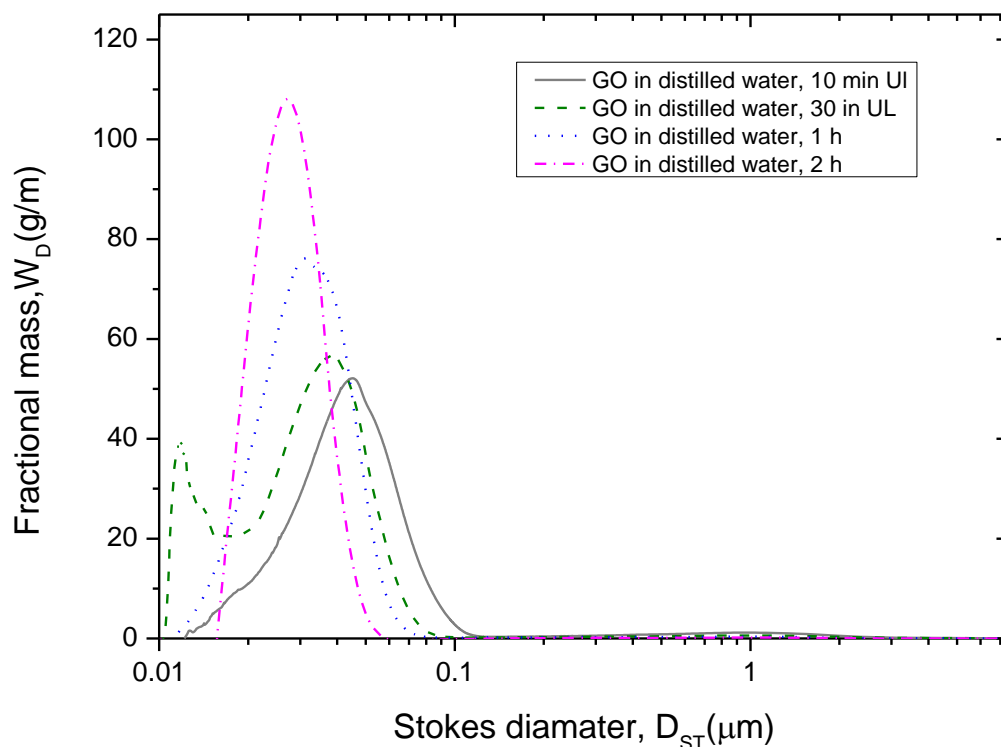


Figure 32 - Result of analysing the dispersion of GO in distilled water in disc centrifuge after treatment with ultrasonic horn for different time intervals. Stokes diameter corresponds to particle size.

The results (Figure 32) show a bimodal pattern which unifies in a single peak around 30 nm as time goes by. The results show that the GO particles in the distilled water are smaller, a larger amount of particles is detected, and the bimodal pattern is less prominent compared to the dispersion of GO particles in acetone.

Based on the results from the disc centrifuge of the dispersions with acetone, was a good alternative as solvent, but due to visual observations, the acetone dispersion seemed to be less stable over time compared to distilled water. GO particles dispersed in acetone seemed to

sediment faster compared to GO particles dispersed in distilled water. Dispersions of GO in distilled water could apparently stand for several days without signs of sedimentation. Two hours of ultrasonic treatment with horn-type sonicator seemed to give well defined particle size distributions, and this duration was therefore used for the following experiments with composites. The EXGO dispersed in MIBK and MIBK with Disperbyk were almost similar, and the Disperbyk didn't appear to give improvements in the dispersion of EXGO. MIBK were not used further in the experiments as a dispersant, as the dispersions didn't appear to be stable over time.

The amplitude of the ultrasonic horn was set to 20 %. The amplitude on the ultrasonic horn was set low to prevent degradation of the sample as other research has shown that degradation is a problem when the amplitude exceeds 70 % [38;62;62]. A different behaviour of the particles has also been observed at amplitude above 40 % [38;62]. It could maybe have been advantageous to increase the amplitude to get even better dispersions. To the author's knowledge, there is no research on the system used in this thesis, but it was presumed that the same conditions as for example CNT's would be applicable.

When analysing the different dispersions using the disc centrifuge, the refractive index was kept constant at the same value. Incorrect refractive index can potentially be a source of error because it can cause the measured amount of particles to be wrong. The particle size, however, is not dependent on the refractive index.

It is important to keep in mind that the GO particles are not spherical, but flake like, and this means that the alignment of the flakes play a role in the size measured in the disc centrifuge. Thin flakes sediment differently based on size and shape. Thin flakes have low weight and sediment slowly. Particles which are not spherical sediment even more slowly due to the higher friction factor [63]. Since the GO particles are more flake-like, the size of the particles can be perceived as smaller than they actually are because they sediment more slowly.

It is also important to be aware of possible artefacts when operating with particles in nano scale. Drift in the baseline, degradation of the density gradient in the spin fluid, temperature differences, or different sedimentation time for the samples, can give fluctuations in the signal. In addition, the instrument can miss some of the smallest particles because of the low light scattering efficiency of very small particles [38].

4.2 X-Ray photoelectron spectroscopy

The analysis of different functionalized graphene oxide samples in order to determine whether the GO was really functionalized, and to test if one of the methods was better compared to the other, was planned. Unfortunately, due to lack of instruments and operator it was not possible to have more samples analysed, and only one sample of FGO was analysed with XPS. A sample of FGO (PPDA) in distilled water was dried and analysed with XPS to see if functionalization had occurred. This sample was compared with a XPS analysis performed in the specialization project performed by the author during the autumn of 2013[30].

4.2.1 Surface composition

The XPS results obtained of the as-prepared GO made during the specialization project the autumn of 2013 is included in Figure 33[30]. Figure 34 shows the survey XPS spectrum of FGO (PPDA) with surface composition with the different elements marked.

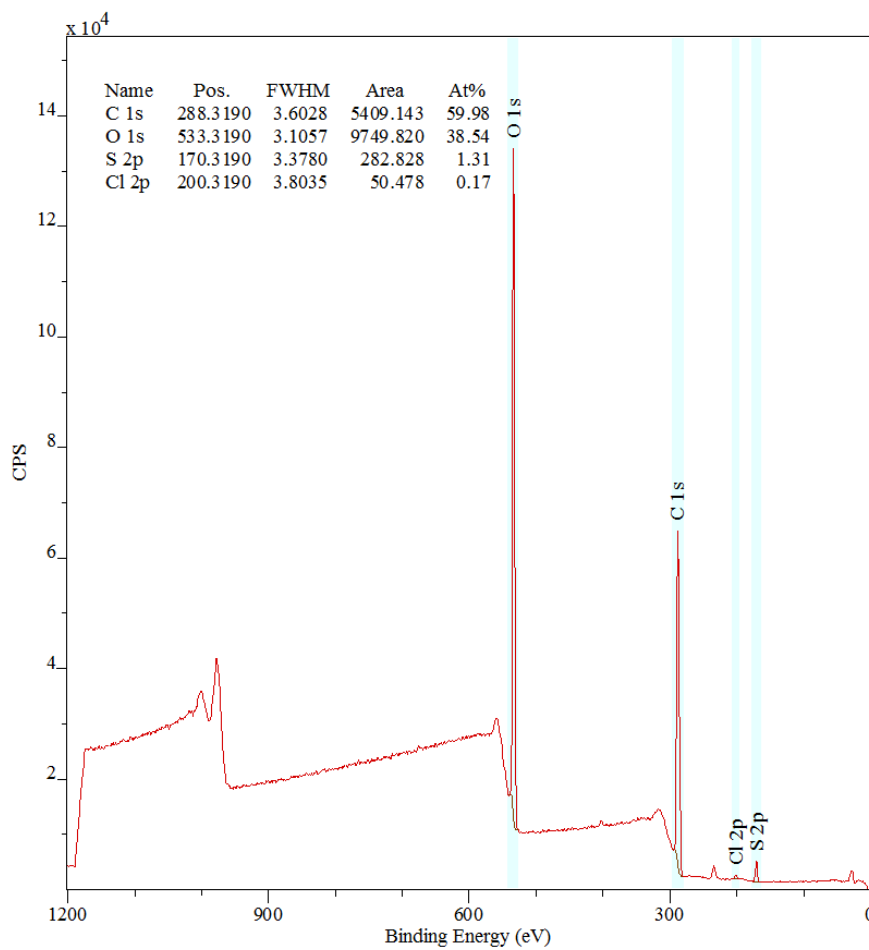


Figure 33 – Survey scan of as-prepared GO from the specialization project performed during the fall of 2013[30].

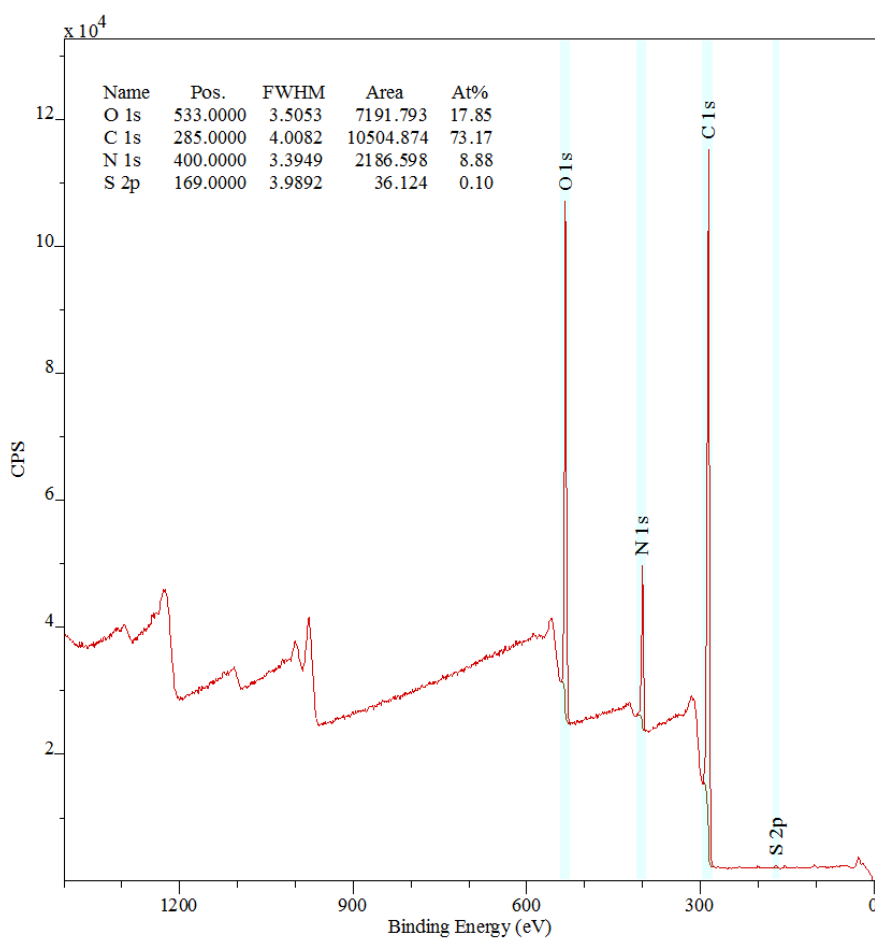


Figure 34 – Survey scan of FGO (PPDA) dispersed in distilled water and dried.

The surface compositions of as-prepared GO (autumn 2013), and FGO (PPDA) are summarized in Table 3. Tables of various characteristic binding energies and chemical shifts are attached in Appendix G.

Table 3 – Surface composition in at. % of as-prepared GO and FGO (PPDA) as determined with XPS.

	O (%)	C (%)	N (%)	Cl (%)	S (%)
As prepared GO (2013)[30]	38.54	59.98	-	0.17	1.31
FGO (PPDA)	17.85	73.17	8.88	-	0.10

As-prepared GO was analysed by XPS as a part of the specialization project performed during the autumn of 2013[30].The same procedure for the preparation of as- prepared GO was used in this thesis, and the XPS results obtained in 2013 are therefore presumed to be applicable.

The content of oxygen and carbon was in accordance with results from previous study of as-prepared GO by XPS, which indicates a successful production of as-prepared GO [29;64]. For example, Brodie got a carbon content of 61.04 and an oxygen content of 37.1 during his analysis [29], and this corresponds well with 59.98 carbon and 38.54 oxygen as found in the specialization project[30].

The results of the XPS (Table 3) showed some content of chlorine and sulphur in the sample with as prepared GO, which indicated remaining sulphuric acid and hydrochloric acid from the preparation procedure. The sample should have been cleaned more efficiently with water to remove the remaining sulphur and chlorine. The FGO shows no presence of chlorine and the amount of sulphur is also low; this is probably caused by additional washing steps after the functionalization with diamine. Another possibility is that the chlorine or sulphur have reacted with the excess diamine and followed it during the washing steps.

The main differences between the as-prepared GO and the FGO are the content of oxygen, carbon and nitrogen. The amount of carbon and nitrogen has increased, while oxygen is lowered in the FGO sample compared to the as-prepared GO sample. The increased carbon content is probably caused by the addition of PPDA which contains six carbon atoms. The PPDA contains two amino groups which explain the nitrogen content in the FGO. These results indicate that the amino groups have reacted with the GO as wanted. A successful reaction of PPDA with GO is also indicated by the high resolution spectra following in Section 4.2.2.

4.2.2 Functional groups

The high resolution de-convoluted C1s XPS spectrum of FGO is presented in Figure 35 with characteristic binding energies for the most probable functional groups.

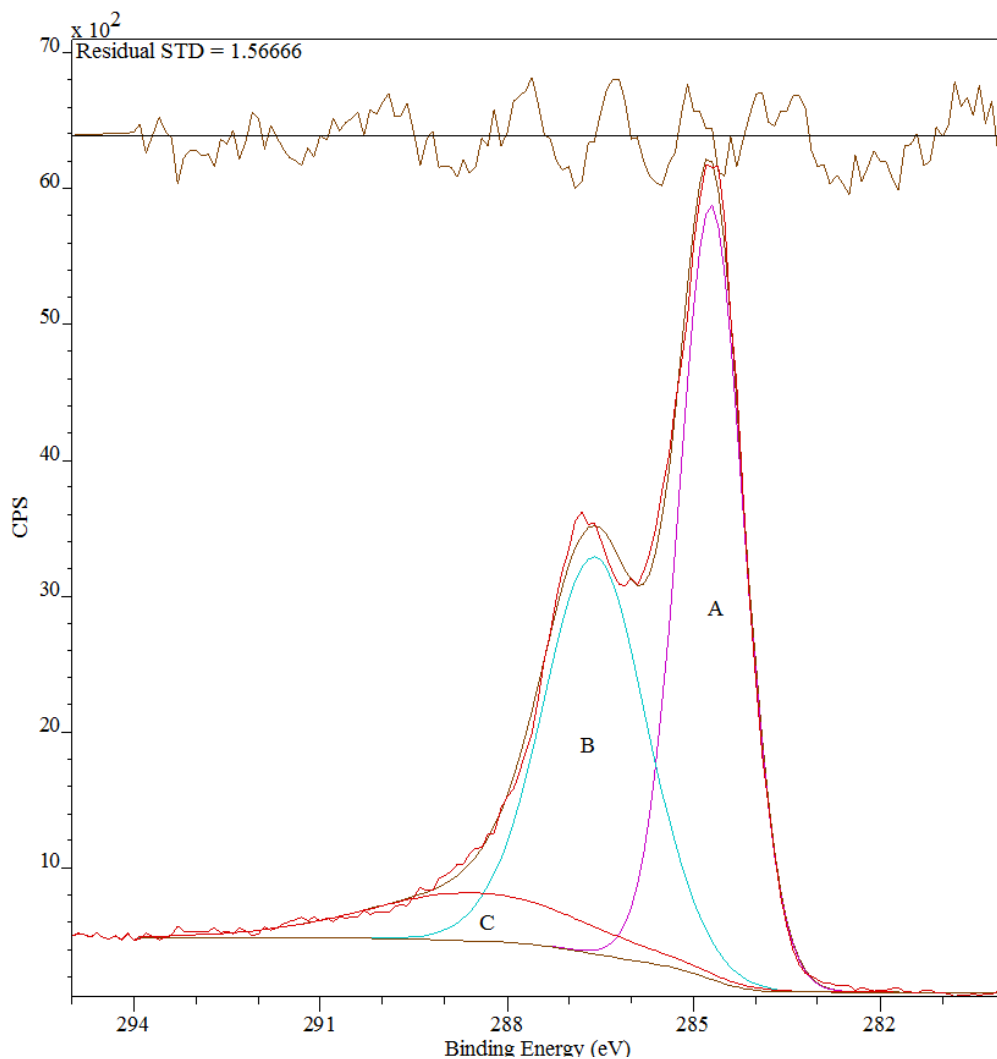


Figure 35 - High resolution C1s XPS spectrum (Carbon peak) of FGO.

The scan (Figure 35) shows at least three chemical states, in which correspond to carbon atoms in different functional groups. The binding energies at 284.714 eV (Peak A) are attributed to C-C (sp^2), C-C (sp^3) and C from diamine (benzene ring) [59;63]. Moreover, the binding energies of 286.586 eV (Peak B) and 288.413 eV (Peak C) correspond to C=O and O=C-OH groups respectively [34;65]. A table of various characteristic binding energies for XPS can be found in Appendix G.

High resolution N1s XPS spectrum of FGO is presented in Figure 36.

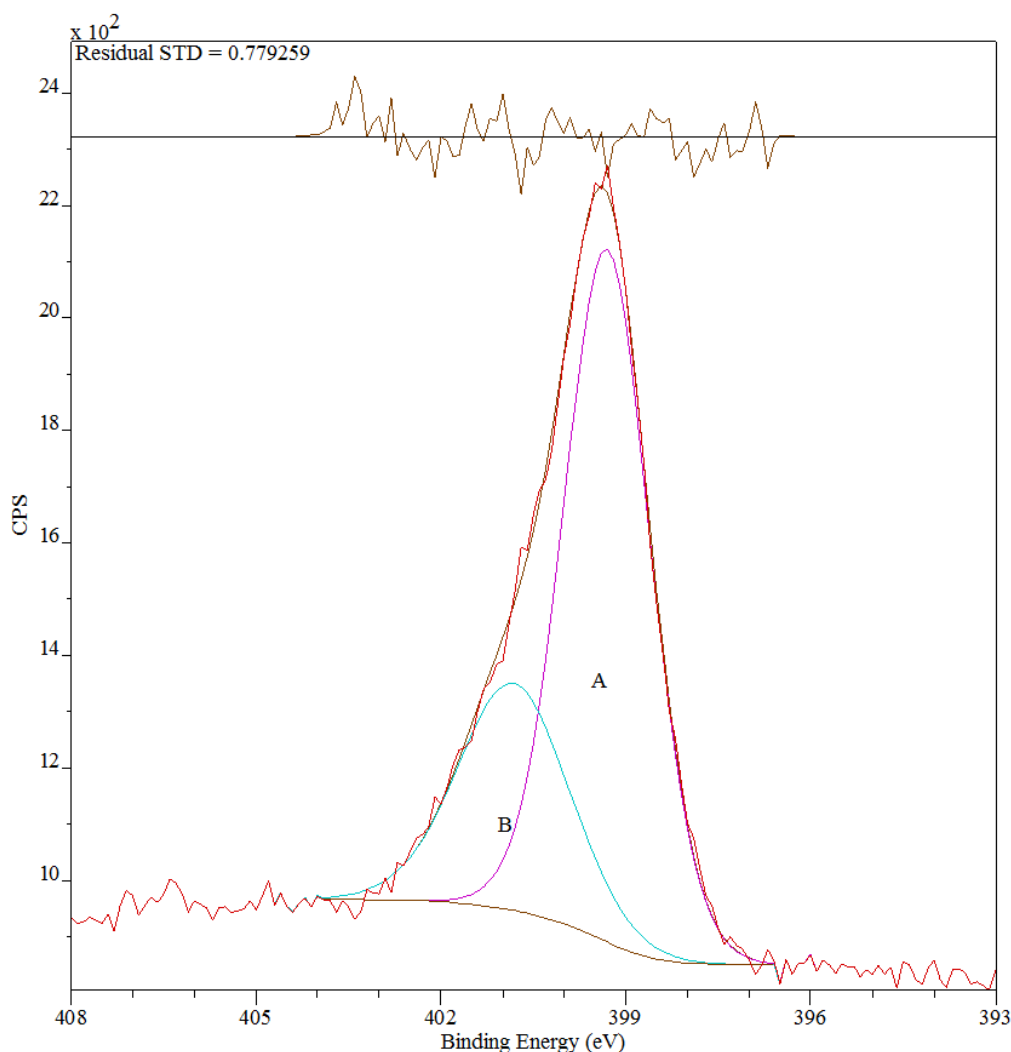


Figure 36 – High resolution N1s XPS spectrum (Nitrogen peak) of FGO.

The high resolution N1s spectrum (Figure 36) shows that nitrogen is found in two different chemical states with a 70 % (Peak A): 30 % (Peak B) distribution of the two forms. It is assumed that one form exists in independent diamine, while the other is bound to graphene oxide. A hypothesis is that the peak at 400.822 eV (Peak B) corresponds to N-C(O) bindings, which means nitrogen from PPDA that is bound to GO through ring opening of epoxy groups on GO. While the peak at 399.305 eV (Peak A) corresponds to unreacted PPDA and PPDA that has partly reacted or is in a middle state as $\text{NH}_3^+\text{-C}$ groups, as a counter ion to the carboxyl functional groups (in other words; ammonium carboxylate formation) [47]. The PPDA was added in excess, and remaining unreacted diamine could potentially be reflected in

this peak (peak A). The hypothesis is that 30 % out of the 70 % peak (Peak A) corresponds to the unreacted diamine group in the diamine, and that the remaining 40 % is the middle state reaction/counter ion to the carboxyl functional group. Peak B indicates that 30 % of diamine has reacted on the GO surface and the study of Gudarzi et al. supports these statements/claims [47].

High resolution O1s XPS spectrum of FGO is presented in Figure 37.

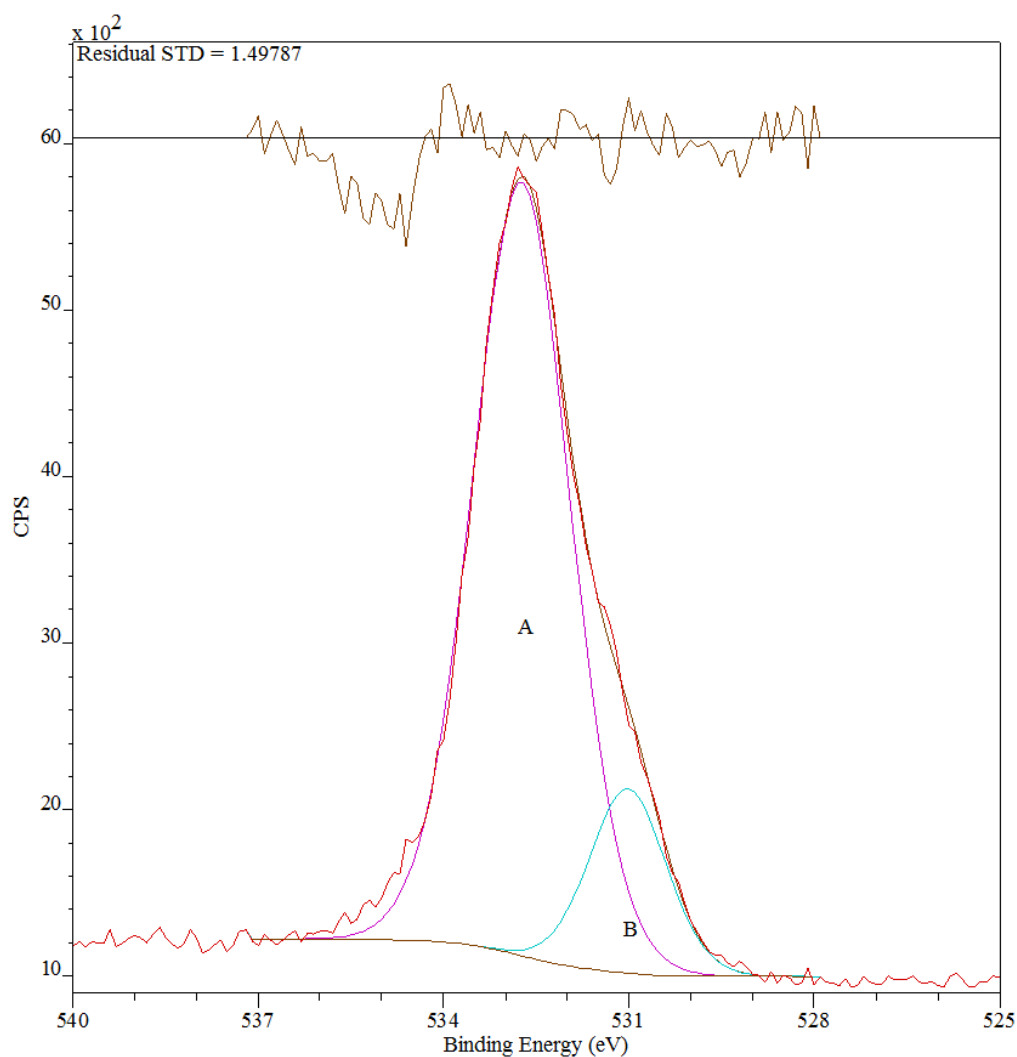


Figure 37 - High resolution O1s XPS spectrum (Oxygen peak) of FGO.

The high resolution O1s spectrum (Figure 37) shows that two oxygen peaks are present, and this indicates that the oxygen exists in at least two chemical states, with an 83.63% (Peak A):

16.37 % (Peak B) distribution of the two forms. The peak at 531.02 eV (Peak B) can possibly correspond to water or –OH functional groups. The –OH functional groups can potentially exist as carboxyl counter ion (Appendix G). If the peak corresponds to water, it can be remaining water in the sample after drying. The biggest peak at approximately 532.738 eV (Peak A) may correspond to the various oxygen groups in GO.

Table 4 shows the different peaks from the nitrogen, oxygen, and carbon spectrum with the distribution of the different peaks in atomic percentage, and binding energy for each peak.

Table 4 – The atomic percentage and the binding energy of the different components.

Component	Nitrogen		Oxygen		Carbon		
	A	B	A	B	A	B	C
Concentration (at. %)	70.44	29.56	84.18	15.82	49.52	40.18	10.31
Binding energy (eV)	399.305	400.822	532.738	531.02	284.714	286.584	288.479

The obtained survey spectra of the FGO (PPDA) sample indicated that functionalization of GO with PPDA had been successful. Increased carbon and nitrogen content enhances the probability of a successful functionalization. The functional groups present in the high resolution de-convoluted carbon, nitrogen, and oxygen spectrums showed binding energies that confirmed the content of amine and possible reactions with GO.

4.3 Effect of pH

When PPDA was added to a GO/distilled water solution, the colour of the solution changed from light brown to black/dark purple. A simple test was performed to find out if the change in colour was a pH effect, or a result of a possible reaction between GO and diamine. For this purpose NaOH (0.1 M) was added to the GO/water solution which resulted in a darker brown colour, (Figure 38), but the black/dark purple colour didn't appear. Additional drops of NaOH were added, until the pH reached 10, but the colour change was minimal. The same experiment was attempted with both concentrated dispersion and on a diluted dispersion without any effect.

Figure 38 shows the result of the pH adjustment with NaOH. The sample in the middle shows a darker colour compared to the sample without GO, while the diluted sample shows little change in colour.



Figure 38 – pH adjustment of GO with NaOH.

The same experiment was done with ammonia with a new sample of GO/water solution, resulting in the same. Nor did this have any effect on the colour at pH 10. These tests therefore indicated that the change in colour when PPDA is added to the GO/distilled water solution primarily is caused by a chemical reaction between the GO/distilled water solution and the PPDA. One hypothesis is that the amine reacts with the epoxy group on GO.

4.4 Zeta potential

A dispersion with GO functionalised with PPDA in distilled water was measured to check the stability of the FGO (PPDA) in distilled water at various pH. The zeta potential can give important information about how well dispersed particles are in a solution. The Zeta potential for a sample of FGO (PPDA) dispersed in distilled water is plotted as function of pH and is shown in Figure 39.

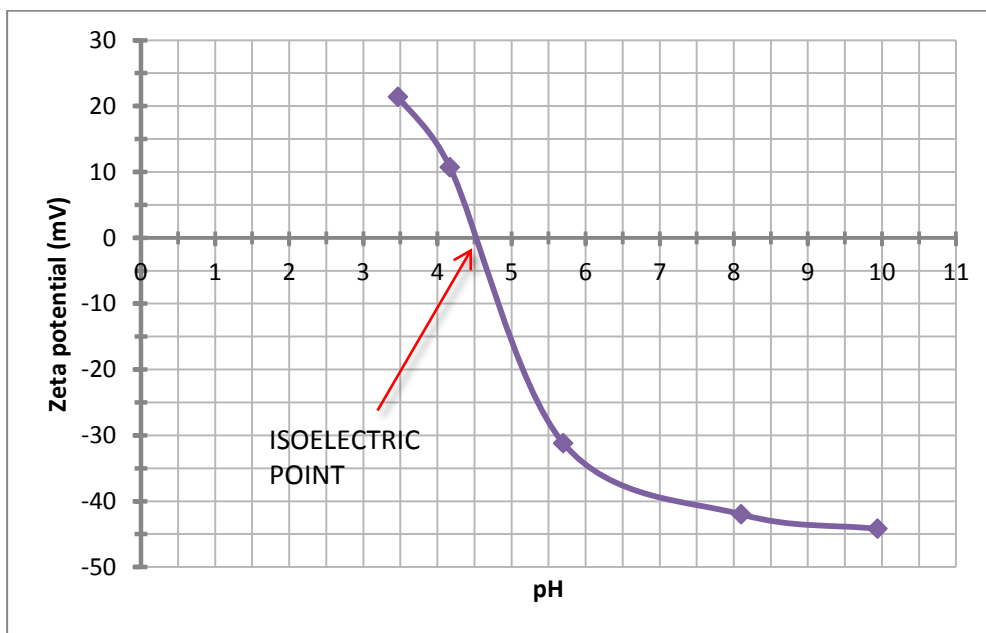


Figure 39 – Zeta potential with isoelectric point for the FGO (PPDA)/distilled water solution.

The isoelectric point was found to be located at pH 4.5 (Figure 39). As can be seen from the figure the Zeta potential became negative at increased pH. The negative Zeta potential will indicate that the FGO(PPDA) particles in the solution will be more stable. The likelihood of the particles to form agglomerates is lower at a negative zeta potential because particles with negative charge will repel each other, and it is therefore a desire to have a pH giving a negative Zeta Potential. The pH was measured by a pH meter every time ammonia was added, but the measurement can give some inaccuracy because of the low buffer capacity of distilled water. pH was measured every now and then and it seemed to be around pH 6-7 in the PPDA/distilled water dispersions used during the thesis, which indicated that no pH adjustment should be necessary to have a stable dispersion. The print-outs of the results from the analysis of the Zeta Potential can be studied in Appendix D.

4.5 Surface tension and interfacial tension

The surface and interfacial tensions were measured to see if surface active groups were present in the epoxy resin, after an epoxy/distilled water test was performed. Surface active groups can potentially give a certain stabilization effect of water in epoxy. If an emulsion with water and epoxy was formed it could maybe be difficult to remove this if surface and active groups were present. A measurement of the surface and interfacial tension could give an indication if surface active groups were present at the epoxy.

The surface tension of epoxy in air is presented as a graph in Figure 40.

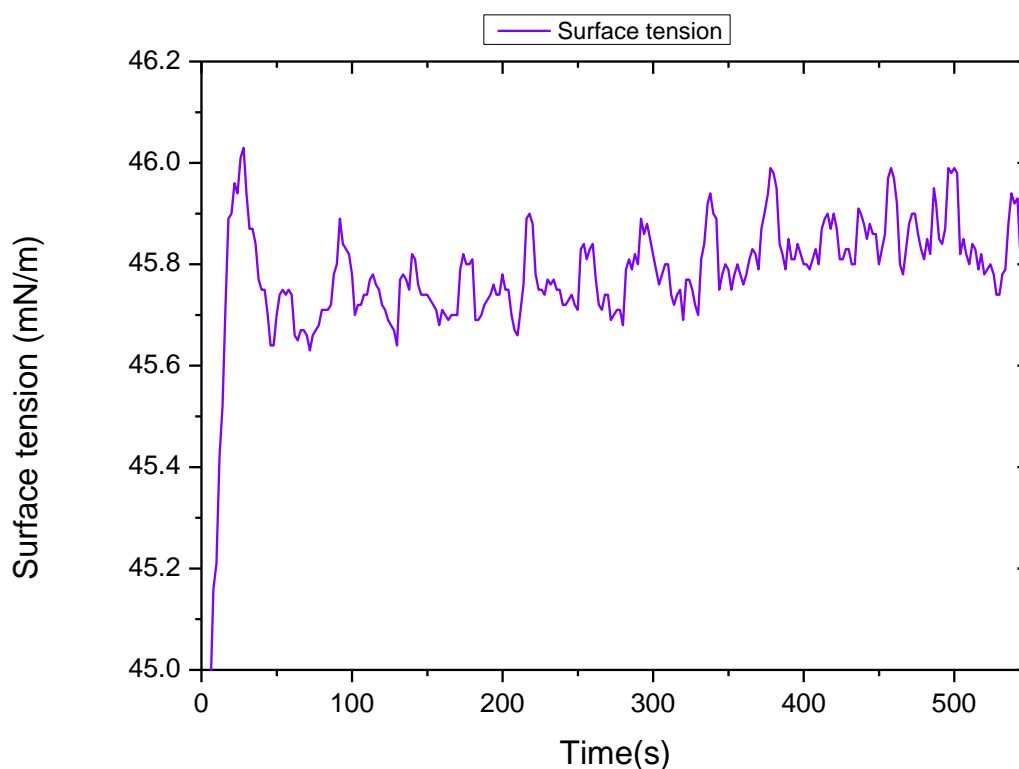


Figure 40 – Surface tension of epoxy in air.

Figure 41 shows the result of the measurement of the interfacial tension of epoxy in water.

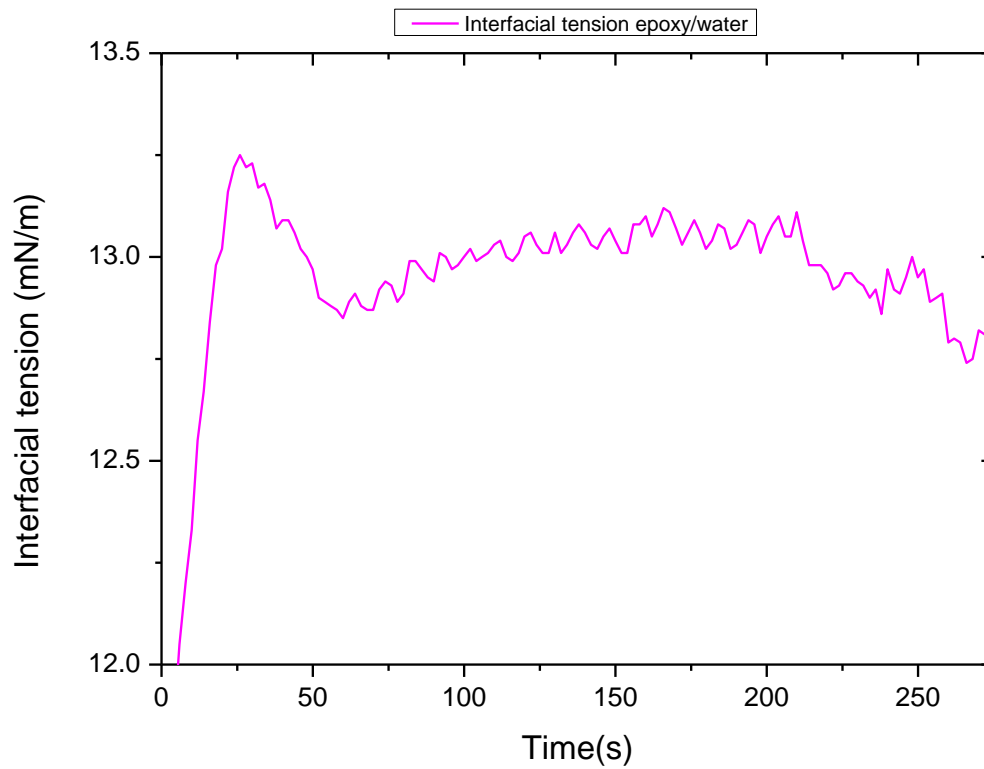


Figure 41- Interfacial tension of epoxy in water.

The surface tension of epoxy in air was found to be 46 mN/m, while the interfacial tension of epoxy in water was 13 mN/m. These results were in accordance with literature for other similar components at 20 °C (Appendix F, Figure F 1 and Figure F 2). The interfacial tension of 13 mN/m is in the border line, meaning that surface active groups could be present. A stable water/epoxy emulsion is undesirable, because it can make complete water removal difficult. The results (Figure 40 and Figure 41) show that the water epoxy emulsion would probably not be very stable.

4.6 Optical microscope

The structure and dispersion of as prepared GO, EXGO and FGO in acetone or distilled water was regularly observed by a conventional optical microscope. Pictures were captured to show the visual difference between the various dispersions, to see if the GO particles were homogenously dispersed, and to see if all solvent were removed.

4.6.1 GO in acetone

Figure 42 shows optical micrographs of as-prepared GO dispersed in acetone.

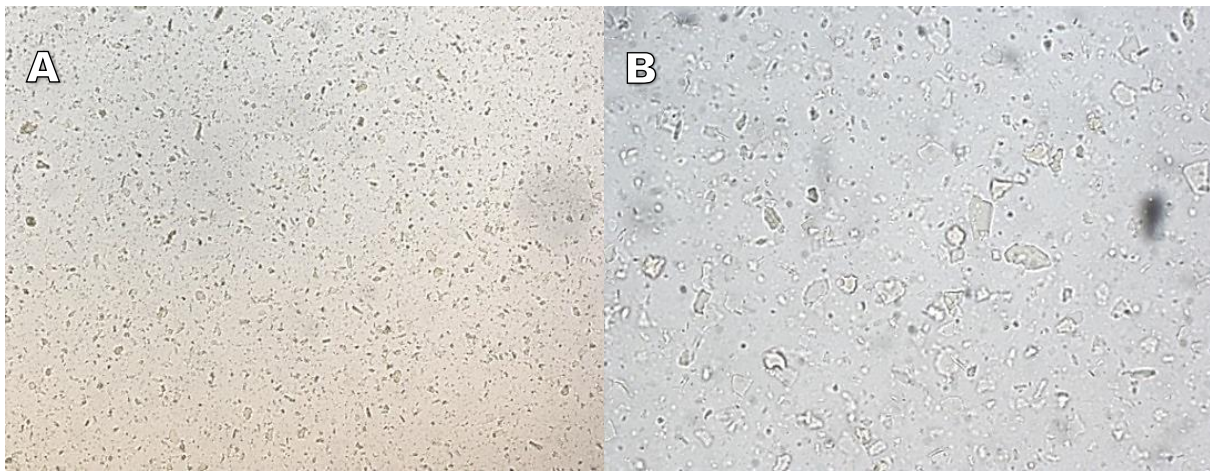


Figure 42- As prepared GO dispersed in acetone, A: 10 X magnification, B: 40 X magnification.

The pictures (Figure 42) show almost transparent GO flakes which remind of ice flakes or crushed glass. The GO flakes vary in size but are quite evenly distributed in the acetone. The different colours of the pictures may be caused by different light and microscope settings, or various elements of nanoparticles that is not possible to see with the optical microscope.

4.6.2 Epoxy with FGO (XB3473) in distilled water

Optical micrographs of epoxy with FGO (XB3473) in distilled water are shown in Figure 43. The pictures show remaining water bubbles and flocculated FGO particles.

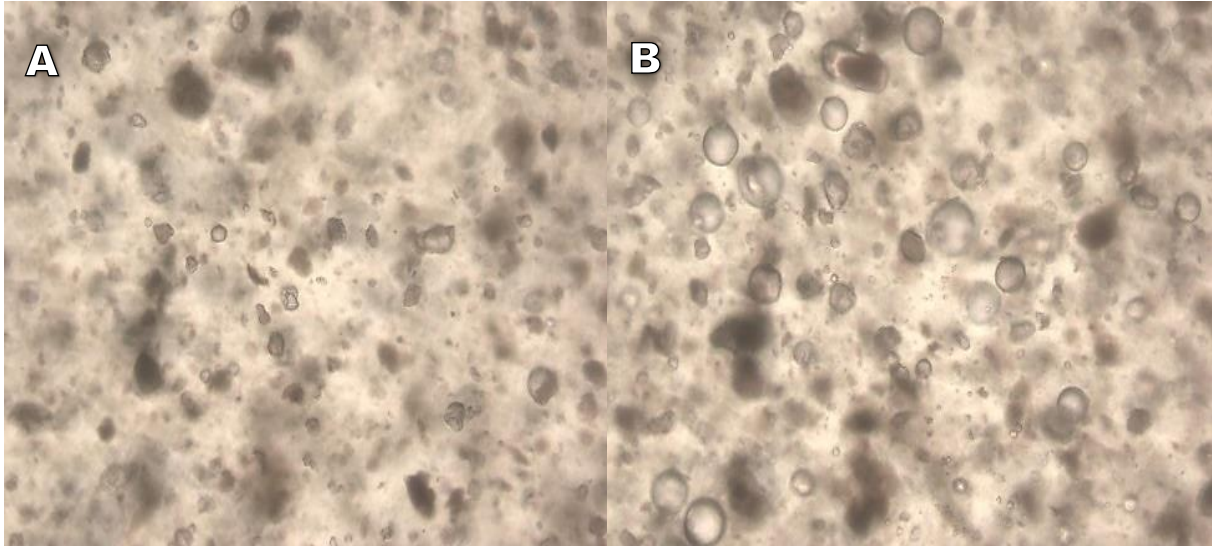


Figure 43 – Epoxy with FGO (XB3473) in distilled water, A: 10 X magnification, B: 40 X magnification.

Figure 44 shows optical micrographs of epoxy with FGO (XB3473) in distilled water before removing all water in the epoxy sample. The pictures show that distinct water bubbles are still left in the epoxy.

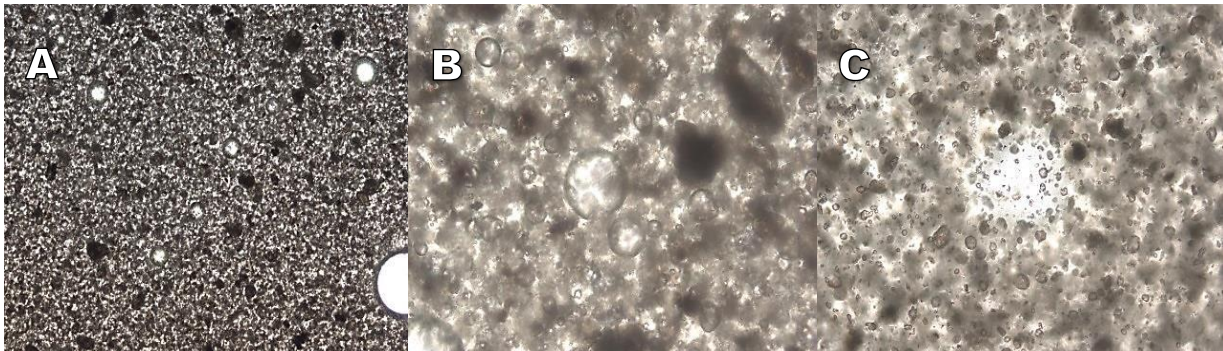


Figure 44 – Epoxy with FGO (XB3473) in distilled water, remaining water bubbles are shown in the pictures, A: 10 X magnification, B: 40 X magnification, C: 40 X magnification.

Optical micrographs of epoxy with FGO (XB3473) after curing are shown in Figure 45. The pictures show a non-homogenous distribution with flocculated FGO.

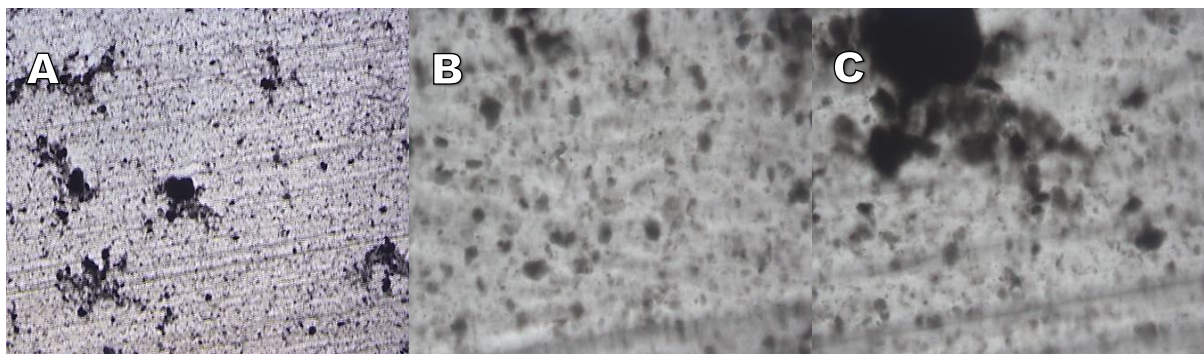


Figure 45 –Epoxy with FGO (XB3473) after removal of distilled water and curing with hardener. This thin flake is remaining parts in the metal moulds. A: 10 X magnification, B: 40 X magnification, C: 40 X magnification.

4.6.3 Epoxy with FGO (PPDA) in acetone

Figure 46 show FGO (PPDA) dispersed in acetone before addition of epoxy. The pictures show that the GO particles are flocculated in the acetone.

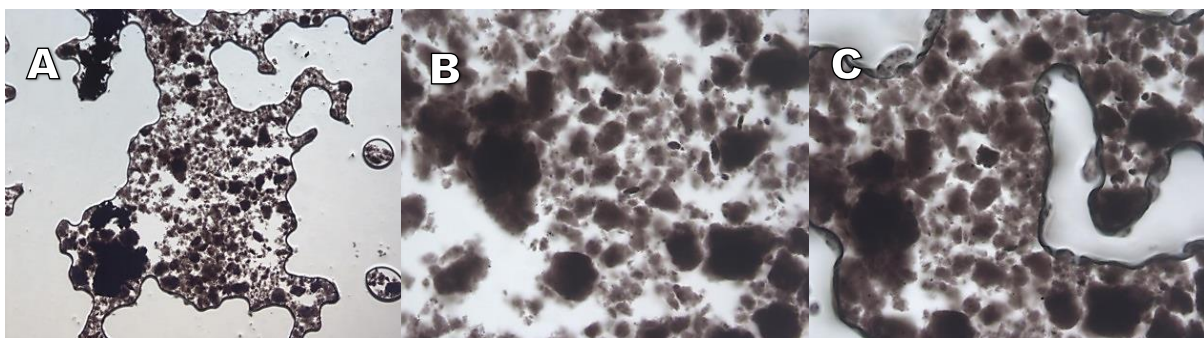


Figure 46 – FGO (PPDA) dispersed in acetone, A: 10 X magnification, B: 40 X magnification, C: 40 X magnification.

Optical micrographs of FGO (PPDA) dispersed in acetone after addition of epoxy and removing acetone are presented in Figure 47. The pictures show well mixed and evenly distributed FGO (PPDA) in the epoxy, but some of the FGO is flocculated and the distribution is thus not homogenous. All acetone and air bubbles are removed.

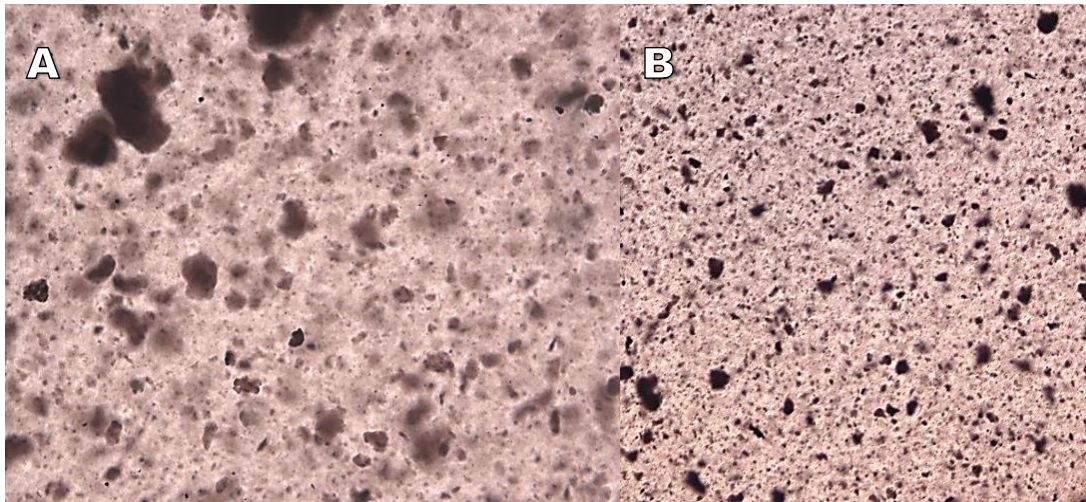


Figure 47 – FGO (PPDA)/acetone after addition of epoxy. A: 40 X magnification, B 10 X magnification.

4.6.4 EXGO (1000 °C) in distilled water and SDS

Figure 48 shows optical micrographs of EXGO (1000 °C) dispersed in distilled water with SDS. The EXGO is varying in size and contains flake like particles that are transparent and consist of several layers.

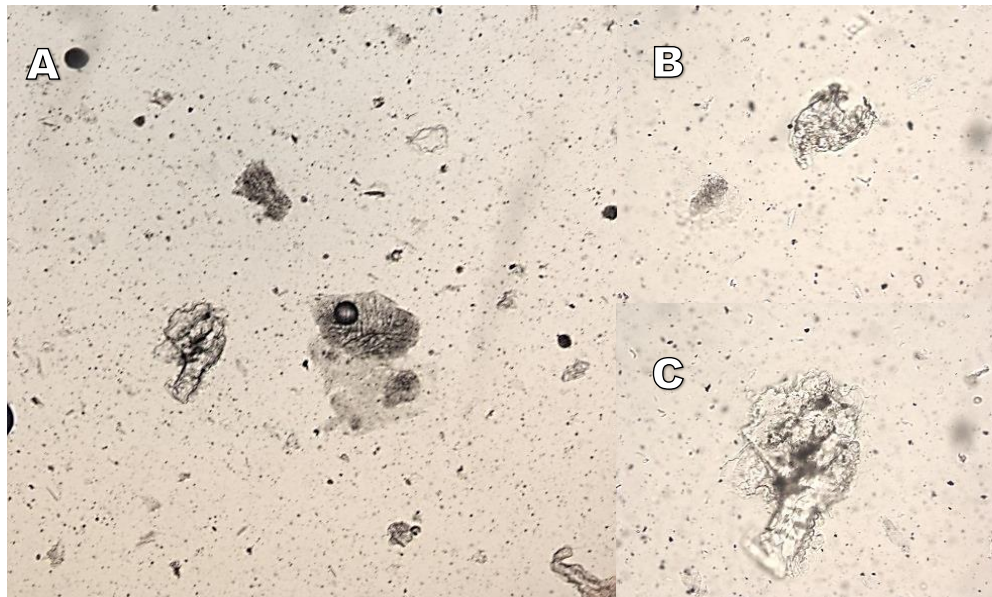


Figure 48 - EXGO (1000 °C) in distilled water and SDS epoxy. A: 10 X magnification, B: 40 X magnification, C: 40 X magnification.

4.6.5 EXGO (300 °C) in acetone

EXGO (300 °C) dispersed in acetone before addition of epoxy resin is shown as optical micrographs in Figure 49. These EXGO particles are more opaque than the EXGO (1000 °C). The EXGO are gathered in clusters or flocculates and are not evenly distributed.

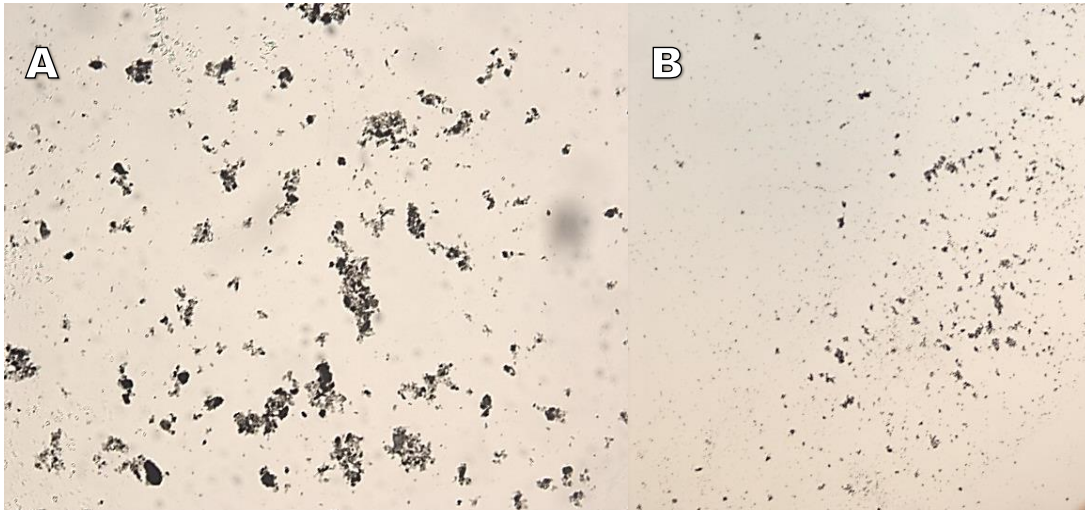


Figure 49 - EXGO (300 °C) in acetone (before addition of epoxy). A: 40 X magnification, B: 10 X magnification.

4.6.6 FGO (PPDA) in distilled water (XB3473/LY556)

GO dispersed in water and later functionalization with PPDA is presented in the following pictures to show the progress and appearance of the FGO (PPDA) during the preparation process. GO in distilled water after 2 hours of treatment in ultrasonic horn and addition of PPDA is presented in Figure 50. The pictures show that the GO particles are fluffy, opaque, and aggregated.

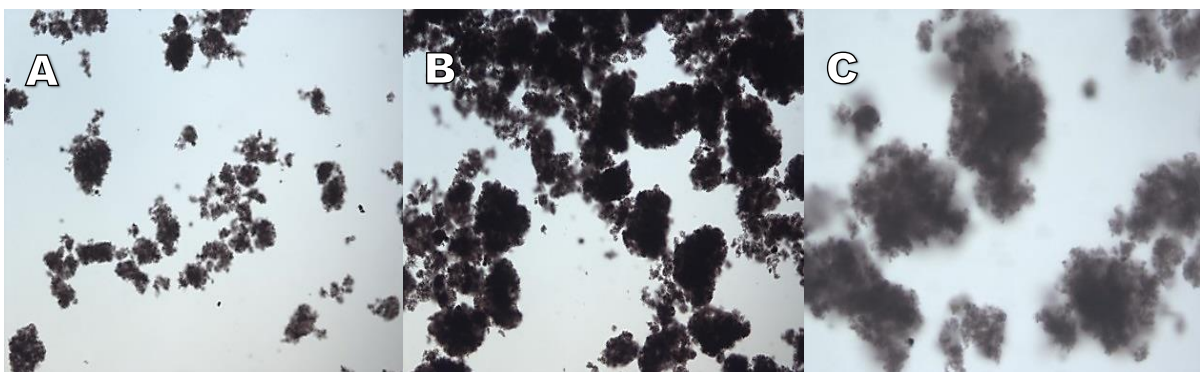


Figure 50 - G.O. and amine before washing, A: 10X magnification, 10 X magnifications, and 40 X magnification.

FGO and amine dispersed in distilled water after several washing steps are presented as optical micrographs in Figure 51. The pictures indicate that some of the aggregated particles have loosened.

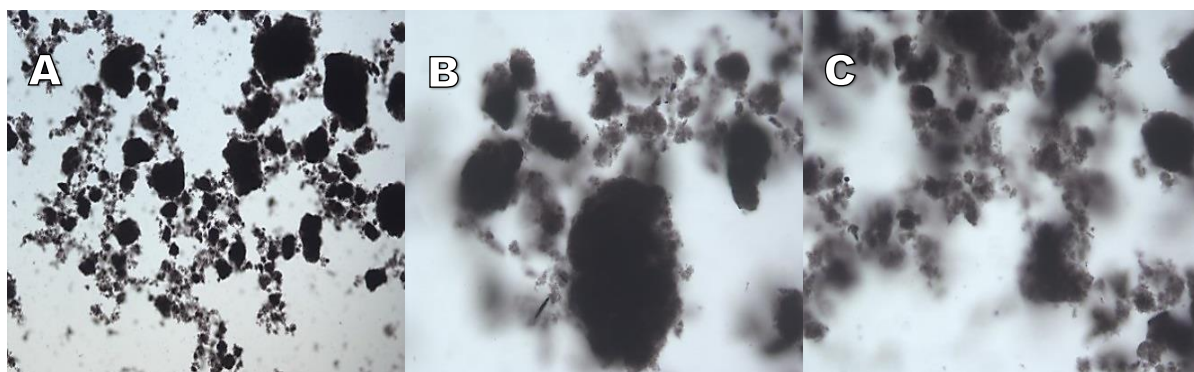


Figure 51 – FGO (PPDA) after washing, A: 10 X magnification, B: 40 X magnification, C: 10 X magnification

Optical micrographs of FGO dispersed in distilled water after several washing steps and one hour of treatment with ultrasonic horn are revealed in Figure 52. The pictures show that the particles are even fluffier, and seem less opaque.

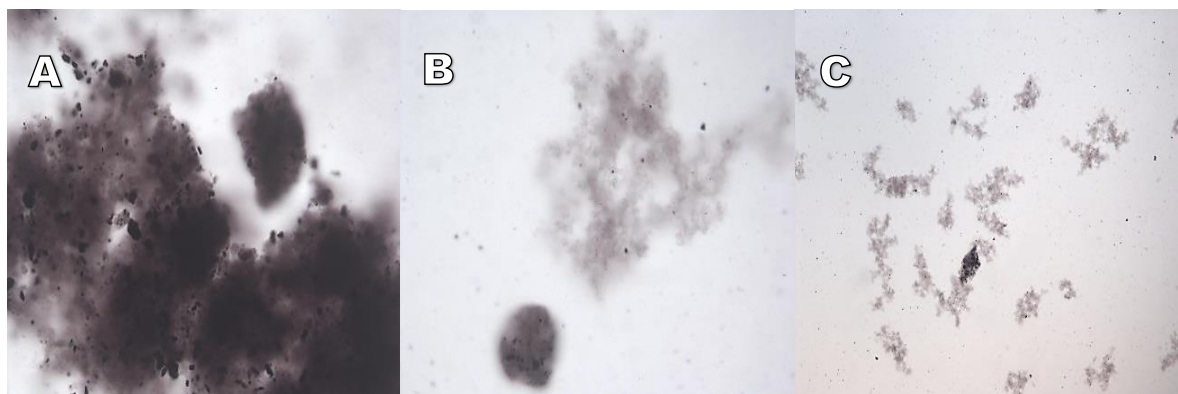


Figure 52 – FGO (PPDA) after washing and 1 hour UL horn, A: 40 X magnification, B: 40 X magnification, C: 10 X magnification.

Figure 53 illustrates FGO (PPDA) after washing and 1.5 hour treatment in ultrasonic horn. The size and shape of the particles vary. Some of the particles are transparent, while some are small and black.



Figure 53- FGO (PPDA) in distilled water after washing and 1.5 hour UL horn, A: 10 X magnification, 40 X magnification, 40 X magnification.

Figure 54 shows optical micrographs of FGO (PPDA) in epoxy with remaining water bubbles. The light circle in picture A shows a big water bubble.

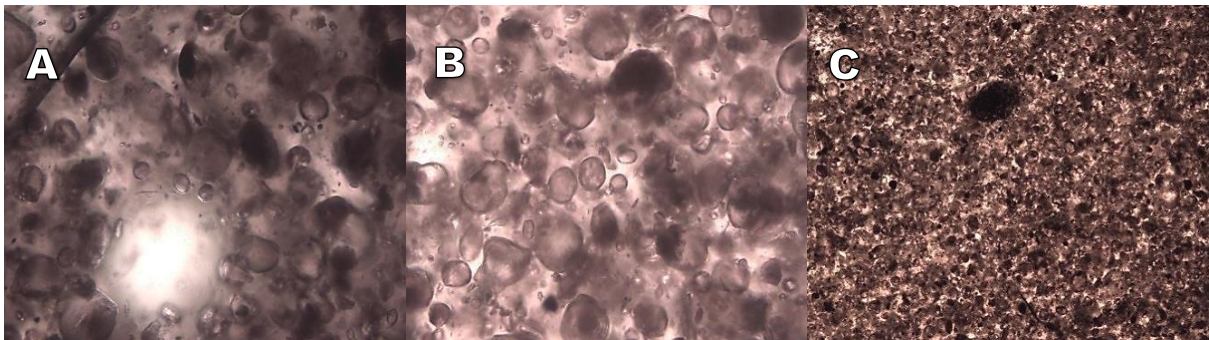


Figure 54 - Addition of epoxy, FGO (PPDA), A: 40 X magnification, B: 40 X magnification, 10 X magnification.

Epoxy and FGO (PPDA) after additional 60 °C in vacuum oven overnight are shown in Figure 55. Water bubbles are still left in the epoxy mix.

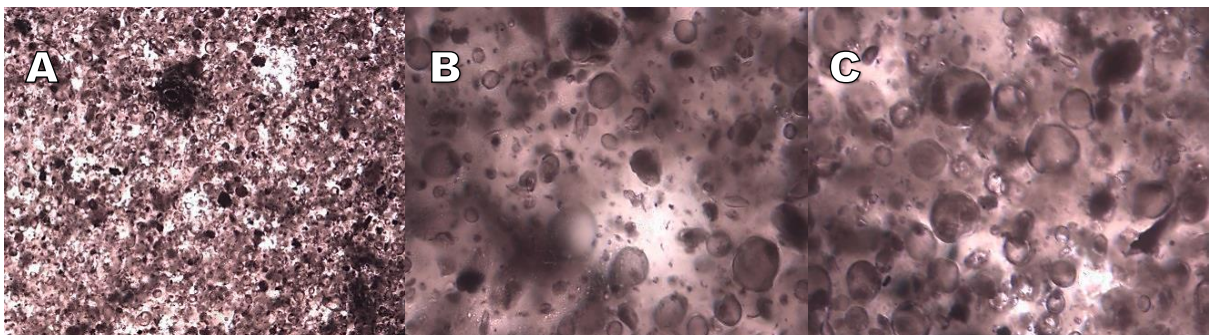


Figure 55 – Epoxy and FGO (PPDA) after 60 °C in vacuum oven, A: 10 X magnification, B: 40 X magnification, C: 40 X magnification.

Optical micrographs of epoxy with FGO (PPDA) after additional 70 °C in vacuum are presented in Figure 56. All residual water is removed.

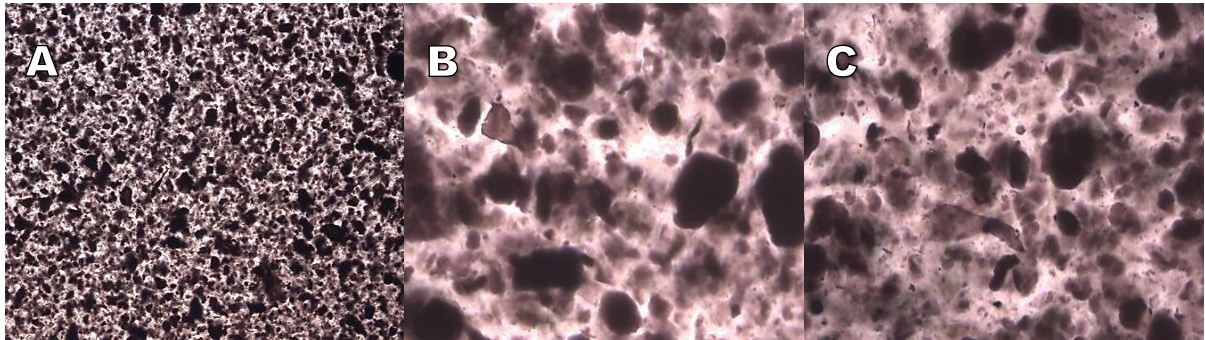


Figure 56 - Epoxy, FGO (PPDA) before addition of hardener. A: 10 X magnification, B: 40 X magnification, C: 40 X magnification.

Figure 57 shows optical micrographs of epoxy with FGO (PPDA) after 5 min treatment with ultrasonic horn, before addition of hardener. The distribution of particles is quite good, but aggregated FGO (PPDA) still makes the dispersion inhomogeneous.

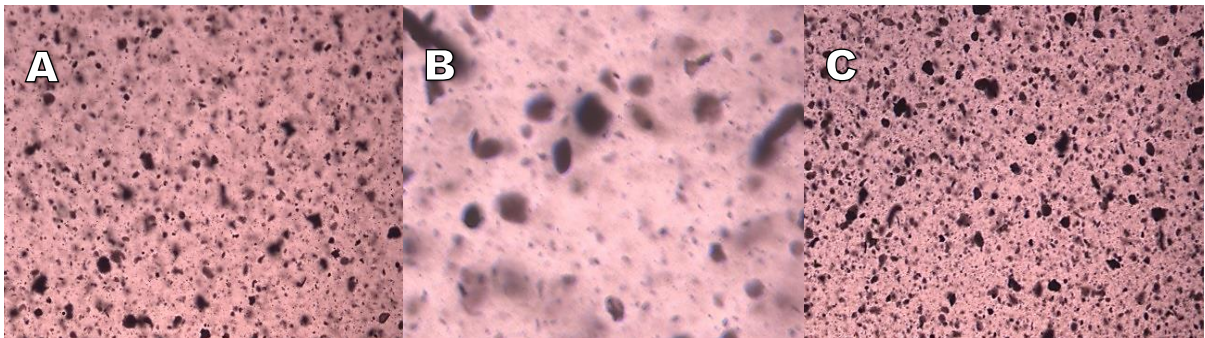


Figure 57 - Epoxy, FGO (PPDA) after additional 5 min UL horn, before addition of hardener. A: 10 X magnification, B: 40 X magnification, C: 10 X magnification.

4.6.7 FGO (PPDA) in distilled water (IPDA/LY556)

GO dispersed in water and later functionalization with PPDA is presented in the following pictures to show the progress and look of the FGO during the preparation process. Optical micrographs of GO in distilled water after 2 hours of treatment in ultrasonic horn before addition of PPDA are presented by Figure 58.

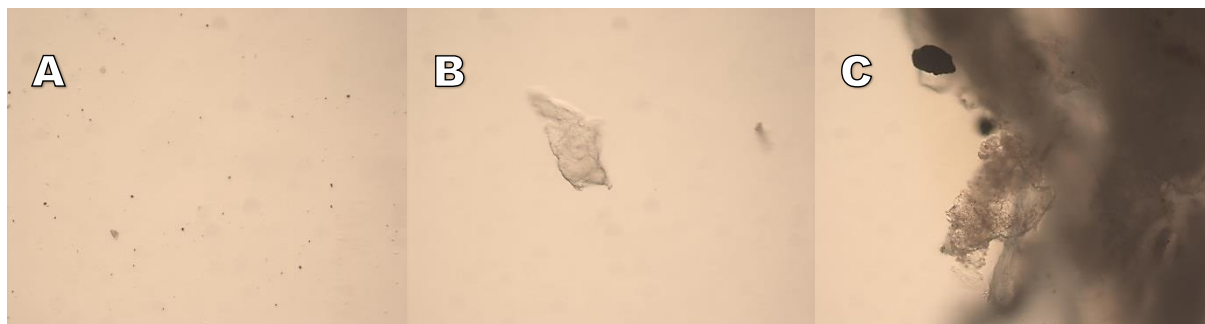


Figure 58 – GO in distilled water after 2 hours of treatment in ultrasonic horn. A: 10 X magnification, B: 40 X magnification, C: 40 X magnification different area.

Figure 59 show the FGO, which is GO that has been functionalised with PPDA.

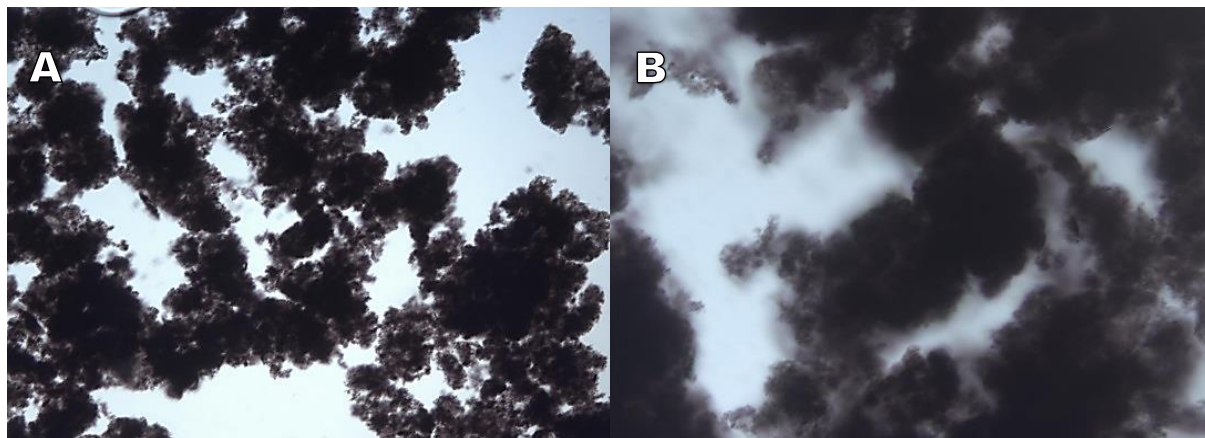


Figure 59 – FGO, GO in distilled water after functionalization with PPDA. A: 10 X magnification, B: 40 X magnification.

FGO (PPDA) after going through several washing steps is shown as optical micrographs in Figure 60.

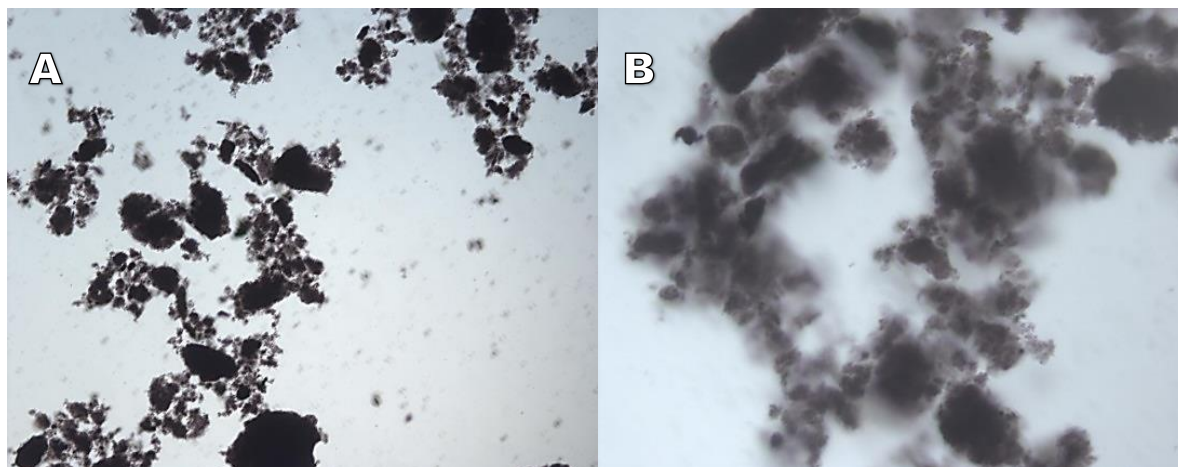


Figure 60 - FGO (PPDA) after washing steps. A: 10 X magnification, B: 40 X magnification.

Optical micrographs of FGO (PPDA) after standing for several weeks are presented in Figure 61. The pictures show that the GO particles are agglomerated and vary in size and shape.

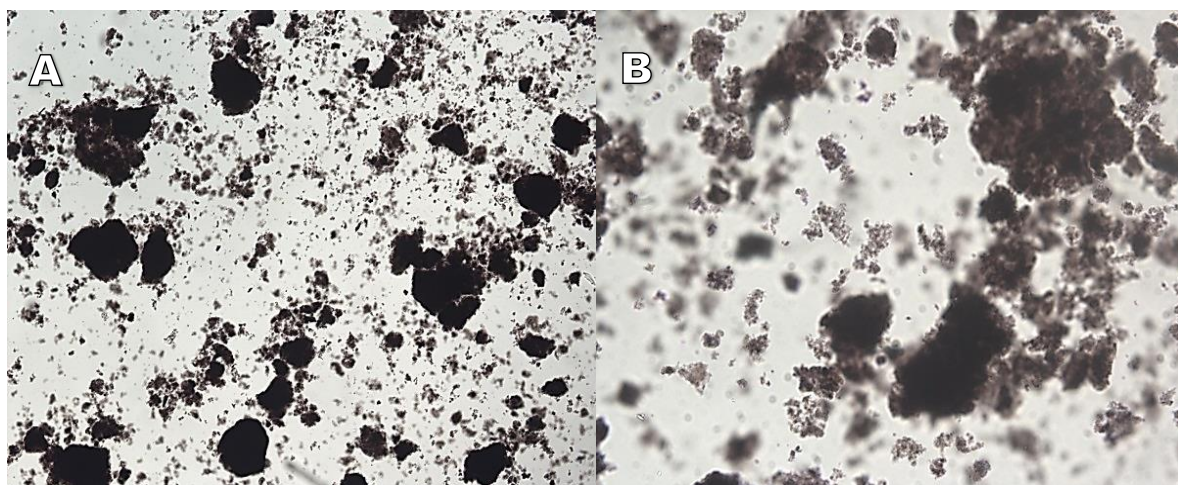


Figure 61 – FGO (PPDA) after standing still for several weeks. A: 10 X magnification, B: 40 X magnification.

FGO (PPDA) dispersed in distilled water after additional 5 minutes of treatment with ultrasonic horn are displayed in Figure 62. The pictures show that many of the agglomerates have disappeared. The ultrasonic treatment obviously have separated the agglomerated FGO particles, and the pictures show more evenly distributed particles.

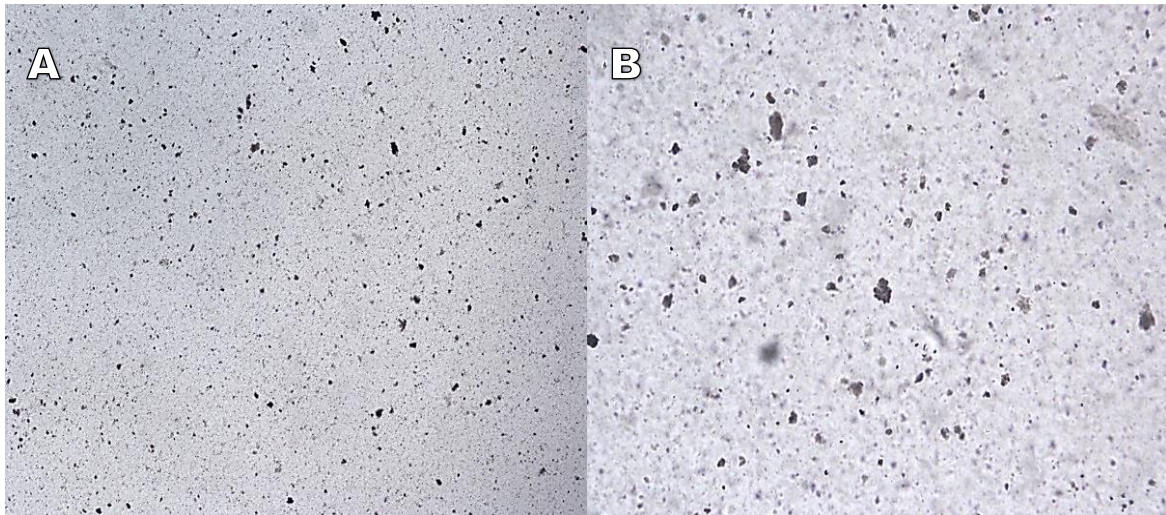


Figure 62 – FGO (PPDA) after 5 min UL horn, A: 10X magnification, B: 40 X magnification

Additional 5 minutes of treatment with ultrasonic horn of FGO (PPDA) in distilled water are presented as optical micrographs in Figure 63. The pictures show little change from the pictures in Figure 62. However, some aggregates are present in the pictures in Figure 63 and other particles seem less opaque.

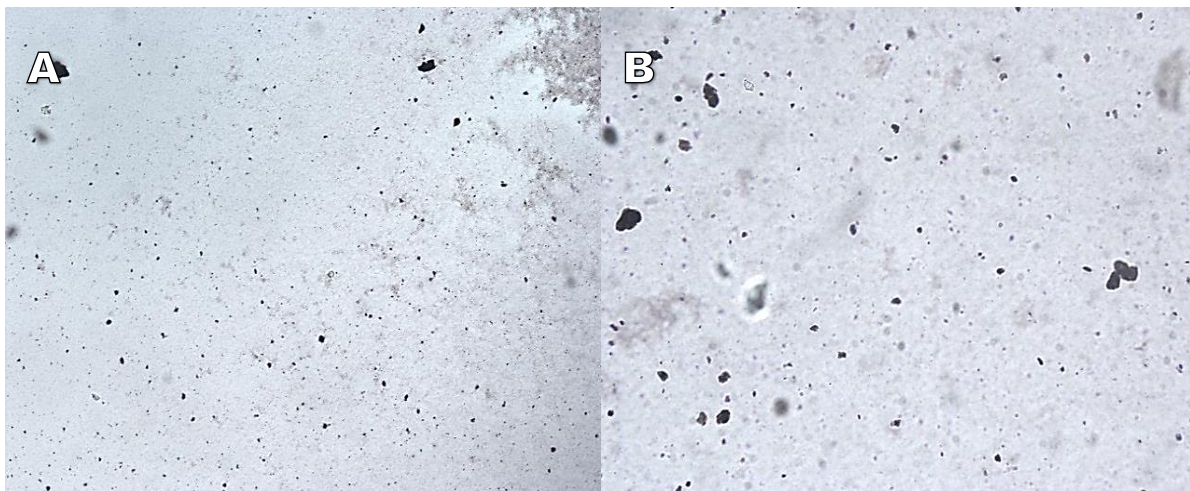


Figure 63 - FGO (PPDA) after 2 x 5 min UL horn, A: 10 X magnification, B: 40 X magnification.

FGO (PPDA) after dispersion in epoxy and removal of water with rotavapor and vacuum oven are showed as optical micrographs in Figure 64. Remaining water can be seen as white bubbles or circles.

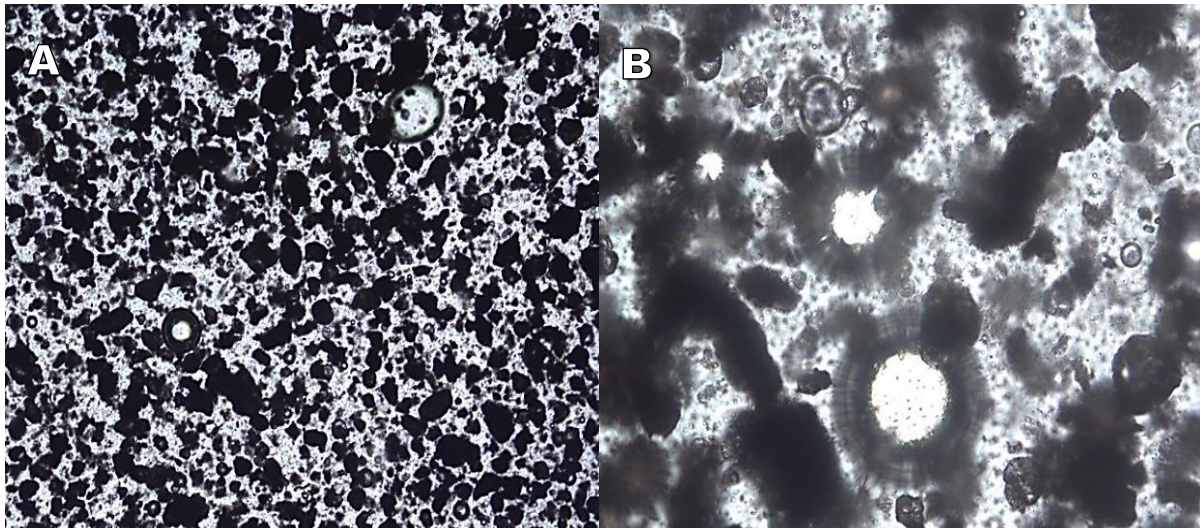


Figure 64 – FGO (PPDA) in epoxy, visible water bubbles left, A: 10 X magnification, B: 40 X magnification.

Figure 65 show optical micrographs of FGO (PPDA) in epoxy after additional heat and vacuum. No remaining water is visible in the sample.

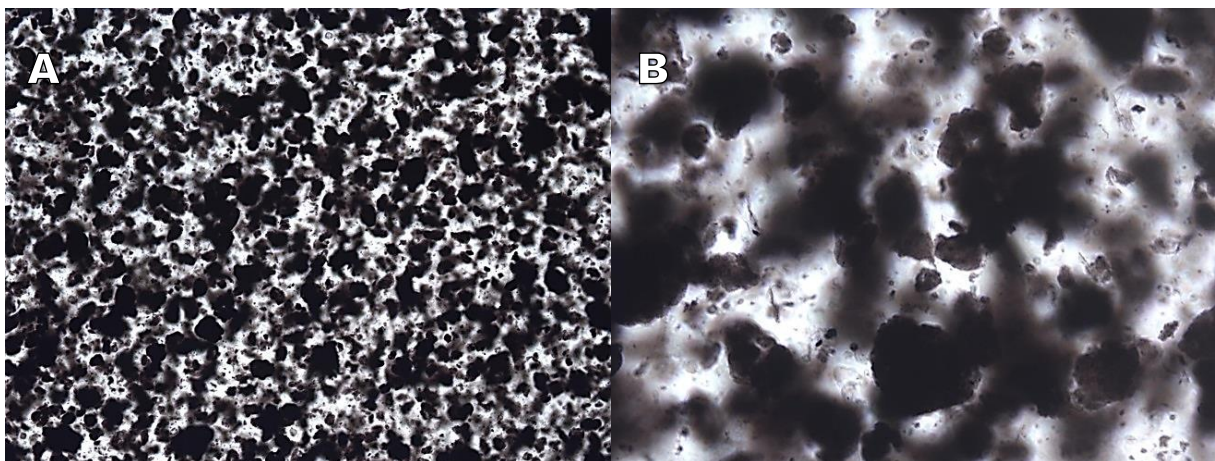


Figure 65 – FGO (PPDA) in epoxy, water bubbles removed, A: 10 X magnification, B: 40 X magnification.

After removing all of remaining water, the epoxy/FGO (PPDA) blend was exposed to additional 5 minutes of ultrasonic horn treatment to secure a properly mixing of FGO in the epoxy. The result was studied in the optical microscope, and pictures of the result can be studied in Figure 66.

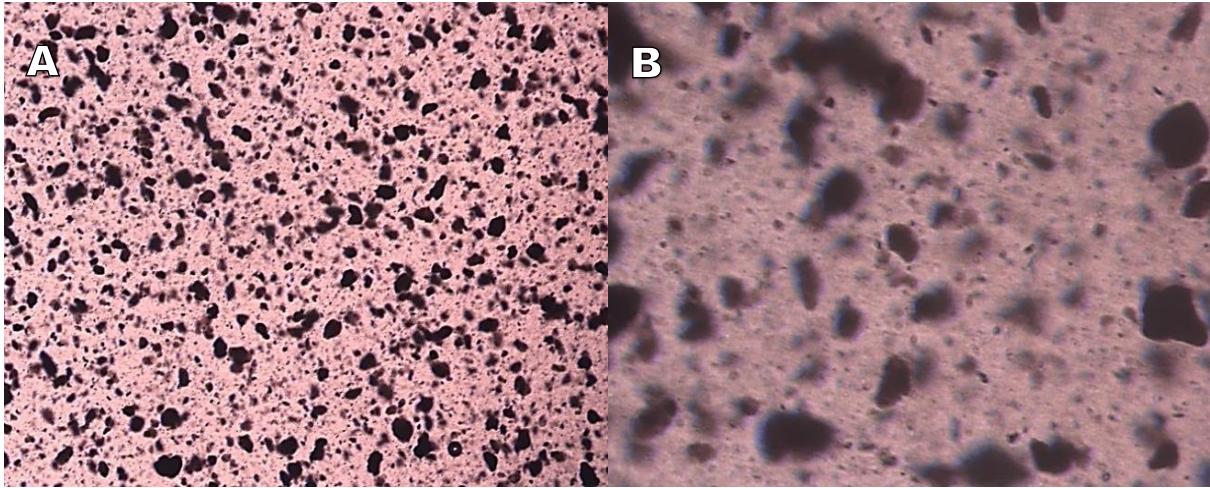


Figure 66 – FGO (PPDA) in epoxy, after 5 min UL horn, A: 10 X magnification, B: 40 X magnification.

Remaining composite in the metal mould after curing was inspected in the optical microscope, and the result can be studied in the optical micrographs that are presented in Figure 67. The pictures show clusters or agglomerates of FGO (PPDA) particles, which give a non-homogenous epoxy.

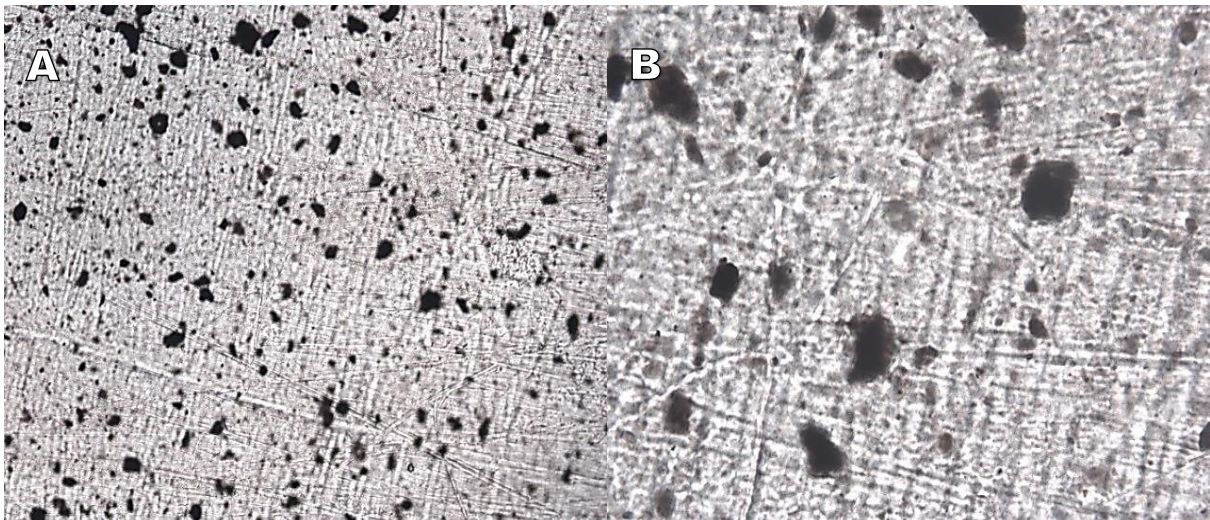


Figure 67 – FGO (PPDA) in epoxy and hardener after curing, A: 10 X magnification, B: 40 X magnification, sample of remaining composite in curing moulds.

4.7 Dynamic mechanical analysis and three-point flexural bending test

All the different composites and neat epoxy were tested for mechanical properties by DMA and three-point flexural bending test to compare their mechanical properties, and to investigate the effect of the addition of GO, EXGO or FGO when added to the composite.

An example of a typical curve from the DMA analyses is presented in Figure 68. The rest of the curves obtained during the DMA analysis are attached in Appendix A. The green line represents the storage modulus, the blue line is the loss modulus, and the red line is the Tan delta function. T_g was found from the peak of the loss modulus, while the value of the storage modulus was found at 35 °C. A temperature of 35 °C was used to be able to compare the results of the various composites.

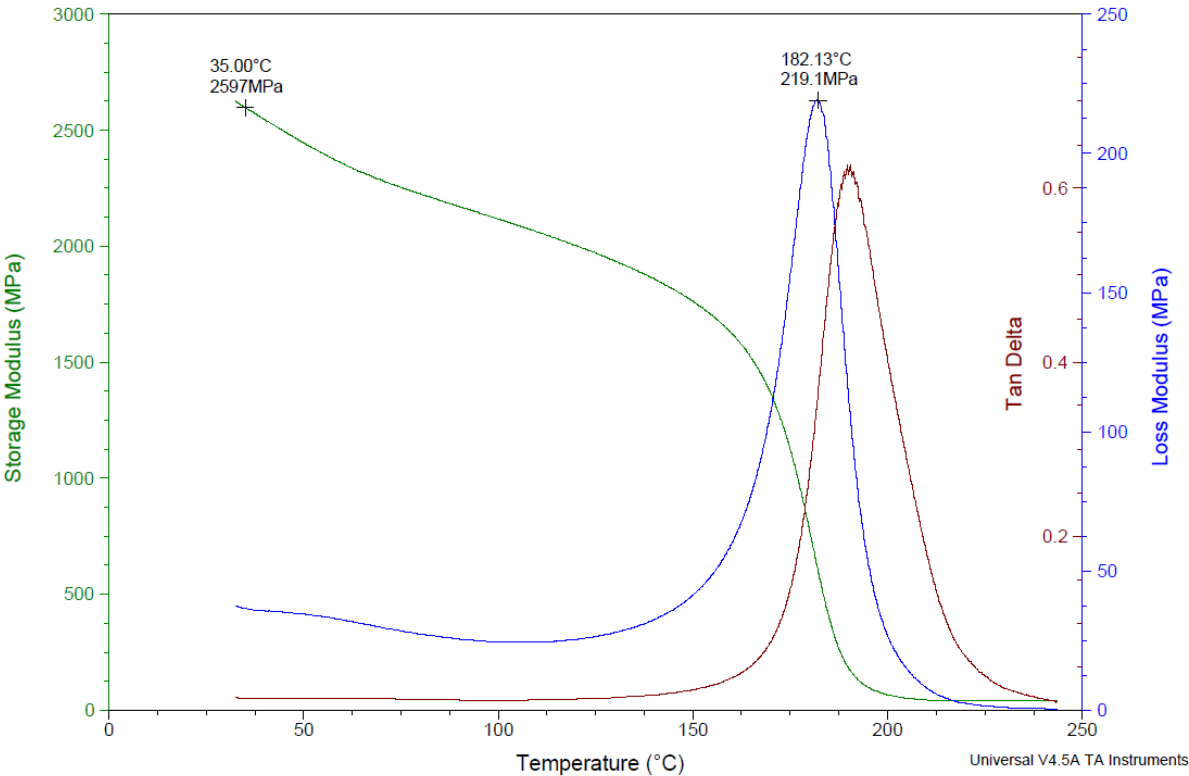


Figure 68 – Typical DMA curve obtained from testing of the neat epoxy polymer analysed by DMA. T_g is marked on the peak of the loss modulus, and the storage modulus is found at 35 °C.

An example of a typical curve obtained in three-point flexural bending test is presented in Figure 69. The rest of the curves obtained by the three-point flexural bending tests are attached in Appendix B. Flexural modulus (E_f), flexural strength (σ_{fM}), and flexural strain (ϵ_{fB}) are marked in the figure.

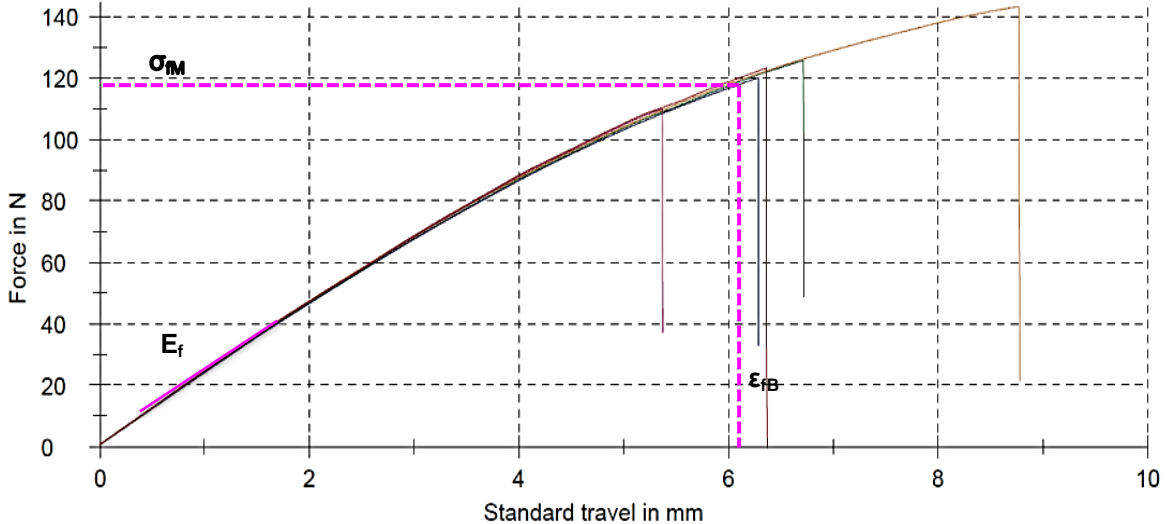


Figure 69- An example of a curve of five specimens obtained from the three-point flexural bending test. E_f , σ_{fM} , and ϵ_{fB} are marked in the figure.

The results from the DMA and three-point flexural bending test are summarized and presented in Table 5 with standard deviations.

Table 5 – Results from DMA and three-point bending test with standard deviations.

Sample	E _f (MPa) (Flexural modulus)	σ _{fM} (MPa) (Flexural strength)	ε _{fB} (%) (Flexural strain)	E' (MPa) (Storage modulus) at 35 °C	T _g (°C)
LY556/XB3473 reference standard 1 *	2520 ± 26	128 ± 8	7.5 ± 1.6	2717 ± 20	161.7 ± 3.2
LY556/XB3473 reference standard 2	2460 ± 56	101 ± 9	5.3 ± 1.0	2524 ± 71	182.0 ± 0.3
LY556/XB3473 dH ₂ O blank	2387 ± 44	116 ± 6	6.5 ± 0.7	2567 ± 28	172.8 ± 0.6
LY556/XB3473 acetone blank	2310 ± 40	102 ± 15	5.6 ± 1.6	2624 ± 46	172.8 ± 1.2
LY556/XB3473 acetone GO	2444 ± 58	89 ± 18	4.3 ± 1.2	2731 ± 69	167.2 ± 1.0
LY556/XB3473 acetone EXGO (300°C)	2091 ± 47	76 ± 8	4.0 ± 0.6	2579 ± 33	179.1 ± 0.1
LY556/XB3473 acetone FGO (PPDA)	2282 ± 18	114 ± 6	6.9 ± 1.2	2625 ± 59	159.2 ± 1.3
LY556/XB3473 dH ₂ O EXGO(1000°C) + SDS	2018 ± 45	45 ± 5	2.3 ± 0.3	2498 ± 48	182.5 ± 1.0
LY556/XB3473 FGO (XB3473) dH ₂ O	2336 ± 42	90 ± 10	4.3 ± 0.7	2594 ± 25	179.1 ± 0.1
LY556/XB3473 FGO (PPDA) dH ₂ O	1672 ± 14	79 ± 16	5.7 ± 1.6	2539 ± 11	172.9 ± 4.2
LY556/IPDA reference standard 1 **	2212 ± 36	95 ± 19	5.0 ± 2.0	3266 ± 23	102.2 ± 0.3
LY556/IPDA reference standard 2	2670 ± 75	88 ± 26	3.6 ± 1.3	2771 ± 21	151.5 ± 0.3
LY556/IPDA FGO (PPDA) dH ₂ O	2740 ± 45	90 ± 35	5.0 ± 3.8	2709 ± 67	130.2 ± 0.3

*This reference standard is wrong and not included in the further results.

** This reference standard went through a different curing cycle and temperature compared to standard 2.

The LY556/IPDA reference standard 1 have a different curing cycle than the LY556/IPDA reference standard 2 and the composite LY556/IPDA with FGO (PPDA), and is just included to show how the different mechanical properties are affected by a different curing cycles. The LY556/IPDA standard and composite with FGO (PPDA) cannot be directly compared with the LY556/XB3473 because of the different hardener and different curing cycle, but they are still included in the same graph to be able to compare all the variations that has been done during the experimental work.

All the results from DMA and three-point bending tests(

Table 5) are plotted as column charts with error bars representing the standard deviation for each series in Figure 70 - Figure 74.

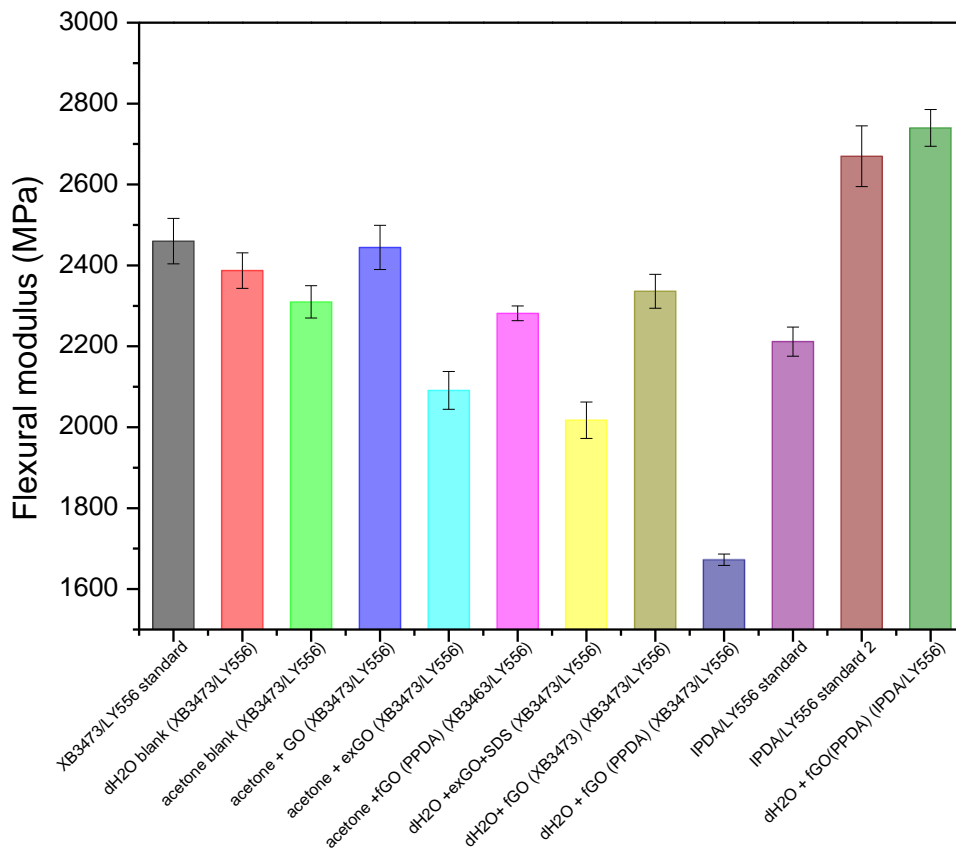


Figure 70 - Flexural modulus. The standard deviation is presented by error bars. dH2O corresponds to distilled water.

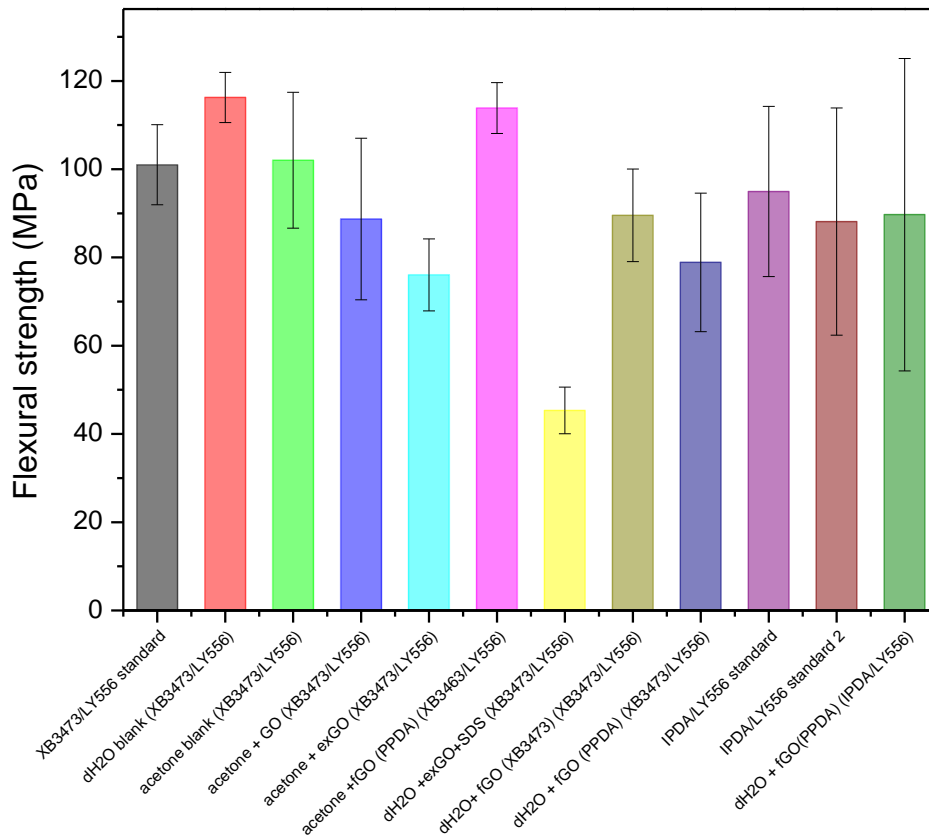


Figure 71- Flexural strength. The standard deviation is presented by error bars. dH2O corresponds to distilled water.

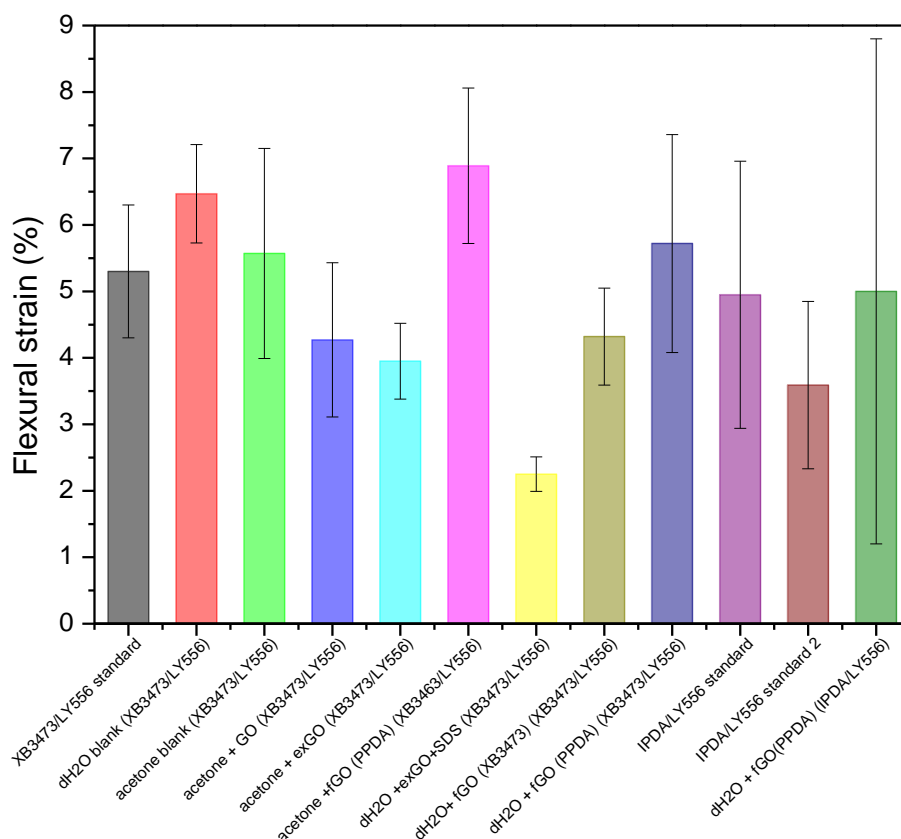


Figure 72 - Flexural strain. The standard deviation is presented by error bars. dH2O corresponds to distilled water.

The graph of the flexural strain (Figure 72) represents the mean value of the maximum strain, which is the value where a sample breaks. The graph of the flexural strength (Figure 71) represents the highest stress value and gives the strength of the material. These two graphs show high standard deviations between the specimens in the different sample series. The graph representing the flexural modulus (Figure 70) shows rather low standard deviations. The flexural modulus is measured in the linear area of the curve. As can be seen from the attached original plot results (Appendix B), most of the specimens in each series are similar in the linear area, but the specimen varies outwards in the graph. The flexural strain and the flexural strength curves show that the specimen break at different point on the graph and this makes the standard deviation high.

For some reason, the distance between the support spans was too large during some of the three-point flexural tests. This was registered after a while of testing, and corrected. Unfortunately, the specimens that were already tested got too low values, especially the flexural modulus. For example, the epoxy/IPDA reference standard 2 showed a value of approximately 1990 MPa when the distance was too long (50.7mm) instead of 48 mm which was set as a parameter in the data programme. A test was performed where the distance between the support spans were decreased to 45.6 mm and the flexural modulus became 3038 MPa. The real value when the support spans had the correct distance, however, showed a flexural modulus of approximately 2700 MPa. These values show that small variation in distance between the support spans gives errors in the measurements of the flexural modulus. Regrettably, the specimens of some of the composites were already tested, and there were not enough specimens left to test new ones with correct distance between the support spans. The tests performed, however, indicate that most of the flexural modulus values reported should have been higher because of having too long a distance between the support spans, compared the beforehand set value in the data programme.

The measured mechanical properties of a sample can be severely influenced by defects in the sample. The epoxy rod is both undergoing bending and stretching during testing. Deformations on the lower surface of an epoxy rod are especially a problem because crack formation and breakage will occur fast due to the downward force pushing on the upper surface which causes stretching at the lower surface. The most probable reason for the different break points of the samples is inhomogeneity of the specimens. Inhomogeneity is generally caused by air bubbles or agglomerates in the specimens. Presence of air bubbles is often a problem if the epoxy is not degassed properly, and especially for dark, opaque samples where air bubbles are difficult to discover. Air bubbles can cause weak points which increase the probability for crack formation. Air bubbles in the samples lead to reduced values, and if this was known to be the reason of the low values, the highest value obtained could have been regarded as the correct value. If the varying results are caused by agglomerates, however, this cannot be assumed. Non-homogenous samples can cause varieties of mechanical properties in a composite, where some parts are reinforced and some are not. The high results could thus have been obtained by being lucky having specimens that were more homogenous than others, and thus avoid hitting agglomerates with weak points. The flexural modulus is not

highly affected by defects like inhomogeneity, but the flexural strain and flexural stress are highly dependent of this as demonstrated in the results from the three-point flexural tests.

Figure 73 and Figure 74 presents the results of the DMA test with storage modulus and Tg respectively.

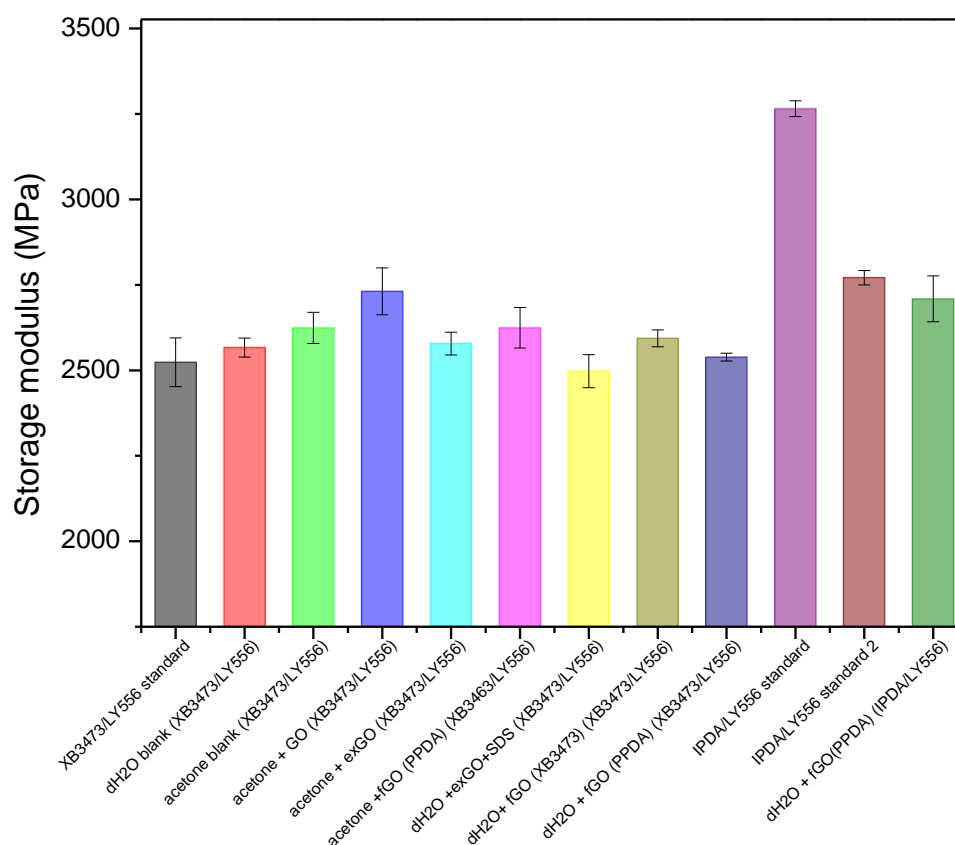


Figure 73 - Storage modulus. The standard deviation is presented by error bars. dH2O corresponds to distilled water.

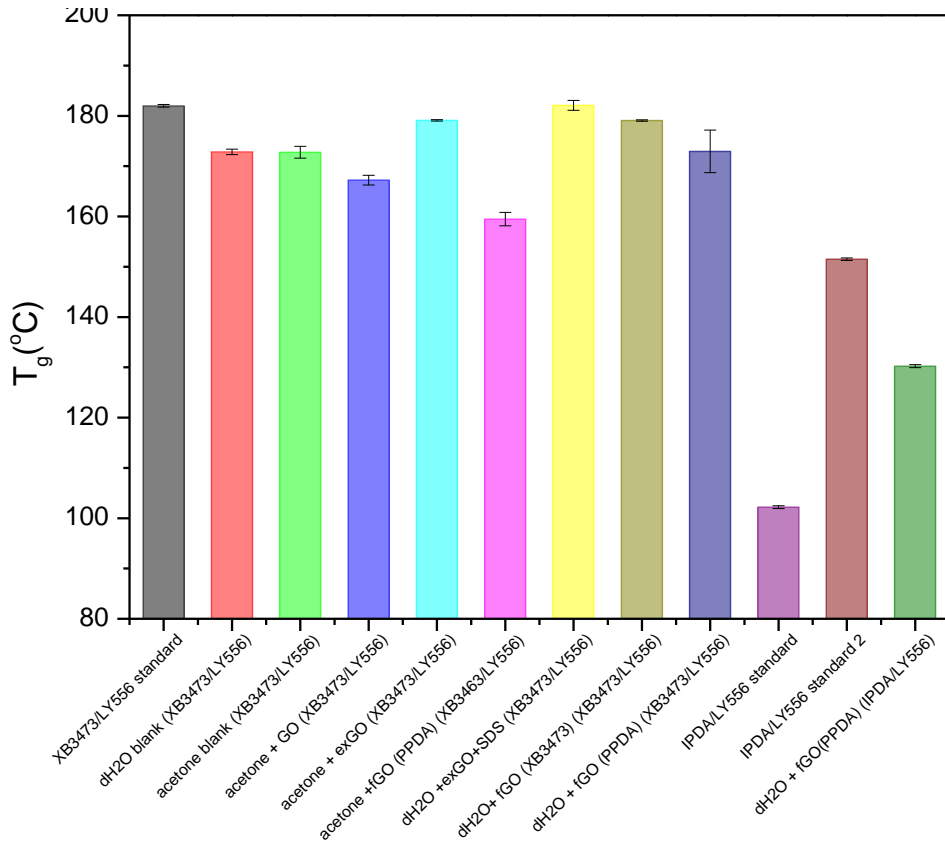


Figure 74 - Glass transition temperature. The standard deviation is presented by error bars. dH2O corresponds to distilled water.

The diagram showing the T_g of the different composite series (Figure 74) generally have low standard deviations, but some of the samples show reduced T_g . Reduction in T_g can be caused by a number of different factors. Residual water or solvent in the composite can cause a reduction in T_g . The removal of all solvent from the composite was a major problem during the experiments, and remaining water or acetone in some of the samples is likely. Errors in the mixture ratio of epoxy resin and hardener, and differences in the curing cycle between the composites can also cause variations in T_g . Another possible explanation for variations in T_g is that some of the hardener could have reacted with some of the functional groups on GO. Some of the sample specimens also showed high T_g and lowered storage modulus. A highly increased T_g , but simultaneously reduced storage modulus often indicates a brittle composite.

Influential factors during a DMA test include among others specimen geometry, measuring parameters, temperature program, clamps, type of load, and frequency. Machining of the

specimen can potentially give differences in geometry, and these differences influence on the storage modulus [15].

The DMA results are less dependent of the positioning of the sample, compared to the three-point flexural test. The results also show better correlation and lower standard deviation between the specimens in the different test series, compared to the three-point flexural test. The results from the DMA are therefore more trustworthy than the results from the three-point flexural test.

Some of the graphs obtained during the DMA analysis showed irregular pattern (Appendix A), which e.g. stopped before the set temperature was reached or showed jagged curves. These results may be caused by either stiff or soft, flexible specimens, because full contact between specimen and specimen fixture is not obtained, or the polymer melts.

The results from DMA and three-point flexural test are reported as the average value with standard deviations. The standard deviation is reported as the deviation between the samples. The values of the different calculated mechanical properties, also consists of equations were many parameters are used. The different parameters like geometry and distances also have varieties and a standard deviation which should have been taken into account during the calculations. The standard deviation is therefore inaccurate from a statistical point of view, but will give a good indication of how much the variations between each sample are. Some of the samples were varying a lot, and more samples were tested when additional samples were available. All samples are reported, which means that if one sample becomes very different from the other samples it will in some cases give a high value of the standard deviation.

4.8 Preparation of composites

Different composites and neat epoxies were made during the experimental work of the thesis. The different variations were made to check for possible effects on the epoxy systems.

The first epoxy polymer made, was an epoxy polymer with LY556, XB3473 and distilled water, without GO. This epoxy polymer was made as a test sample to learn to handle epoxy resin and hardener, and to find methods for mixing and methods for the removal of solvent. The polymer was examined by DMA and three-point flexural test. The results from the DMA

test (Appendix A, Figure A 1, Figure A 15, and Figure A 16) showed that the polymer was weak. The first broke in the DMA, and the other samples melted, became bent and deformed. It is suspected that the poor results were caused by residual water in the sample, as remaining solvent in polymer materials can cause severe reduction in mechanical properties of a composite. When water and epoxy resin were mixed, a white milk-like emulsion was formed. High temperature was used between two mixing steps, and a hypothesis was that the water reacted with the epoxy, and formed hydrogen bonds that were later difficult to remove. The high temperature which was used during removal of solvent could also maybe favour these bindings and make the removal of water more difficult.

Figure 75 shows epoxy rods from the water test. The epoxy rods were tested in DMA, and were bent, deformed, and did even break during the test.

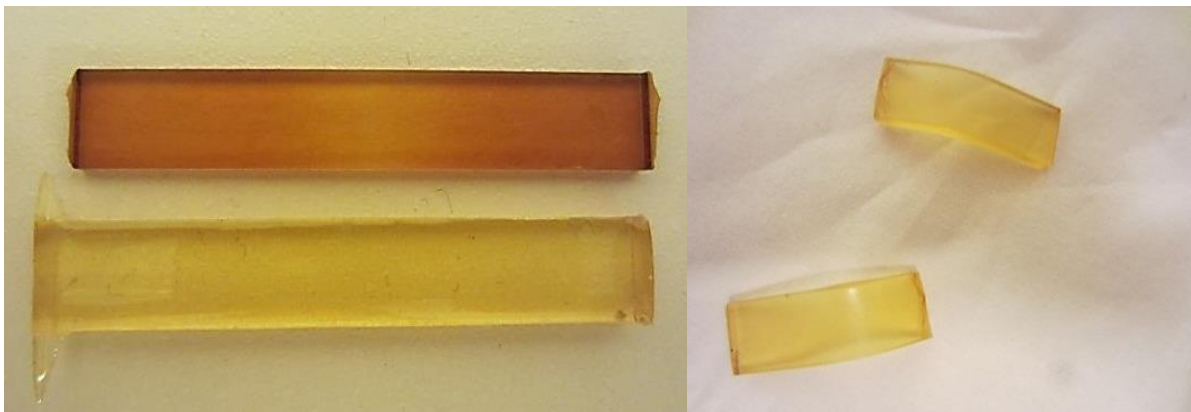


Figure 75 - Left: Epoxy rods before and after DMA testing. Right: Epoxy rod after DMA, this is from the water test and it broke in the DMA test.

It was decided to make a new epoxy/distilled water polymer with the same resin and hardener (LY556/XB3473) as the epoxy/water test. The difference from the first epoxy/water test was that the heating step during mixing was removed and during evaporation in rotavapor the temperature was maintained at a temperature as low as possible (around 40 °C). An epoxy polymer with just water was also needed to see if the water did cause any decrease in the mechanical properties of the epoxy. During testing in DMA and three-point flexural test of the epoxy/distilled water the measurements showed much better results. The samples did not break and the values of storage modulus, T_g, flexural modulus, flexural strain and flexural stress became more similar to what was expected due to known values of the epoxy system without water.

During the specialization project performed during the autumn of 2013, different versions of exfoliated GO was made [30]. Some small amount of the different exfoliated GO still remained, and it was decided to try this out in a composite during the M.Sc. thesis because other studies had obtained good results with EXGO in epoxy based composites [52;55]. One composite where a small amount of EXGO (300 °C) dispersed in acetone was transferred into epoxy was made. Another composite with EXGO (1000 °C) dispersed in distilled water with added SDS were also made. The addition of SDS was thought to give a more homogenous dispersion of EXGO solution, and that was also the case before the epoxy was added. However, when the epoxy resin was added, it was almost impossible to get rid of the water in the rotavapor. SDS was added in a 1:1 ratio, and it became apparent this was too high a quantity, because the solution produced a lot of foam. During the evaporation of water, the epoxy mix showed heavy foaming (Figure 76), and it was difficult to prevent bumpy boiling. After 2 hours in the rotavapor, much water was still left in the epoxy. The epoxy mix was therefore put in a vacuum oven at 90 °C overnight, to get rid of the remaining water.



Figure 76 – EXGO and SDS in distilled water. Left picture is before removal of distilled water, Right picture shows the solution during evaporation of distilled water in the rotavapor. The picture shows lot of foam and bubbles.

The foam formation made it difficult to remove the water, and in addition the homogenous dispersion didn't remain when the EXGO was transferred to the epoxy resin. After curing, some residual foam was visible on the top of the cured epoxy rods (Figure 77).

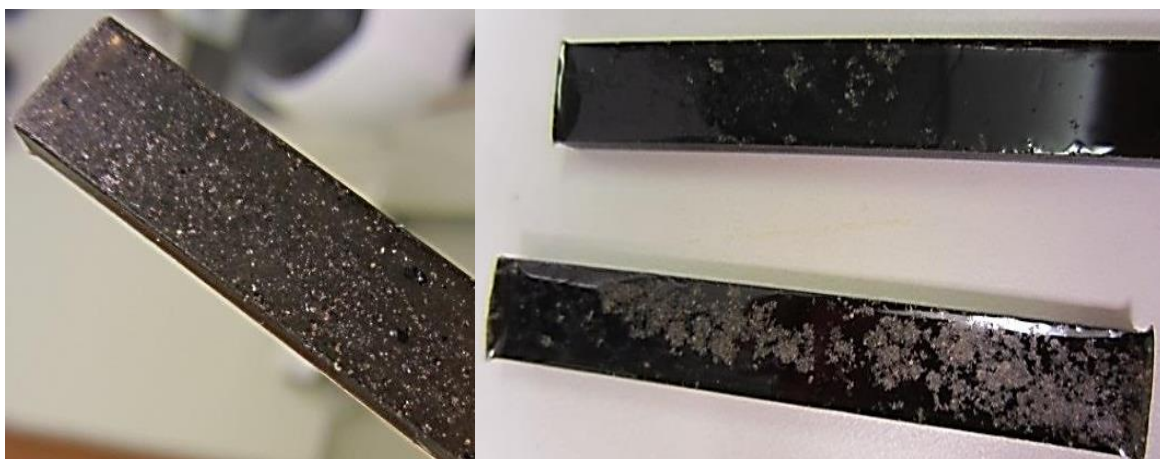


Figure 77 – EXGO (1000 °C) + SDS and distilled water; epoxy rods.

The epoxy rods are transparent with black clods of EXGO. There were also obvious agglomerations and some sediment in the samples. The epoxy rods were transparent with black lumps of agglomerated GO. It also seemed to be sedimentation on the bottom of the samples. The results in DMA and three-point flexural bending tests were not very bad; however, it is unknown whether the result would have been better or worse if the amount of EXGO added to the epoxy had been increased. Another problem with addition of EXGO is that the exact amount of EXGO added was difficult to know. EXGO is fluffy and electrostatically charged and difficult to weigh. It was necessary to use a radioactive source to de-ionize the EXGO particles, to even obtain a reading of the weight on the electronic balance.

An epoxy polymer with acetone was made to investigate the possible effect of acetone on the epoxy. Like the epoxy/water polymer, it was important to have efficient removal of solvent to avoid remaining solvent in the sample. The actual epoxy system is well investigated, and acetone was already known to function well together with the epoxy system. The difference was maybe the method that was used in the experiments in this thesis. The results from the DMA actually showed better results for the storage modulus compared to the reference standard, but this can be caused by the slightly low value of the reference standard. The T_g showed some decrease, but this was expected due to difficulties of completely removal of solvent which often causes reduction in T_g . The three point flexural test showed a small decrease in flexural modulus, flexural stress and flexural strain.

A neat epoxy polymer of the system LY556/XB3473 was made as reference for further experiments. It was also made as a control to see if the epoxy was handled correctly and if the results of mechanical testing were consistent with values in the data sheets of the manufacturer. The values obtained on DMA and three points flexural test were in good accordance with the data sheet (Appendix E), but both the storage modulus and the flexural modulus were slightly lower compared to the values in the data sheets. The curing cycle used in the experiments in this M.Sc. thesis is somewhat different than the curing cycle used by the manufacturer. Differences in curing cycle can give differences in the results, but usually this affects T_g more than storage modulus. Differences in geometry and alignment of the sample could be probable causes of the differences in the modulus.

4.9 Discussion/Summary

The results from the DCS test of the GO dispersions in distilled water and acetone showed similar results for distilled water and acetone. Due to better stability of the distilled water dispersion, however, most of the composites were made with GO dispersed in distilled water.

The XPS results indicated successful functionalization of GO with PPDA. Unfortunately, the FGO with XB3473 functionalization was not analysed in XPS, and it is therefore not possible to tell if this functionalization was successfully performed or not. A comparison of the two different diamines used for functionalization of GO was done by comparing the results from the DMA and the three-point flexural bending test. The DMA and three-point flexural test showed similar results for the two diamines used for the functionalization. The low value of the flexural modulus of the FGO (PPDA) in distilled water is caused by the error in span distance as mentioned earlier.

In light of the study of surface and interfacial tensions, some of the difficulties with the removal of water from the epoxy could potentially have been aggravated by the presence of surface active groups in the epoxy, but this was probably not the main cause for the difficulties with complete water removal. During the experiments with epoxy and water, the temperature was raised to 70 °C, while the tables (Appendix F) give the values of interfacial tension and surface tension at 20 °C. An increase in temperature will cause a lower interfacial tension, which could lead to a more stable emulsion. However, in addition to an increase in

the interfacial tension, the viscosity decreases, the water becomes easier to evaporate, and the temperature rise was necessary to be able to remove the water [26]. It was decided to keep the temperature as low as possible during evaporation in rotavapor and vacuum as a precaution.

As - prepared GO was wet transferred in acetone to the epoxy resin. Research has shown better dispersion of GO particles in the epoxy matrix when being wet transferred compared to addition of particles in dry state directly into the matrix [47]. Acetone is commonly used at FFI as a dispersant for nanoparticles because it is soluble and interacts well with epoxy. In addition, acetone is easier to evaporate. Acetone was therefore chosen as solvent instead of distilled water in the first experiment with GO particles.

A research study performed by Gudarzi et al. was chosen as a template for further experiments [47]. However, when the first composite with fGO was made, XB3473 was used as diamine and hardener instead of PPDA, to try a new variation. It was difficult to remove the water because the GO particles increased the chances for bumpy boiling during the evaporation in the rotavapor, and the results of the DMA and three-point flexural bending test showed that the FGO didn't appear to give the wanted improvement of the composite properties.

Since the removal of water was an issue, it was decided to make a new attempt with an FGO reinforced composite, where acetone was used instead of water and to change the diamine to PPDA instead of XB3473. The hypothesis was that the acetone was easier to evaporate and thus would give better results than obtained with water as dispersant.

It was decided to make an attempt to follow the receipt of making FGO epoxy as made by Gudarzi et al. [47], to check if the same impressive results were obtained. The same epoxy resin (LY556) and hardener (XB3473) as used on the other composites, however, were still used as a difference from Gudarzi et al. This epoxy system was continued because this is a good system that is well known and used at FFI, and if addition of FGO particles should be worth continuing with, it will be most advantageous if an already good system could have been even better. Nor this composite gave the wanted improvements in the properties of the composite.

One hypothesis after making many different composites with as prepared GO, EXGO, and FGO, was that the high temperature during curing causes re-flocculation of GO particles, or maybe causes some form of chemical reaction that is not advantageous. All the composites were made with the same hardener and same curing procedure, and it was therefore decided to use a different hardener with lower curing temperature. A research study performed by Gudarzi et al. proposed good results when using IPDA as a hardener, with a curing time of 24 hours in room temperature followed by 2 hours at 100 °C [47]. It was decided to follow this procedure, still using the same epoxy resin (LY556). A LY556/IPDA reference standard was made. Unfortunately, the low temperature did not seem to be enough. When testing in three point flexural bending tests, the results became weak, and the test in DMA indicated a low T_g and very high storage modulus. During the DMA it seemed like the composite rods were continuing their curing during the analysis. The same specimen was run several times, and between the first and second run, T_g increased considerably, while the storage modulus decreased. These observations indicate that the curing was incomplete and that the curing temperature was too low.

Based on the poor results from the LY556/IPDA epoxy reference standard 1, it was decided that a new reference standard with another curing temperature and – cycle would be made. Different research and data sheets were studied, and a curing time and temperature was set after these specifications [66-68]. It was still a desire to keep the curing temperature low in the first hours and later below 160 °C because of the suspicion about a potential reaction with GO at high temperatures. This epoxy showed a completely different behaviour in both DMA and three point flexural tests. T_g increased and the storage modulus showed results as expected according to standards and literature [66-68].

A composite with the low temperature hardener and FGO (PPDA) were made to find out if the FGO could make any improvement of this epoxy system. The other composites failed in improving the properties, and if this composite gave better results, it could indicate that the hypothesis about the high curing temperature was on to something. The results showed that there was a small increase in storage modulus, flexural modulus, flexural strength and flexural strain, compared to the reference standard. The T_g of the composite, however, was reduced compared to the reference standard. Other studies have shown variable effects on T_g when using GO as reinforcement, some reports an increase in T_g [69], other reports little or no

effect [70], while other have found a decrease in T_g [64;71;72]. The influence on reaction conversion and molecular confinement affects T_g of composites. Stiffer composites have the tendency to reduce T_g . A reaction between the functional groups of GO and curing agent may cause an interference with the epoxy curing reaction, and have an impact on the optimal ratio of epoxy and curing agent. The polymer cross linkage may be reduced by errors in epoxy/hardener ratio, and the polymer chain mobility may be increased [64].

A lowered T_g can also be caused by remaining solvent in the composite. Variations in the ratio of curing agent and the epoxy in the composite can potentially lead to a decrease in glass transition temperature. The epoxy and curing agent are based on cross bindings during curing and the ratio between the components will have significant influence on the structure of the polymer, and thus the glass temperature.

Previous research claim that GO was homogeneously dispersed in the polymer matrix [25]. However, a homogenous dispersion was not obtained in the present work. Nano particles have a higher tendency to agglomerate compared to micro sized particles. When agglomerates are formed, the size of the interface between the particles and surrounding medium will decrease, and the mechanical properties will not take fully advantage of the nano size of the particles.

The improvement in the properties of the nanocomposites depends on the distribution of graphene layers in the polymer matrix as well as interfacial bonding between the graphene layers and polymer matrix. If the compatibility is poor, the particles will not be able to carry external load, and the composite material will not be able to achieve higher strength than the neat epoxy. Pristine graphene is not compatible with organic polymers and does not form homogeneous composites. In contrast, graphene oxide sheets are heavily oxygenated. Because of the functional groups, GO can be more compatible with organic polymers because the functional groups (hydroxyl, epoxide, diols, ketones and carboxyl) can alter the van der Waals interactions significantly. Graphene oxide also has a hydrophilic character, which makes it less soluble in epoxy resin. The amount of filler compared to epoxy and curing agent has to be correct, and is strongly dependent on size, shape and type of filler. None of the studied research has used the same epoxy resin as in the present thesis, and the use of rotavapor for the evacuation of water is not found in other research. A different source of graphite was also

used in this work. The reason for the absent in improving results of the composites made in this thesis is unknown, but may be caused by among other having different curing cycle- and temperature, epoxy resin, graphite source, or dispersion method.

In a macroscopic point of view, a random distribution of GO particles in the epoxy matrix is presumed, and the composite is in general considered as isotropic. However, by itself each GO particle is anisotropic meaning that the strength varies in different directions. In theory, it is possible to arrange the GO particles in such a way that they become parallel. This would give a material which has direction dependent properties. Fibres basically have low strength across the fibre direction, while the strength along the fibre direction is higher. It is possible to make an ordered distribution by using various techniques like electric fields or electron spin methods. During this work, the GO particles were not aligned, and isotropic composites are presumed.

In the view of the performed experiments and obtained results, the author's knowledge in mechanics has been insufficient. The author had too much focus on the chemistry part of the study, and too little knowledge of mechanics. With hindsight, the author should have studied the principles behind mechanical testing before starting the mechanical testing. Small differences in the parameters made a major impact on the results. Unfortunately, many of the experiments were performed before knowledge in mechanical testing was obtained, and this is reflected in the results of the mechanical testing, especially in the results from the three point flexural bending test. Although there were some sources of error in the mechanical experiments, the results could be used to differentiate between the different epoxy polymers with incorporated GO. The results of the mechanical tests showed that incorporation of the various GO particles did not make any notable improvements in mechanical properties like T_g , flexural strength, flexural modulus or flexural strain. The main reason why the improvements did not materialize, is most probably inhomogeneous composites due to the problems with dispersion of GO. Remaining solvent in some of the composites, and inaccuracies in the mechanical testing may also have been influential.

The biggest gain/profit that can be obtained for a composite is to increase the adsorption between epoxy matrix and carbon fibre, to minimize delamination and improve the total

mechanical strength of the overall composite. Although the mechanical properties of the epoxy were not improved, the adhesion to carbon fibers might have been improved by the addition of GO particles. Hence, one could have obtained an increase in the mechanical strength for the overall composite. Experiments with carbon fiber composites were not performed in this work, but such experiments are interesting for future work.

4.10 Future work

Unfortunately, there was not enough time and equipment to perform more research on other variations of nanocomposites reinforced with GO during the M.Sc. thesis. Many unanswered questions still remain, and these questions and hypotheses may form the basis for new experiments in future work.

- During the M.Sc. thesis only one (two (EXGO)) concentration of GO were added, and even though other researchers have made some attempts, the effect of changing the amount of GO in the composite should be studied in future work.
- The main problem during the M.Sc. thesis was to get a homogenous dispersion, and it was not possible to get a dispersion that remained homogenous when added to epoxy resin and cured. A new method for the dispersion of GO in epoxy should thus be found. In addition, curing time and curing temperature could be optimized. Other solvents could be tried out, thermal exfoliated GO can be studied in more detail with larger amount, and different amines for functionalization of GO can be tested.
- Previous research has shown different properties and characteristics of GO for different graphite sources and manufacturing methods, and another graphite source or manufacturing method could potentially give different and better results. It would therefore be interesting to try another graphite source for the processing of GO, and maybe also use another method for the production of GO.
- During the M. Sc. thesis, one surfactant (SDS) was tried out to see if it could make the dispersion of GO more stable and homogenous, but the results were rather bad. Other surfactants can be tried out to see if these have more effect on the dispersion.
- Lastly, it could have been interesting to investigate if addition of GO to the epoxy matrix could have made an increase in the adhesion between the epoxy matrix and carbon fibre, despite the fact that the epoxy itself was not improved by the incorporation of GO, maybe the strength of the total composite could be improved

5 Conclusion

Recent research has shown potential for increased strength and stiffness of epoxy based nanocomposites when adding GO as reinforcement. During this M.Sc. thesis, different epoxy based composites were made with GO as reinforcement. GO was added in different chemical variations; as prepared, exfoliated, and functionalised with different diamines (PPDA and XB3473). In addition, two types of hardeners were used; XB3473 and IPDA. The XPS indicated that GO was successfully functionalised with PPDA. However, the results of the composites in this M.Sc. thesis were not as promising as results from previous research, even though a variety of systems were tested. The GO particles were possibly not dispersed homogenously enough because of re-flocculation during manufacturing.

6 References

- [1] D. Galpaya, M. Wang, M. Liu, N. Motta, E. R. Waclawik, and C. Yan, "Recent advances in fabrication and characterization of graphene-polymer nanocomposites", vol.1,no.2,pp.30-49,2012.
- [2] P. P. Sambarkar, P. P. Patewekar, and B. M. Dudhgaonkar, "Polymer nanocomposites: An overview" *International Journal of Pharmacy and Pharmaceutical Sciences*, vol. 4, no. 1,pp. 60-65, 2012.
- [3] B. Wetzel, P. Rosso, F. Hauptert, and K. Friedrich, "Epoxy nanocomposites - fracture and toughening mechanisms" *Engineering fracture mechanics*, vol. 73, no. 16, pp. 2375-2398, 2006.
- [4] F. Hussain, M. Hojjati, M. Okamoto, and R. E. Gorga, "Review article: Polymer-matrix Nanocomposites, Processing, Manufacturing, and Application: An Overview" *Journal of Composite Materials*, vol. 40, no. 17, pp. 1511-1575, 2006.
- [5] P. Song, Z. Cao, Y. Cai, L. Zhao, Z. Fang, and S. Fu, "Fabrication of exfoliated graphene-based polypropylene nanocomposites with enhanced mechanical and thermal properties" *Polymer*, vol. 52, no. 18, pp. 4001-4010, 2011.
- [6] A. Taylor, "Adhesives with Nanoparticles" in *Handbook of Adhesion Technology*. L. da Silva, A.Öchsner, and R. Adams, Eds. Springer Berlin Heidelberg, pp. 1437-1460, 2011.
- [7] E. T. Thostenson, C. Li, and T. W. Chou, "Nanocomposites in context" *Composites Science and Technology*, vol. 65, no. 3-4, pp. 491-516, 2005.
- [8] F. C. Campbell, "Introduction to Composite materials" in *Structural composite materials*,USA, ASM International, p.599, 2010.
- [9] D. R. Paul and L. M. Robeson, "Polymer nanotechnology: Nanocomposites" *Polymer*, vol. 49, no. 15, pp. 3187-3204, 2008.

- [10] B. W. Kim and A. H. Mayer, "Influence of fiber direction and mixed-mode ratio on delamination fracture toughness of carbon/epoxy laminates" *Composites Science and Technology*, vol. 63, no. 5, pp. 695-713, 2003.
- [11] V. Singh, D. Joung, L. Zhai, S. Das, S. I. Khondaker, and S. Seal, "Graphene based materials: Past, present and future" *Progress in Materials Science*, vol. 56, no. 8, pp. 1178-1271, 2011.
- [12] I. Srivastava, M. A. Rafiee, F. Yavari, J. Rafiee, and N. Koratkar, "Epoxy Nanocomposites: Graphene a Promising Filler" *Graphite, Graphene, and Their Polymer Nanocomposites*, p. 315, 2012.
- [13] M. M. Boyle, C. J. Martin, and J. D. Neuner, "Epoxy Resins" in *ASM Handbook Composites*. ASM International, Ed. Ohio: ASM International, Material Park, pp. 78-89, 2001.
- [14] M. S. Bhatnagar, "Epoxy Resins (Overview)" , USA ,CRC Press, pp. 1-11, 1996.
- [15] B. B. Johnsen and T. Olsen, "Material properties of plastics and carbon fibre-reinforced plastics-experimental methods and results", Norwegian Defence Research Establishment (FFI), 2010/00539, 2011.
- [16] A. A. Azeez, K. Y. Rhee, S. J. Park, and D. Hui, "Epoxy clay nanocomposites - processing, properties and applications: A review" *Composites Part B: Engineering*, vol. 45, no. 1, pp. 308-320, 2013.
- [17] A. K. Geim and K. S. Novoselov, "The rise of graphene" *Nature Materials*, vol. 6, no. 3, pp. 183-191, 2007.
- [18] H. Kim, A. A. Abdala, and C. W. Macosko, "Graphene/polymer nanocomposites" *Macromolecules*, vol. 43, no. 16, pp. 6515-6530, 2010.
- [19] M. Terrones, O. Martín, M. González, J. Pozuelo, B. Serrano, J. C. Cabanelas, S. M. Vega-Díaz, and J. Baselga, "Interphases in Graphene Polymer-based Nanocomposites: Achievements and Challenges" *Advanced Materials*, vol. 23, no. 44, pp. 5302-5310, 2011.

- [20] J. Du and H.-M. Cheng, "The fabrication, properties, and uses of graphene/polymer composites" *Macromolecular Chemistry and Physics*, vol. 213, no. 10-11, pp. 1060-1077, 2012.
- [21] P. Mukhopadhyay and R. Gupta, "Trends and frontiers in graphene-based polymer nanocomposites" *Plastics Engineering*, pp.32 -42, 2013.
- [22] O. C. Compton and S. T. Nguyen, "Graphene Oxide, Highly Reduced Graphene Oxide, and Graphene: Versatile Building Blocks for Carbon-Based Materials" *Small*, vol. 6, no. 6, pp. 711-723, 2010.
- [23] R. J. Young, I. A. Kinloch, L. Gong, and K. S. Novoselov, "The mechanics of graphene nanocomposites: A review" *Composites Science and Technology*, vol. 72, no. 12, pp. 1459-1476, 2012.
- [24] H. Bai, C. Li, and G. Shi, "Functional Composite Materials Based on Chemically Converted Graphene" *Advanced Materials*, vol. 23, no. 9, pp. 1089-1115, 2011.
- [25] S. Pei and H. M. Cheng, "The reduction of graphene oxide" *Carbon*, vol. 50, no. 9, pp. 3210-3228, 2012.
- [26] H. J. Salavagione, G. Martínez, and G. Ellis, "Graphene-Based Polymer Nanocomposites" in *Physics and applications of Graphene- Experiments*, 1 ed. S. Mikhailov, Spain, Institute of Polymer Science and Technology, Spanish National Research Council, pp. 169-192, 2011.
- [27] W. S. Hummers and R. E. Offeman, "Preparation of Graphitic Oxide" *Journal of the American Chemical Society*, vol. 80, no. 6, p. 1339, 1958.
- [28] D. C. Marcano, D. V. Kosynkin, J. M. Berlin, A. Sinitskii, Z. Sun, A. Slesarev, L. B. Alemany, W. Lu, and J. M. Tour, "Improved Synthesis of Graphene Oxide" *ACS Nano*, vol. 4, no. 8, pp. 4806-4814, 2010.
- [29] D. R. Dreyer, S. Park, C. W. Bielawski, and R. S. Ruoff, "The chemistry of graphene oxide" *Chemical Society Reviews*, vol. 39, no. 1, pp. 228-240, 2010.

- [30] E. M. Svendsen, "Preparation and characterization of graphene oxide" Norwegian University of Science and Technology, Faculty of Natural Science and Technology, Department of Chemical Engineering, 2013.
- [31] J. R. Potts, D. R. Dreyer, C. W. Bielawski, and R. S. Ruoff, "Graphene-based polymer nanocomposites" *Polymer*, vol. 52, no. 1, pp. 5-25, 2011.
- [32] M. A. Rafiee, J. Rafiee, Z. Wang, H. Song, Z. Z. Yu, and N. Koratkar, "Enhanced Mechanical Properties of Nanocomposites at Low Graphene Content" *ACS Nano*, vol. 3, no. 12, pp. 3884-3890, 2009.
- [33] R. Verdejo, M. M. Bernal, L. J. Romasanta, and M. A. Lopez-Manchado, "Graphene filled polymer nanocomposites" *Journal of Materials Chemistry*, vol. 21, no. 10, pp. 3301-3310, 2011.
- [34] O. Akhavan, "The effect of heat treatment on formation of graphene thin films from graphene oxide nanosheets" *Carbon*, vol. 48, no. 2, pp. 509-519, 2010.
- [35] C. Zhang, W. Lv, X. Xie, D. Tang, C. Liu, and Q. H. Yang, "Towards low temperature thermal exfoliation of graphite oxide for graphene production" *Carbon*, vol. 62, pp. 11-24, 2013.
- [36] P. C. Mørk, *Overflate og kolloidkjemi*. Trondheim, NTNU, Institutt for kjemisk prosessteknologi, p. 307, 2004
- [37] M. Nadler, T. Mahrholz, U. Riedel, C. Schilde, and A. Kwade, "Preparation of colloidal carbon nanotube dispersions and their characterisation using a disc centrifuge" *Carbon*, vol. 46, no. 11, pp. 1384-1392, 2008.
- [38] T. R. Frømyr, F. K. Hansen, and T. Olsen, "The Optimum Dispersion of Carbon Nanotubes for Epoxy Nanocomposites: Evolution of the Particle Size Distribution by Ultrasonic Treatment" *Journal of Nanotechnology*, vol. 2012, 2012.
- [39] B. B. Johnsen, T. R. Frømyr, T. Thorvaldsen, and T. Olsen, "Preparation and characterisation of epoxy/alumina polymer nanocomposites" *Composite Interfaces*, vol. 20, no. 9, pp. 721-740, 2013.

- [40] K. L. Lu, R. M. Lago, Y. K. Chen, M. L. H. Green, P. J. F. Harris, and S. C. Tsang, "Mechanical damage of carbon nanotubes by ultrasound" *Carbon*, vol. 34, no. 6, pp. 814-816, 1996.
- [41] M. Helbæk and S. Kjelstrup, *Fysikalsk kjemi*, Trondheim, Fagbokforlaget, p. 796, 2006.
- [42] Malvern Instruments Ltd, "Zeta Potential An Introduction in 30 Minutes, technical note" Malvern Instrumens Ltd., 2014. Last accessed: 02.06.2014, Available at: <http://www3.nd.edu/~rroeder/ame60647/slides/zeta.pdf>
- [43] R. J. Hunter, *Zeta Potential in Colloid Science: Principles and Applications*, 3rd ed., Academic Press, p.386, 1988.
- [44] Y. Li, D. Pan, S. Chen, Q. Wang, G. Pan, and T. Wang, "In situ polymerization and mechanical, thermal properties of polyurethane/graphene oxide/epoxy nanocomposites" *Materials & Design*, vol. 47, pp. 850-856, 2013.
- [45] S. Stankovich, D. A. Dikin, G. H. B. Dommett, K. M. Kohlhaas, E. J. Zimney, E. A. Stach, R. D. Piner, S. T. Nguyen, and R. S. Ruoff, "Graphene-based composite materials" *Nature*, vol. 442, no. 7100, pp. 282-286, 2006.
- [46] M. M. Gudarzi and F. Sharif, "Molecular level dispersion of graphene in polymer matrices using colloidal polymer and graphene" *Journal of Colloid and Interface Science*, vol. 366, no. 1, pp. 44-50, 2012.
- [47] M. M. Gudarzi and F. Sharif, "Enhancement of dispersion and bonding of graphene-polymer through wet transfer of functionalized graphene oxide" *Express Polymer Letters*, vol. 6, no. 12, pp. 1017-1031, 2012.
- [48] Y. J. Wan, L. C. Tang, D. Yan, L. Zhao, Y. B. Li, L. B. Wu, J. X. Jiang, and G. Q. Lai, "Improved dispersion and interface in the graphene/epoxy composites via a facile surfactant-assisted process" *Composites Science and Technology*, vol. 82, pp. 60-68, 2013.

- [49] L. C. Tang, Y. J. Wan, D. Yan, Y. B. Pei, L. Zhao, Y. B. Li, L. B. Wu, J. X. Jiang, and G. Q. Lai, "The effect of graphene dispersion on the mechanical properties of graphene/epoxy composites" *Carbon*, vol. 60, pp. 16-27, 2013.
- [50] B. A. Rozenberg and R. Tenne, "Polymer-assisted fabrication of nanoparticles and nanocomposites" *Progress in Polymer Science*, vol. 33, no. 1, pp. 40-112, 2008.
- [51] P. C. Painter and M. M. Coleman, *Fundamentals of Polymer Science: An Introductory Text*, Lancaster, Technomic Publishing Company, p.478, 1997.
- [52] M. A. Rafiee, J. Rafiee, I. Srivastava, Z. Wang, H. Song, Z. Z. Yu, and N. Koratkar, "Fracture and Fatigue in Graphene Nanocomposites" *Small*, vol. 6, no. 2, pp. 179-183, 2010.
- [53] H. Yang, C. Shan, F. Li, Q. Zhang, D. Han, and L. Niu, "Convenient preparation of tunably loaded chemically converted graphene oxide/epoxy resin nanocomposites from graphene oxide sheets through two-phase extraction" *Journal of Materials Chemistry*, vol. 19, no. 46, pp. 8856-8860, 2009.
- [54] Y. J. Wan, L. X. Gong, L. C. Tang, L. B. Wu, and J. X. Jiang, "Mechanical properties of epoxy composites filled with silane-functionalized graphene oxide" *Composites Part A: Applied Science and Manufacturing*, vol.64, pp. 79-89, 2014.
- [55] S. Chandrasekaran, N. Sato, F. Tölle, R. Mülhaupt, B. Fiedler, and K. Schulte, "Fracture toughness and failure mechanism of graphene based epoxy composites" *Composites Science and Technology*, vol. 97, pp. 90-99, 2014.
- [56] Sigma-Aldrich, "p-Phenylenediamine,". Sigma-Aldrich, 2014. Last accessed: 02.06.2014, Available at: <http://www.sigmaaldrich.com/catalog/product/sigma/p6001?lang=en®ion=NO>
- [57] Sigma- Aldrich, "3-Aminomethyl-3,5,5-trimethylcyclohexylamine, IPDA,". Sigma-Aldrich, 2014, Last accessed:02.06.2014, Available at: <http://www.sigmaaldrich.com/catalog/product/fluka/59180?lang=en®ion=NO>
- [58] G. Øye, "Lecture notes sedimentation and diffusion". Ugelstad Laboratory, Norwegian University of Science and Technology, 2013.

- [59] A. Bratt and A. R. Barron, "XPS of carbon nanomaterials,". Connexions, Last accessed: 27.05.2014, Available at: <http://webcache.googleusercontent.com/search?q=cache:http://cnx.org/content/m34549/1.2/>, Connexions, 2013.
- [60] I. Jung, M. Vaupel, M. Pelton, R. Piner, D. A. Dikin, S. Stankovich, J. An, and R. S. Ruoff, "Characterization of Thermally Reduced Graphene Oxide by Imaging Ellipsometry" *Journal of Physical Chemistry*, vol. 112, no. 23, pp. 8499-8506, 2008.
- [61] ASTM International, "ASTM D 790-03 Standard Test method for Flexural properties of Unreinforced and reinforced Plastics and Electrical Insulating Materials", ASTM International, 2003.
- [62] S. Halder and P. K. Gosh, "Mechanism of nanoparticle dispersion via acoustic cavitation in highly viscous fluid," 2013., Last accessed: 02.06.2014, Available at: http://www.nacomm2013.org/Papers/041-inacomm2013_submission_230.pdf
- [63] K. Haubner, J. Murawski, P. Olk, L. M. Eng, C. Ziegler, B. Adolphi, and E. Jaehne, "The Route to Functional Graphene Oxide" *ChemPhysChem*, vol. 11, no. 10, pp. 2131-2139, 2010.
- [64] D. Galpaya, M. Wang, C. Yan, M. Liu, N. Motta, and E. R. Waclawik, "Fabrication and mechanical and thermal behaviour of graphene oxide/epoxy nanocomposites" *Journal of Multifunctional Composites*, pp. 91-98, 2013.
- [65] S. Stankovich, D. A. Dikin, R. D. Piner, K. A. Kohlhaas, A. Kleinhammes, Y. Jia, Y. Wu, S. T. Nguyen, and R. S. Ruoff, "Synthesis of graphene-based nanosheets via chemical reduction of exfoliated graphite oxide," *Carbon*, vol. 45, no. 7, pp. 1558-1565, 2007.
- [66] F. Fraga, E. C. Vazquez, E. Rodríguez-Núñez, and J. M. Martínez-Ageitos, "Curing kinetics of the epoxy system diglycidyl ether of bisphenol A/isophorone diamine by Fourier transform infrared spectroscopy" *Polymers for Advanced Technologies*, vol. 19, no. 11, pp. 1623-1628, 2008.

- [67] Momentive, "Technical Data Sheet, EPIKURE Curing Agent 3300," Momentive, 2007, Last accessed: 02.06.2014, Available at: <http://www.momentive.com/Products/TechnicalDataSheet.aspx?id=3543>
- [68] D. Zilli, C. Chilotte, M. M. Escobar, V. Bekeris, G. R. Rubiolo, A. L. Cukierman, and S. Goyanes, "Magnetic properties of multi-walled carbon nanotube - epoxy composites" *Polymer*, vol. 46, no. 16, pp. 6090-6095, 2005.
- [69] T. Liu, Z. Zhao, W. W. Tjiu, J. Lv, and C. Wei, "Preparation and characterization of epoxy nanocomposites containing surface-modified graphene oxide" *Journal of Applied Polymer Science*, vol. 131, no. 9, 2014.
- [70] D. R. Bortz, E. G. Heras, and I. Martin-Gullon, "Impressive fatigue life and fracture toughness improvements in graphene oxide/epoxy composites" *Macromolecules*, vol. 45, no. 1, pp. 238-245, 2011.
- [71] C. Bao, Y. Guo, L. Song, Y. Kan, X. Qian, and Y. Hu, "In situ preparation of functionalized graphene oxide/epoxy nanocomposites with effective reinforcements" *Journal of Materials Chemistry*, vol. 21, no. 35, pp. 13290-13298, 2011.
- [72] Q. Liu, X. Zhou, X. Fan, C. Zhu, X. Yao, and Z. Liu, "Mechanical and thermal properties of epoxy resin nanocomposites reinforced with graphene oxide" *Polymer-Plastics Technology and Engineering*, vol. 51, no. 3, pp. 251-256, 2012.

APPENDICES

Appendix A: Results DMA.....	II
Appendix B: Results of the three-point flexural bending test.....	XXV
Appendix C: Risk assessment.....	XXXIV
Appendix D: Zeta potential.....	XXXVI
Appendix E: Data sheet epoxy system LY556/XB3473.....	XLII
Appendix F: Tables of surface tension and interfacial tension.....	XLVI
Appendix G: Characteristic binding energies and chemical shifts for XPS analyses	XLVIII

APPENDIX A - RESULTS DMA

Figure A 1 - Figure A 46 show the graphs of all the composites that were analysed by DMA during the M.Sc. thesis.

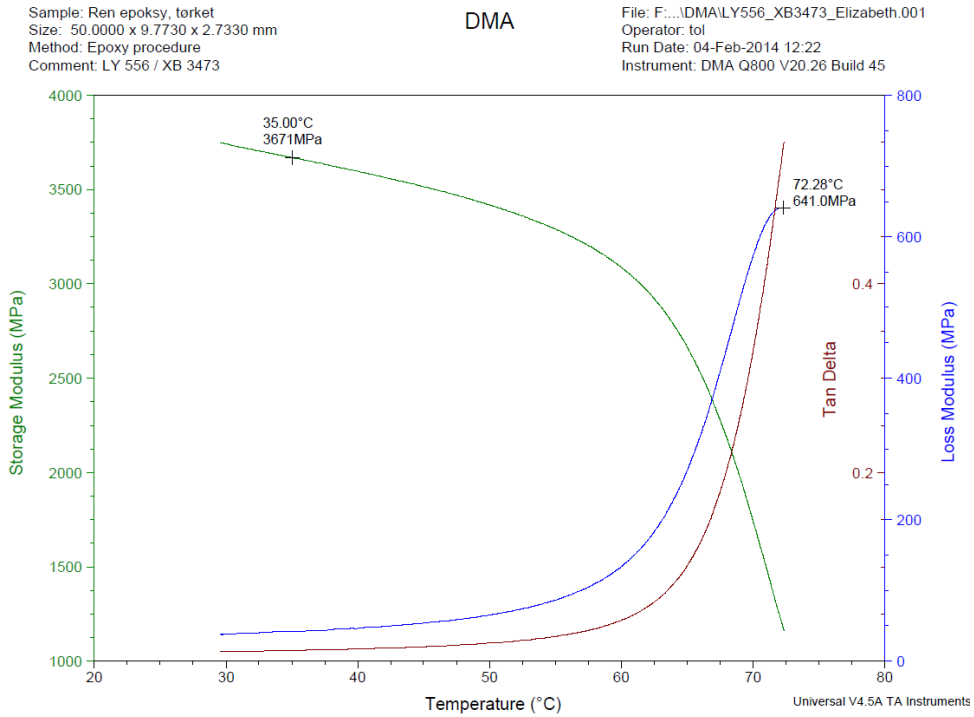


Figure A 1 – Epoxy /distilled water test, sample 1.

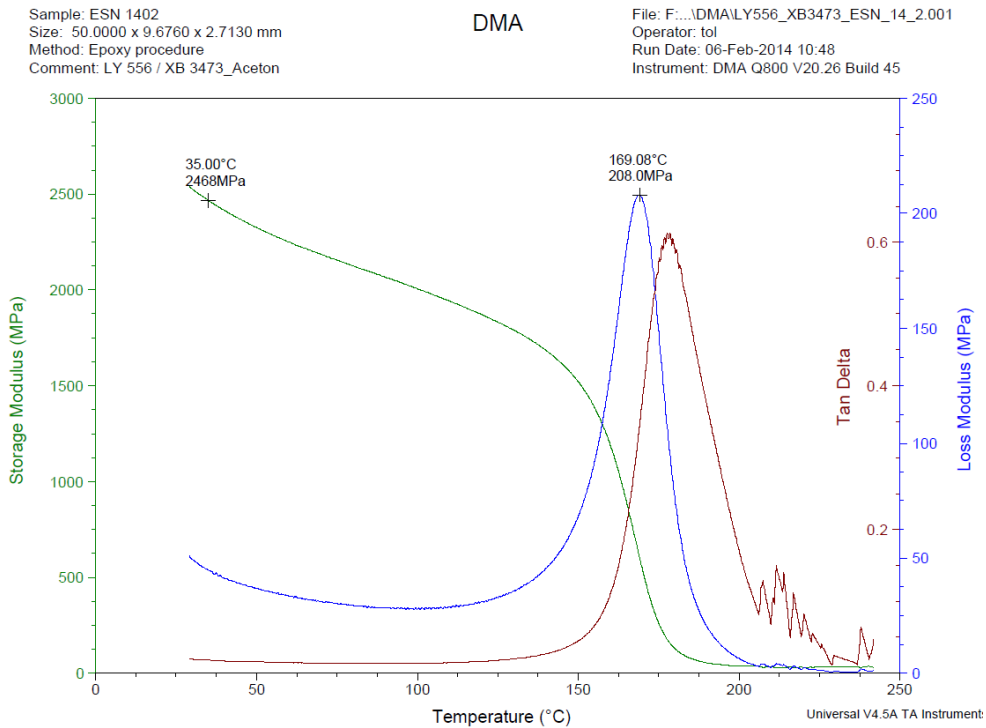


Figure A 2 – Epoxy acetone and GO, sample 1.

Sample: ESN 1403
Size: 50.0000 x 9.6659 x 2.6763 mm
Method: Epoxy procedure
Comment: LY 556 / XB 3473_Aceton

DMA

File: F:\...DMALY556_XB3473_ESN_14_3.001
Operator: esn
Run Date: 06-Feb-2014 13:31
Instrument: DMA Q800 V20.26 Build 45

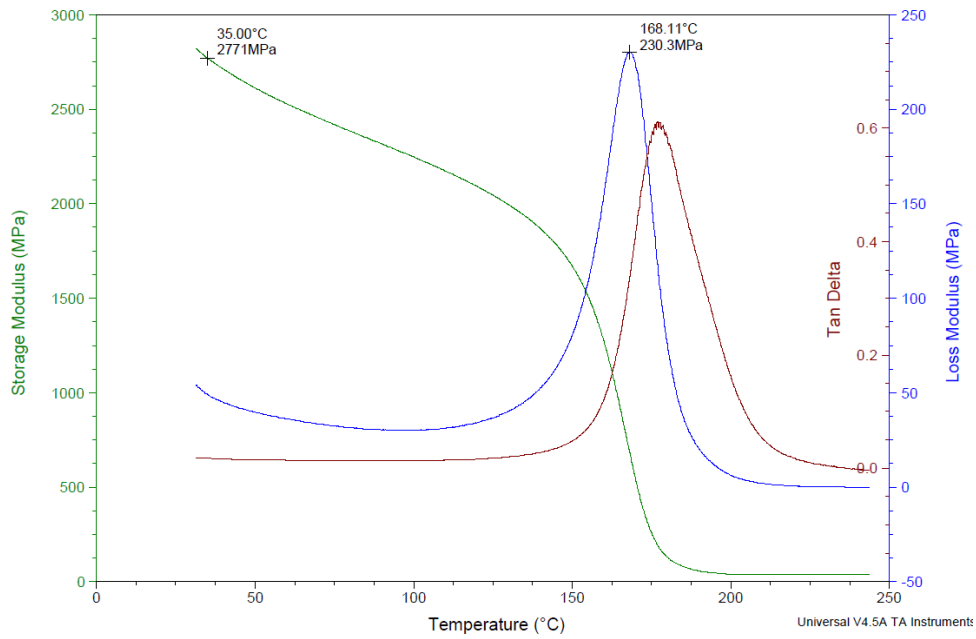


Figure A 3 – Epoxy acetone and GO, sample 2.

Sample: ESN 1404
Size: 50.0000 x 9.6990 x 2.6810 mm
Method: Epoxy procedure
Comment: LY 556 / XB 3473_Aceton

DMA

File: F:\...DMALY556_XB3473_ESN_14_4.002
Operator: esn
Run Date: 06-Feb-2014 15:07
Instrument: DMA Q800 V20.26 Build 45

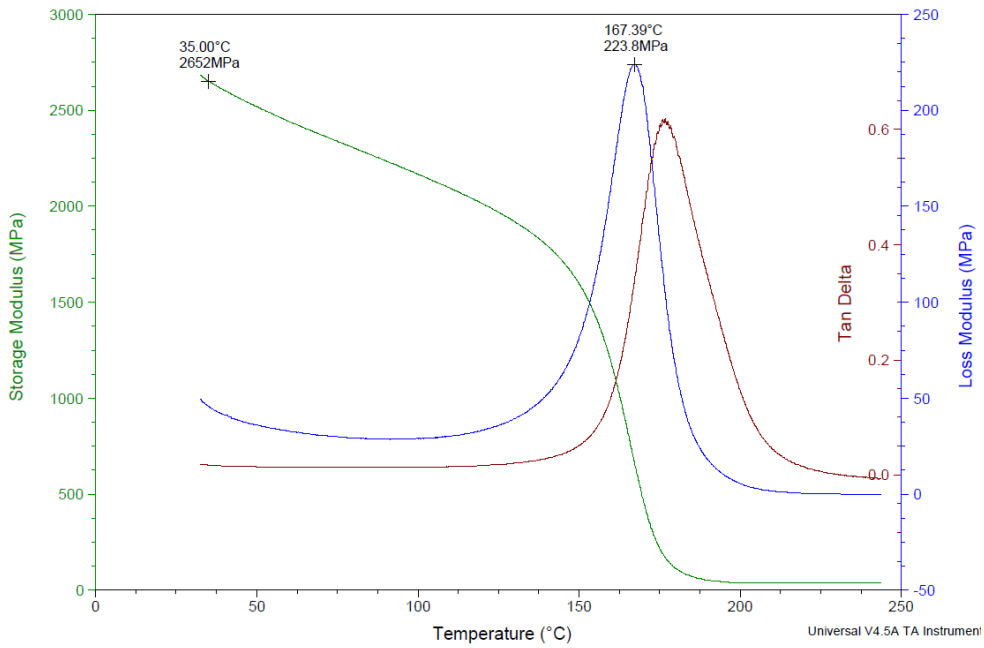


Figure A 4 - Epoxy acetone and GO, sample 3.

Sample: ESN 1405
 Size: 50.0000 x 9.6990 x 2.6810 mm
 Method: Epoxy procedure
 Comment: LY 556 / XB 3473_Aceton

DMA

File: F:\...DMA\LY556_XB3473_ESN_14_005.001
 Operator: esn
 Run Date: 13-Feb-2014 10:34
 Instrument: DMA Q800 V20.26 Build 45

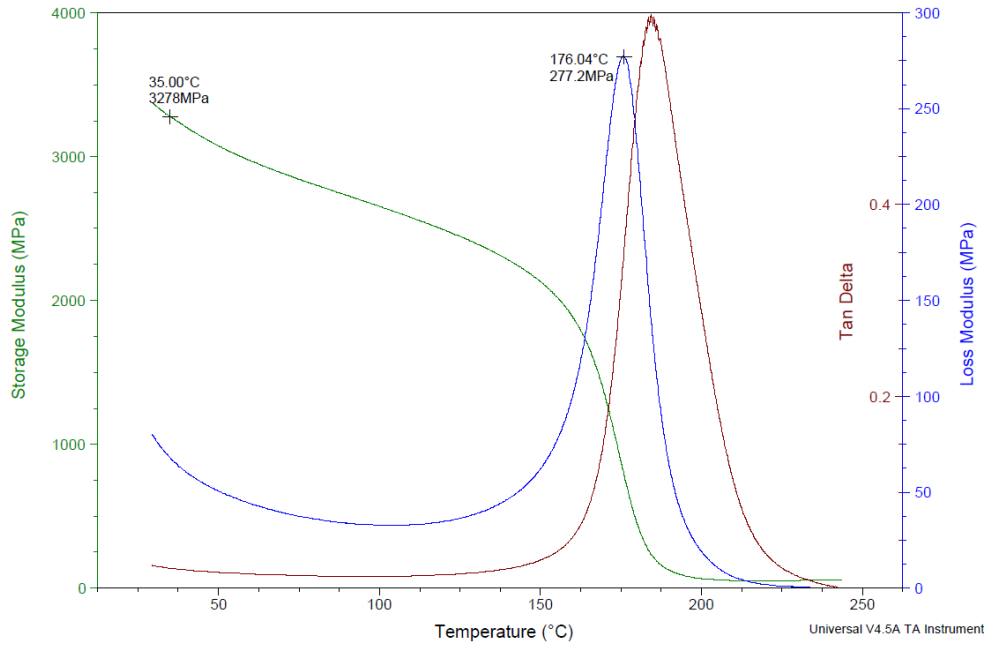


Figure A 5 – Epoxy and acetone blank, sample 1.

Sample: ESN 1406
 Size: 50.0000 x 9.7110 x 2.6250 mm
 Method: Epoxy procedure
 Comment: LY 556 / XB 3473_Aceton

DMA

File: F:\...DMA\LY556_XB3473_ESN_14_006.002
 Operator: esn
 Run Date: 13-Feb-2014 12:37
 Instrument: DMA Q800 V20.26 Build 45

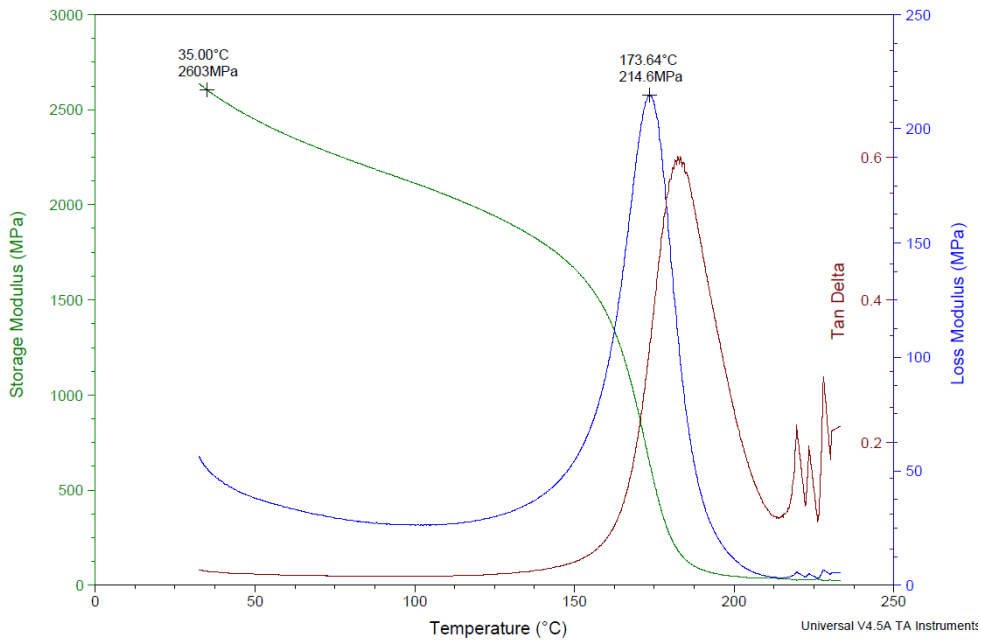


Figure A 6 - Epoxy and acetone blank, sample 2.

Sample: ESN 1407
Size: 50.0000 x 9.6740 x 2.5730 mm
Method: Epoxy procedure
Comment: LY 556 / XB 3473_Aceton

DMA

File: F:\DMA\LY556_XB3473_ESN_14_007.002
Operator: esn
Run Date: 13-Feb-2014 15:31
Instrument: DMA Q800 V20.26 Build 45

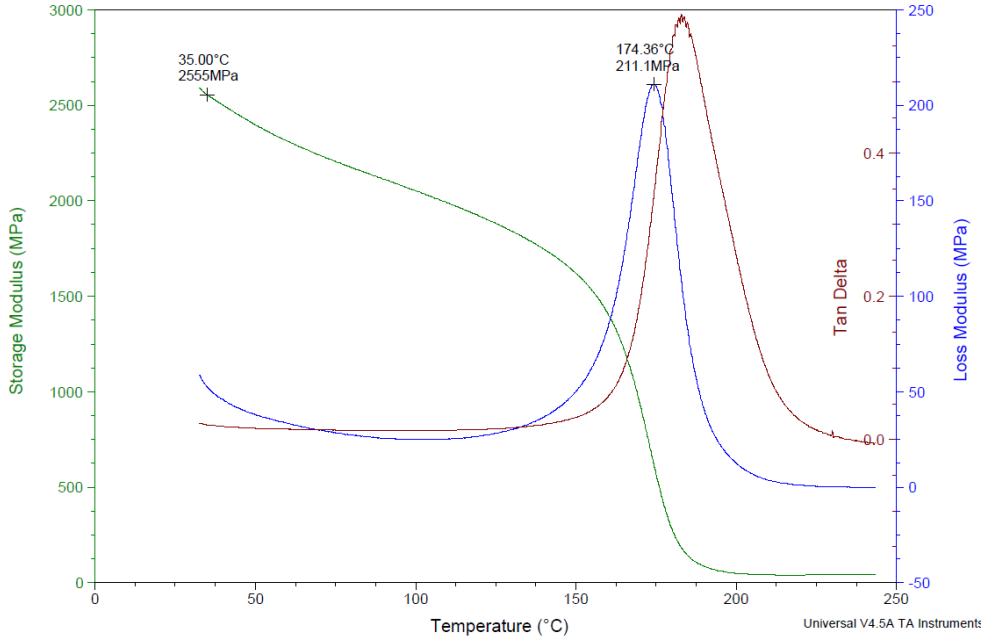


Figure A 7 - Epoxy and acetone blank, sample 3.

Sample: ESN 1408
Size: 50.0000 x 9.7180 x 2.6530 mm
Method: Epoxy procedure
Comment: LY 556 / XB 3473_Destillert vann

DMA

File: F:\DMA\LY556_XB3473_ESN_14_008.001
Operator: esn
Run Date: 14-Feb-2014 09:09
Instrument: DMA Q800 V20.26 Build 45

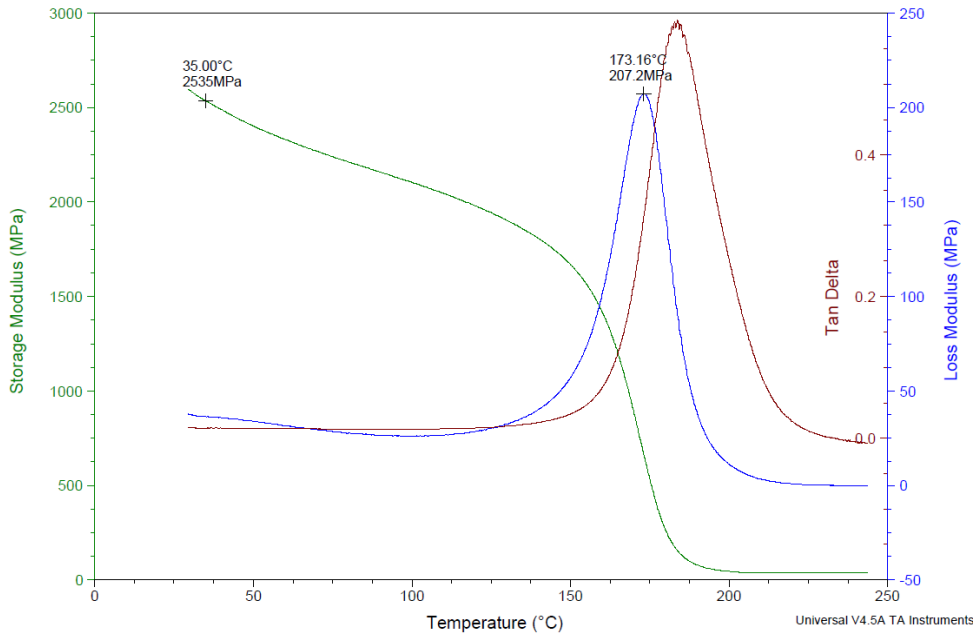


Figure A 8 - Epoxy and distilled water blank, sample 1.

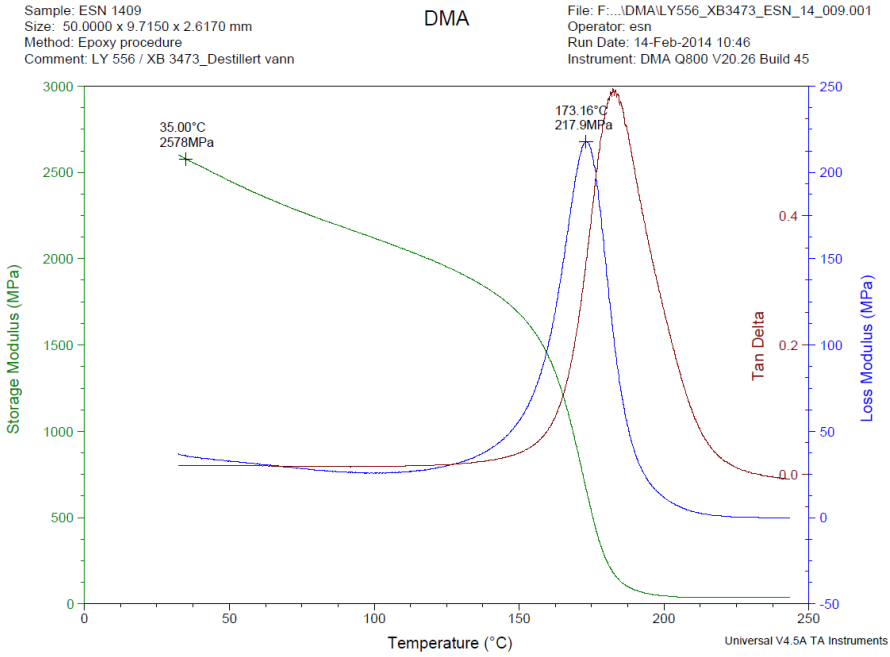


Figure A 9 - Epoxy and distilled water blank, sample 2.

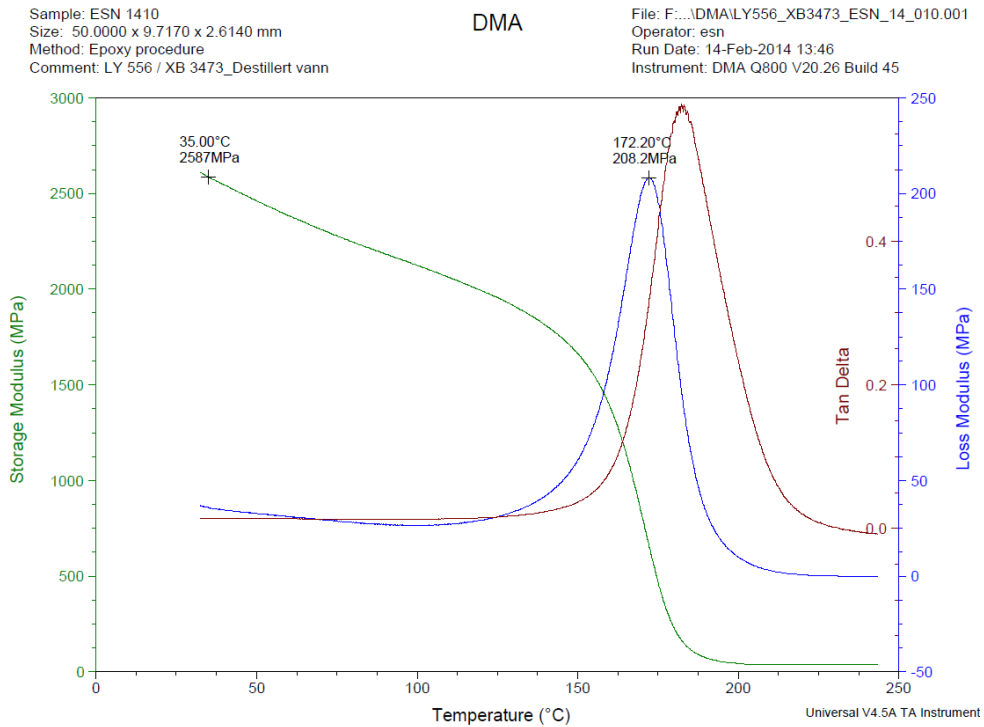


Figure A 10 - Epoxy and distilled water blank, sample 3.

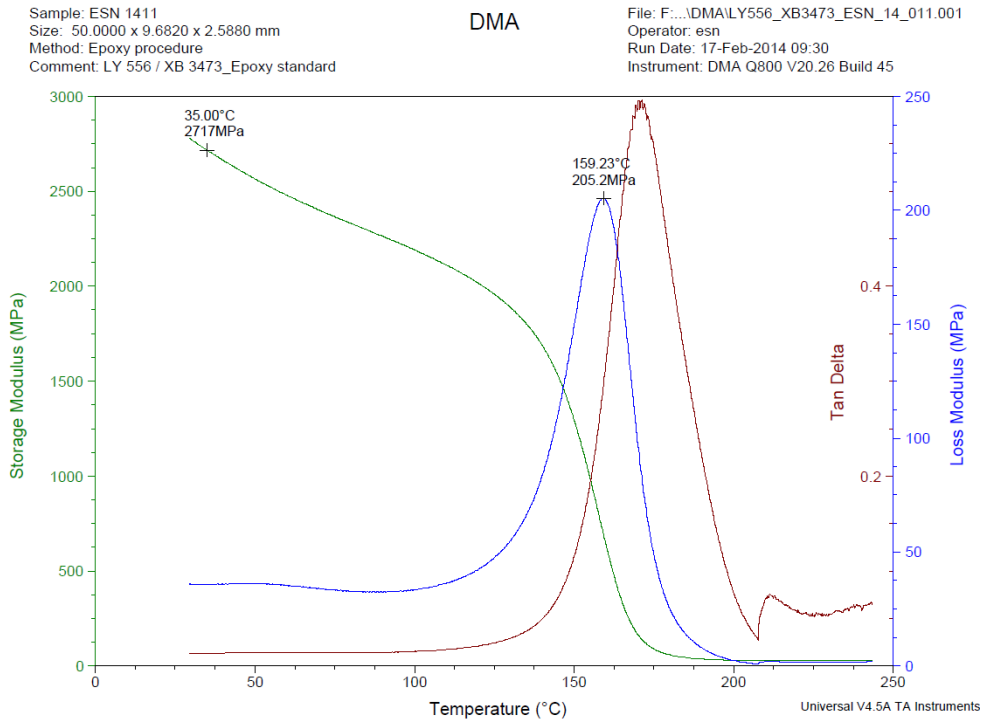


Figure A 11 - Epoxy standard, LY556/XB3473, sample 1

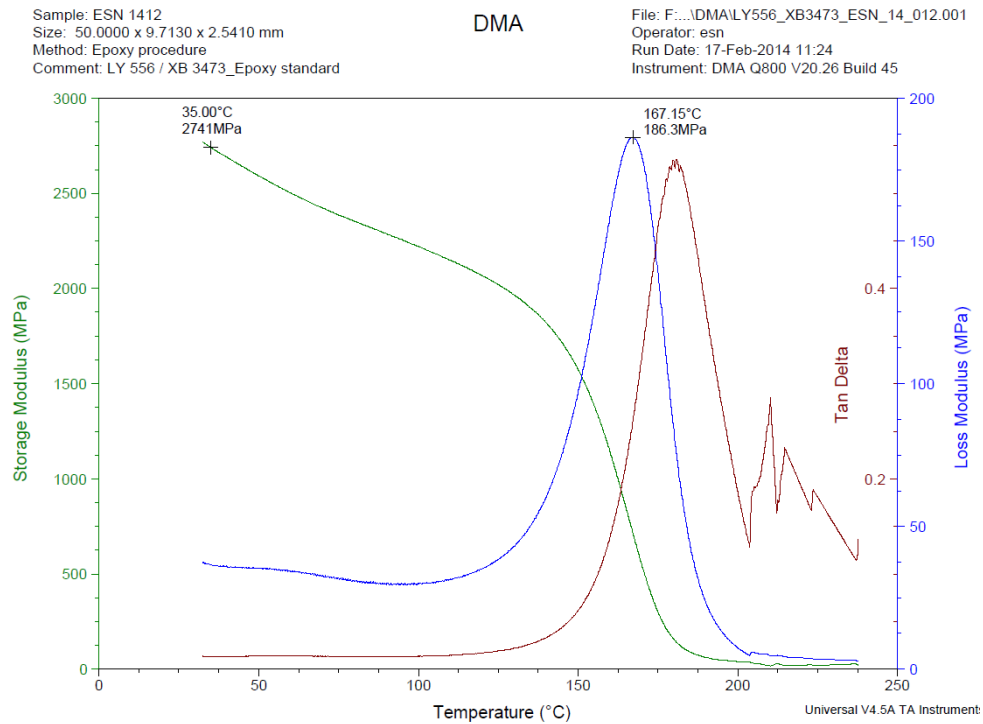


Figure A 12 – Epoxy standard, LY556/XB3473, sample 2

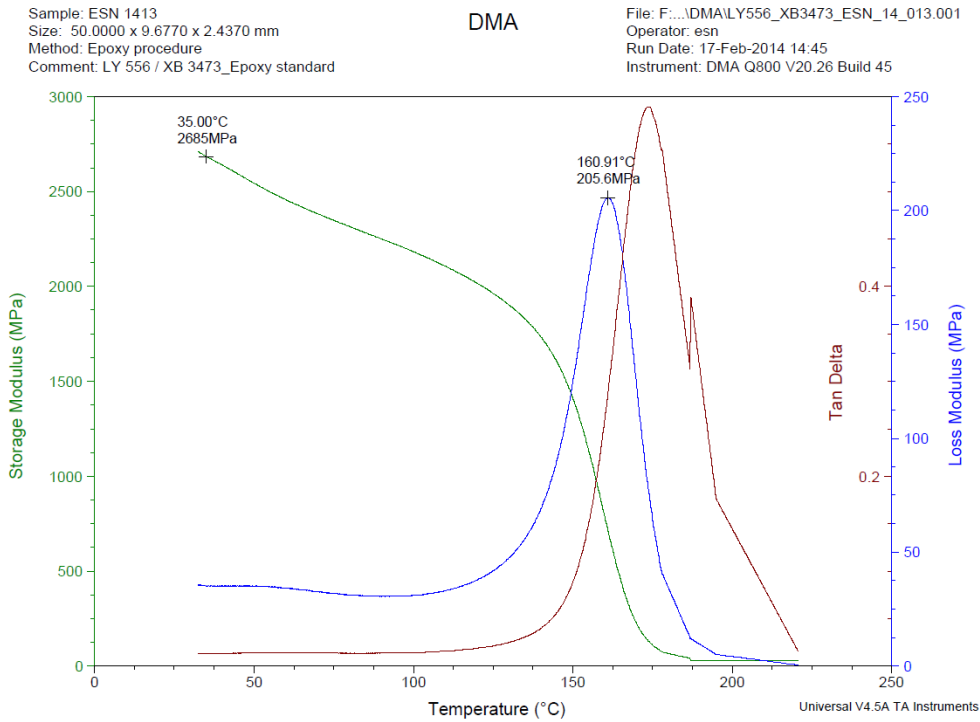


Figure A 13 – Epoxy standard, LY556/XB3473, sample 3.

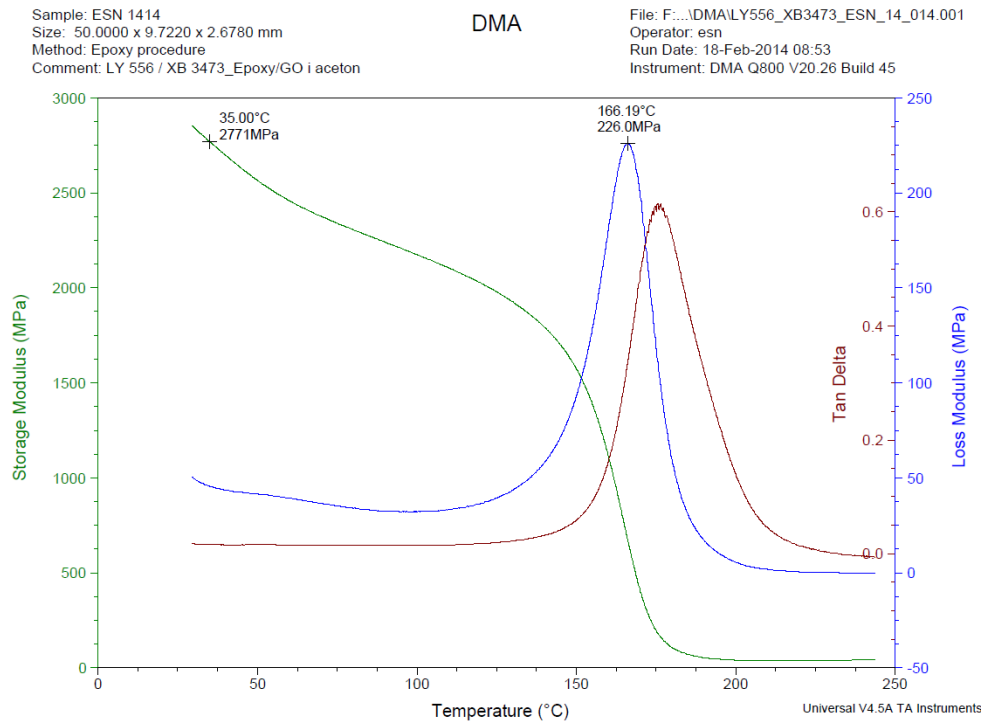


Figure A 14 – Epoxy with acetone and GO, sample 4.

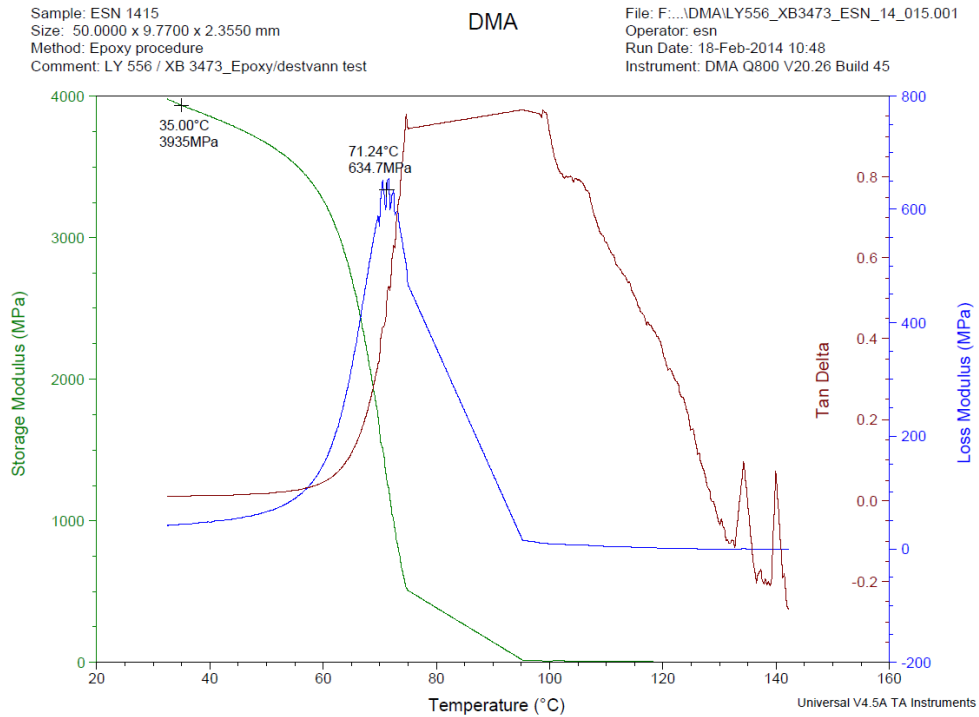


Figure A 15 – Epoxy/distilled water test, sample 2.

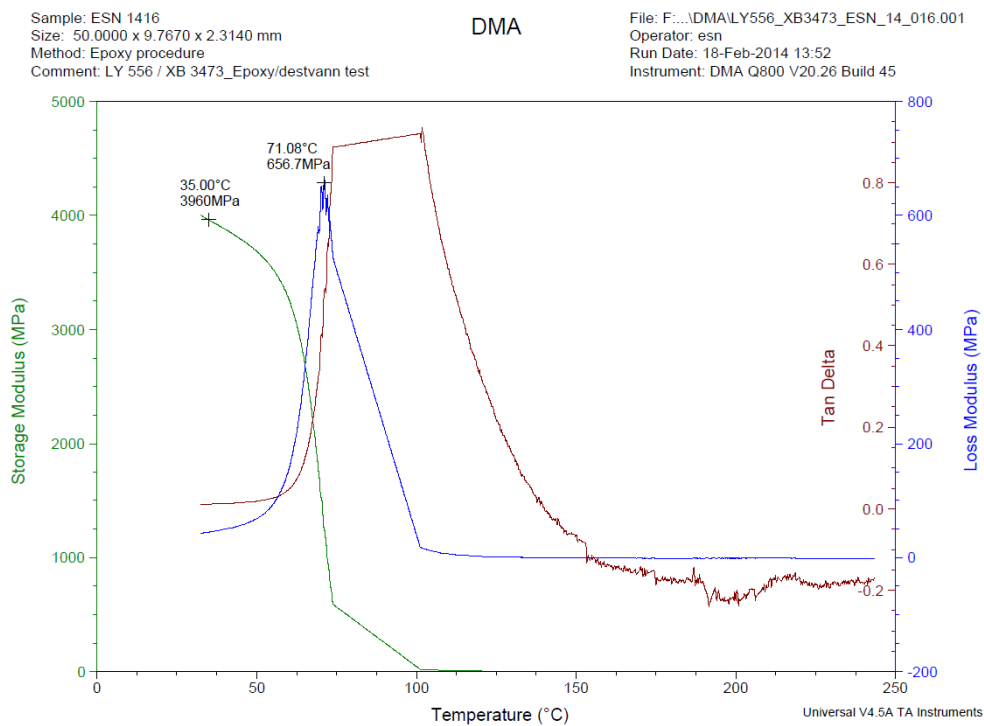


Figure A 16 - Epoxy /distilled water test, sample 3.

Sample: ESN 1417
Size: 50.0000 x 9.7210 x 2.1310 mm
Method: Epoxy procedure
Comment: LY 556 / XB 3473_Epoxy standard

DMA

File: F:\...DMA\LY556_XB3473_ESN_14_017.001
Operator: esn
Run Date: 19-Feb-2014 08:57
Instrument: DMA Q800 V20.26 Build 45

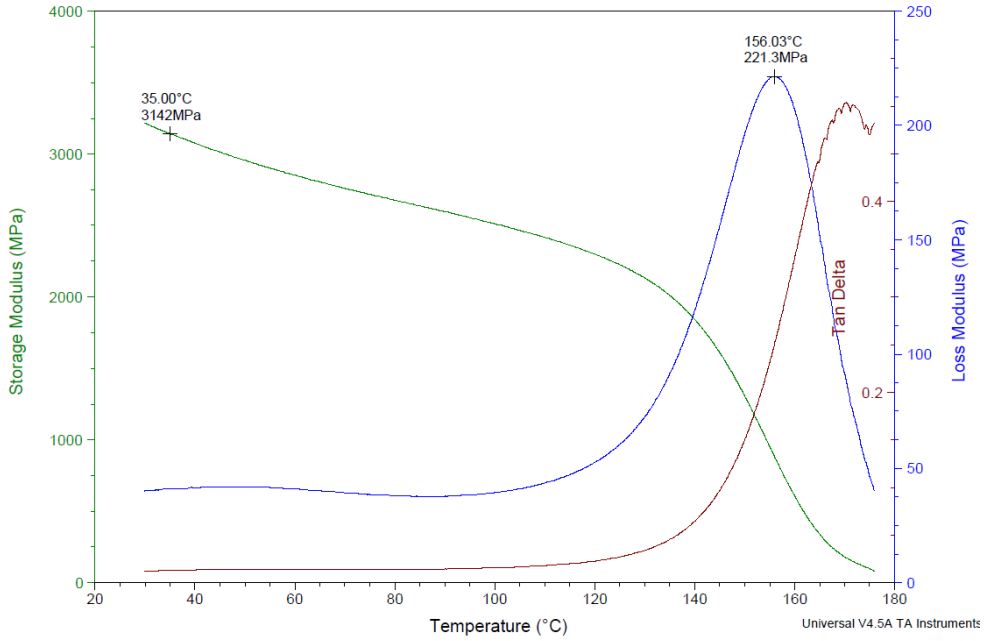


Figure A 17 – Epoxy standard, LY556/XB3473, sample 4.

Sample: ESN 1418
Size: 50.0000 x 9.6750 x 2.9950 mm
Method: Epoxy procedure_2002_2014
Comment: LY 556 / XB 3473_Epoxy fGO i dH2O

DMA

File: F:\...DMA\LY556_XB3473_ESN_14_018.001
Operator: esn
Run Date: 24-Feb-2014 10:30
Instrument: DMA Q800 V20.26 Build 45

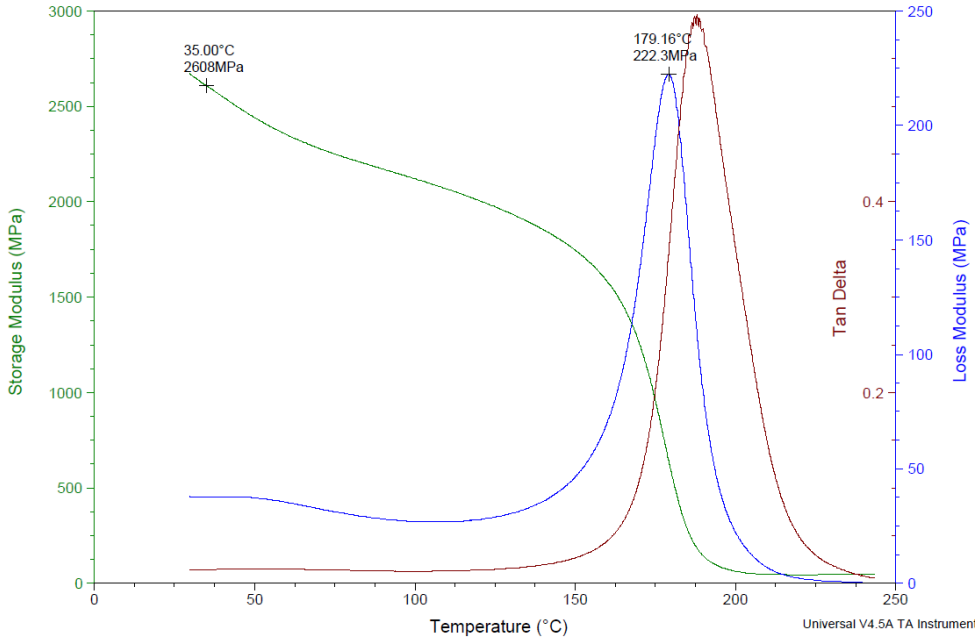


Figure A 18 – Epoxy with FGO(XB3473) in distilled water, sample 1.

Sample: ESN 1419
Size: 50.0000 x 9.6730 x 3.0320 mm
Method: Epoxy procedure_2002_2014
Comment: LY 556 / XB 3473_Epoxy fGO i dH2O

DMA

File: F:\...DMAILY556_XB3473_ESN_14_019.001
Operator: esn
Run Date: 24-Feb-2014 12:16
Instrument: DMA Q800 V20.26 Build 45

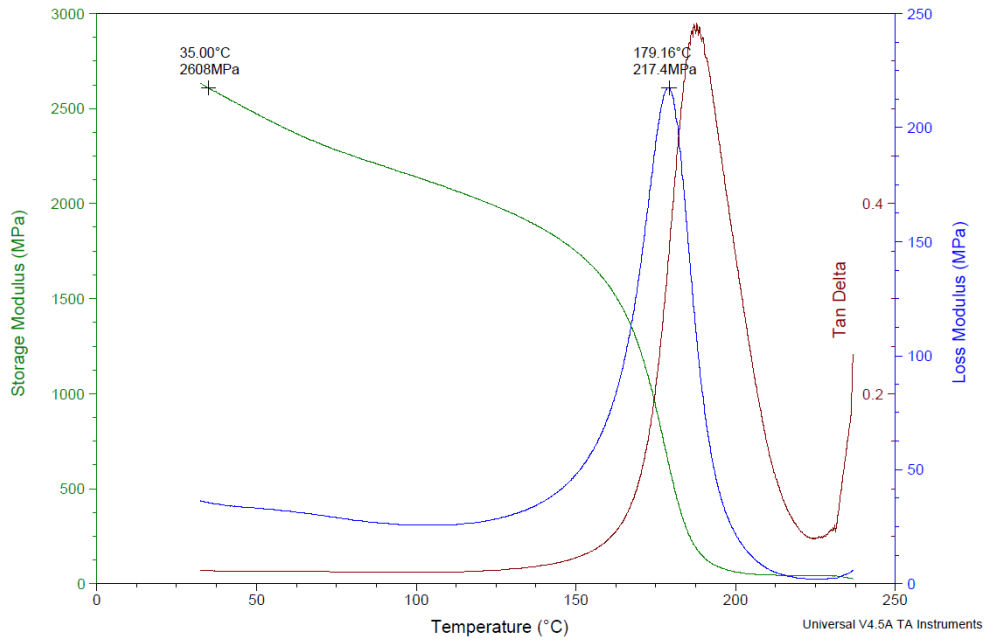


Figure A 19 - Epoxy with FGO (XB3473) in distilled water, sample 2.

Sample: ESN 1420
Size: 50.0000 x 9.6760 x 2.9930 mm
Method: Epoxy procedure_2002_2014
Comment: LY 556 / XB 3473_Epoxy fGO i dH2O

DMA

File: F:\...DMAILY556_XB3473_ESN_14_020.001
Operator: esn
Run Date: 24-Feb-2014 15:46
Instrument: DMA Q800 V20.26 Build 45

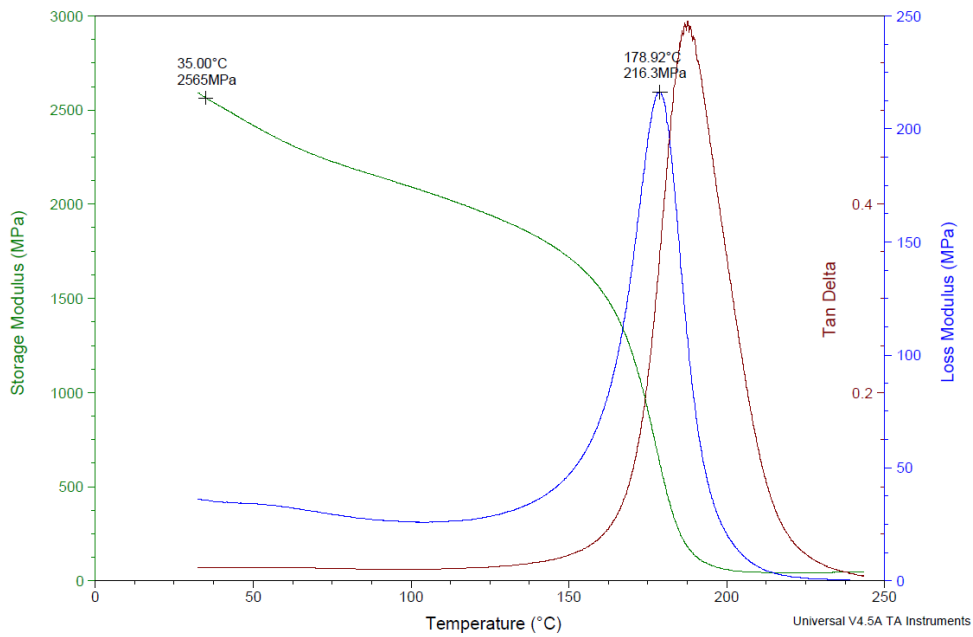


Figure A 20 - Epoxy with FGO (XB3473) in distilled water, sample 3.

Sample: ESN 1421
Size: 50.0000 x 9.7140 x 3.0970 mm
Method: Epoxy procedure_2002_2014
Comment: LY 556 / XB 3473_Epoxy fGO2 i acetone

DMA

File: F:\DMALY556_XB3473_ESN_14_021.001
Operator: esn
Run Date: 26-Feb-2014 09:12
Instrument: DMA Q800 V20.26 Build 45

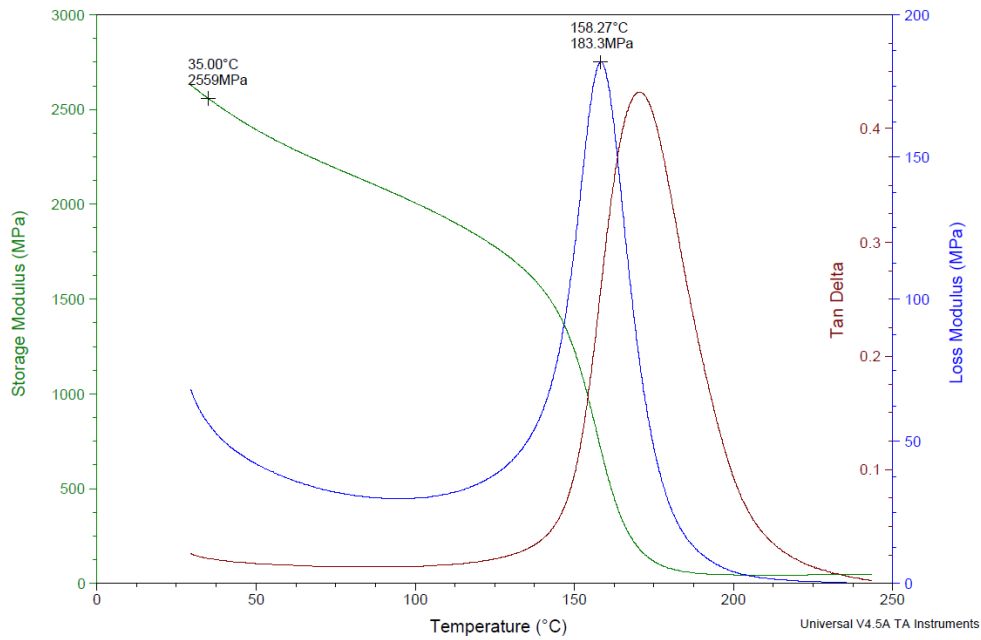


Figure A 21 - Epoxy with FGO (PPDA) in acetone, sample 1.

Sample: ESN 1422
Size: 50.0000 x 9.7160 x 3.0250 mm
Method: Epoxy procedure_2002_2014
Comment: LY 556 / XB 3473_Epoxy fGO2 i acetone

DMA

File: F:\DMALY556_XB3473_ESN_14_022.001
Operator: esn
Run Date: 26-Feb-2014 11:12
Instrument: DMA Q800 V20.26 Build 45

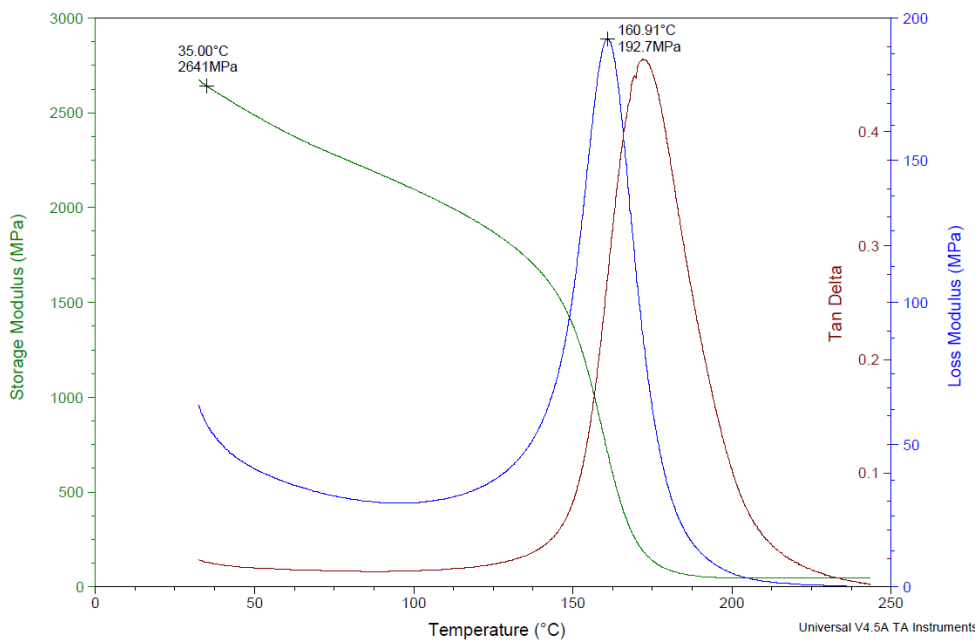


Figure A 22 - Epoxy with FGO (PPDA) in acetone, sample 2.

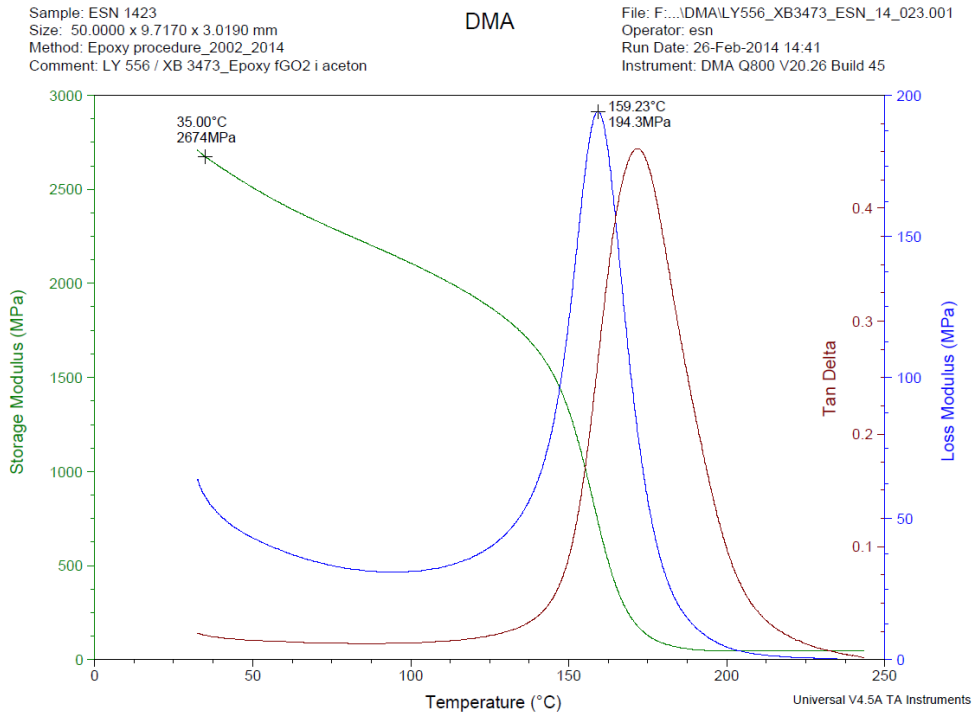


Figure A 23 - Epoxy with FGO (PPDA) in acetone, sample 3.

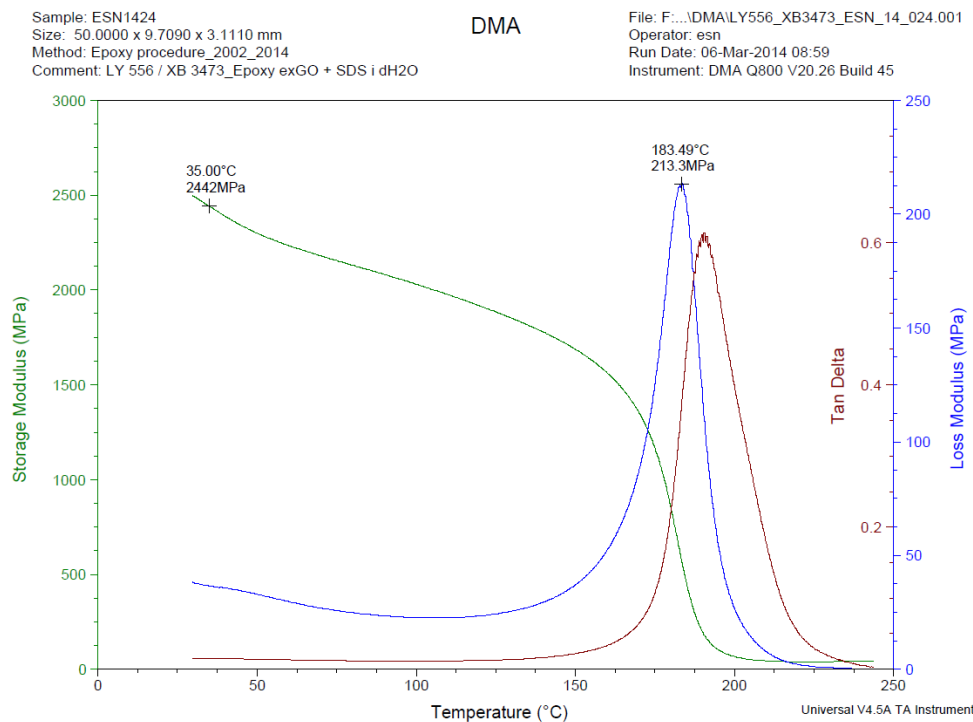


Figure A 24 – Epoxy with EXGO (1000°C) and SDS in distilled water, sample 1.

Sample: ESN1425
Size: 50.0000 x 9.7060 x 2.9950 mm
Method: Epoxy procedure_2002_2014
Comment: LY 556 / XB 3473_Epoxy exGO + SDS i dH2O

DMA

File: F:\...DMAILY556_XB3473_ESN_14_025.001
Operator: esn
Run Date: 06-Mar-2014 14:16
Instrument: DMA Q800 V20.26 Build 45

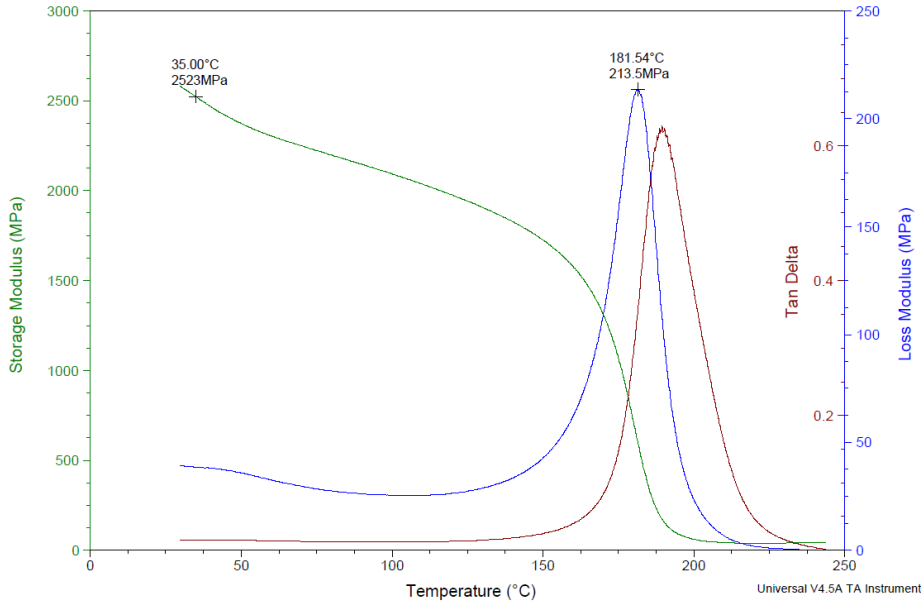


Figure A 25 - Epoxy with EXGO (1000°C) and SDS in distilled water; sample 2.

Sample: ESN1426
Size: 50.0000 x 9.6700 x 2.7060 mm
Method: Epoxy procedure_2002_2014
Comment: LY 556 / XB 3473_Epoxy exGO + SDS i dH2O

DMA

File: F:\...DMAILY556_XB3473_ESN_14_026.001
Operator: esn
Run Date: 06-Mar-2014 17:11
Instrument: DMA Q800 V20.26 Build 45

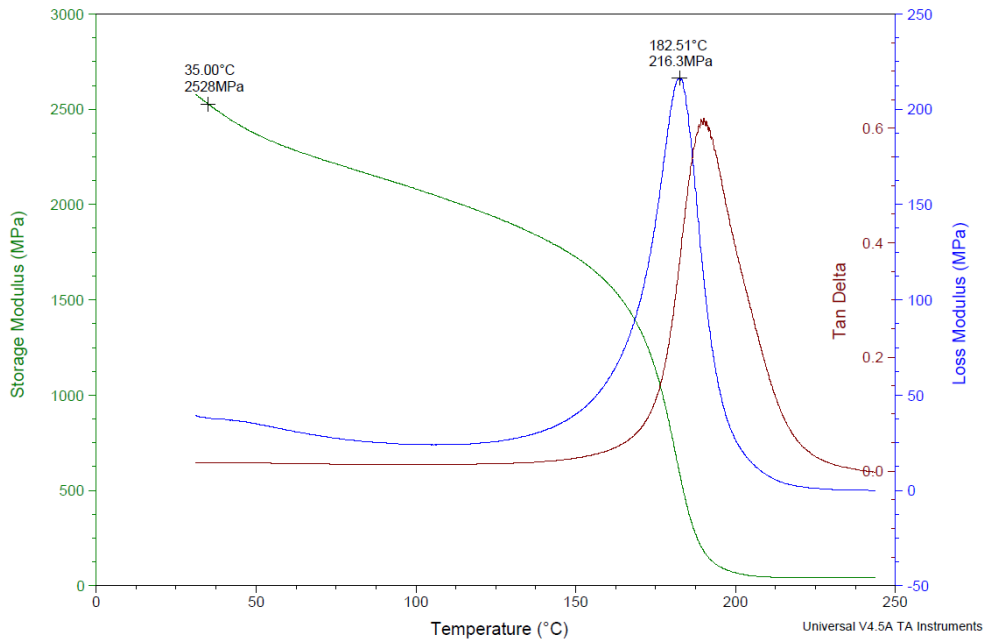


Figure A 26 - Epoxy with EXGO (1000°C) and SDS in distilled water; sample 3.

Sample: ESN1427
Size: 50.0000 x 9.7100 x 2.9530 mm
Method: Epoxy procedure_2002_2014
Comment: LY 556 / XB 3473_Epoxy exGO i acetone

DMA

File: F:\...DMA\LY556_XB3473_ESN_14_027.001
Operator: esn
Run Date: 07-Mar-2014 09:42
Instrument: DMA Q800 V20.26 Build 45

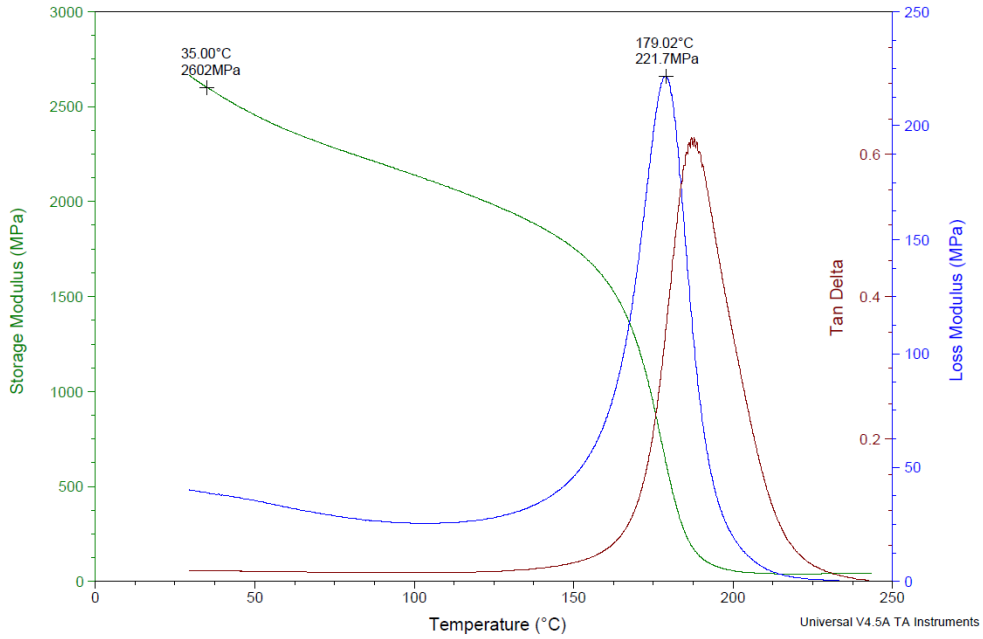


Figure A 27 – Epoxy with EXGO (300°C) in acetone, sample 1.

Sample: ESN1428
Size: 50.0000 x 9.7100 x 3.0070 mm
Method: Epoxy procedure_2002_2014
Comment: LY 556 / XB 3473_Epoxy exGO i acetone

DMA

File: F:\...DMA\LY556_XB3473_ESN_14_028.001
Operator: esn
Run Date: 07-Mar-2014 11:37
Instrument: DMA Q800 V20.26 Build 45

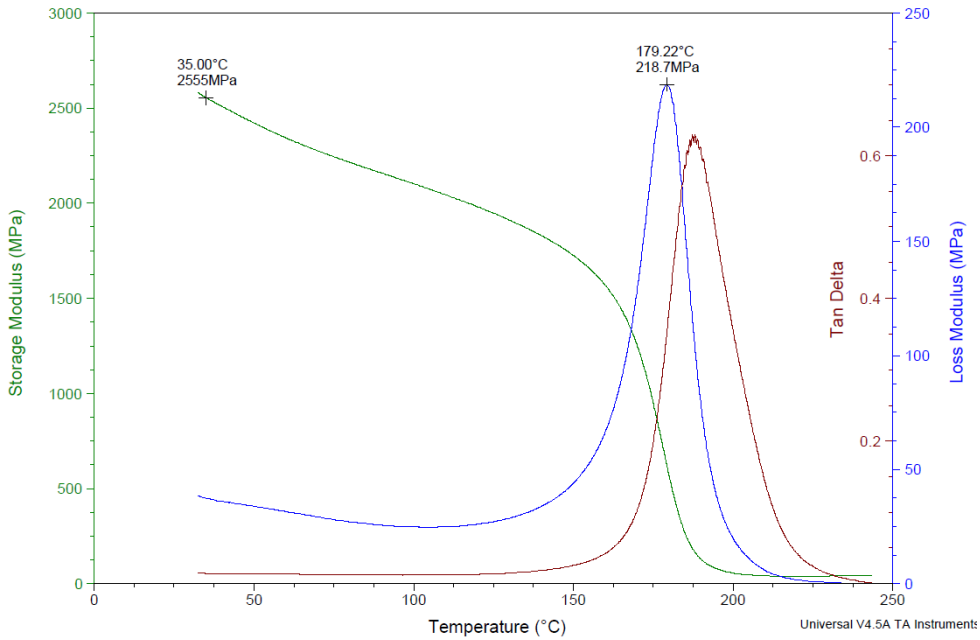


Figure A 28 - Epoxy with EXGO (300°C) in acetone, sample 2.

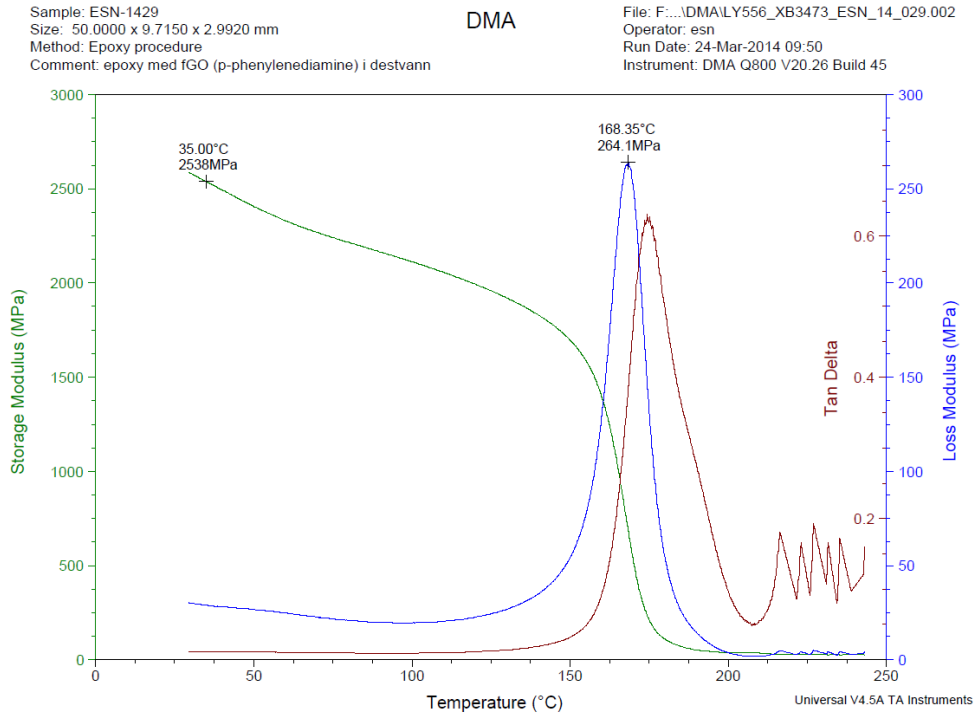


Figure A 29 – Epoxy with FGO (PPDA) in distilled water, sample 1.

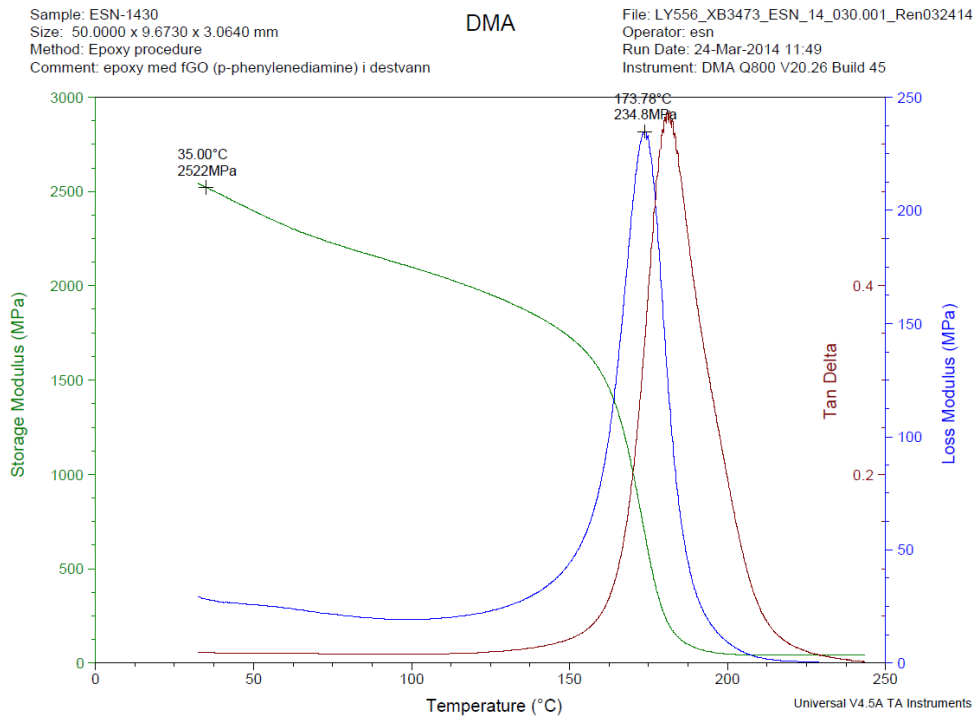


Figure A 30 – Epoxy with FGO (PPDA) in distilled water, sample 2.

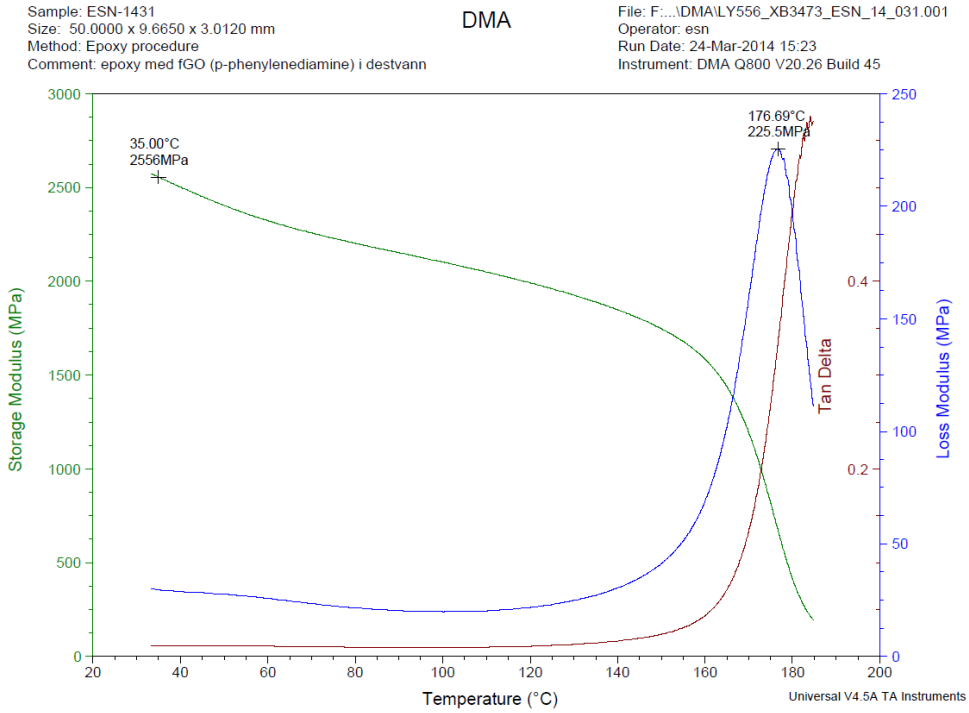


Figure A 31 – Epoxy with FGO (PPDA) in distilled water, sample 3.

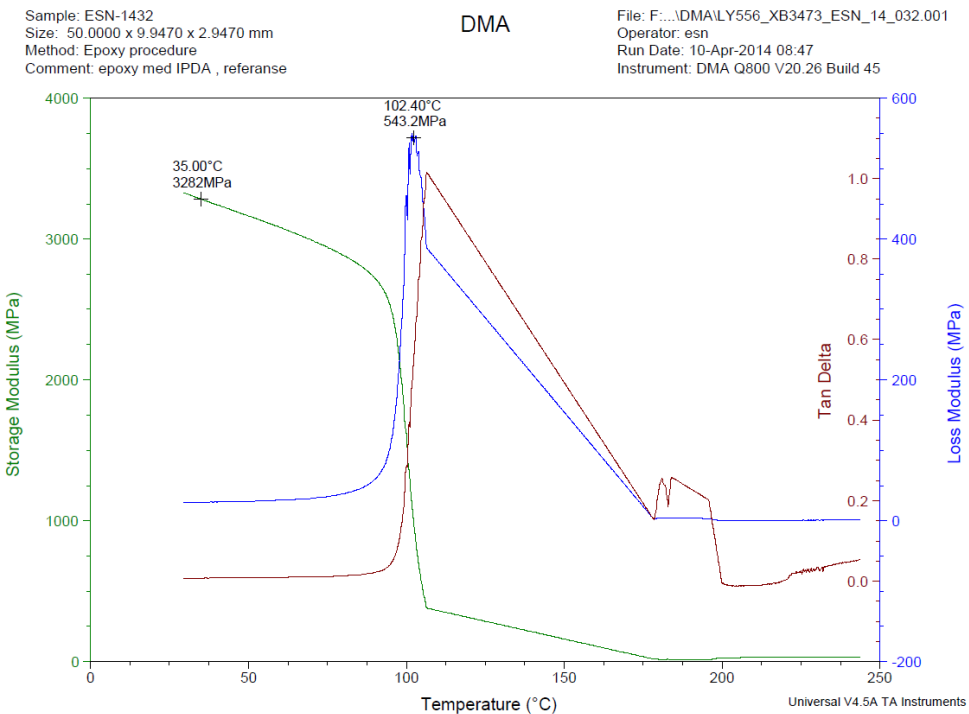


Figure A 32 – Epoxy LY556/IPDA reference standard, sample 1.

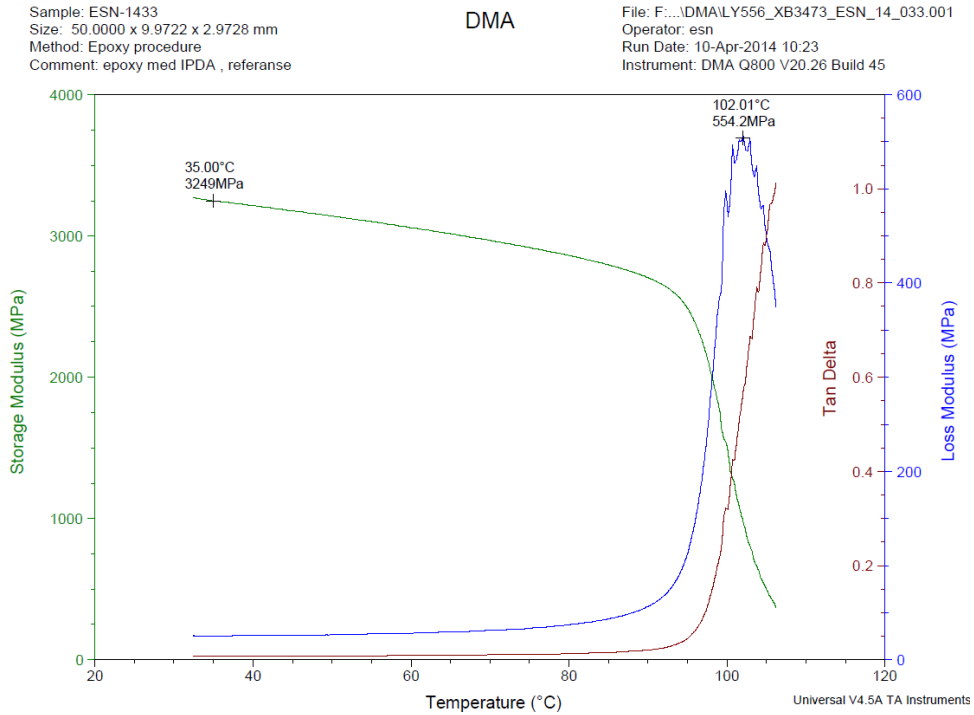


Figure A 33 – Epoxy LY556/IPDA reference standard, sample 2.

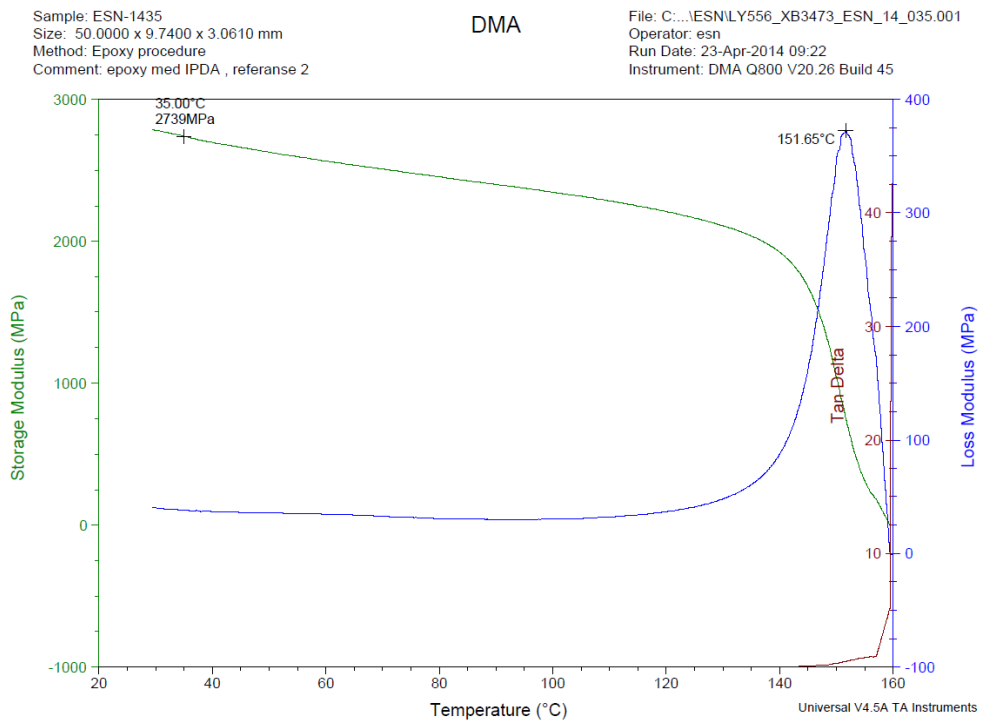


Figure A 34 – Epoxy LY556/IPDA reference standard 2, sample 1.

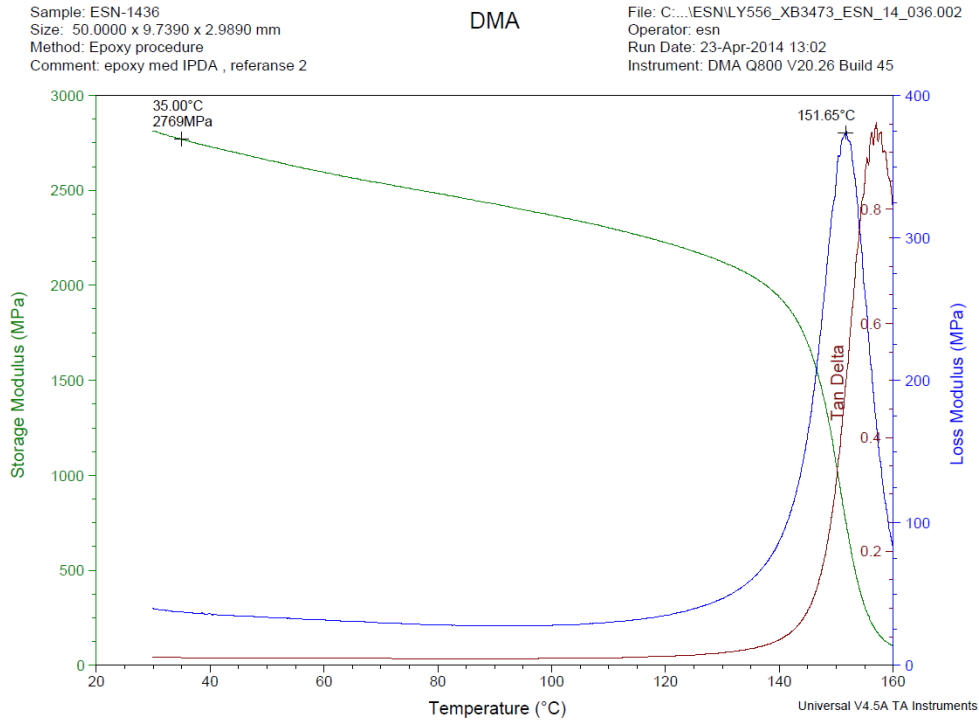


Figure A 35 - Epoxy LY556/IPDA reference standard 2, sample 2.

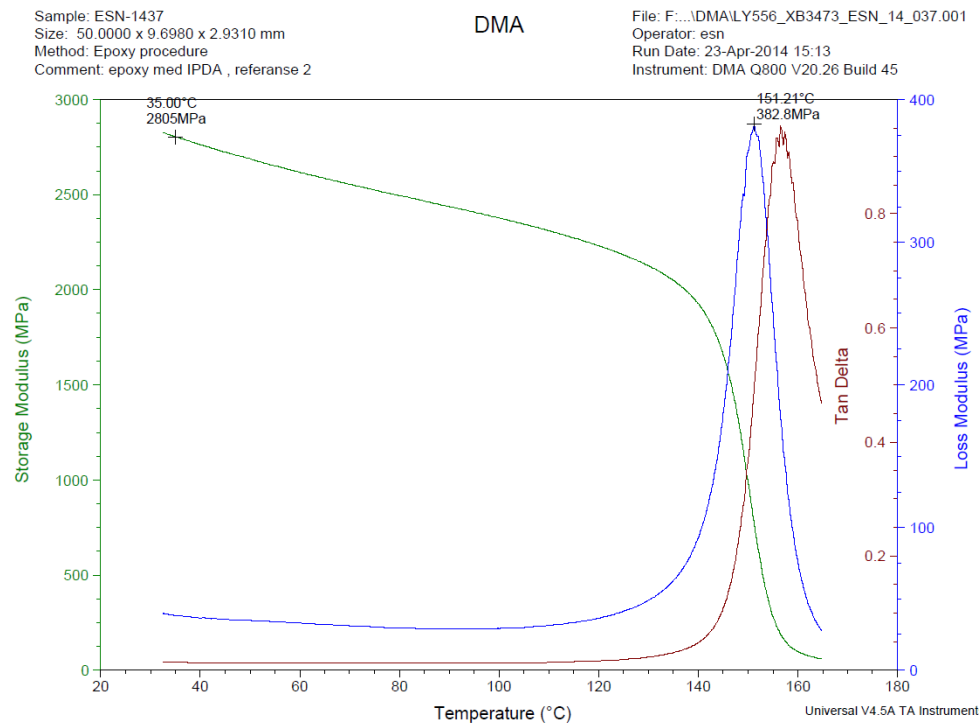


Figure A 36 – Epoxy LY556/IPDA reference standard 2, sample 3.

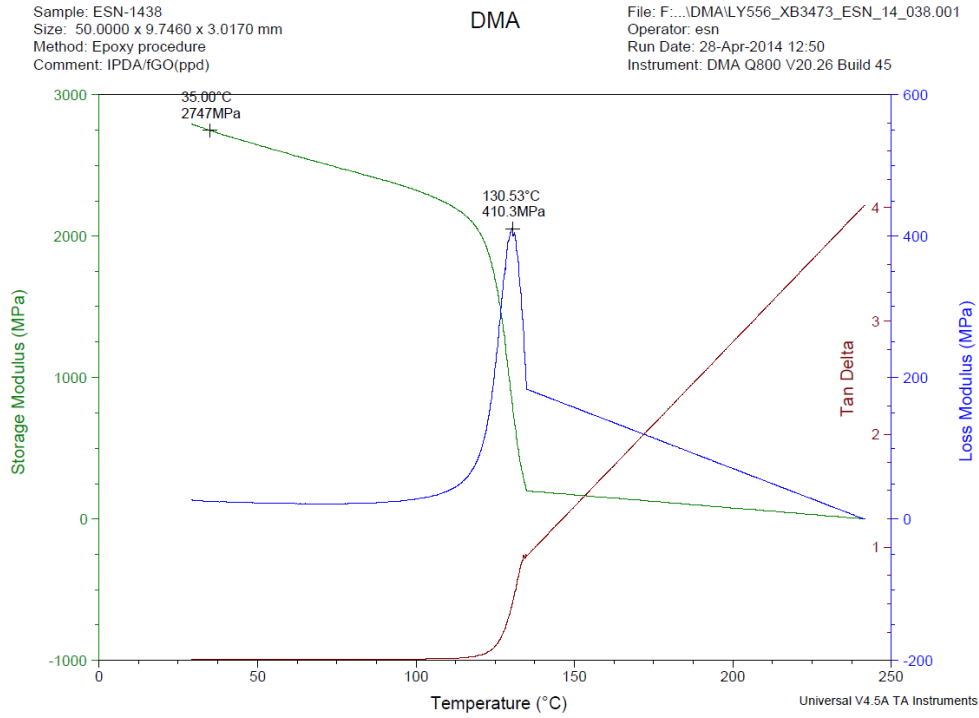


Figure A 37 – Epoxy (LY556/IPDA) with FGO (PPDA), sample 1.

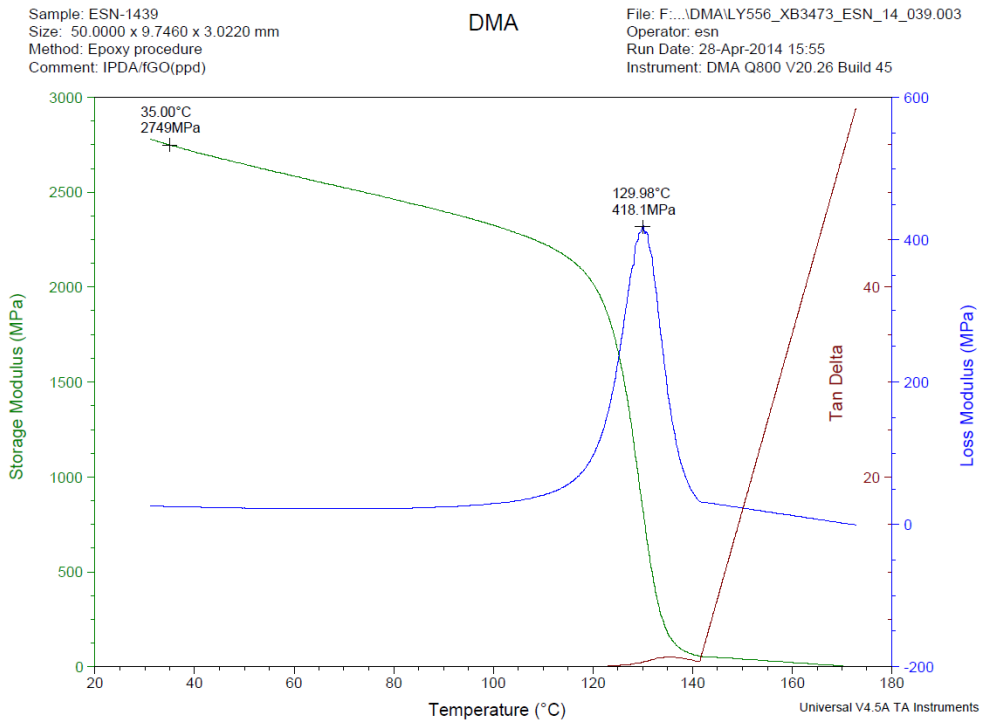


Figure A 38 – Epoxy (LY556/IPDA) with FGO (PPDA), sample 2.

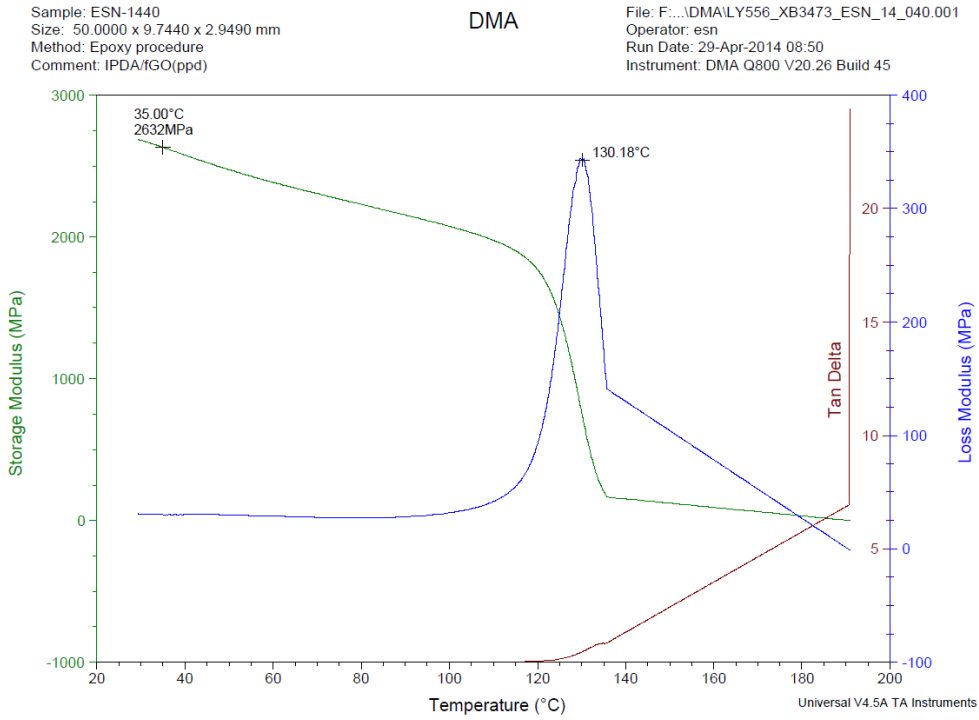


Figure A 39 – Epoxy (LY556/IPDA) with FGO (PPDA), sample 3.

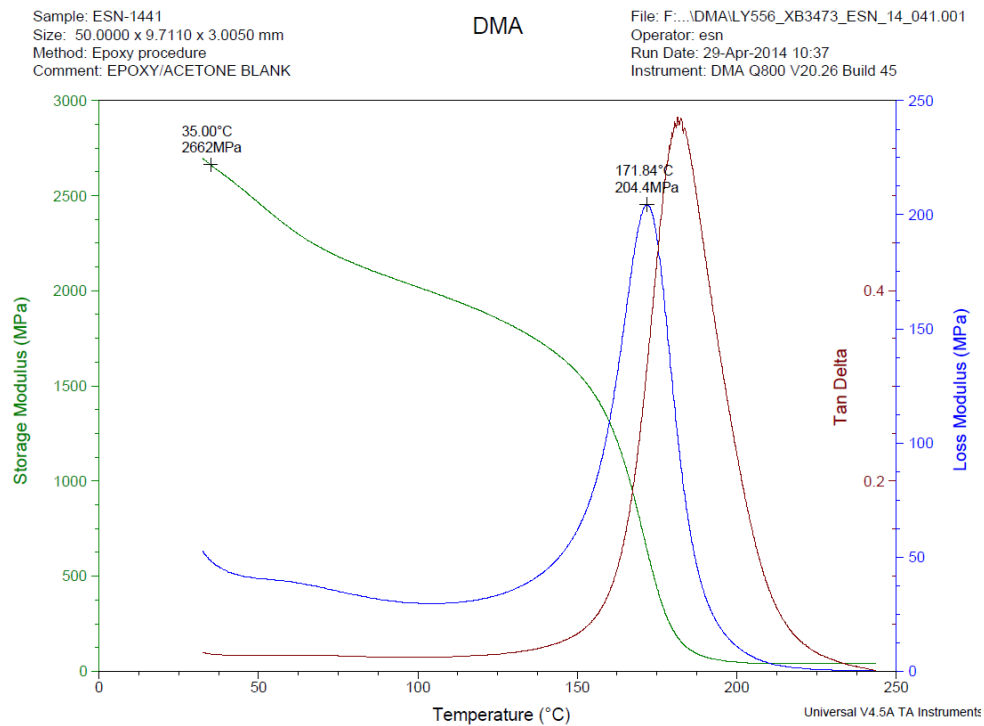


Figure A 40 – Epoxy/acetone blank, (LY556/XB3473), sample 5.

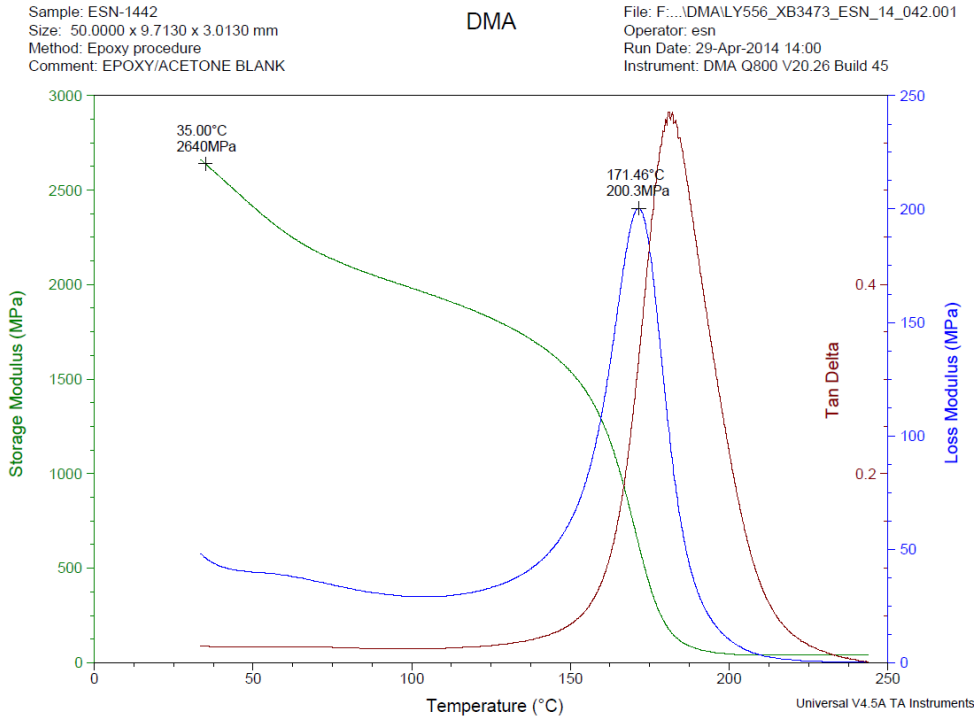


Figure a 41–Epoxy/acetone blank, (LY556/XB3473), sample 6.

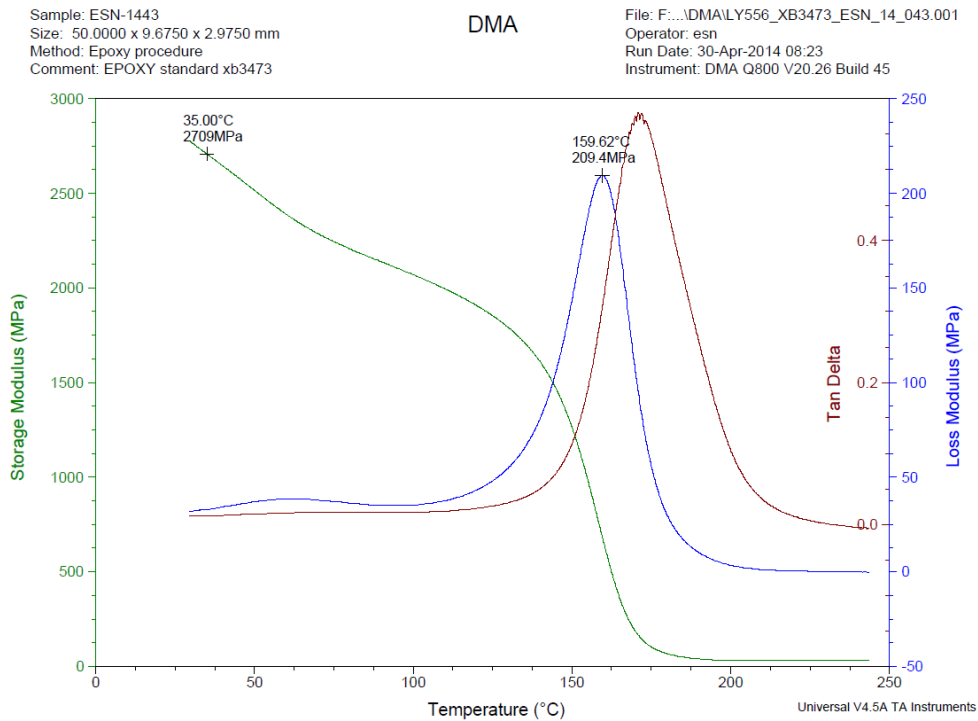


Figure A 42– Epoxy reference standard (LY556/XB3473), sample 5.

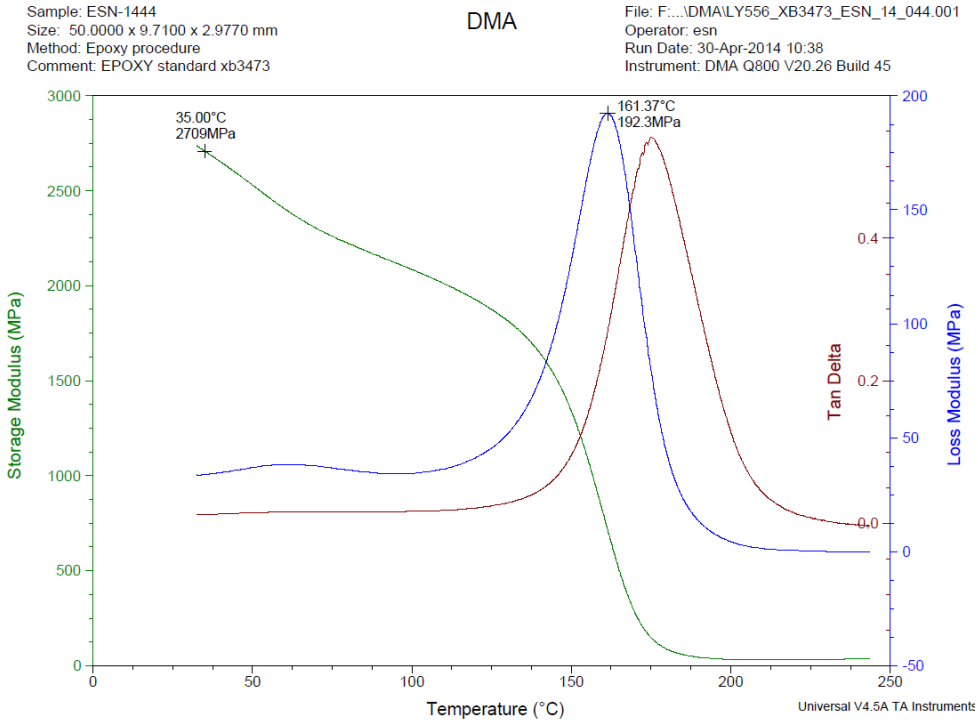


Figure A 43 – Epoxy reference standard (LY556/XB3473), sample 6.

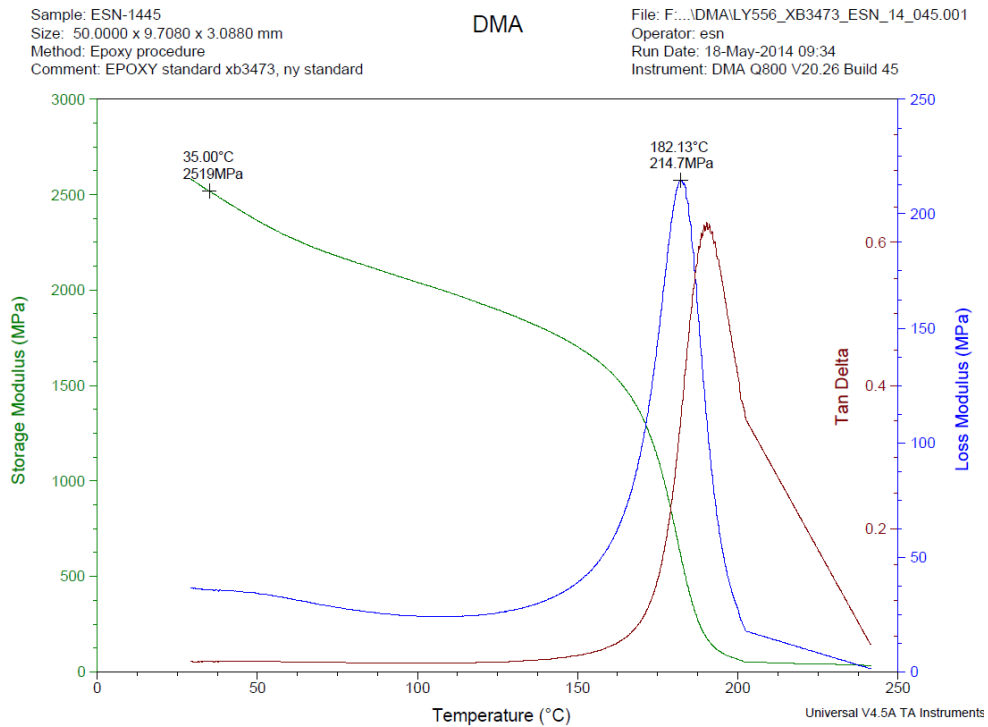


Figure A 44 – LY556/XB3473 reference standard 2, sample 1.

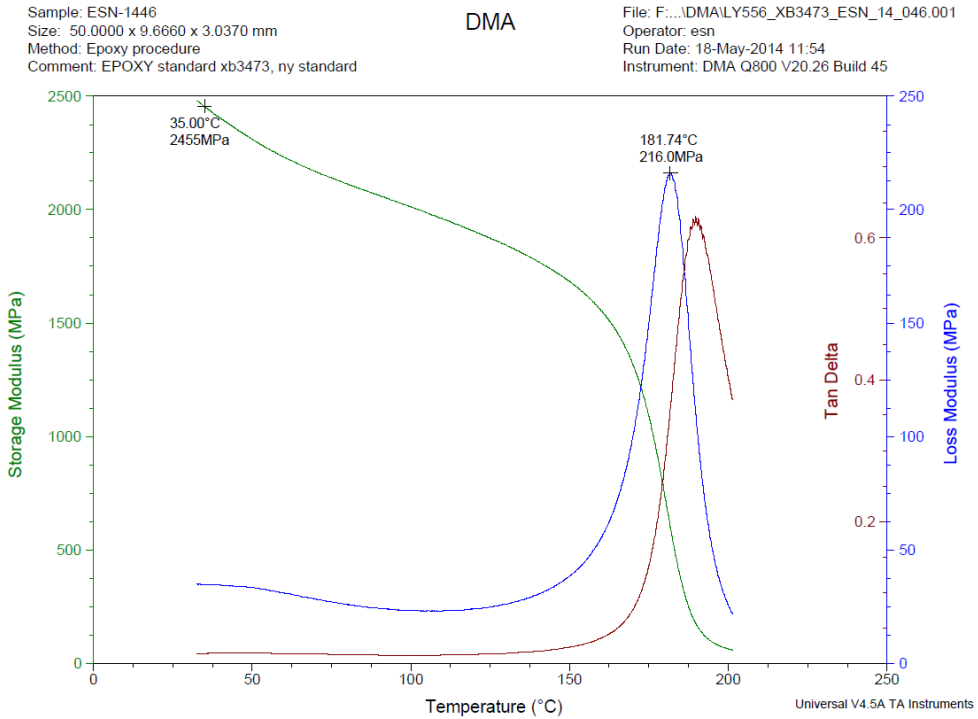


Figure A 45 - LY556/XB3473 reference standard 2, sample 2.

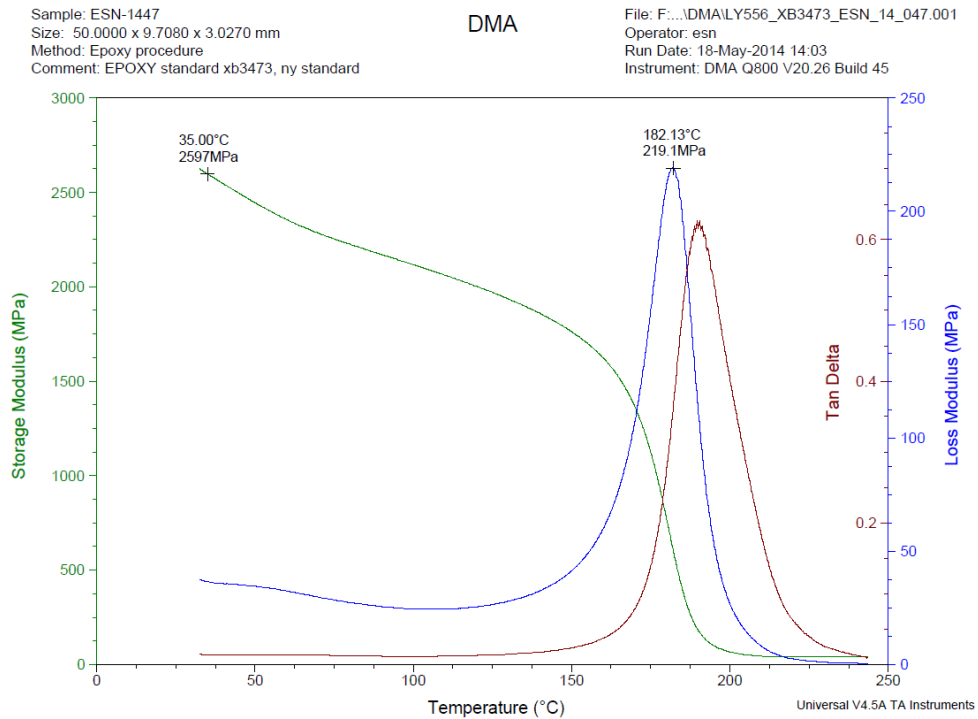


Figure A 46 – LY556/XB3473 reference standard, sample 3.

APPENDIX B – Results of the three-point flexural bending test

Figure B 1-Figure B 13 and Table B 1-Table B 14 presents the results of the analysis in the three-point flexural bending test for all the composites.

Epoxy acetone blank

Table B 1 – Epoxy acetone blank.

Specimen no.	E_f	σ_{fM}	ϵ_{fB}	h	b	A_0
	MPa	MPa	%	mm	mm	mm ²
1	2334.043	82.53867	3.880223	3.003	9.675	29.05403
2	2344.093	97.67607	4.874884	2.971	9.67	28.72957
3	2338.17	94.63739	4.647414	2.997	9.69	29.04093
4	2274.191	115.9	6.906128	2.991	9.68	28.95288
5	2259.11	119.4428	7.560165	2.996	9.67	28.97132

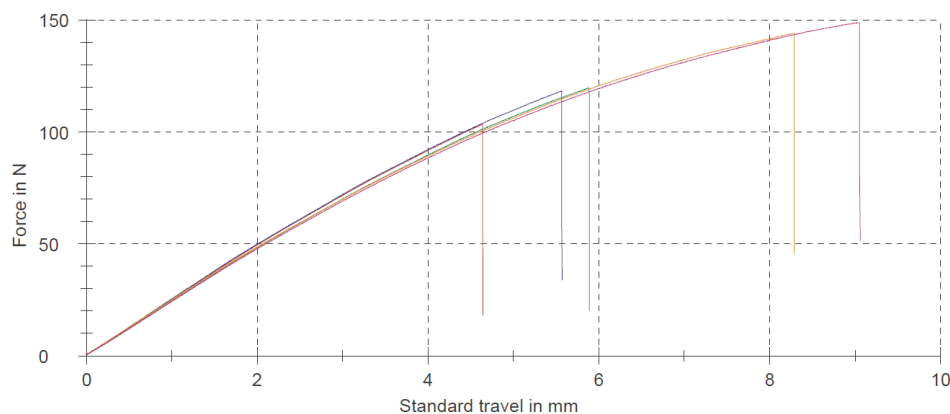


Figure B 1 - Epoxy acetone blank, three-point flexural test.

Epoxy in distilled water blank

Table B 2 – Epoxy in distilled water blank.

Specimen no.	E_f	σ_{fM}	ϵ_{fB}	h	b	A_0
	MPa	MPa	%	mm	mm	mm ²
1	2441.72	111.4703	5.693612	2.978	9.68	28.82704
2	2370.914	122.6385	7.576648	2.975	9.71	28.88725
3	2406.629	117.9602	6.496492	3.018	9.68	29.21424
4	2393.576	119.9664	6.662202	3.053	9.67	29.52251
5	2323.628	109.2767	5.919651	3.084	9.71	29.94564

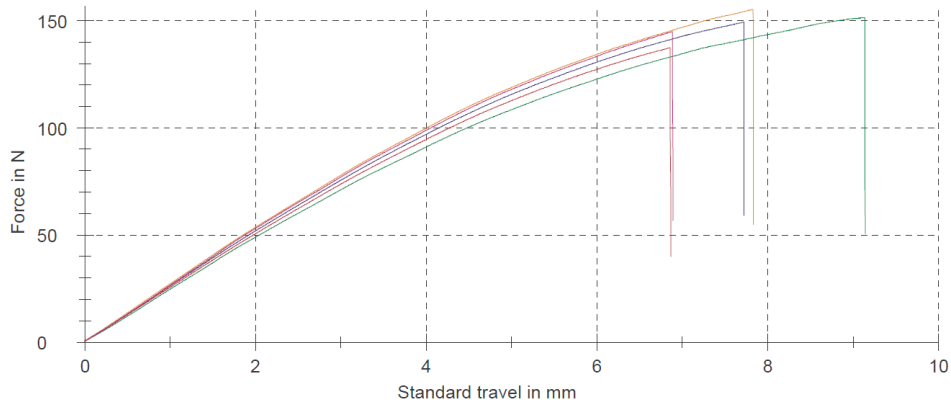


Figure B 2 - Epoxy in distilled water blank three-point flexural test.

Epoxy in acetone and EXGO (1000 C)

Table B 3 – Epoxy in acetone and EXGO (1000 C).

Specimen no.	E_f	σ_{fM}	ϵ_{fB}	h	b	A_0
	MPa	MPa	%	mm	mm	mm ²
1	2024.657	85.91167	4.783522	3.032	9.668	29.31338
2	2111.18	79.51254	4.096752	2.912	9.705	28.26096
3	2141.269	70.0276	3.461469	2.914	9.709	28.29203
4	2062.829	65.53657	3.362639	2.921	9.67	28.24607
5	2115.273	79.24178	4.04847	2.907	9.707	28.21825

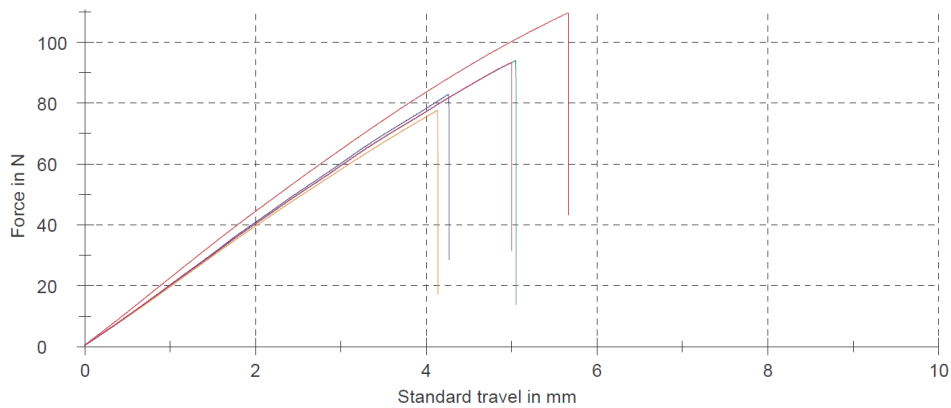


Figure B 3 - Epoxy in acetone and EXGO (1000 C) three-point flexural test.

FGO in acetone epoxy

Table B 4- FGO in acetone epoxy.

Specimen no.	E_f	σ_{fM}	ε_{fB}	h	b	A_0
	MPa	MPa	%	mm	mm	mm ²
1	2279.163	122.9289	8.875512	3.013	9.67	29.13571
2	2277.51	114.7288	6.944635	2.982	9.68	28.86576
3	2266.145	110.7113	6.309306	3.06	9.67	29.5902
4	2271.953	107.5714	5.874031	3.068	9.71	29.79028
5	2312.786	113.3463	6.448153	2.964	9.68	28.69152

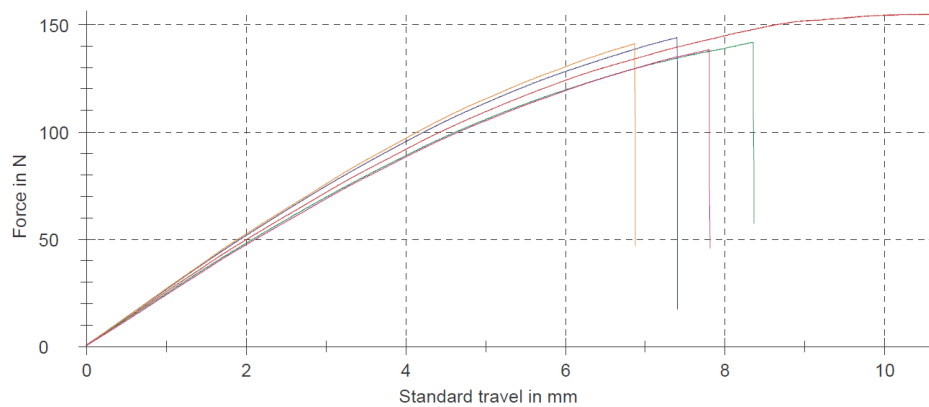


Figure B 4 - FGO in acetone epoxy three-point flexural test

FGO (XB3473) in distilled water epoxy

Table B 5 – FGO (XB3473) in distilled water epoxy

Specimen no.	E_f	σ_{fM}	ε_{fB}	h	b	A_0
	MPa	MPa	%	mm	mm	mm ²
1	2343.597	74.97258	3.384066	2.983	9.71	28.96493
2	2339.6	94.98448	4.660854	3.004	9.71	29.16884
3	2351.813	97.35846	4.757906	2.994	9.71	29.07174
4	2266.284	98.46176	5.075187	3.029	9.67	29.29043
5	2379.059	81.97381	3.718712	2.99	9.7	29.003

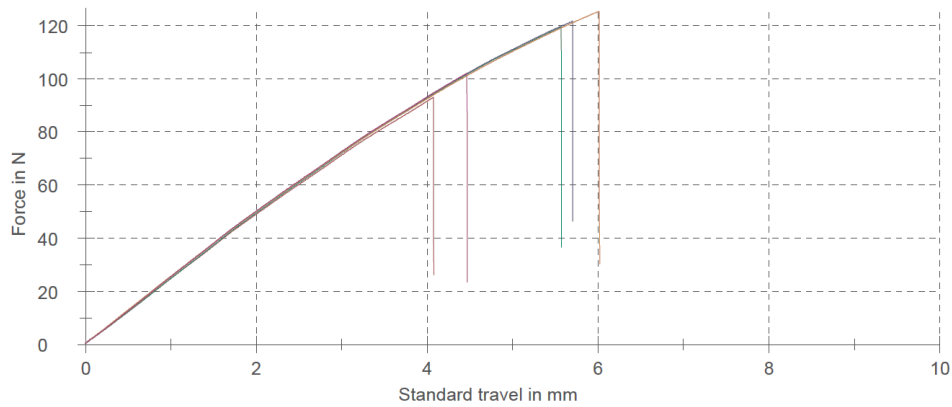


Figure B 5 – FGO (XB3473) in distilled water epoxy three-point flexural test

GO in acetone epoxy

Table B 6 – GO in acetone epoxy

Specimen no.	E_f	σ_{fM}	ε_{fB}	h	b	A_0
	MPa	MPa	%	mm	mm	mm ²
1	2417.648	104.6754	5.367882	2.848	9.68	27.56864
2	2488.957	57.27169	2.340299	2.812	9.71	27.30452
3	2435.658	96.49696	4.712065	2.738	9.67	26.47646
4	2372.227	94.51267	4.775529	2.741	9.68	26.53288
5	2507.513	90.57692	4.147957	2.68	9.7	25.996

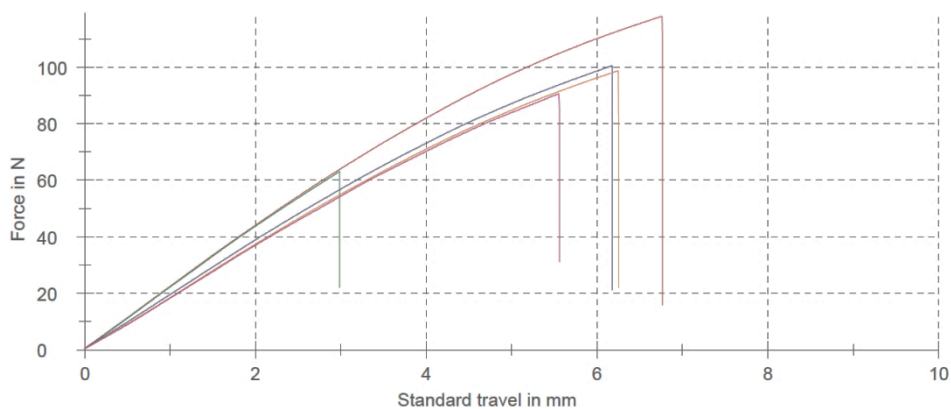


Figure B 6 - GO in acetone epoxy three-point flexural test

Epoxy in distilled water and EXGO (300° C)

Table B 7 – Epoxy in distilled water and EXGO (300°C)

Specimen no.	E_f	σ_{fM}	ϵ_{fB}	h	b	A_0
	MPa	MPa	%	mm	mm	mm ²
1	1980	47.8	2.4			
2	2020	39.0	1.9			
3	1990	43.4	2.2			
4	2080	51.1	2.5			

FGO (PPDA) in distilled water epoxy

Table B 8 – FGO (PPDA) in distilled water epoxy

Specimen no.	E_f	σ_{fM}	ϵ_{fB}	h	b	A_0
	MPa	MPa	%	mm	mm	mm ²
1	1670.935	94.09951	7.520723	3.014	9.715	29.28101
2	1666.689	80.87206	5.691954	3.053	9.717	29.666
3	1696.683	54.41741	3.340296	2.995	9.717	29.10242
4	1665.893	74.66643	5.116529	2.99	9.714	29.04486
5	1661.778	90.3306	6.937421	3.003	9.715	29.17415

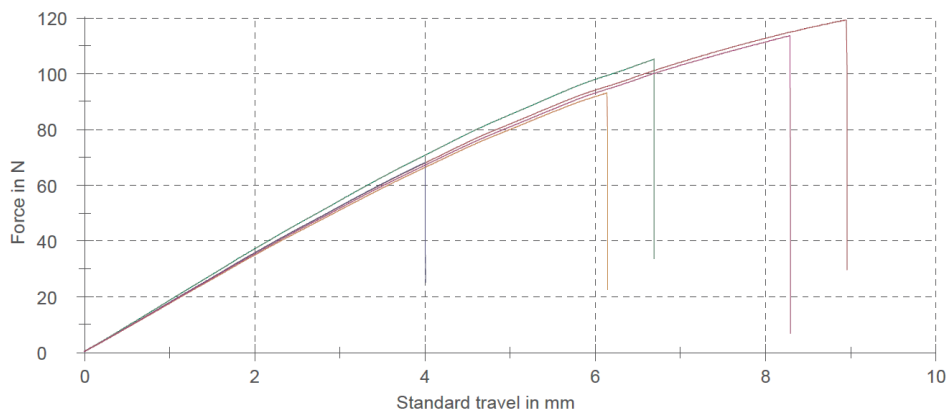


Figure B 7 – FGO (PPDA) in distilled water epoxy result three-point flexural test

Epoxy/IPDA reference

Table B 9 – Epoxy/IPDA standard, low temperature curing

Specimen no.	E_f	σ_{fM}	ε_{fB}	h	b	A_0
	MPa	MPa	%	mm	mm	mm ²
1	2158.535	86.66795	4.190898	3.004	9.724	29.2109
2	2200.267	88.64421	4.155558	3.037	9.722	29.52571
3	2218.217	81.01216	3.718264	3.049	9.758	29.75214
4	2257.357	128.934	8.540655	3.044	9.724	29.59986
5	2223.217	89.43132	4.161225	3.049	9.765	29.77349

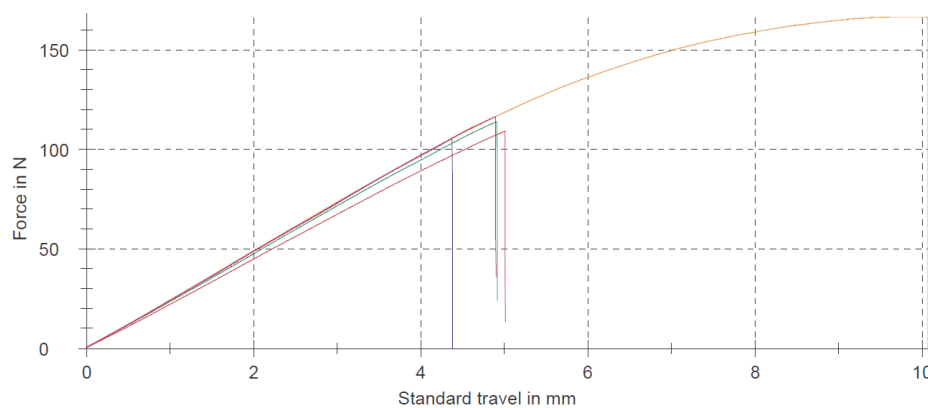


Figure B 8 – IPDA reference standard results from three-point flexural test

Epoxy/IPDA reference 2

Table B 10 – Epoxy/IPDA reference standard 2, wrong span (too long)

Specimen no.	E_f	σ_{fM}	ε_{fB}	h	b	A_0
	MPa	MPa	%	mm	mm	mm ²
1	1993.388	83.7661	4.551335	3.061	9.696	29.67946
2	1956.114	58.99815	3.082027	3.084	9.699	29.91172
3	1990.003	92.28209	5.241564	3.017	9.74	29.38558

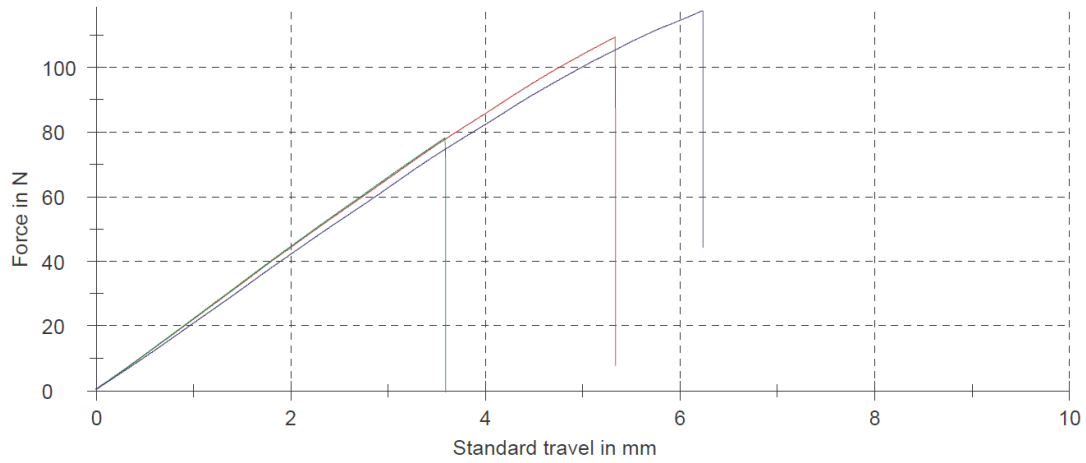


Figure B 9 – Epoxy/IPDA reference standard, wrong span (too long).

Table B 11 - Epoxy/IPDA reference standard 2, wrong span (too short)

Specimen no.	E_f	σ_{fM}	ϵ_{fB}	h	b	A_0
	MPa	MPa	%	mm	mm	mm ²
1	3038.456	82.51476	2.753028	3.009	9.742	29.31368

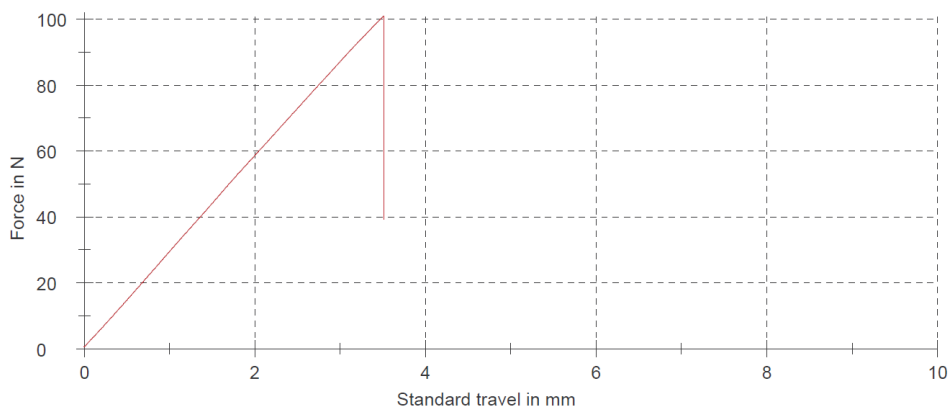


Figure B 10 – Epoxy/IPDA reference standard 2, wrong span (too short).

Table B 12 – Epoxy/IPDA reference standard 2, correct distance

Specimen no.	E_f	σ_{fM}	ϵ_{fB}	h	b	A_0
	MPa	MPa	%	mm	mm	mm ²
1	2719.777	120.177	5.345671	2.998	9.74	29.20052
2	2648.806	89.66214	3.563198	3.049	9.701	29.57835
3	2728.168	98.77388	3.883635	3.09	9.693	29.95137
4	2704.725	49.75889	1.82123	3.041	9.736	29.60718
5	2547.64	82.28575	3.349173	2.995	9.702	29.05749

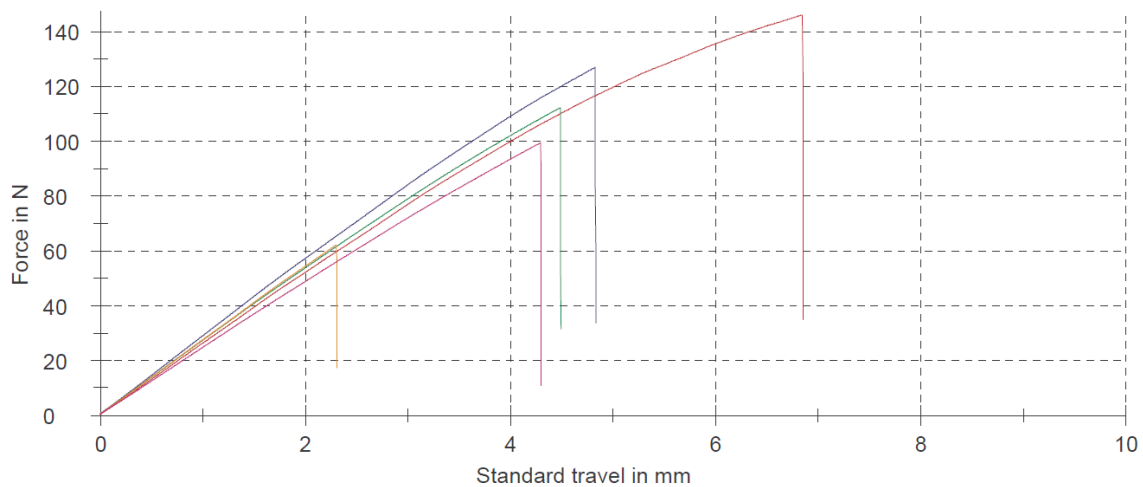


Figure B 11 – Epoxy /IPDA reference standard 2 results three-point flexural test. Correct distance.

IPDA + FGO (PPDA)

Table B 13 – Results of three point flexural test, IPDA/FGO (PPDA)

Specimen no.	E_f	σ_{fM}	ϵ_{fB}	h	b	A_0
	MPa	MPa	%	mm	mm	mm ²
1	2692.515	126.6931	11.75228	2.981	9.703	28.92464
2	2685.038	60.44254	2.262247	2.985	9.704	28.96644
3	2772.307	62.46311	2.266291	2.97	9.708	28.83276
4	2716.096	95.72111	3.818756	3.013	9.706	29.24418
5	2792.46	124.2276	5.688556	2.989	9.744	29.12482
6	2788.454	80.471	2.976337	3.026	9.74	29.47324
7	2800.00	36.90248	1.338055	2.993	9.739	29.3619
8	2762.324	131.0201	9.702153	3.027	9.7	29.3619

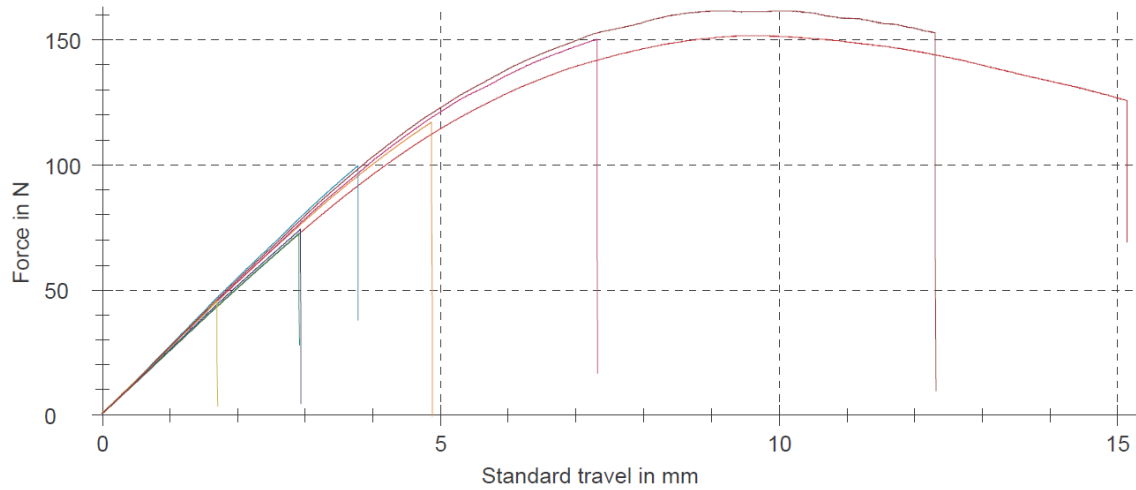


Figure B 12 - Results of three point flexural test, IPDA/FGO (PPDA).

LY556/XB3473 reference standard

Table B 14 – Results from three point flexural test, LY556/XB3473 reference standard 2.

Specimen no.	E_f	σ_{fM}	ϵ_{fB}	h	b	A_0
	MPa	MPa	%	mm	mm	mm ²
1	2503.651	101.2353	4.98149	3.006	9.708	29.18225
2	2453.59	103.0935	5.277519	3.016	9.659	29.13154
3	2380.42	96.66496	4.977077	3.041	9.671	29.40951
4	2426.072	115.2694	6.953749	3.042	29.42831	
5	2517.222	90.83613	4.193131	2.997	9.71	29.10087

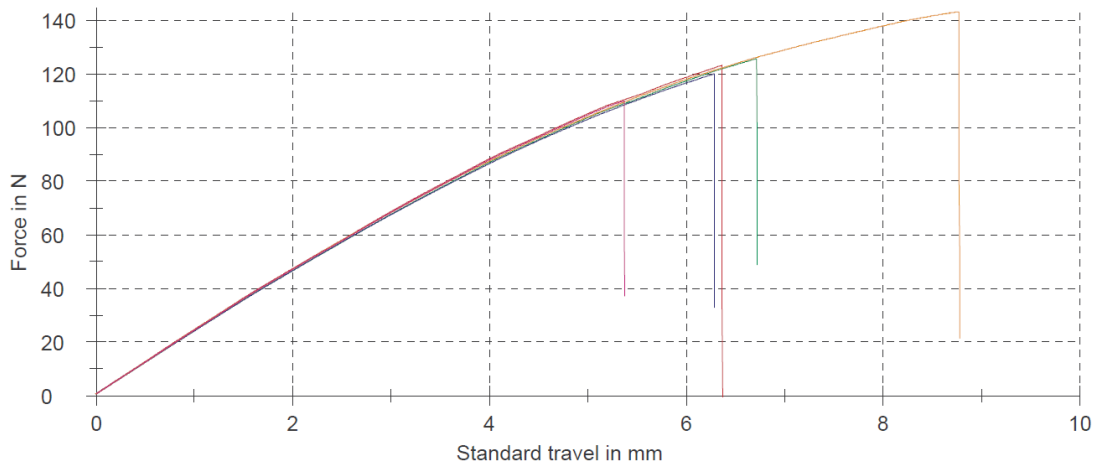


Figure B 13 - Results from three point flexural test, LY556/XB3473 reference standard 2.

APPENDIX C – RISK ASSESSMENT

NTNU	Risk assessment			Prepared by	Number	Date
				HSE/KS	HSE section	HMSRV2603E
			Approved by		Replaces	
			The Rector			01.12.2006

Unit: *Chemical engineering*
 Line manager: *Edd A. Blekkan*
 Participants in the identification process (including their function): *Elizabeth M. Svendsen, student and Finn Knut Hansen, co-supervisor*
 Short description of the main activity/main process: *Master project for student Elizabeth M. Svendsen, Project title: Graphene and graphene oxide in nanocomposites*

Date: *27.03.2014*

Signatures: Responsible supervisor: *F. Blekkan* Student: *Elizabeth M. Svendsen*

Activity from the identification process form	Potential undesirable incident/strain	Likelihood: Likelihood (1-5)	Consequence:		Risk Value (human)	Comments/status Suggested measures
			Human (A-E)	Environment (A-E)		
Chemicals, preparation of graphene oxide(GO), preparation of GO/epoxy composite, amines	Overheating, spillage of chemicals, eye- or skin damage	3	B	B	3B	Fumehood, gloves, safety glasses, coat
Ultrasonication bath/horn	Hearing impairment	2	C	A	2C	Hearing protection
DMA		1	A	A	1A	
Disk centrifuge	Spillage of chemicals	1	A	A	1A	Fumehood, gloves, safety glasses, coat
Three point bending test	Eye damage,	3	B	B	3B	Safety glasses, cover the sample with paper to prevent flying parts
Grinding machine for epoxy rods		2	A		2A	Do not wear loose sweaters, bracelets or big necklaces

Likelihood, e.g.:
 1. Minimal
 2. Low
 3. Medium
 4. High
 5. Very high

Consequence, e.g.:
 A. Safe
 B. Relatively safe
 C. Dangerous
 D. Critical
 E. Very critical

Risk value (each one to be estimated separately):
 Human = Likelihood x Human Consequence
 Environmental = Likelihood x Environmental consequence
 Financial/material = Likelihood x Consequence for Economy/material

NTNU	Hazardous activity identification process			Prepared by	Number	Date
 HSE				HSE section	HMSRV-28/01	09.01.2013
		Approved by		Replaces		
		The Rector		01.12.2008		

Unit: Chemical engineering

Date: 27.03.2014

Line manager: Edd A. Blekkan

Participants in the identification process (including their function): Elizabeth M. Svendsen, student and Finn Knut Hansen, co-supervisor

Short description of the main activity/main process: Master project for student Elizabeth M. Svendsen, Project title: Graphene and graphene oxide in nanocomposites

Is the project work purely theoretical? (YES/NO): NO

Signatures: Responsible supervisor: F. Ulstein

Student: Elizabeth M. Svendsen

ID nr.	Activity/process	Responsible person	Existing documentation	Existing safety measures	Laws, regulations etc.	Comment
1	Chemicals, preparation of graphene oxide(GO), exfoliation of GO, preparation of GO/epoxy composite, amines	Elizabeth Svendsen/Finn Knut Hansen	Data sheets	Fumehood, gloves, safety glasses, coat		Hazardous if spilled or consumed, can overheat, high pressure and temperature, amines can potentially give allergic reactions to the skin
2	Ultrasonication bath/horn	Finn Knut Hansen				Harmful noise
3		Bernt B. Johnsen	Instrument folder			Heat
4	DMA	Tomas R. Frømyr	Instrument folder			Heat, spillage of chemicals
5	Disk centrifuge Three point bending test	Bernt B. Johnsen		Fumehood, gloves, safety glasses, coat Safety glasses		Flying parts
6	Grinding machine for epoxy rods	Torbjørn Oisen				Rotating parts

APPENDIX D – ZETA POTENTIAL

Figure D 1- Figure D 6 show the print- outs with the results of FGO (PPDA) dispersed in distilled water analysed in Zetasizer at different pH's.

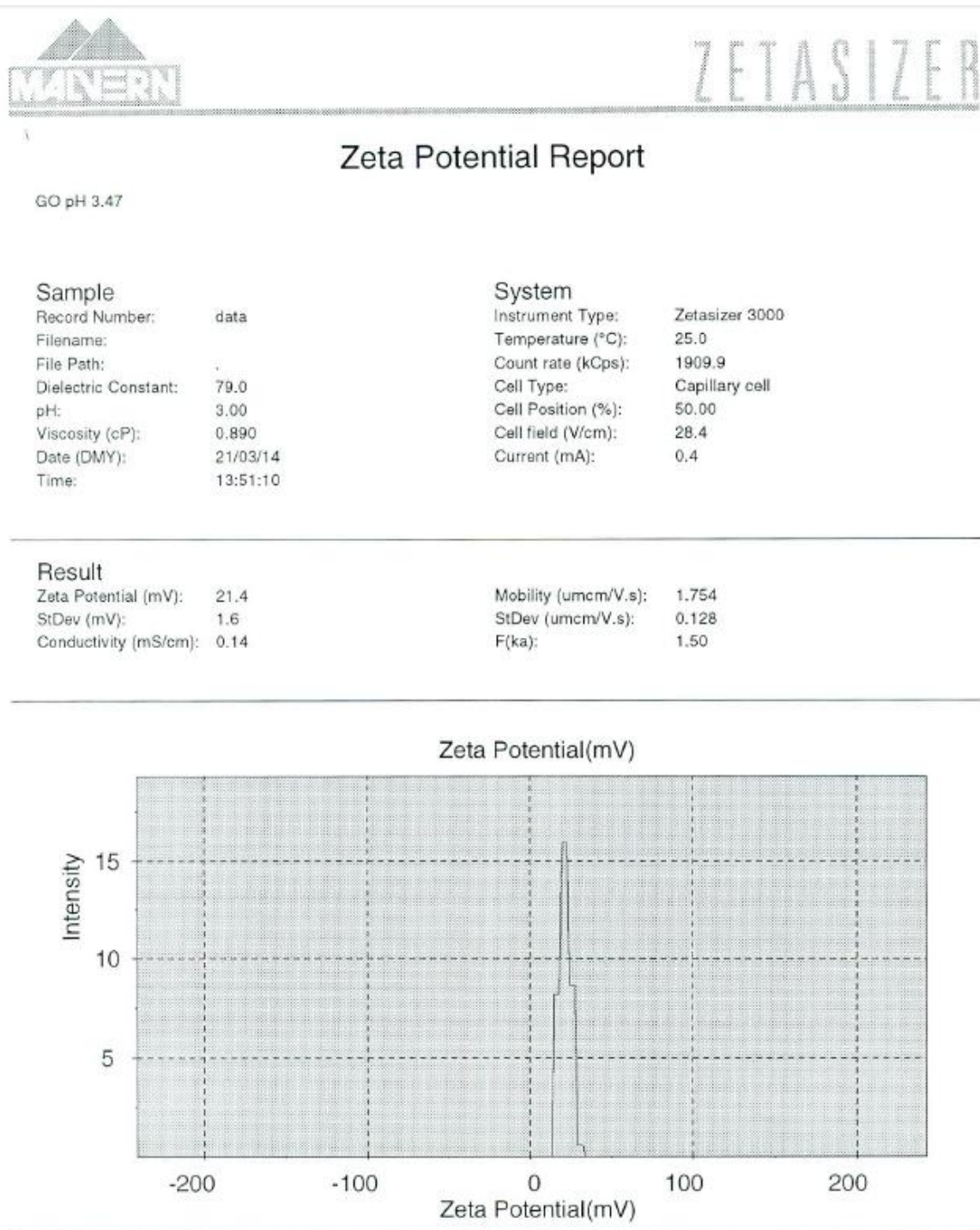


Figure D 1 – Zeta potential of FGO (PPDA) at pH =3.47.



Zeta Potential Report

GO pH 4.17

Sample

Record Number: data
Filename:
File Path: .
Dielectric Constant: 79.0
pH: 3.00
Viscosity (cP): 0.890
Date (DMY): 21/03/14
Time: 13:32:45

System

Instrument Type: Zetasizer 3000
Temperature (°C): 25.0
Count rate (kCps): 1939.4
Cell Type: Capillary cell
Cell Position (%): 50.00
Cell field (V/cm): 28.3
Current (mA): 0.1

Result

Zeta Potential (mV): 10.7
StDev (mV): 1.6
Conductivity (mS/cm): 0.03

Mobility (umcm/V.s): 0.880
StDev (umcm/V.s): 0.129
F(ka): 1.50

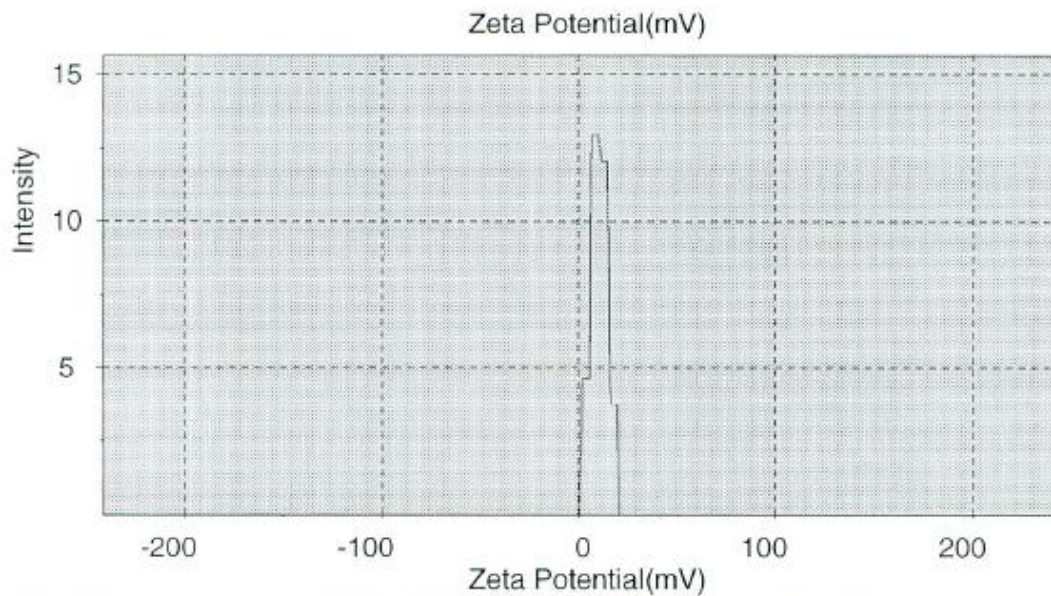


Figure D 2 - Zeta potential of FGO (PPDA) at pH = 4.17.

Zeta Potential Report

Default sample name

Sample

Record Number: data
 Filename:
 File Path:
 Dielectric Constant: 79.0
 pH: 3.09
 Viscosity (cP): 0.890
 Date (DMY): 21/03/14
 Time: 11:38:01

System

Instrument Type: Zetasizer 3000
 Temperature (°C): 25.0
 Count rate (kCps): 328.0
 Cell Type: Capillary cell
 Cell Position (%): 50.00
 Cell field (V/cm): 28.5
 Current (mA): 0.1

Result

Zeta Potential (mV): 19.5
 StDev (mV): 71.6
 Conductivity (mS/cm): 0.03
 Mobility (umcm/V.s): 1.476
 StDev (umcm/V.s): 5.619
 F(ka): 1.50

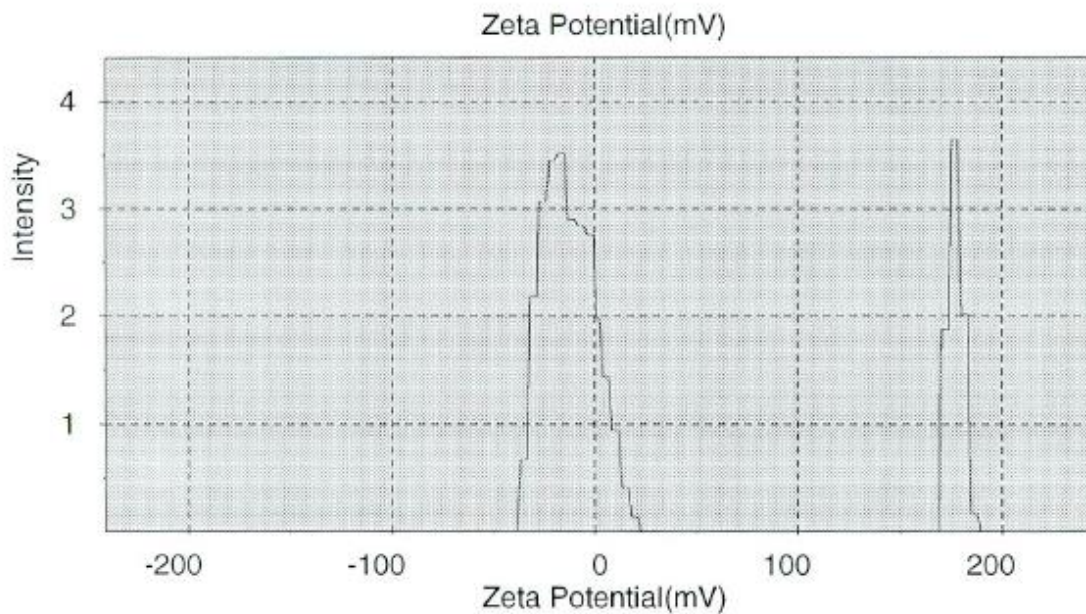


Figure D 3 - Zeta potential of FGO (PPDA) at pH =4.26.

Zeta Potential Report

GO pH 5.7

Sample

Record Number: data
 Filename:
 File Path:
 Dielectric Constant: 79.0
 pH: 2.99
 Viscosity (cP): 0.890
 Date (DMY): 21/03/14
 Time: 13:39:11

System

Instrument Type: Zetasizer 3000
 Temperature (°C): 25.0
 Count rate (kCps): 1816.9
 Cell Type: Capillary cell
 Cell Position (%): 50.00
 Cell field (V/cm): 28.2
 Current (mA): 0.1

Result

Zeta Potential (mV):	-31.2	Mobility (umcm/V.s):	-2.406
StDev (mV):	1.6	StDev (umcm/V.s):	0.129
Conductivity (mS/cm):	0.03	F(ka):	1.50

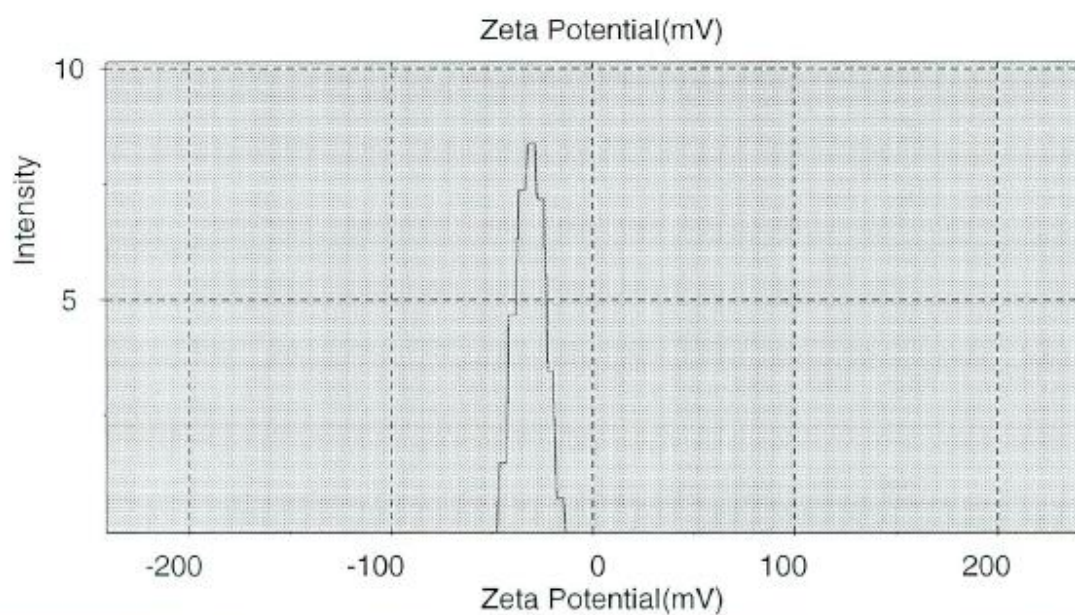


Figure D 4 - Zeta potential of FGO (PPDA) at pH =5.7.

Zeta Potential Report

GO pH8.1

Sample

Record Number: data
 Filename:
 File Path:
 Dielectric Constant: 79.0
 pH: 3.06
 Viscosity (cP): 0.891
 Date (DMY): 21/03/14
 Time: 12:11:54

System

Instrument Type: Zetasizer 3000
 Temperature (°C): 25.0
 Count rate (kCps): 1798.1
 Cell Type: Capillary cell
 Cell Position (%): 50.00
 Cell field (V/cm): 28.2
 Current (mA): 0.1

Result

Zeta Potential (mV):	-42.0	Mobility (umcm/V.s):	-3.294
StDev (mV):	1.6	StDev (umcm/V.s):	0.129
Conductivity (mS/cm):	0.04	F(ka):	1.50

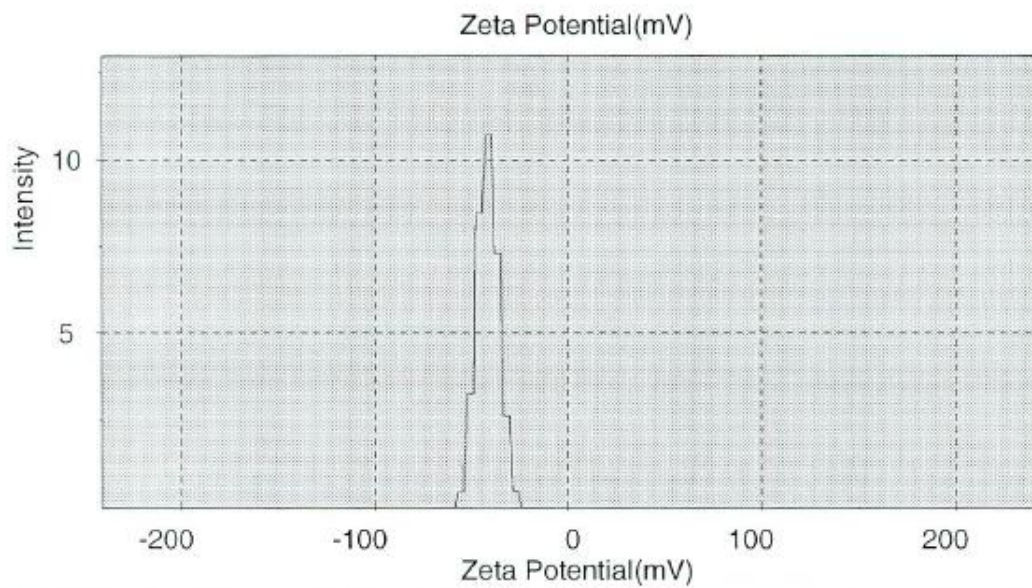


Figure D 5 - Zeta potential of FGO (PPDA) at pH =8.1.

Zeta Potential Report

GO pH 9.94

Sample

Record Number: data
 Filename:
 File Path:
 Dielectric Constant: 79.0
 pH: 3.06
 Viscosity (cP): 0.890
 Date (DMY): 21/03/14
 Time: 12:31:40

System

Instrument Type: Zetasizer 3000
 Temperature (°C): 25.0
 Count rate (kCps): 1813.4
 Cell Type: Capillary cell
 Cell Position (%): 50.00
 Cell field (V/cm): 28.2
 Current (mA): 0.2

Result

Zeta Potential (mV):	9.5	Mobility (umcm/V.s):	0.695
StDev (mV):	1.6	StDev (umcm/V.s):	0.129
Conductivity (mS/cm):	0.09	F(ka):	1.50

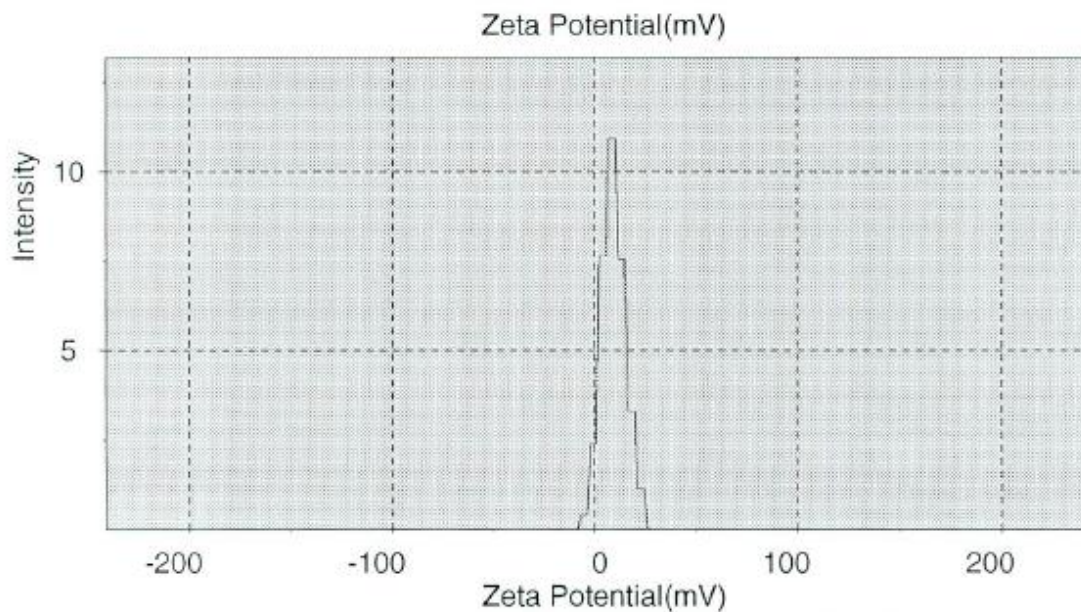


Figure D 6 - Zeta potential of FGO (PPDA) at pH =9.94.

APPENDIX E - DATA SHEETS EPOXY SYSTEM LY556/XB3473

Hot curing epoxy system based on Araldite LY 556 / Hardener XB 3473

Advanced Materials



Structural Composites

DATA SHEET

Hot curing epoxy system based on Araldite® LY 556* / Hardener XB 3473*																																								
Araldite LY 556 is an epoxy resin Hardener XB 3473 is a formulated amine hardener																																								
Applications	<ul style="list-style-type: none"> • Industrial composites • Structural composites 																																							
Properties	Laminating system																																							
Processing	<ul style="list-style-type: none"> • Filament Winding • Resin Transfer Moulding (RTM) • Pressure Moulding • Pultrusion 																																							
Key data	<table border="1"> <thead> <tr> <th colspan="3">Araldite LY 556</th> </tr> </thead> <tbody> <tr> <td>Aspect (visual)</td> <td>clear, pale yellow liquid</td> <td></td> </tr> <tr> <td>Colour (Gardner, ISO 4630)</td> <td>≤ 2</td> <td></td> </tr> <tr> <td>Viscosity at 25 °C (ISO 12058-1)</td> <td>10000 - 12000</td> <td>[mPa s]</td> </tr> <tr> <td>Density at 25 °C (ISO 1675)</td> <td>1.15 - 1.2</td> <td>[g/cm³]</td> </tr> <tr> <td>Flash point (ISO 2719)</td> <td>> 200</td> <td>[°C]</td> </tr> <tr> <td>Storage temperature (see expiry date on original container)</td> <td>2 - 40</td> <td>[°C]</td> </tr> <tr> <th colspan="3">Hardener XB 3473</th> </tr> <tr> <td>Aspect (visual)</td> <td>clear yellow to brown liquid</td> <td></td> </tr> <tr> <td>Viscosity at 25 °C (ISO 12058-1)</td> <td>95 - 145</td> <td>[mPa s]</td> </tr> <tr> <td>Density at 25 °C (ISO 1675)</td> <td>0.99 - 1.02</td> <td>[g/cm³]</td> </tr> <tr> <td>Flash point (ISO 2719)</td> <td>121</td> <td>[°C]</td> </tr> <tr> <td>Storage temperature (see expiry date on original container)</td> <td>2 - 40</td> <td>[°C]</td> </tr> </tbody> </table>	Araldite LY 556			Aspect (visual)	clear, pale yellow liquid		Colour (Gardner, ISO 4630)	≤ 2		Viscosity at 25 °C (ISO 12058-1)	10000 - 12000	[mPa s]	Density at 25 °C (ISO 1675)	1.15 - 1.2	[g/cm ³]	Flash point (ISO 2719)	> 200	[°C]	Storage temperature (see expiry date on original container)	2 - 40	[°C]	Hardener XB 3473			Aspect (visual)	clear yellow to brown liquid		Viscosity at 25 °C (ISO 12058-1)	95 - 145	[mPa s]	Density at 25 °C (ISO 1675)	0.99 - 1.02	[g/cm ³]	Flash point (ISO 2719)	121	[°C]	Storage temperature (see expiry date on original container)	2 - 40	[°C]
Araldite LY 556																																								
Aspect (visual)	clear, pale yellow liquid																																							
Colour (Gardner, ISO 4630)	≤ 2																																							
Viscosity at 25 °C (ISO 12058-1)	10000 - 12000	[mPa s]																																						
Density at 25 °C (ISO 1675)	1.15 - 1.2	[g/cm ³]																																						
Flash point (ISO 2719)	> 200	[°C]																																						
Storage temperature (see expiry date on original container)	2 - 40	[°C]																																						
Hardener XB 3473																																								
Aspect (visual)	clear yellow to brown liquid																																							
Viscosity at 25 °C (ISO 12058-1)	95 - 145	[mPa s]																																						
Density at 25 °C (ISO 1675)	0.99 - 1.02	[g/cm ³]																																						
Flash point (ISO 2719)	121	[°C]																																						
Storage temperature (see expiry date on original container)	2 - 40	[°C]																																						
Storage	<p>Provided that Araldite LY 556 and Hardener XB 3473 are stored in a dry place in their original, properly closed containers at the above mentioned storage temperatures they will have the shelf lives indicated on the labels. Partly emptied containers should be closed immediately after use.</p>																																							

* In addition to the brand name product denomination may show different appendices, which allows us to differentiate between our production sites: e.g., BD = Germany, US = United States, IN = India, CI = China, etc.. These appendices are in use on packaging, transport and invoicing documents. Generally the same specifications apply for all versions. Please address any additional need for clarification to the appropriate Huntsman contact.

Processing data

Mix ratio	<i>Components</i>	<i>Parts by weight</i>	<i>Parts by volume</i>
	Araldite LY 556	100	100
	Hardener XB 3473	23	27
<p>We recommend that the components are weighed with an accurate balance to prevent mixing inaccuracies which can affect the properties of the matrix system. The components should be mixed thoroughly to ensure homogeneity. It is important that the side and the bottom of the vessel are incorporated into the mixing process.</p> <p>When processing large quantities of mixture the pot life will decrease due to exothermic reaction. It is advisable to divide large mixes into several smaller containers.</p>			
Initial mix viscosity (cone/plate viscosimeter)		<i>[°C]</i>	<i>[mPa s]</i>
	LY 556/XB 3473	at 25	5200 - 6000
		at 40	700 - 900
Pot life (Tecam, 23°C, 65 % RH)		<i>[g]</i>	<i>[h]</i>
	LY 556/XB 3473	100	32 - 37
Gel time (Hot plate)		<i>[°C]</i>	<i>[min]</i>
	LY 556/XB 3473	at	68 - 78
		120	35 - 43
		at	18 - 23
		140	9 - 13
		at	
		160	
		at 180	
<p>The values shown are for small amounts of pure resin/hardener mix. In composite structures the gel time can differ significantly from the given values depending on the fibre content and the laminate thickness.</p>			

Properties of the cured, neat formulation

Glass transition temperature (IEC 1006, DSC, 10 K/min)	<i>Cure:</i> 4 h 80°C + 4 h 160°C 2 h 120°C + 4 h 180°C 2 h 120°C + 2 h 160°C + 2h 200°C 2 h 120°C + 2 h 160°C + 2h 200°C + 4h 220°C	T_g [°C] [°C] [°C] [°C]	LY 556 XB 3473 162 - 168 185 - 194 185 - 193 187 - 195
Glass transition temperature (ISO 6721, DMA, 2 K/min)	<i>Cure:</i> 2 h 120°C + 2 h 140°C + 2h 180°C	T_g [°C]	LY 556 XB 3473 175 - 185
Flexural test (ISO 178)	<i>Cure:</i> 2 h 120°C + 2 h 140°C + 2 h 180°C		
	Flexural strength	[MPa]	110 - 120
	Elongation at flexural strength	[%]	5,5 - 6,5
	Ultimate strength	[MPa]	110 - 120
	Ultimate elongation	[%]	5,5 - 6,5
	Flexural modulus	[MPa]	2700 - 2900
Fracture properties	<i>Cure:</i>		
Bend notch test (PM 258-0/90)	2 h 120°C + 2 h 140°C + 2 h 180°C		
	Fracture toughness K_{Ic}	[MPa \sqrt{m}]	0,70 - 0,85
	Fracture energy G_{Ic}	[J/m 2]	190 - 220

Properties of the cured, reinforced formulation

	Short beam: Laminate comprising 12 layers unidirectional E-glass fabric (425 g/m 2) Laminate thickness $t = 3.1 - 3.3$ mm Fibre volume content: 63 - 65 %		
Interlaminar shear strength (ASTM D 2344)	<i>Cure:</i> 2 h 120 °C + 2 h 140 °C + 2 h 180 °C		
	Shear strength	[MPa]	62 - 66
Flexural test (ISO 178)	<i>Cure:</i> 2 h 120 °C + 2 h 140 °C + 2 h 180 °C		
	Flexural strength	[MPa]	1050 - 1250
	Ultimate elongation	[%]	2.4 - 2.8
	Flexural modulus	[MPa]	40000 - 44000

Handling precautions	<p>Mandatory and recommended industrial hygiene procedures should be followed whenever our products are being handled and processed. For additional information please consult the corresponding product safety data sheets and the brochure "Hygienic precautions for handling plastics products".</p> <p>Personal hygiene</p> <p><i>Safety precautions at workplace</i></p> <table border="0"> <tr> <td>protective clothing</td> <td>yes</td> </tr> <tr> <td>gloves</td> <td>essential</td> </tr> <tr> <td>arm protectors</td> <td>recommended when skin contact likely</td> </tr> <tr> <td><u>goggles/safety glasses</u></td> <td>yes</td> </tr> </table> <p><i>Skin protection</i></p> <table border="0"> <tr> <td>before starting work</td> <td>Apply barrier cream to exposed skin</td> </tr> <tr> <td><u>after washing</u></td> <td>Apply barrier or nourishing cream</td> </tr> </table> <p><i>Cleansing of contaminated skin</i></p> <p>Dab off with absorbent paper, wash with warm water and alkali-free soap, then dry with disposable towels. Do not use solvents</p> <p><i>Disposal of spillage</i></p> <p>Soak up with sawdust or cotton waste and deposit in plastic-lined bin</p> <p><i>Ventilation</i></p> <table border="0"> <tr> <td>of workshop</td> <td>Renew air 3 to 5 times an hour</td> </tr> <tr> <td>of workplaces</td> <td>Exhaust fans. Operatives should avoid inhaling vapours</td> </tr> </table>	protective clothing	yes	gloves	essential	arm protectors	recommended when skin contact likely	<u>goggles/safety glasses</u>	yes	before starting work	Apply barrier cream to exposed skin	<u>after washing</u>	Apply barrier or nourishing cream	of workshop	Renew air 3 to 5 times an hour	of workplaces	Exhaust fans. Operatives should avoid inhaling vapours
protective clothing	yes																
gloves	essential																
arm protectors	recommended when skin contact likely																
<u>goggles/safety glasses</u>	yes																
before starting work	Apply barrier cream to exposed skin																
<u>after washing</u>	Apply barrier or nourishing cream																
of workshop	Renew air 3 to 5 times an hour																
of workplaces	Exhaust fans. Operatives should avoid inhaling vapours																
First aid	<p>Contamination of the eyes by resin, hardener or mix should be treated immediately by flushing with clean, running water for 10 to 15 minutes. A doctor should then be consulted.</p> <p>Material smeared or splashed on the <i>skin</i> should be dabbed off, and the contaminated area then washed and treated with a cleansing cream (see above). A doctor should be consulted in the event of severe irritation or burns. Contaminated clothing should be changed immediately.</p> <p>Anyone taken ill after <i>inhaling</i> vapours should be moved out of doors immediately.</p> <p>In all cases of doubt call for medical assistance.</p>																
Note	<p>Araldite® is a registered trademark of Huntsman LLC or an affiliate thereof in one or more countries, but not all countries.</p>																

<p>Huntsman LLC</p> <p>®Registered trademark</p> 	<p>IMPORTANT: The following supersedes Buyer's documents. SELLER MAKES NO REPRESENTATION OR WARRANTY, EXPRESS OR IMPLIED, INCLUDING OF MERCHANTABILITY OR FITNESS FOR A PARTICULAR PURPOSE. No statements herein are to be construed as inducements to infringe any relevant patent. Under no circumstances shall Seller be liable for incidental, consequential or indirect damages for alleged negligence, breach of warranty, strict liability, tort or contract arising in connection with the product(s). Buyer's sole remedy and Seller's sole liability for any claims shall be Buyer's purchase price. Data and results are based on controlled or lab work and must be confirmed by Buyer by testing for its intended conditions of use. The product(s) has not been tested for, and is therefore not recommended for, uses for which prolonged contact with mucous membranes, abraded skin, or blood is intended; or for uses for which implantation within the human body is intended.</p>
--	---

APPENDIX F – Tables of surface tension and interfacial tension

Figure F 1 and Figure F 2 show tables of surface tension and interfacial tensions. The tables are borrowed by the supervisor Professor Finn Knut Hansen (UiO/FFI).

Liquid	t (°C)	γ (mN/m)	Boiling pt. (°C)
Pentane	20	16.0	36.1
Diethyl ether	20	17.0	34.5
Polydimethylsiloxanes			
Tetramer	20	17.6	
Dodecamer	20	19.6	
Hexane	20	18.4	68.7
Heptane	20	20.1	98.4
Octane	20	21.1	125.7
Ethanol	20	22.3	78.3
Methanol	20	22.5	64.7
Methyl isobutyl ketone	20	23.6	116.5
Ethyl acetate	20	23.7	77.1
1-Propanol	20	23.7	97.2
Decane	20	23.7	174.9
Acetone	25	24.0	56.3
Methyl ethyl ketone	25	24.0	79.6
1-Butanol	20	24.6	117.7
Cyclohexane	20	25.2	80.7
Dodecane	20	25.3	216.3
1,1,1-Trichloroethane	20	25.6	74.0
1-Pentanol	20	25.6	137.8
1-Octanol	20	26.1	195.2
Tetrahydrofuran	25	26.4	66.0
Carbon tetrachloride	25	26.4	76.7
Chloroform	25	26.7	61.2
Acetic acid	20	27.4	117.9
Methylene chloride	20	27.8	39.7
Cellosolve	25	28.2	135.6
Toluene	20	28.5	110.6
Benzene	20	28.9	80.1
Octanoic acid	20	29.2	239.9
Methyl cellosolve	15	31.8	124.6
Oleic acid	20	32.8	360 (decomposes)
p-Dioxane	15	34.4	101.3
Cyclohexane	20	34.5	155.6
Bromobenzene	20	36.5	155.9
Benzaldehyde	20	38.8	178.9
Aniline	20	42.9	184.4
Nitrobenzene	20	43.9	210.8
Ethylene glycol	20	46.5	197.3
Methylene iodide	20	50.8	182 (decomposes)
Glycerol	20	63.3	290
Water	20	72.9	100.0
Water	30	71.3	100.0
Water	60	67.0	100.0
Mercury	20	484	356.6

Surface tensions and boiling points of some liquids.

Figure F 1– Surface tensions and boiling point of some liquids.

	Liquid	t (°C)	γ_{12} (mN/m)	W^a_{12} (mN/m) ¹⁸
Interfacial tensions and work of adhesion of some organic liquids against water	Hexane	20	51.1	40.1
	Heptane	20	50.2	42.7
	Octane	20	50.8	43.4
	Decane	20	51.2	45.3
	Carbon tetrachloride	20	45.0	54.2
	Toluene	20	36.1	65.2
	Benzene	20	35.0	66.7
	Chloroform	20	31.6	67.9
	Bromobenzène	20	38.1	71.2
	Methylene chloride	20	28.3	72.6
	Methylene iodide	20	48.5	75.0
	Diethyl ether	20	10.7	79.1
	Ethyl acetate	20	6.8	89.7
	Oleic acid	20	15.7	89.9
	1-Octanol	20	8.5	90.4
	Nitrobenzene	20	25.7	91.0
	Octanoic acid	20	8.5	93.5
	1-Pentanol	20	4.4	94.0
	1-Butanol	20	1.8	95.6
	Benzaldehyde	20	15.5	96.1
Aniline	20	5.8	109.9	
Mercury	25	427	130	

Figure F 2– Interfacial tensions and work of adhesion of some organic liquids against water.

APPENDIX G – Characteristic binding energies and chemical shifts for XPS analyses

Table G 1- Table G 3 were received from Spyros Diplas at SINTEF/UiO and show characteristic binding energies and chemical shifts for different chemical compounds for XPS analyses.

Table G 1 – Primary C1s Chemical shifts (eV) relative to saturated hydrocarbon (C1s=285.00 eV)

APPENDIX 1 PRIMARY C 1s CHEMICAL SHIFTS (eV) RELATIVE TO SATURATED HYDROCARBON (C 1s = 285.00 eV)				
Table A1 Oxygen functions				
Functional group	Chemical shift			Number of examples
	Min.	Max.	Mean	
C-O-C	1.13	1.75	1.45	18
C-OH	1.47	1.73	1.55	5
C-O-C	1.12	1.98	1.64	21
	—	—	2.02	1
C=O ^a	2.81	2.97	2.90	3
O-C-O	2.83	3.06	2.93	5
C-O-C*	3.64	4.23	3.99	21
HO-C-	4.18	4.33	4.26	2
O-C-O	4.30	4.34	4.32	2
Table A1 (continued)				
Functional group	Chemical shift			Number of examples
	Min.	Max.	Mean	
	4.36	4.46	4.41	3
	5.35	5.44	5.40	2
^a Neglecting aromatic carboxylic esters, mean of 18 is 1.72, min. 1.48. ^b PEEK significantly lower: shift = 2.10 (BE referenced to aromatic CH C 1s = 284.70 eV). ^c Neglecting aromatic carboxylic esters, mean of 18 is 4.05, min. 3.84.				

Table G 2 – Chemical shifts for XPS analysis.

Table A2 Nitrogen functions				Table A3 Miscellaneous and halogen functions					
Functional group	Chemical shift			Number of examples	Functional group	Chemical shift			Number of examples
	Min.	Max.	Mean			Min.	Max.	Mean	
C-NO ₂ ^a	—	—	0.76	1	C=C	-0.24	-0.31	-0.27	4
C-N<	0.56	1.41	0.94	9		-0.20	-0.56	-0.34	20
C-N≡	0.99	1.22	1.11	2	C-Si	-0.61	-0.78	-0.67	3
*C-C≡N	1.35	1.46	1.41	2	C-S	0.21 ^b	0.52	0.37	2
-C≡N	1.73	1.74	1.74	2	C-SO ₂	0.31 ^b	0.64	0.38	2
C-ONO ₂	—	—	2.62	1	C-SO ₃ ^{-b}	—	—	0.16	1
N-C-O	—	—	2.78	1	C-Br ^b	—	—	0.74	1
N-C=O	2.97	3.59	3.11	6		0.99	1.07	1.02	3
	3.49	3.61	3.55	2	C-Cl	2.00	2.03	2.02	2
N-C-N	—	—	3.84	1	-CCl ₂	—	—	3.56	1
	—	—	3.84	1	C-F	—	—	2.91	1
N-C-O	—	—	4.60	1	-CF ₂	—	—	5.90	1
	—	—	4.60	1	-CF ₃	7.65	7.72	7.69	2

^a C in phenyl ring.

^b Average of C atoms not directly bonded to substituent X.
^c In this example bonded C atom is in phenyl ring.

Table G 3 – O1s binding energies (eV) in Cho polymers relative to saturated hydrocarbon (C1s=285 eV).

APPENDIX 3.1 O 1s BINDING ENERGIES (eV) IN CHO POLYMERS RELATIVE TO SATURATED HYDROCARBON (C 1s = 285.00 eV)

Functional group	Binding energy			Number of examples	Functional group	Binding energy			Number of examples	
	Min.	Max.	Mean			Min.	Max.	Mean		
C-O-C (aliphatic)	532.47	532.83	532.64	8	Aromatic	1	531.62	531.70	531.65	3
(aromatic) ^a	532.98	533.45	533.25	3	O ² -C-Ar	2	533.06	533.22	533.14	
C-OH (aliphatic)	532.74	533.09	532.89	4		1	532.52	532.81	532.64	3
(aromatic) ^b	—	—	533.64	1	2	533.86	534.02	533.91		
	—	—	533.13	1	O ² -C-O ²	1	532.33	532.44	532.38	2
O-C-O	532.94	533.51	533.15	5	2	533.88	533.97	533.93		
O-C-O	532.95	533.02	532.99	2						
	—	—	—	—						
C=O (aliphatic)	532.30	532.37	532.33	3						
(aromatic) ^c	—	—	531.25	1						
Aliphatic	1	531.96	532.43	532.21	20					
O ² -C-C	2	533.24	533.86	533.59						
	—	—	—	—						

^a One or both carbon atoms in phenyl ring (PMS, PDMPO, PEEK).
^b Carbon atom in phenyl ring (PHS).
^c Carbonyl group bonded to phenyl ring (PEEK).

For PEEK and PET BE are referenced to aromatic CH C 1s = 284.70 eV.

A table of characteristic binding energies for carbon functional groups from XPS analysis is given in Table G 4.

Table G 4 – Characteristic binding energies for XPS analyses [59].

Bond/Group	Binding Energy (eV)
C-C	284.0-286.0
C-C (sp ²)	284.3-284.6
C-C (sp ³)	285.0-286.0
C-N	285.2-288.4
C-NR ₂ (amine)	285.5-286.4
O=C-NH (amide)	287.9-288.6
-C=N (nitrile)	266.3-266.8
C-O	286.1-290.0
O=C-OH (carboxyl)	288.0-289.4
-C-O (epoxy)	286.1-287.1
-C-OH (hydroxyl)	286.4-286.7
-C-O-C- (ether)	286.1-288.0
-C=O (aldehyde/ketone)	287.1-288.1
C-F	287.0-293.4
-C-F (covalent)	287.7-290.2
-C-F (ionic)	287.0-287.4
C-C-F	286.0-287.7
C-F ₂	291.6-292.4
C-F ₃	292.4-293.4
C-S	285.2-287.5
C-Cl	287.0-287.2